frontiers | Research Topics

Torpor and hibernation: Metabolic and physiological paradigms

Edited by
Sylvain Giroud, Robert Henning, Yoshifumi Yamaguchi and Jérémy Terrien

Published in
Frontiers in Physiology

ISSN 1664-8714
ISBN 978-2-8325-5062-5
DOI 10.3389/978-2-8325-5062-5

About Frontiers

Frontiers is more than just an open access publisher of scholarly articles: it is a pioneering approach to the world of academia, radically improving the way scholarly research is managed. The grand vision of Frontiers is a world where all people have an equal opportunity to seek, share and generate knowledge. Frontiers provides immediate and permanent online open access to all its publications, but this alone is not enough to realize our grand goals.

Frontiers journal series

The Frontiers journal series is a multi-tier and interdisciplinary set of open-access, online journals, promising a paradigm shift from the current review, selection and dissemination processes in academic publishing. All Frontiers journals are driven by researchers for researchers; therefore, they constitute a service to the scholarly community. At the same time, the *Frontiers journal series* operates on a revolutionary invention, the tiered publishing system, initially addressing specific communities of scholars, and gradually climbing up to broader public understanding, thus serving the interests of the lay society, too.

Dedication to quality

Each Frontiers article is a landmark of the highest quality, thanks to genuinely collaborative interactions between authors and review editors, who include some of the world's best academicians. Research must be certified by peers before entering a stream of knowledge that may eventually reach the public - and shape society; therefore, Frontiers only applies the most rigorous and unbiased reviews. Frontiers revolutionizes research publishing by freely delivering the most outstanding research, evaluated with no bias from both the academic and social point of view. By applying the most advanced information technologies, Frontiers is catapulting scholarly publishing into a new generation.

What are Frontiers Research Topics?

Frontiers Research Topics are very popular trademarks of the *Frontiers journals series*: they are collections of at least ten articles, all centered on a particular subject. With their unique mix of varied contributions from Original Research to Review Articles, Frontiers Research Topics unify the most influential researchers, the latest key findings and historical advances in a hot research area.

Find out more on how to host your own Frontiers Research Topic or contribute to one as an author by contacting the Frontiers editorial office: frontiersin.org/about/contact

Torpor and hibernation: Metabolic and physiological paradigms

Topic editors

Sylvain Giroud – Northern Michigan University, United States
Robert Henning – University Medical Center Groningen, Netherlands
Yoshifumi Yamaguchi – Hokkaido University, Japan
Jérémy Terrien – Muséum National d'Histoire Naturelle, France

Citation

Giroud, S., Henning, R., Yamaguchi, Y., Terrien, J., eds. (2024). *Torpor and hibernation: Metabolic and physiological paradigms*. Lausanne: Frontiers Media SA. doi: 10.3389/978-2-8325-5062-5

Table of contents

frontiers | Frontiers in Physiology

TYPE Editorial
PUBLISHED 18 June 2024
DOI 10.3389/fphys.2024.1441872

OPEN ACCESS

EDITED AND REVIEWED BY
Kamal Rahmouni,
The University of Iowa, United States

*CORRESPONDENCE
Sylvain Giroud,
sgiroud@nmu.edu

RECEIVED 31 May 2024
ACCEPTED 07 June 2024
PUBLISHED 18 June 2024

CITATION
Giroud S, Yamaguchi Y, Terrien J and Henning RH (2024), Editorial: Torpor and hibernation: metabolic and physiological paradigms.
Front. Physiol. 15:1441872.
doi: 10.3389/fphys.2024.1441872

Editorial: Torpor and hibernation: metabolic and physiological paradigms

Sylvain Giroud[1]*, Yoshifumi Yamaguchi[2,3], Jeremy Terrien[4] and Robert H. Henning[5]

[1]Energetics Lab, Department of Biology, Northern Michigan University, Marquette, MI, United States, [2]Hibernation Metabolism, Physiology, and Development Group, Institute of Low Temperature Science, Hokkaido University, Sapporo, Japan, [3]Graduate School of Environmental Science, Hokkaido University, Sapporo, Japan, [4]Unité Mécanismes Adaptatifs et Evolution (MECADEV), Muséum National d'Histoire Naturelle, Centre National de la Recherche Scientifique Unité Mixte de Recherche 7179, Brunoy, France, [5]Department of Clinical Pharmacy and Pharmacology, University Medical Center Groningen, Groningen, Netherlands

KEYWORDS

heterothermy, seasonality, thermoregulation, body temperature, pathophysiology, mammals, primates, biomimicry (biomimetics)

Editorial on the Research Topic
Torpor and hibernation: metabolic and physiological paradigms

Torpor or heterothermy manifest a state of depressed metabolism and feature specific metabolic, cellular and molecular adaptations that often are seasonal (Jastroch et al., 2016; Giroud et al., 2021). The exact mechanisms and functioning of these extraordinary adaptations are poorly understood. Yet their unraveling will advance our understanding of the orchestration of hibernation and may inspire research related to obesity and metabolic syndrome (Martin, 2008), cardiovascular and metabolic dysfunctions (Nelson and Robbins, 2015; Bonis et al., 2018), ischemia-reperfusion injuries (Drew et al., 2001; Kurtz et al., 2006), immune depression (Bouma et al., 2010), and longevity of animal species (Keil et al., 2015). Collectively, the Research Topic covers three main aspects on metabolic and physiological changes associated to the phenotype of torpor across several heterothermic species: (i) seasonal metabolic and somatic changes in hibernators; (ii) thermogenic mechanisms, cryoprotection and resistance to metabolic depression; and (iii) mechanisms enabling the induction of a torpid state or "synthetic torpor."

Hibernators undergo marked seasonal changes in energy metabolism with large differences between an active reproductive season and a period of metabolic depression conveying winter survival. To accommodate seasonal fluctuations, fat-storing hibernators particularly master the circannual cycle of promoting storage or mobilizing lipids. The energy balance of hibernators is regulated by several hormones notably during pre-hibernation fattening (Florant and Healy, 2012). Insulin control of carbohydrate and lipid metabolism is central in regulating cycles of intermittent fasting in mammalian hibernators. Blanco et al. examine glucose and insulin dynamics across the feast-fast cycle in fat-tailed dwarf lemurs (*Cheirogaleus medius*), the only obligate hibernator among primates, showing mechanisms involved in lean-season insulin resistance. In the same vein, Heinis et al. highlight the main metabolic pathways occurring during hibernation by reporting the polar metabolomic profile of white adipose tissue isolated from active and hibernating thirteen-lined ground squirrels (*Ictidomys tridecemlineatus*).

While hibernation interrupts the reproductive cycle in many heterothermic mammals, some hibernating bats engage in mating during hibernation. Sato et al. report males of little horseshoe bats (*Rhinolophus cornutus*) retaining sexual behavior and copulating with females during hibernation. Forced mating appears to increase chances of male bats to obtain a mate while avoiding pre-mating female selection, whereas forced copulations induced arousal in torpid females, which then cannot opt for higher-quality males. The seasonal metabolic changes occurring in hibernators are also associated with changes in individuals' somatic maintenance such as variations in telomeres, the protective endcap of chromosomes. During hibernation, periodic rewarming, known as interbout arousals, are associated with high metabolic costs including telomeres shortening which can be lengthened in case of extra-energy available during the winter (Giroud et al., 2023) or during the active season (Hoelzl et al., 2016). Galindo-Lalana et al. investigate telomerase activity, a key mechanism in telomere elongation, in the garden dormouse (*Eliomys quercinus*) that shows high telomerase activity across seasons except prior to hibernation due to diversion of resources to increase fat reserves before overwintering.

Besides their seasonal adaptations to overcome challenging conditions, hibernators display powerful metabolic and protective mechanisms, including thermogenesis and cold resistance, to accommodate the physiological extremes and metabolic depression. During arousals, body temperature rapidly rises from 1°C to 40°C requiring tight thermoregulation to maintain rheostasis. Hunstiger et al. reveal differential timing of protein and metabolite abundance of non-shivering thermogenic pathways across different organs in Arctic ground squirrels (*Urocitellus parryii*), indicating distinct thermogenic functions. To extent the understanding of thermoregulatory mechanisms and activation of pro-survival factors during hibernation, Emser et al. studied the mitochondrial single-nucleotide polymorphism m.3017C>T in the evolutionarily conserved gene MT-SHLP6. In-silico analysis indicates the protein truncating polymorphism to be more abundant in heterotherms. Transcript abundance of MT-SHLP6 in thirteen-lined ground squirrel's brown adipose tissue, a key thermogenic organ, is also high before hibernation and during arousal and low during torpor and after hibernation.

Most mammals adapt thermal physiology to normothermic temperatures with large deviations leading to organ dysfunction and death. Conversely, hibernators resist long-term cold states, a current knowledge which is now summarized by Sone and Yamaguchi. During torpor, hibernators also suppress blood clotting to survive prolonged periods of immobility and decreased blood flow that would otherwise lead to potentially lethal clots. Yet, upon arousal hibernators must quickly restore normal clotting activity to avoid excess bleeding. De Vrij et al. review the mechanisms underlying inhibition of hemostasis in multiple species of hibernating mammals in perspective of medical applications to improve cold preservation of platelets and antithrombotic therapy.

The induction of a torpid state in humans, named "synthetic torpor," holds large potential for either long distance space travel or treatments of specific medical conditions, and constitutes an active line of research. To identify underlying mechanisms of torpor, the brain is thought to orchestrate various physiological changes within the organism (Drew et al., 2001). The physiological mechanisms facilitating the switch from an active state to a hibernation phenotype remain to be elucidated. The Siberian chipmunk, a food-storing hibernator, activates AMPK, a protein playing a central role in feeding behavior and metabolic regulation in response to starvation. Kamata et al. report phosphorylation of AMPK in brain of hibernating chipmunks and absence of such in the non-hibernating phenotype, corresponding with differences in lifespan. In the same vein, hyperphosphorylated Tau protein is the hallmark of neurodegeneration. Squarcio et al. elucidate the molecular mechanisms underlying reversible hyperphosphorylation of brain Tau protein during a hypothermic state of "synthetic torpor." Although still far from application in larger non-heterothermic species, such as swine or humans, the overall similarity in Tau and microglia regulation between natural and "synthetic torpor" offers perspective on safe metabolic reduction in non-hibernating species.

Collectively, this Research Topic summarizes key relevant knowledge into understanding the state of hibernation by highlighting various adaptations associated with cryoprotection and resistance to metabolic depression. We hope that this Research Topic will constitute a solid ground for future collaborative and multidisciplinary research efforts toward the understanding of the hibernation phenotype leading to unravel the mechanisms of torpor induction and maintenance in homeotherms for the development of a state of "synthetic torpor" applicable to humans and other non-heterotherms for therapeutic treatments.

Author contributions

SG: Conceptualization, Funding acquisition, Writing–original draft, Writing–review and editing. YY: Conceptualization, Writing–review and editing. JT: Conceptualization, Writing–review and editing. RH: Conceptualization, Writing–review and editing.

Funding

The author(s) declare that financial support was received for the research, authorship, and/or publication of this article. SG was financially supported by the Austrian Science Fund (FWF, Grant No. P31577-B25) and a Faculty Research Grant from Northern Michigan University (NMU, FRG FY2024).

Acknowledgments

The authors would like to thank all authors for their valuable contributions to this Research Topic.

Conflict of interest

The authors declare that the research was conducted in the absence of any commercial or financial relationships that could be construed as a potential conflict of interest.

The author(s) declared that they were an editorial board member of Frontiers, at the time of submission. This had no impact on the peer review process and the final decision.

Publisher's note

References

Bonis, A., Talhouarne, G., Schueller, E., Unke, J., Krus, C., Stokka, J., et al. (2019). Cardiovascular resistance to thrombosis in 13-lined ground squirrels. *J. Comp. Physiology B* 189, 167–177. doi:10.1007/s00360-018-1186-x

Bouma, H. R., Carey, H. V., and Kroese, F. G. M. (2010). Hibernation: the immune system at rest? *J. Leukoc. Biol.* 88, 619–624. doi:10.1189/jlb.0310174

Drew, K., Rice, M., Kuhn, T., and Smith, M. (2001). Neuroprotective adaptations in hibernation: therapeutic implications for ischemia-reperfusion, traumatic brain injury and neurodegenerative diseases. *Free Radic. Biol. Med.* 31 (5), 563–573. doi:10.1016/s0891-5849(01)00628-1

Florant, G. L., and Healy, J. E. (2012). The regulation of food intake in mammalian hibernators: a review. *J. Comp. Physiol. B* 182, 451–467. doi:10.1007/s00360-011-0630-y

Giroud, S., Habold, C., Nespolo, R. F., Mejías, C., Terrien, J., Logan, S. M., et al. (2021). The torpid state: recent advances in metabolic adaptations and protective mechanisms. *Front. Physiol.* 11, 623665. doi:10.3389/fphys.2020.623665

Giroud, S., Ragger, M. T., Baille, A., Hoelzl, F., Smith, S., Nowack, J., et al. (2023). Food availability positively affects the survival and somatic maintenance of hibernating garden dormice (*Eliomys quercinus*). *Front. Zoology* 20 (19), 19. doi:10.1186/s12983-023-00498-9

Hoelzl, F., Cornils, J. S., Smith, S., Moodley, Y., and Ruf, T. (2016). Telomere dynamics in free-living edible dormice (*Glis glis*): the impact of hibernation and food supply. *J. Exp. Biol.* 219, 2469–2474. doi:10.1242/jeb.140871

Jastroch, M., Giroud, S., Barrett, P., Geiser, F., Heldmaier, G., and Herwig, A. (2016). Seasonal control of mammalian energy balance: recent advances in the understanding of daily torpor and hibernation. *J. Neuroendocrinol.* 28. doi:10.1111/jne.12437

Keil, G., Cummings, E., and de Magalhaes, J. P. (2015). Being cool: how body temperature influences ageing and longevity. *Biogerontology* 16, 383–397. doi:10.1007/s10522-015-9571-2

Kurtz, C. C., Lindell, S. L., Mangino, M. J., and Carey, H. V. (2006). Hibernation confers resistance to intestinal ischemia-reperfusion injury. *Am. J. Physiol. Gastrointest. Liver Physiol.* 291, G895–G901. doi:10.1152/ajpgi.00155.2006

Martin, S. (2008). Mammalian hibernation: a naturally reversible model for insulin resistance in man? *Diabetes Vasc. Dis. Res.* 5, 76–81. doi:10.3132/dvdr.2008.013

Nelson, O. L., and Robbins, C. T. (2015). Cardiovascular function in large to small hibernators: bears to ground squirrels. *J. Comp. Physiol. B* 185, 265–279. doi:10.1007/s00360-014-0881-5

frontiers | Frontiers in Physiology

TYPE Original Research
PUBLISHED 09 March 2023
DOI 10.3389/fphys.2023.1129278

OPEN ACCESS

EDITED BY
Jérémy Terrien,
Muséum National d'Histoire Naturelle, France

REVIEWED BY
Chunmei Xia,
Fudan University, China
Zhe Shi,
Hunan University of Chinese Medicine, China

*CORRESPONDENCE
Marco Luppi,
marco.luppi@unibo.it

†These authors have contributed equally to this work and share first authorship

SPECIALTY SECTION
This article was submitted to Metabolic Physiology, a section of the journal Frontiers in Physiology

RECEIVED 21 December 2022
ACCEPTED 28 February 2023
PUBLISHED 09 March 2023

CITATION
Squarcio F, Hitrec T, Piscitiello E, Cerri M, Giovannini C, Martelli D, Occhinegro A, Taddei L, Tupone D, Amici R and Luppi M (2023), Synthetic torpor triggers a regulated mechanism in the rat brain, favoring the reversibility of Tau protein hyperphosphorylation. *Front. Physiol.* 14:1129278. doi: 10.3389/fphys.2023.1129278

Synthetic torpor triggers a regulated mechanism in the rat brain, favoring the reversibility of Tau protein hyperphosphorylation

Fabio Squarcio[1†], Timna Hitrec[1†], Emiliana Piscitiello[1,2], Matteo Cerri[1], Catia Giovannini[3,2], Davide Martelli[1], Alessandra Occhinegro[1,2], Ludovico Taddei[1], Domenico Tupone[1,4], Roberto Amici[1] and Marco Luppi[1,2]*

[1]Department of Biomedical and Neuromotor Sciences, University of Bologna, Bologna, Italy, [2]Centre for Applied Biomedical Research—CRBA, St. Orsola Hospital, University of Bologna, Bologna, Italy, [3]Department of Experimental, Diagnostic and Specialty Medicines, University of Bologna, Bologna, Italy, [4]Department of Neurological Surgery, Oregon Health and Science University, Portland, OR, United States

Introduction: Hyperphosphorylated Tau protein (PPTau) is the hallmark of tauopathic neurodegeneration. During "synthetic torpor" (ST), a transient hypothermic state which can be induced in rats by the local pharmacological inhibition of the Raphe Pallidus, a reversible brain Tau hyperphosphorylation occurs. The aim of the present study was to elucidate the – as yet unknown – molecular mechanisms underlying this process, at both a cellular and systemic level.

Methods: Different phosphorylated forms of Tau and the main cellular factors involved in Tau phospho-regulation were assessed by western blot in the parietal cortex and hippocampus of rats induced in ST, at either the hypothermic nadir or after the recovery of euthermia. Pro- and anti-apoptotic markers, as well as different systemic factors which are involved in natural torpor, were also assessed. Finally, the degree of microglia activation was determined through morphometry.

Results: Overall, the results show that ST triggers a regulated biochemical process which can dam PPTau formation and favor its reversibility starting, unexpectedly for a non-hibernator, from the hypothermic nadir. In particular, at the nadir, the glycogen synthase kinase-β was largely inhibited in both regions, the melatonin plasma levels were significantly increased and the antiapoptotic factor Akt was significantly activated in the hippocampus early after, while a transient neuroinflammation was observed during the recovery period.

Discussion: Together, the present data suggest that ST can trigger a previously undescribed latent and regulated physiological process, that is able to cope with brain PPTau formation.

Abbreviations: aCSF, artificial cerebrospinal fluid; AT8, Tau protein phosphorylated at S202 and T205; C, control group; ER, early recovery; Hip, hippocampus; IF, immunofluorescence; MI, morphological index; MTs, microtubules; N, nadir of hypothermia; NND, nearest neighboring distance; P-Cx, parietal cortex; PPTau, hyperphosphorylated tau protein; R3, 3h after ER; R6, 6h after ER; RPa, Raphe Pallidus; Ta, ambient temperature; Tau-1, Tau protein with no phosphorylation within residues 189-207; Tb, deep brain temperature; WB, western-blot.

KEYWORDS

deep hypothermia, microtubules, melatonin, glycogen synthase kinase 3β, hippocampus, parietal cortex

1 Introduction

The Tau protein has a fundamental function in neurons (Wang and Mandelkow, 2016), the name itself deriving from the very first description of the key role it plays in the assembly and stabilization of microtubules (MTs) (Weingarten et al., 1975). When it is hyperphosphorylated, Tau (PPTau) loses its primary function: Tau monomers detach from MTs, showing a tendency to aggregate in oligomers and then evolve toward the formation of neurofibrillary tangles (Gerson et al., 2016; Wang and Mandelkow, 2016). This mechanism represents the main pathological marker of neurological diseases that are also termed as tauopathies (Kovacs, 2017), including Alzheimer's disease (AD) and other neurodegenerative disorders (Wang and Mandelkow, 2016; Kovacs, 2017).

The formation of PPTau is not exclusive to neurodegenerative diseases. As a matter of fact, in response to hypothermic conditions, PPTau is also abundantly expressed in the brain. This is the case of hibernation (Arendt et al., 2003; Arendt et al., 2015), deep anesthesia (Planel et al., 2007; Whittington et al., 2013), and "synthetic torpor" (ST) (Luppi et al., 2019), a condition the rat, a non-hibernator, enters into in response to pharmacological inhibition of thermogenesis (Cerri et al., 2013; Cerri, 2017). In almost all these cases, with the only exclusion of anesthesia-induced hypothermia in transgenic mice models of tauopathy (Planel et al., 2009), Tau hyperphosphorylation is reversible and not apparently leading to neurodegeneration. Since mice are facultative heterotherms, able to enter torpor if necessary (Hudson and Scott, 1979; Oelkrug et al., 2011; Hitrec et al., 2019), the PPTau reversibility observed during ST in the non-hibernator (Luppi et al., 2019; Hitrec et al., 2021) appears of particular relevance from a translational point of view.

The physiological mechanisms responsible for Tau hyperphosphorylation at a low body temperature, and its return to normality in euthermic conditions, are not yet well understood. The PPTau formation could be theoretically explained by simply considering the physical chemistry of the two main enzymes involved in Tau phospho-regulation: glycogen-synthase kinase 3β (GSK3β) and protein-phosphatase 2A (PP2A) (Planel et al., 2004; Su et al., 2008). In accordance with the Arrhenius equations (*cf.* Gutfreund, 1995; Marshall, 1997), the lowering of the temperature reduces the reaction rate of both enzymes. However, PP2A has been observed to reduce its reaction rate earlier than GSK3β (Planel et al., 2004; Su et al., 2008). Thus, at temperatures below the physiological level GSK3β might act on Tau filaments without being fully counter-balanced by PP2A. However, the only effect described by the Arrhenius equations cannot explain the rather fast dephosphorylation of PPTau observed during recovery from ST (Luppi et al., 2019; Hitrec et al., 2021).

The aim of the present work was to verify that the hyperphosphorylation and subsequent dephosphorylation of Tau, during and after ST, come from active molecular mechanisms triggered by deep hypothermia, at both cellular and systemic levels, not only being the result of temperature-dependent enzymatic activity modifications. Therefore, levels of different cellular factors in the parietal cortex (P-Cx) and in the hippocampus (Hip) of animals in ST and in normothermic conditions were compared. These brain structures were chosen since they are commonly affected by tauopathies (Padurariu et al., 2012; Kovacs, 2017; Ugolini et al., 2018). In particular, we determined levels of: 1) AT8 (p[S202/T205]-Tau; Malia et al., 2016) and Tau-1 (non-phosphorylated Tau); 2) GSK3β (total and inhibited form); 3) Akt (total and activated form; also known as protein-kinase B); 4) PP2A. Moreover, since Tau can be phosphorylated at different residues (Wang and Mandelkow, 2016), the levels of p[T205]-Tau form, which has been shown to have a neuroprotective role (Ittner et al., 2016), was also determined. Neuroinflammation, an important feature of tauopathies (Ransohoff, 2016; Nilson et al., 2017), was also assessed by analyzing the degree of microglia activation, together with that of pro-apoptotic and anti-apoptotic factors. Furthermore, considering that melatonin and noradrenaline might have a neuroprotective role (Herrera-Arozamena et al., 2016; Shukla et al., 2017; Benarroch, 2018) and their release is strongly affected, respectively, in hibernators during arousal from torpid bouts (Stanton et al., 1986; Willis and Wilcox, 2014), and, in general, during a strong thermogenic activation (e.g., such as that needed when returning to euthermia) (Braulke and Heldmaier, 2010; Cerri et al., 2013; Cerri et al., 2021), we considered these systemic factors worth studying. Therefore, plasma levels of melatonin and noradrenaline, together with those of adrenaline, dopamine, cortisol, and corticosterone were also determined. The finding of any relevant change in these systemic factors induced by such a dramatic physiological perturbation as represented by ST may lead to new studies aimed at finding a possible link between such factors and the molecular modifications induced by ST at a neuronal level. Moreover, these data will eventually strengthen the parallelism between ST and natural torpor (Stanton et al., 1986; Willis and Wilcox, 2014).

In this study we confirm that ST is associated with the hyperphosphorylation of Tau and that this process is reversed during the return to euthermia. Moreover, the return to normal phosphorylation levels of Tau is not merely due to temperature changes but is also associated with an active neuroprotective biochemical process characterized by the inhibition of GSK3β, the activation of Akt and an increase in plasma levels of melatonin. This biochemical process is triggered by deep hypothermia, since rapidly elicited at the lowest brain temperature reached during ST. Lastly, it results that microglia cells were probably activated in response to ST, but modifications were mild and transitory.

2 Material and methods

2.1 Animals

A total of 30 male Sprague–Dawley rats (250–350 gr; Charles River) were used. After their arrival, animals were housed in pairs in Plexiglas cages (Techniplast) under normal laboratory conditions: ambient temperature (Ta) set at 24°C ± 0.5°C; 12 h:12 h light-dark

(LD) cycle (L: 09:00 h–21:00 h; 100–150 lux at cage level); food and water *ad libitum*. All the experiments were conducted following approval by the National Health Authority (decree: No. 262/2020-PR), in accordance with the DL 26/2014 and the European Union Directive 2010/63/EU, and under the supervision of the Central Veterinary Service of the University of Bologna. All efforts were made to minimize the number of animals used and their pain and distress.

Since ST is a new and yet unstudied animal model, at present it has been induced on male rats only (Cerri et al., 2013; Luppi et al., 2019; Tinganelli et al., 2019). For this reason and to avoid additional variability in this explorative step, we conducted the following experiments only on male rats.

2.2 Surgery

After 1 week of adaptation, rats underwent surgery as previously described (Cerri et al., 2013). Briefly, deeply anesthetized rats (Diazepam, 5 mg/kg i.m.; Ketamine-HCl, Imalgene 1000, Merial, 100 mg/kg, i.p.) were placed in a stereotaxic apparatus (David Kopf Instruments) and surgically implanted with: 1) electrodes for electroencephalogram (EEG); 2) a thermistor (Thermometrics Corporation) mounted inside a stainless steel needle (21 gauge) and placed beside the left anterior hypothalamus to record the deep brain temperature (Tb); 3) a microinjection guide cannula (C315G-SPC; Plastics One; internal cannula ex-tension below guide: +3.5 mm), targeted to the brainstem region involved in thermogenic control, the Raphe Pallidus (RPa), at the following coordinates from lambda: on the midline, 3.0 mm posterior and 9.0 ventral to the dorsal surface of the cerebellum (Paxinos and Watson, 2007; Morrison and Nakamura, 2019). Since reports showed that the inhibition of RPa neurons causes vasodilation (Blessing and Nalivaiko, 2001), the increase of tail temperature subsequent to the injection of GABA-A agonist muscimol (1 mM) in RPa was used as proof of the correct positioning of the guide cannula.

After surgery, rats received 0.25 mL of an antibiotic solution (penicillin G and streptomycin-sulfate, i.m.), analgesics (Carprofen—Rimadyl, Pfizer, 5 mg/kg, i.m.), and 20 mL/kg saline subcutaneously.

Animals were constantly monitored until they regained consciousness and then left to recover for at least 1 week under standard laboratory conditions. The animal's pain, distress, or suffering symptoms were constantly evaluated using the Humane End Point (HEP) criteria. 24 h prior to the experimental session, rats underwent an adaptation period in a cage positioned within a thermoregulated and sound-attenuated box, at low Ta (15°C).

2.3 Synthetic torpor

To induce ST, we used a consolidated protocol (Cerri et al., 2013; Luppi et al., 2019; Tinganelli et al., 2019). Briefly, a microinjecting cannula was inserted into the previously implanted guide cannula. Then, 100 nL of muscimol (1 mM) was injected once an hour, six consecutive times. Following the last injection, Tb reached values of around 22°C (Cerri et al., 2013). The control group, conversely, was injected with artificial cerebrospinal fluid (aCSF; EcoCyte Bioscience). During the whole experiment, EEG and Tb signals were recorded, after being opportunely amplified, filtered, and digitalized (Cerri et al., 2013). The EEG registration, in particular, was used since of great help in monitoring brain functioning during ST, as shown by Cerri et al. (2013), and to exactly check for the starting point of the recovery period following ST (see later).

2.4 Experimental procedure

Animals were randomly assigned to five different experimental groups and were sacrificed at different times following the injection of either muscimol or aCSF (first injection at 11.00 a.m.). The experimental groups were the following (Figure 1).

- C → Control, injected with aCSF and sacrificed at around 17.00 h, exactly matching the N condition (n = 6).
- N → Nadir, sacrificed 1 h after the last injection, at 17:00 h, when Tb reached the lowest temperature (i.e., the nadir) during hypothermia (n = 6; Tb = 22.8°C ± 1.3°C).
- ER → Early Recovery; sacrificed when Tb reached 35.5°C after ST, at around 19:00 h (n = 6).
- R3 → 3 h Recovery, sacrificed 3 h after ER, at around 22: 00 h (n = 6).
- R6 → 6 h Recovery, sacrificed 6 h after ER, at around 1: 00 h (n = 6).

The ER condition was empirically considered as the exact conclusion of the hypothermic period, since in this condition animals start to show normal EEG signals, including clear physiological signs of sleep (Cerri et al., 2013).

Blood was collected transcardially from each animal after induction of deep anesthesia, and was centrifuged at 3000 g for 15 min at 4°C; plasma was then separated for subsequent ELISAs. Three animals per condition were transcardially perfused with paraformaldehyde 4% (w/v) as previously described (Luppi et al., 2019; Hitrec et al., 2021), and brain excised for immunofluorescence (IF); three animals per condition were sacrificed by decapitation, and the fresh brain was extracted for subsequent Western blot (WB) analysis. All samples were stored at −80 °C until assayed.

2.5 Immunofluorescence

The procedure has been described in detail in Luppi et al. (2019). Briefly, extracted fixed brains were post fixed for 2 h by immersion in the same solution used for the perfusion and put in a 30% (w/v) sucrose solution in phosphate buffer saline (PBS) and sodium-azide 0.02% (w/v) overnight for cryoprotection (Luppi et al., 2019). Thereafter, tissue samples were cut into 35 µm-thick coronal slices, using a cryostat microtome (Frigocut 2800) set at −22.0 °C. All the slices were then stored at −80°C in a cryoprotectant solution: 30% (w/v) sucrose, 30% (v/v) ethylene glycol, 1% (w/v) polyvinylpyrrolidone in PBS.

Slices from approximately Bregma −2.0/-4.0 were used for free-floating immunostaining. These levels were chosen so that each slice

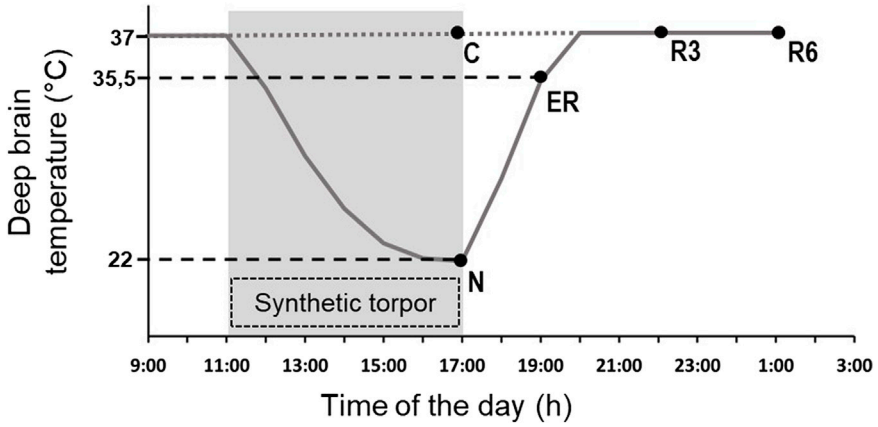

FIGURE 1
Schematic representation of the experimental conditions. The solid line indicates the progress of deep brain temperature (Tb) throughout the experiment. The dotted line refers to the control group (C; i.e., injected with artificial cerebrospinal fluid). The shaded area represents the period when synthetic torpor (ST) was induced (i.e., by injecting muscimol within the Raphe Pallidus). N, samples taken at nadir of hypothermia, during ST; ER, early recovery, samples taken when Tb reached 35.5 °C following ST; R3, samples taken 3 h after ER; R6, samples taken 6 h after ER. See Methods for details.

would contain both a portion of the parietal cortex (P-Cx) and the hippocampus (Hip). Slices were rinsed twice in PBS and then incubated for 2 h in 1% (v/v) normal donkey serum. Slices were incubated overnight with polyclonal rabbit Anti-p[T205]-Tau (Thermo Fisher; 1:400) probed with a Donkey Anti-rabbit IgG conjugated with Alexa-594 (Thermo Fisher; 1:500).

Microglia activation was also assessed using the rabbit polyclonal Anti-Iba1 anti-body (Wako Chemicals; 1:800) and the secondary antibody Donkey Anti-rabbit IgG conjugated with Alexa-594 (Thermo Fisher; 1:500), as previously described. Activation level was measured (ImageJ software, following appropriate calibration) using established morphometric parameters of microglia cells (Davis et al., 2017; Baldy et al., 2018): 1) Soma area; 2) Arborization area; 3) Morphological index (MI): Soma area/arborization area ratio; 4) Microglial density (counting the number of cells in every picture taken); 5) Nearest neighbor distance (NND). This analysis was conducted on samples from the P-Cx and on only the CA3 field of Hip, since it represents the most vulnerable cortical field of the Hip in AD development (Padurariu et al., 2012).

Finally, endogenous levels of the large fragment (17/19 kDa) of activated Caspase-3, resulting from cleavage adjacent to Asp175, were detected using the rabbit polyclonal antibody for cleaved-Caspase 3 (Asp175) (Cell Signaling, 1:300), followed by a Donkey Anti-rabbit IgG conjugated with Alexa-594 (Thermo Fisher; 1:500).

Images were obtained with a Nikon eclipse 80i equipped with Nikon Digital Sight DS-Vi1 color camera, using ×10 objective (×20 for the microglia staining).

2.6 Western blots

After extraction, fresh brains were quickly transferred to a Petri dish filled with ice cold PBS. P-Cx and Hip were then isolated, homogenized by ice-assisted sonication in lysis buffer condition [RIPA Buffer: 50 mM Tris buffer, 150 mM NaCl, 10% (v/v) NP-40, containing a cocktail of protease and phosphatase inhibitors (Sigma Aldrich), 1 mM dithiothreitol (DTT) and 1 mM PMSF]. The extract was centrifuged at 12000 *g* for 30 min at 4°C and stored at −80°C. The protein concentration was determined using the Bio-Rad DC protein assay kit (Bio-Rad Laboratories). Aliquots were thawed on ice and then denatured in a sample buffer [containing: 500 mM DTT, lithium dodecyl sulfate (LDS)] with Coomassie G250 and phenol red (Invitrogen™ NuPAGE) at 65 °C for 10 min. Then, protein samples (20 µg) were loaded and separated electrophoretically using a 1.0 mm thick 4%–12% Bis-Tris gel together with NuPAGE MOPS SDS Running Buffer (both by Invitrogen™ NuPAGE). The gels were then electrotransferred onto nitrocellulose membranes (Hybond C Extra, Amersham Pharmacia) *via* wet transfer. Membranes were blocked using 5% (w/v) not-fat dry milk in 0.1% (v/v) tween-20 in PBS (PBST) for at least 40 min at room temperature, and then incubated overnight at 4°C with the different primary antibodies indicated in Table 1.

Bound antibodies were detected using horseradish peroxidase-conjugated Anti-rabbit and Anti-mouse secondary antibodies. The uniformity of sample loading was confirmed *via* Ponceau S staining and immunodetection of β-actin, used as a loading control. ChemiDoc™XRS+ (Image Lab™Software, Bio-Rad) was used to acquire digital images through a chemiluminescence reaction (ECL reagents, Amersham). A semi-quantitative measurement of the band intensity was performed using the same computer software and expressed as a ratio of band intensity with respect to the loading control, normalizing the different gels according to a randomly chosen sample used as an internal control (i.e., a sample taken from a single rat that was run on every gel for the different determinations).

2.7 ELISA determinations

For each experimental condition the plasma samples from three animals, randomly chosen, were pooled in order to obtain a

TABLE 1 Primary antibodies employed in this study.

Antibody	Type	Species	Specificity	MW (kDa)	Source and dilution
Anti-Total Tau	Mono-	M	several Tau protein isoforms between 50 and 70 kDa	50–70	Merck Millipore; WB 1:5000
Anti-Tau-1	Mono-	M	non-phosphorylated 189–207 residues	52–68	Merck Millipore; WB 1:5000
AT8	Mono-	M	p-Tau (S202/T205)	68–70	Thermo Fisher; WB 1:1000
Anti-p-Tau (T205)	Poly-	R	p-Tau (T205)	68–70	Thermo Fisher; IF 1:400; WB 1:1000
Anti-GSK3β	Mono-	R	GSK3β	46	Cell Signaling Technology; WB 1:3000
Anti-p-GSK3β	Mono-	R	p-GSK3β (S9)	46	Cell Signaling Technology; WB 1:3000
Anti-Akt	Poly-	R	Total Akt1, Akt2, Akt3	56–60	Cell Signaling; WB 1:2000
Anti-p-Akt	Poly-	R	p-Akt1 (S473), p-Akt2 (S473), p-Akt3 (S473)	56–60	Cell Signaling; WB 1:2000
Anti-GRP78	Mono-	R	GRP78	78	Cell Signaling; WB P-Cx 1:5000; WB Hip 1:3000
Anti-XIAP	Mono-	M	XIAP	54	Santa Cruz Biotechnology; WB 1:1000
Anti-PP2A Catalytic *a*	Mono-	M	PP2A	36	BDT Transduction Laboratories™; WB 1:5000
Anti-cleaved-Caspase 3	Poly-	R	Cleaved Caspase 3 (A175)	17–19	Cell Signaling; IF 1:300; WB P-Cx 1:250; WB Hip 1:500
Anti-β-actin	Mono-	M	β-actin	42	Thermo Fisher; WB 1:5000

Abbreviations: Mono-, monoclonal; Poly-, polyclonal; M, mouse; R, rabbit; MW, molecular weight; p-, phosphorylated; IF, immunofluorescence; WB, Western blot; P-Cx, Parietal Cortex; Hip, Hippocampus.

sufficient volume to be assessed and with the aim to reduce the individual variability due to the relatively small number of animals. Therefore, we obtained two "grand-samples," each assayed twice. Commercially available ELISA kits were used to measure plasma levels of melatonin (IBL International, RE54021), dopamine (IBL International, RE59161), adrenaline/noradrenaline (IBL International, RE59242), cortisol (IBL International, RE52061), and corticosterone (Abnova, KA0468). All procedures were run following the manufacturer's recommendations. Optical density was red with a spectrophotometer (Spark® microplate reader, Tecan).

2.8 Statistical analysis

Statistical analysis was carried out using SPSS software (25.0). Western blot and ELISA results were analyzed using the Mann-Whitney non-parametric test, comparing every experimental condition with the relative C level. Microglia morphometric results were tested with a one-way ANOVA. In the case that ANOVA was significant, means of the different experimental conditions were compared with the relative C level, using the modified *t*-test (t*).

3 Results

3.1 Tau levels in the brain

The induction of ST did not induce changes in total Tau levels (Figure 2A), while AT8 (p[S202/T205]-Tau) and p[T205]-Tau showed a significantly higher peak in both P-Cx and Hip ($p < 0.05$; for all comparisons), compared to C (Figures 2B, D). Interestingly, Figure 3 shows that the high level of p[T205]-Tau found in the Hip was specifically limited to the CA3 field (Paxinos and Watson, 2007), not involving CA1 and CA2 fields.

Moreover, during this condition Tau-1 (i.e., the non-phosphorylated form of Tau protein; Table 1) mirrored the trend described for the phosphorylated forms, being significantly lower in both brain structures ($p < 0.05$; for all comparisons) compared to control levels, as shown in Figure 2C.

During the early stage of recovery (ER) AT8 returned to normal conditions (Figure 2B), while p[T205]-Tau level remained significantly higher than C (see Figure 2D) in both the brain structures studied ($p < 0.05$; for all comparisons). Tau-1 levels returned to a normal condition in the P-Cx but was still significantly lower than control values in the Hip ($p < 0.05$; Figure 2C). During the rest of the recovery period (R3 and R6) all the values affected by ST returned to normal levels (Figures 2B–D). In these recovery conditions, and only for P-Cx, total-Tau expression was found to be significantly higher than C ($p < 0.05$; for both comparisons).

3.2 Levels of kinases and phosphatases in the brain

Deep hypothermia induced different effects on GSK3β levels (Figure 4A), depending on the brain structure considered. In fact, the expression of GSK3β was significantly lower in the P-Cx (N vs. C, $p < 0.05$), but only showed an increasing trend in the Hip, that reached a significant level in ER ($p < 0.05$). Consistently with what had been observed during ST, and in contrast with Hip, in P-Cx at ER the level of GSK3β was still lower than in C ($p < 0.05$). Differently, results regarding the inhibited form of GSK3β (p

10.3389/fphys.2023.1129278

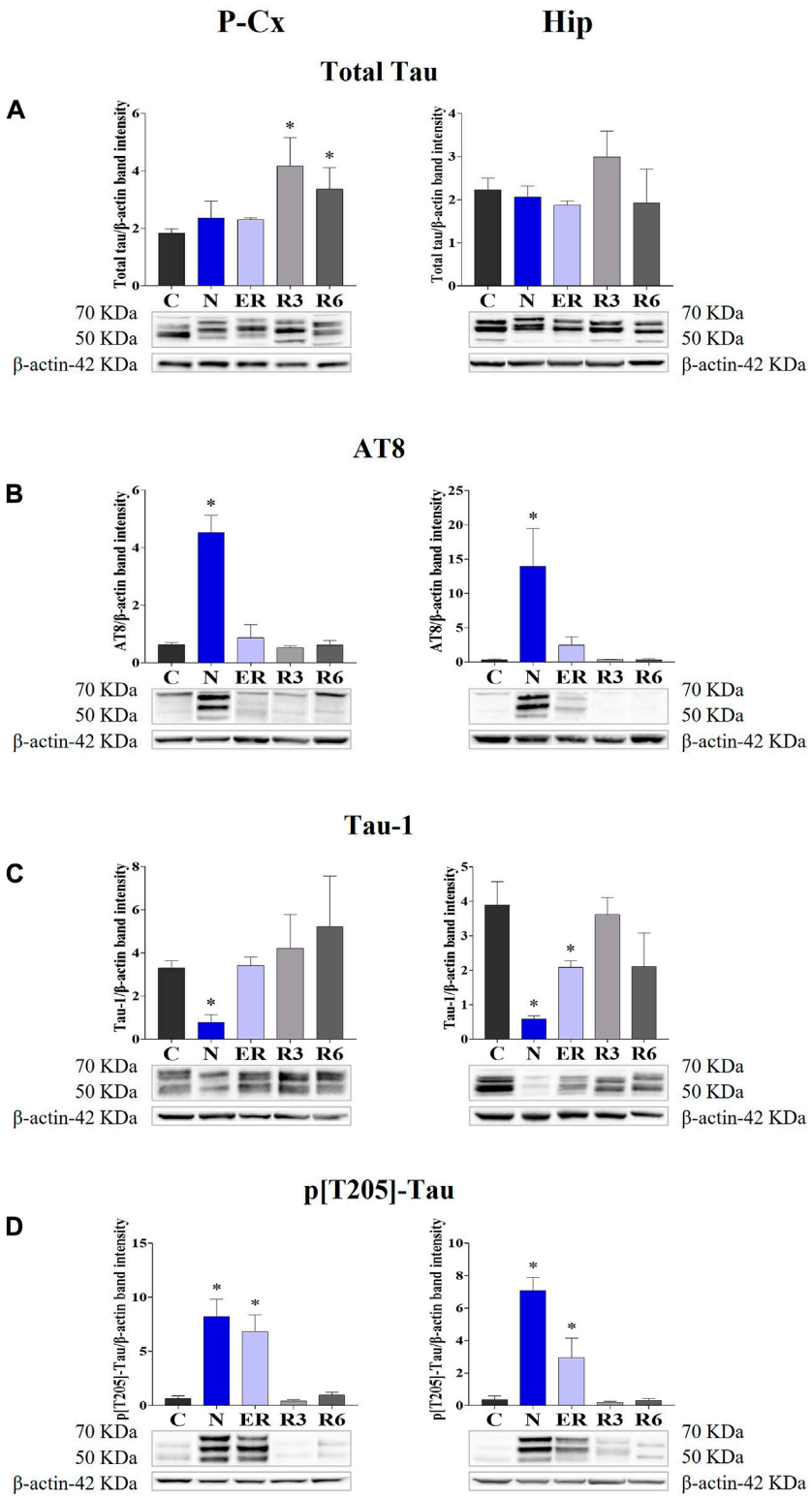

FIGURE 2
Western blot detection of the main enzymes involved in phosphorylation and dephosphorylation of Tau, determined in brain extracts of the parietal cortex (P-Cx) and hippocampus (Hip). Below each histogram, WB representative samples are shown for each experimental condition. **(A)** glycogensynthase kinase-3β (GSK3β), the main kinase targeting Tau; **(B)** p[S9]-GSK3β (inactive form of GSK3β, phosphorylated at Ser9); **(C)** protein phosphatase-2A (PP2A), the main phosphatase targeting Tau; **(D)** different isoforms of Akt (protein kinase-B; Akt 1/2/3), kinases targeting GSK3β at Ser9 and antiapoptotic factors; **(E)** p[S473] Akt, the active form of Akt 1/2/3, phosphorylated at Ser473. Data are normalized by β-actin and expressed as means ± S.E.M., n = 3. *: $p < 0.05$ vs. C. Experimental groups (see Figure 1): C, control; N, samples taken at nadir of hypothermia, during ST; ER, early recovery, samples taken when Tb reached 35.5°C following ST; R3, samples taken 3 h after ER; R6, samples taken 6 h after ER.

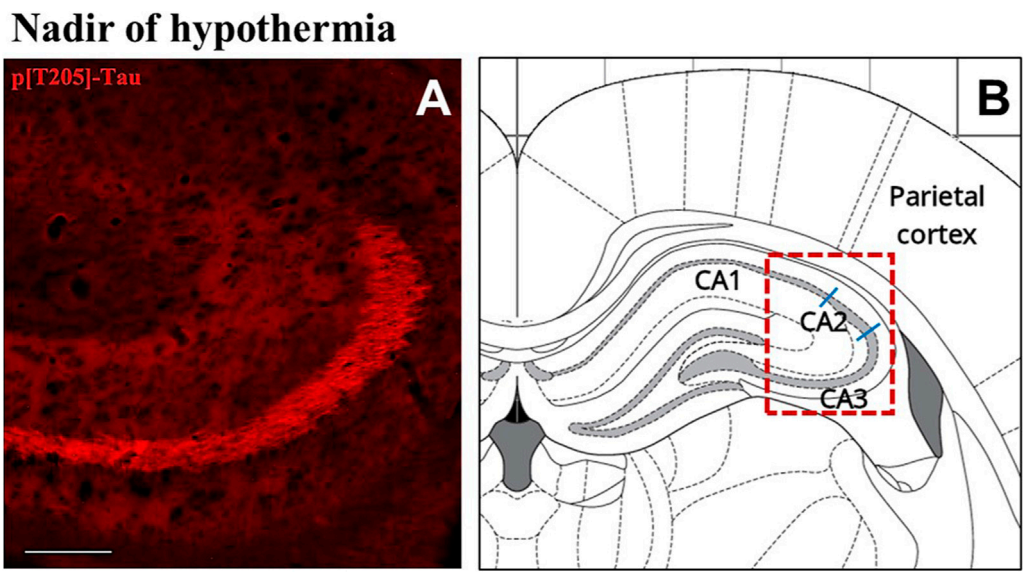

FIGURE 3
Representative pictures showing the hippocampal cortex, specifically stained for p[T205]-Tau, phosphorylated Tau protein in Thr-205 residue (secondary antibody conjugated with Alexa-594; **(A)**. In **(B)** is the correspondent left hippocampal hemicortex field, as represented by the rat brain atlas at Bregma −3.12 mm (Paxinos and Watson, 2007). The dashed red line represents the microscope picture shown in **(A)** and the blue lines represent the boundaries among the hippocampal cortical fields (Paxinos and Watson, 2007). **(A)** shows that p[T205]-Tau immunostaining was positive in the only CA3 area, while CA1 and CA2 areas are not stained. The picture refers to the N condition (samples taken at the nadir of hypothermia, during the induction of synthetic torpor; see Figure 1). Calibration bar: 100 μm.

[S9]-GSK3β; Figure 4B) showed a change, with a similar pattern in both the brain structures studied: values were significantly higher at N ($p < 0.05$; for both P-Cx and Hip) compared to C, slowly returning to normal conditions during the recovery period (Figure 4B).

As expected, PP2A (i.e., the main phosphatase acting on Tau protein) was significantly higher than in C ($p < 0.05$; Figure 4C) during ER in the P-Cx, but such a trend was not observed in the Hip, where PP2A was lower than in C in R3 ($p < 0.05$; Figure 4C).

Figures 4D, E, show total and active forms of Akt, respectively, also known as protein-kinase B, that play a role in neuroprotection and in contrasting apoptosis (Risso et al., 2015; Levenga et al., 2017). Total Akt expression was not affected by ST, and only at R3 and R6 within the P-Cx (Figure 4D) were levels significantly lower than in C ($p < 0.05$; for both comparisons). The activated form of Akt (p[S473]-Akt) was induced only during the early stages of the recovery period ($p < 0.05$; Figure 4E).

3.3 Stressful/protective cellular markers in the brain

Taken together, all the results collected within Figure 5 show whether ST was stressful or protective at a cellular level. In particular: 1) cleaved-Caspase 3 (panel A) is a factor that is commonly considered to be involved in the initiation of apoptosis (Fricker et al., 2018); 2) GRP78 (Glucose regulating protein 78; panel B) is a key factor that regulates the "unfolded protein response," a well-recognized mechanism involved in cellular stress conditions (Ibrahim et al., 2019); 3) XIAP (X chromosome-linked inhibitor of apoptosis; panel C) is a factor that inhibits apoptosis (Holcik and Korneluk, 2001).

These results show that the activated form of Caspase 3 (Figure 5A) was not affected by ST, resulting significantly lower ($p < 0.05$) only in R3 within the P-Cx. GRP78 levels were found to be higher in ER within the Hip ($p < 0.05$), but promptly returned to the normal condition during the rest of the recovery period. In P-Cx, this cellular factor presented significantly lower values in R6 ($p < 0.05$), but maintained almost constant values throughout the other experimental conditions.

Synthetic torpor did not notably affect the neuroprotective factor XIAP. In this case, the only significant difference found was in R6 ($p < 0.05$) within the Hip (Figure 5C), where it was lower than in C; while in the P-Cx XIAP levels were similar across the whole experiment.

Finally, as shown by Figure 6, levels of the neuronal marker NeuN were not affected by the experimental procedure, as determined by WB quantification at the end of the whole procedure in respect to the C condition.

3.4 Systemic factors

Figure 7 shows the results obtained from plasma determinations of the systemic factors measured. While most of the results did not show significant variations across the experiment, melatonin and cortisol did. In particular, melatonin (Figure 5A) was significantly higher in both N and ER, compared to C ($p < 0.05$; for both comparisons), while plasma cortisol (Figure 5E) was significantly lower than in C at ER ($p < 0.05$).

10.3389/fphys.2023.1129278

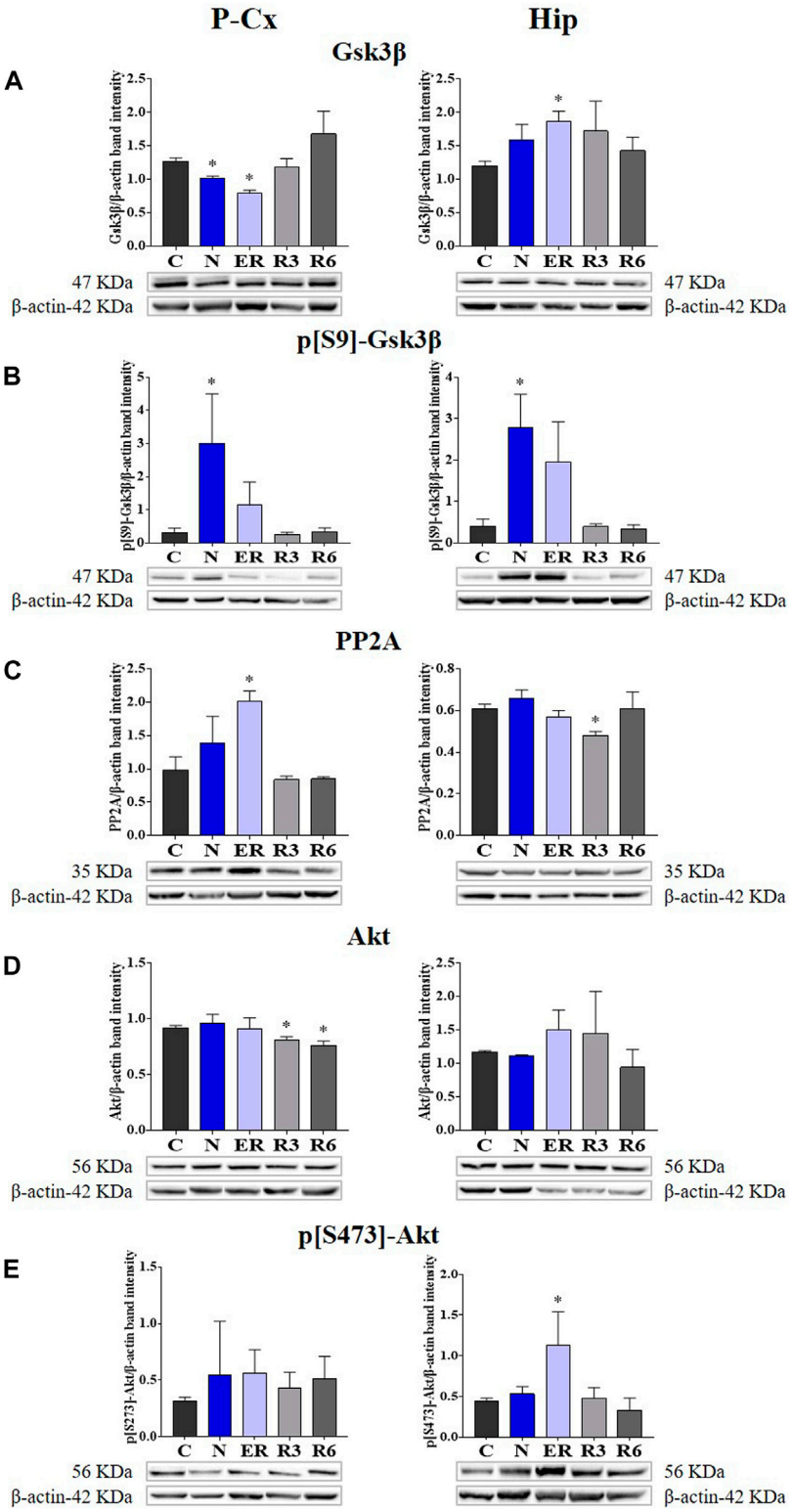

FIGURE 4
Western blot detection of the main enzymes involved in phosphorylation and dephosphorylation of Tau, determined in brain extracts of the parietal cortex (P-Cx) and hippocampus (Hip). Below each histogram, WB representative samples are shown for each experimental condition. **(A)** glycogensynthase kinase-3β (GSK3β), the main kinase targeting Tau; **(B)** p[S9]-GSK3β (inactive form of GSK3β, phosphorylated at Ser9); **(C)** protein phosphatase-2A (PP2A), the main phosphatase targeting Tau; **(D)** different isoforms of Akt (protein kinase-B; Akt 1/2/3), kinases targeting GSK3β at Ser9 and antiapoptotic factors; **(E)** p[S473] Akt, the active form of Akt 1/2/3, phosphorylated at Ser473. Data are normalized by β-actin and expressed as means ± S.E.M., n = 3. *: $p < 0.05$ vs. C. Experimental groups (see Figure 1): C, control; N, samples taken at nadir of hypothermia, during ST; ER, early recovery, samples taken when Tb reached 35.5°C following ST; R3, samples taken 3 h after ER; R6, samples taken 6 h after ER.

10.3389/fphys.2023.1129278

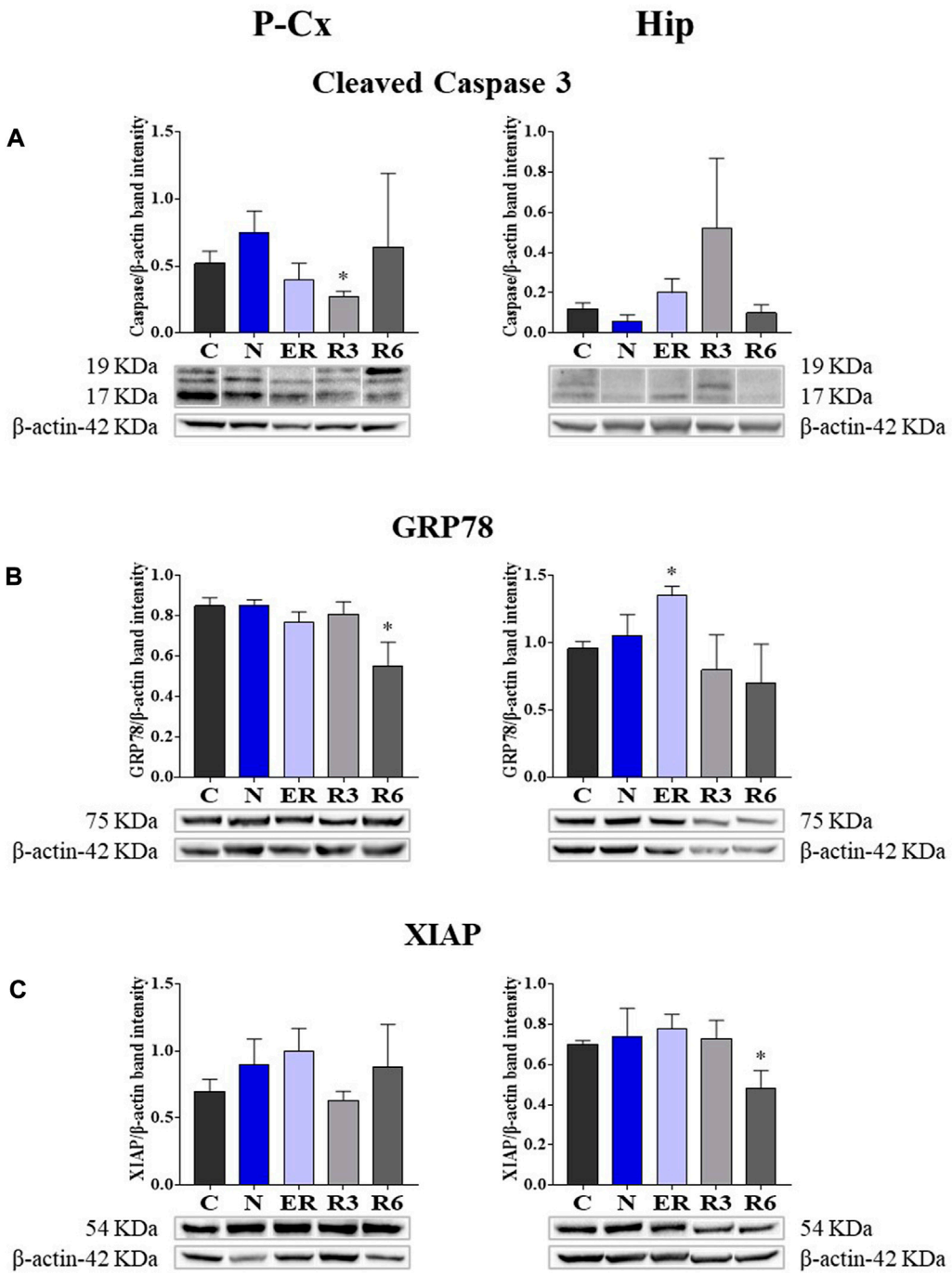

FIGURE 5
Western blot detection of pro- and anti-apoptotic and cell-stress factors in brain extracts of the parietal cortex (P Cx) and hippocampus (Hip). Below each histogram, WB representative samples are shown for each experimental condition. **(A)** cleaved-Caspase 3 (cleaved at Asp175 residue; i.e., the activated form); **(B)** Glucose regulating protein 78 (GRP78); **(C)** X chromosome-linked inhibitor of apoptosis (XIAP). Data are normalized by β-actin and expressed as means ± S.E.M., $n = 3$. *: $p < 0.05$ vs. C. Experimental groups (see Figure 1): C, control; N, samples taken at nadir of hypothermia, during ST; ER, early recovery, samples taken when Tb reached 35.5°C following ST; R3, samples taken 3 h after ER; R6, samples taken 6 h after ER.

3.5 Microglia morphometry

Figure 8 shows pictures taken from P-Cx during the different experimental conditions (see Figure 1), as representative samples of the resulting analysis that is summarized in Table 2. Results show that microglia mildly changed some morphological parameters, but only transiently: all the measured values returned to normal within the considered recovery period.

In particular, the deep hypothermia reached during ST induced smaller soma and arborization areas compared to C ($p < 0.05$; for both parameters) for microglia in the CA3 field of the Hip (Table 2). No differences were found in P-Cx. At the beginning of the recovery

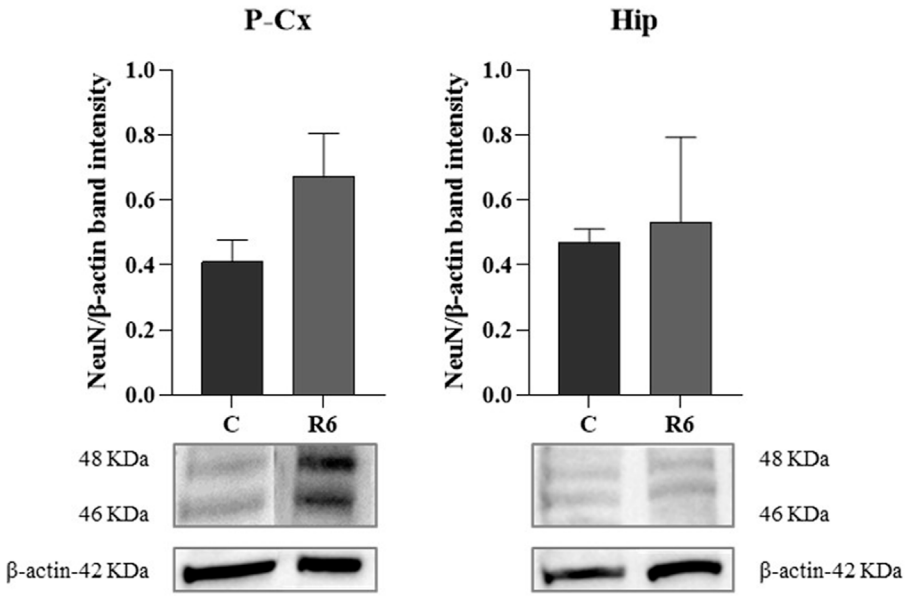

FIGURE 6
Western blot (WB) determinations of NeuN levels (i.e., neuronal marker) in brain extracts of parietal cortex (P-Cx) and hippocampus (Hip). Below each histogram, WB representative sample are shown for each experimental condition. Data are normalized by β-actin and expressed as mean ± S.E.M., n = 3. Experimental groups: C, control; R6, samples taken 6 h after Tb reached 35.5°C following ST (see Figure 1).

period (ER) data showed a lower number of cells compared to C, in both the brain structures studied ($p < 0.05$ for CA3 and $p < 0.001$ for P-Cx). At R3, the arborization area of microglia cells was significantly reduced both in CA3 and P-Cx areas ($p < 0.05$ and $p < 0.001$, respectively), and the NND parameter (i.e., the mean distance between neighboring cells) was lower compared to C ($p < 0.001$), but only in P- Cx. In accordance with these results, at R3 the MI (i.e., morphological index) was also found to be significantly higher in P-Cx ($p < 0.001$) compared to C, and close to statistical significance in CA3 ($p = 0.055$). At the end of the recovery period considered (R6), the soma area was larger than in C in both brain structures ($p < 0.05$ for CA3 and $p < 0.01$ for P-Cx), while the arborization area was greater than in C ($p < 0.05$) only in the P-Cx (Table 2).

4 Discussion

The results of the present work confirm that the reversibility of Tau hyperphosphorylation is not the mere effect of a temperature drop, acting on the physical chemistry characteristics of the enzymatic activity. In fact, the lowering of temperature seems to act as a trigger to elicit an active and regulated biochemical mechanism. Differently from what we supposed, this mechanism does not start to occur during the recovery from ST but it appears to be already clearly activated at the nadir of hypothermia (i.e., the N condition), when Tb is close to 22°C (Cerri et al., 2013). This was unexpected since rats are non-hibernating mammals, and it was not obvious they evolved some biochemical mechanisms that may act at the low Tb reached during ST. Interestingly, the increase in melatonin plasma levels parallels the changes in the regulatory processes of the enzymes responsible for Tau phosphorylation observed during ST and in the following recovery of normothermia, suggesting a possible involvement of melatonin in this recovery process (see later). Another unexpected result was that catecholamine plasma levels were not affected by the experimental procedure, despite the return to euthermia is characterized by thermogenic activation (Cerri et al., 2013; Morrison and Nakamura, 2019). Regarding neuroinflammation, ST induced a mild and transitory activation of microglia cells, suggesting their possible role in sustaining the recovery of normal conditions of Tau protein, as will be better discussed later.

The present results reflect very well what had previously been observed in our lab in terms of IF determinations (Luppi et al., 2019). In particular, a strong accumulation of AT8 (i.e., p[S202/T205]-Tau) was mirrored by reduced levels of Tau-1 (i.e., the non-phosphorylated form of Tau) in the N condition, with both recovering control levels within the following 3 h. Moreover, during the recovery period, high levels of Total Tau were observed, particularly in the P-Cx, indicating a possible stimulating effect of ST on the synthesis of new Tau monomers or, alternatively, a less active turnover or degradation processes. The consequences of an enhanced Tau levels are not easily predictable, since it may be considered a factor that favors either neurotoxicity or cellular neuroprotection (Esclaire et al., 1997; Lesort et al., 1997; Joseph et al., 2017). We believe that, at least in our experimental conditions, the latter is more likely the case. As a matter of fact, p[T205]-Tau form was also shown to be increased at N, also persisting at ER before returning to control levels, and this specific phosphorylated form of Tau protein has been described as having neuroprotective effects (Ittner et al., 2016).

Even though the concomitant high peaks of AT8 and p[T205]-Tau in the N condition could be explained, at least in part, by the

10.3389/fphys.2023.1129278

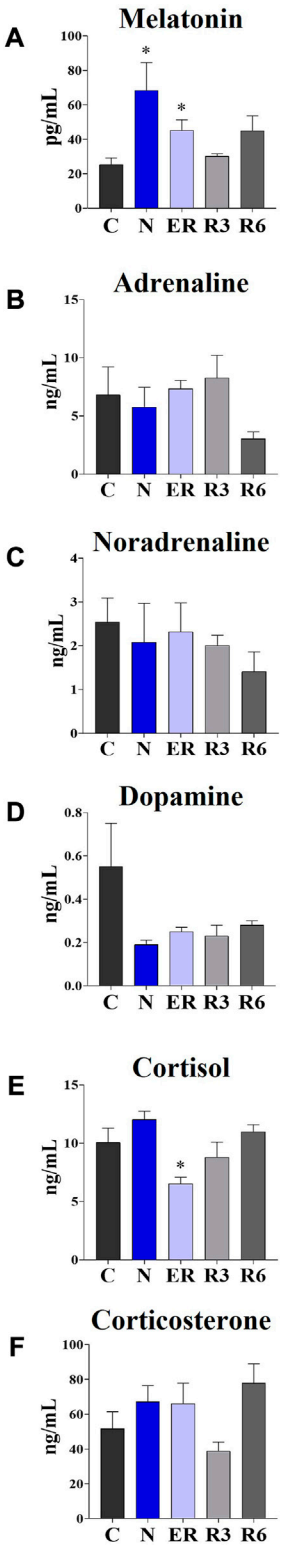

FIGURE 7
Levels of different plasmatic factors. **(A)** Melatonin; **(B)** Adrenaline; **(C)** Noradrenaline; **(D)** Dopamine; **(E)** Cortisol; **(F)** Corticosterone. Data are expressed as means ± S.E.M., $n = 4$ (see Methods for details). *: $p < 0.05$ vs. C. Experimental groups (see Figure 1): C, control; N, samples taken at nadir of hypothermia, during ST; ER, early recovery, samples taken when Tb reached 35.5°C following ST; R3, samples taken 3 h after ER; R6, samples taken 6 h after ER.

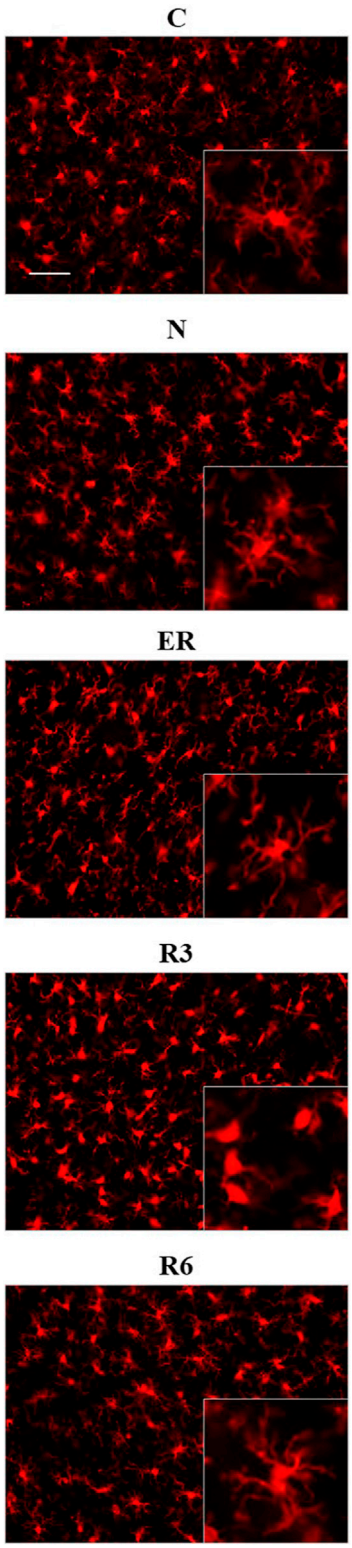

FIGURE 8
Representative pictures showing microglia, stained for Iba1 (secondary antibody conjugated with Alexa-594), in samples from the parietal cortex (P-Cx) randomly taken between Bregma −2.0 and −4.0. The inclusions within panels show representative microglial cell at higher magnification. Experimental groups (see Figure 1): C, control; N, samples taken at nadir of hypothermia, during ST; ER, early recovery, samples taken when Tb reached 35.5°C following ST; R3, samples taken 3 h after ER; R6, samples taken 6 h after ER. Calibration bar: 50 μm.

TABLE 2 Microglia morphometric analysis.

		C		N		ER		R3		R6	
		Mean	*S.E.M.*	Mean	*S.E.M.*	Mean	*S.E.M.*	Mean	*S.E.M.*	Mean	*S.E.M.*
Cell number	*CA3*	84.2	*3.6*	76.3	*5.8*	*56.5	*6.0*	96.2	*12.5*	72.0	*2.6*
	P-Cx	71.8	*3.9*	70.8	*3.6*	*52.7	*4.1*	74.5	*3.7*	63.3	*2.6*
Soma area (μm^2)	*CA3*	47.70	*2.64*	*33.84	*3.12*	40.06	*3.30*	43.34	*2.73*	*58.78	*4.51*
	P-Cx	51.28	*4.52*	40.16	*3.40*	42.89	*1.55*	42.66	*5.31*	*71.37	*6.65*
Arborization area (μm^2)	*CA3*	1076.78	*184.75*	*686.70	*101.39*	805.40	*96.43*	*688.37	*52.55*	1210.46	*83.18*
	P-Cx	1150.20	*62.00*	989.55	*73.81*	1024.71	*94.55*	*613.41	*48.28*	*1456.44	*149.45*
NND	*CA3*	39.59	*2.76*	40.13	*1.49*	43.10	*3.67*	33.65	*3.54*	44.22	*2.45*
	P-Cx	47.03	*1.61*	42.77	*1.75*	42.97	*2.97*	*35.75	*1.76*	45.78	*1.96*
MI	*CA3*	0.054	*0.007*	0.054	*0.004*	0.054	*0.004*	0.073	*0.011*	0.051	*0.003*
	P-Cx	0.047	*0.004*	0.043	*0.003*	0.050	*0.005*	*0.075	*0.007*	0.056	*0.003*

Morphometric parameters for the microglia analysis are shown as means ± S.E.M. NND, is the "nearest neighboring distance" and MI, is the "morphological index" (see Methods for details). This analysis was carried out in the parietal cortex (P Cx) and in the CA3 field of Hip, with the following experimental conditions (see Figure 1): Control C); Nadir of hypothermia N); Early recovery (ER; i.e., as soon as Tb reached 35.5°C during the recovery period following ST); 3 h after reaching ER (R3), 6 h after reaching ER (R6). * vs. C ($p < 0.05$). That the italic values indicates the standard error of the means, as indicated by the relative column headings.

occurrence of a cross reaction of the two primary antibodies with the two antigens [i.e., AT8 recognizes Tau only when phosphorylated at both S202 and T205 (Malia et al., 2016)], the persistence of high levels of p[T205]-Tau at ER represent a sign of a specific ongoing process with neuroprotective effects. This is supported by the peculiar p[T205]-Tau immunostaining of the CA3 field of the Hip, observed during the N condition, with no staining in the CA1 and CA2 fields (see Figure 3). This result is consistent with the different involvement of the various Hip cortical fields described in AD neurodegeneration (Padurariu et al., 2012; Ugolini et al., 2018). Therefore, the possible neuroprotective process triggered by ST within the Hip is apparently region-specific.

In the present work, we decided to focus on the most representative biochemical pathways involved in Tau phospho-regulation (Planel et al., 2004; Su et al., 2008). Overall, the results from the molecular quantifications of GSK3β and PP2A show that ST elicits a temporary neuronal formation of PPTau that is finely regulated at a biochemical level, as already described in hibernators (Su et al., 2008) and mice (Okawa et al., 2003; Planel et al., 2004; Planel et al., 2007). However, it is worth noting that mice are able to spontaneously enter torpor as well (Hudson and Scott, 1979; Oelkrug et al., 2011; Hitrec et al., 2019). When planning the experiments, our hypothesis was that some regulated cellular mechanism, that is able to cope with Tau hyper-phosphorylation, would take place only during the recovery period from ST, since rats do not hibernate and they might have not evolved specific adaptive mechanisms to cope with torpor bouts (Planel et al., 2004; Su et al., 2008). The present results show that even in the N condition, concomitantly with the excessive PPTau formation, there is a massive biochemical inhibition of GSK3β through phosphorylation on S9 residue (Cross et al., 1995). This response was not expected in a non-hibernator, considering that the enzymatic activity is generally depressed at low temperatures (Aloia and Raison, 1989; Marshall, 1997), with the exception of the specifically adaptive modifications in some enzymatic activity described in hibernating animals (Aloia and Raison, 1989; Su et al., 2008). Moreover, the inhibition of GSK3β apparently persisted, evidenced by the tendency to also maintain high levels of p[S9]-GSK3β during ER in both P-Cx and Hip (Figure 4). The ER condition also showed a higher PP2A level in P-Cx, a condition that possibly favors the ongoing PPTau dephosphorylation. Hence, GSK3β and PP2A regulations appeared to be important for the quick recovery of normal Tau phosphorylation levels.

In order to verify whether the mechanism elicited by ST is effectively neuroprotective or potentially neurotoxic, we also quantified some key molecular factors involved in apoptosis (i.e., factors that either stimulate or contrast it) or stressogenic cellular processes. Notably, apoptosis represents the main process that causes neurodegeneration (Fricker et al., 2018). In general, changes related to these factors were mild and transitory, such as, for instance, the peak value shown for GRP78 at ER in Hip. However, it is worth noting that when significant differences compared to control levels were observed in these molecular parameters, they were in a direction which indicated a possible neuroprotective rather than a neurotoxic effect. This trend was also confirmed by the observed decrease in the IF staining of cleaved-Caspase three in P-Cx during R3, shown in Supplementary Figure S1, or the transient and not significant increase in R3 within the Hip (see Figure 5): it is described that when levels of cleaved-Caspase 3 change quickly is a sign of neuroplasticity instead of an initiation of apoptosis (Snigdha et al., 2012). Along the same lines we should consider p[S473]-Akt [i.e., the activated and protective form of Akt (Risso et al., 2015; Levenga et al., 2017)] at ER in Hip and the lack of changes in the quantification of the neuronal marker NeuN, in both P-Cx and Hip, after 6 h of recovery from ST. However, it is worth noting that these data should be only considered as indication of a possible neuroprotection, a process that should be properly investigated with future experiments considering a much longer time window (Fricker et al., 2018) following ST.

Considering the specific patterns of data observed in the two brain structures, some interesting differences emerged between P-Cx and Hip: Tau-1 returned to normal values later in Hip

than in P-Cx, while GRP78 and p[S473]-Akt only peaked in Hip, for instance. These patterns, on the whole, show that Hip seems to regain normal conditions after ST with more difficulty than P-Cx. This is also corroborated by the quantifications that were observed in AT8 levels; they were much higher in Hip than in P-Cx. Higher values of staining intensity in the Hip, compared to P-Cx, were also found in our previous study using IF (Luppi et al., 2019). Therefore, ST appears to be more stressful to Hip compared to P-Cx, and this is in line with the normally observed evolution of tauopathy within the brain (Crary et al., 2014; Busche and Hyman, 2020). However, the difference between the two structures studied in regaining normality was limited to the first few hours of the recovery period; at R6 all the molecular parameters considered returned to normal in both brain areas.

The aim of the present work was also to look for possible systemic factors implicated in the neuronal formation and resolution of PPTau. We mainly focused on plasma melatonin, due to the involvement of this hormone in natural torpor arousal (Willis and Wilcox, 2014) as well as to its capacity to exert neuroprotective effects (Herrera-Arozamena et al., 2016; Shukla et al., 2017). Plasma catecholamines and cortico-steroid levels were also assessed, since they might be affected by the strong sympathetic activation which occurs during the recovery of normothermia following ST (Saaresranta and Polo, 2003; Cerri et al., 2013). However, among all the molecules that were tested, only melatonin was shown to change its plasma levels in relation to the experimental conditions. This strongly suggests a possible involvement of this hormone in the neuroprotective mechanism elicited by ST, although we are aware that further experiments are needed to confirm such a hypothesis. In fact, at N the pineal hormone showed a dramatic increase that was concomitant with the peak of p[S9]-GSK3β, suggesting that melatonin may play a role in the process of phosphorylation/dephosphorylation of Tau observed during and after ST. As a matter of fact, a melatonin mediated neuroprotective effect, leading to GSK3β inhibition and Akt activation, has been described (Liu et al., 2015; Chinchalongporn et al., 2018). The most peculiar aspect shown by the present results, is that the concomitant peaks of p[S9]-GSK3β and melatonin were not observed during the recovery period from ST, as initially supposed, but they were measured in deep hypothermic conditions. Since melatonin by itself did not turn out to be effective in contrasting tauopathies (Sanchez-Barcelo et al., 2017), this may suggest that, at a low body temperature, the pineal hormone could act differently from how it acts during euthermia. Indeed, melatonin mainly acts on neurons by means of specific membrane receptors (Liu et al., 2015), but a small quota may directly cross the cell membrane and interact with different cytoplasmatic targets (Liu et al., 2019). A possible explanation of how a low temperature may emphasize the neuroprotective effect of melatonin is the induction of a functional differentiation between these two action modalities. This possibility is supported by data from Chong and Sugden (1994), who studied the thermodynamics of melatonin-receptor binding processes and found that the best affinity ligand-target is actually reached at 21°C, corresponding with the Tb reached by rats during ST in the N condition. Moreover, these authors also reason that at this temperature plasma membrane is very close to a phase transition (Chong and Sugden, 1994). It follows that, at deep hypothermic condition, melatonin could not cross the cell membrane with the same efficiency shown at euthermia. Hence, the coexistence of a much higher binding affinity with membrane receptors [that trigger neuroprotective/antiapoptotic molecular pathways (Liu et al., 2015)], and the difficulty in crossing the cell membrane, may lead to a functional differentiation that could take place only close to 21°C, and not at 37°C. Moreover, the possible involvement of melatonin as a factor in the neuroprotective mechanism elicited by ST is also corroborated by the specific immunostaining of the CA3 field of Hip for the neuroprotective p[T205]-Tau (Ittner et al., 2016) that we observed in the N condition (see Figure 3): in fact, a different regional distribution of melatonin receptors has been described in the Hip, with a higher density exactly in the CA3 field (Lacoste et al., 2015).

Neuroinflammation represents a key condition in tauopathies (Ransohoff, 2016; Nilson et al., 2017), and is also a possible mechanism that induces, or emphasizes, neurodegeneration (Yu et al., 2021). The relationship between neuroinflammation and neurodegenerative pathology is complex: even though neuroinflammation is linked to amyloidosis and tauopathy, it is not clear whether one triggers the other or *vice versa* (Guerrero et al., 2021). Apparently, neuroinflammation may be protective as an initial response to a newly developing neuropathology, but, undoubtedly, a sustained chronic inflammatory response contributes to the evolution of neurological diseases (Guerrero et al., 2021). Also, at least in a condition of overt tauopathy, microglia cells appear to actively participate in spreading Tau aggregates (Asai et al., 2015). Our results show that ST induces a mild and temporary microglia activation, mainly shown by the higher MI in Hip and smaller arborization areas observed in both P-Cx and Hip in R3. In a previous work, we also observed a transient microgliosis at R6, that returned to normal after 38 h of recovery (Luppi et al., 2019), not confirmed here. Nevertheless, taken together, these results confirm that microglia cells are involved in the resolution of PPTau brain formation during recovery from ST, but microglia activation does not last more than a few hours, since PPTau disappeared. Hence, ST does not trigger a pathological neuroinflammation, but, rather, triggers an apparently acute microglia response that should have a protective role (Webers et al., 2020; Guerrero et al., 2021). This further strengthens the parallelism between ST and hibernation, since a similar pattern of microglia activation has been described in the Syrian hamster (Cogut et al., 2018).

In conclusion, deep hypothermia in rats seems to uncover a latent and evolutionary preserved physiological mechanism that is able to dam brain PPTau formation and to favor its dephosphorylation, apparently counteracting the evolvement towards neurotoxic effects and strongly supporting the similarity between ST and natural torpor. Considering that the pharmacological stabilization of MTs to treat AD has recently been suggested (Fernandez-Valenzuela et al., 2020), but also that these drugs (which are mainly used as anti-cancer treatments) are highly toxic (Majcher et al., 2018), the indirect stabilization of MTs, as apparently occurs following ST, might be a suitable therapeutic alternative (Craddock et al., 2012). Thus, the full understanding of what happens at a molecular level in the regulation of Tau phosphorylation/dephosphorylation in neurons of rats exposed to deep hypothermic conditions may assist in the development of new pharmacological approaches to simulate these processes in euthermic conditions, hopefully opening new avenues for the treatment of tauopathies.

Data availability statement

All the original data are accessible upon reasonable request to the Corresponding author. All the original gel images from western-blot analysis are available on AMS Acta, the Open Science repository of the University of Bologna (http://amsacta.unibo.it/id/eprint/6884 - DOI: 10.6092/unibo/amsacta/6884).

Ethics statement

The animal study was reviewed and approved by the National Health Authority (Ministero della Salute—Direzione Generale della Sanità Animale e dei Farmaci Veterinari).

Author contributions

FS and TH conducted the experiments and collected the results. EP, AO, LT, and CG contributed to *ex-vivo* procedures and prepared the tables and figures. ML performed the statistical analysis. DT and DM contributed in discussing and interpreting results. ML, MC, and RA contributed to conception and design of the study and funding acquisition. ML and RA wrote the first draft of the manuscript. All authors contributed to manuscript revision, read, and approved the submitted version.

Funding

This work has been supported by the Ministero dell'Università e della Ricerca Scientifica (MUR)—Italy, by the University of Bologna and with the contribution of: Fondazione Cassa di Risparmio in Bologna and European Space Agency (Research agreement collaboration 4000123556).

Acknowledgments

The authors wish to thank: Melissa Stott for reviewing the English, and Prof. Michelangelo Fiorentino, director of the Operative Unit of Pathologic Anatomy, Ospedale Maggiore, Bologna (Italy), for making a fluorescence microscope available.

Conflict of interest

The authors declare that the research was conducted in the absence of any commercial or financial relationships that could be construed as a potential conflict of interest.

Publisher's note

All claims expressed in this article are solely those of the authors and do not necessarily represent those of their affiliated organizations, or those of the publisher, the editors and the reviewers. Any product that may be evaluated in this article, or claim that may be made by its manufacturer, is not guaranteed or endorsed by the publisher.

Supplementary material

The Supplementary Material for this article can be found online at: https://www.frontiersin.org/articles/10.3389/fphys.2023.1129278/full#supplementary-material

References

Aloia, R. C., and Raison, J. K. (1989). Membrane function in mammalian hibernation. *Biochim. Biophys. Acta* 988, 123–146. doi:10.1016/0304-4157(89)90007-5

Arendt, T., Stieler, J., and Holzer, M. (2015). Brain hypometabolism triggers PHF-like phosphorylation of Tau, a major hallmark of Alzheimer's disease pathology. *J. Neural. Transm. (Vienna)* 122, 531–539. doi:10.1007/s00702-014-1342-8

Arendt, T., Stieler, J., Strijkstra, A. M., Hut, R. A., Rüdiger, J., Van der Zee, E. A., et al. (2003). Reversible paired helical filament-like phosphorylation of tau is an adaptive process associated with neuronal plasticity in hibernating animals. *J. Neurosci.* 23, 6972–6981. doi:10.1523/JNEUROSCI.23-18-06972.2003

Asai, H., Ikezu, S., Tsunoda, S., Medalla, M., Luebke, J., Haydar, T., et al. (2015). Depletion of microglia and inhibition of exosome synthesis halt Tau propagation. *Nat. Neurosci.* 18, 1584–1593. doi:10.1038/nn.4132

Baldy, C., Fournier, S., Boisjoly-Villeneuve, S., Tremblay, M. È., and Kinkead, R. (2018). The influence of sex and neonatal stress on medullary microglia in rat pups. *Exp. Physiol.* 103, 1192–1199. doi:10.1113/EP087088

Benarroch, E. E. (2018). Locus coeruleus. *Cell Tissue Res.* 373, 221–232. doi:10.1007/s00441-017-2649-1

Blessing, W. W., and Nalivaiko, E. (2001). Raphe magnus/pallidus neurons regulate tail but not mesenteric arterial blood flow in rats. *Neuroscience* 105, 923–929. doi:10.1016/s0306-4522(01)00251-2

Braulke, L. J., and Heldmaier, G. (2010). Torpor and ultradian rhythms require an intact signalling of the sympathetic nervous system. *Cryobiology* 60, 198–203. doi:10.1016/j.cryobiol.2009.11.001

Busche, M. A., and Hyman, B. T. (2020). Synergy between amyloid-β and tau in Alzheimer's disease. *Nat. Neurosci.* 23, 1183–1193. doi:10.1038/s41593-020-0687-6

Cerri, M., Hitrec, T., Luppi, M., and Amici, R. (2021). Be cool to be far: Exploiting hibernation for space exploration. *Neurosci. Biobehav. Rev.* 128, 218–232. doi:10.1016/j.neubiorev.2021.03.037

Cerri, M., Mastrotto, M., Tupone, D., Martelli, D., Luppi, M., Perez, E., et al. (2013). The inhibition of neurons in the central nervous pathways for thermoregulatory cold defense induces a suspended animation state in the rat. *J. Neurosci.* 33, 2984–2993. doi:10.1523/JNEUROSCI.3596-12.2013

Cerri, M. (2017). The central control of energy expenditure: Exploiting torpor for medical applications. *Annu. Rev. Physiol.* 79, 167–186. doi:10.1146/annurev-physiol-022516-034133

Chinchalongporn, V., Shukla, M., and Govitrapong, P. (2018). Melatonin ameliorates Aβ42 -induced alteration of βAPP-processing secretases via the melatonin receptor through the Pin1/GSK3β/NF-κB pathway in SH-SY5Y cells. *J. Pineal Res.* 64, e12470. doi:10.1111/jpi.12470

Chong, N. W., and Sugden, D. (1994). Thermodynamic analysis of agonist and antagonist binding to the chicken brain melatonin receptor. *Br. J. Pharmacol.* 111, 295–301. doi:10.1111/j.14765381.1994.tb14059.x

Cogut, V., Bruintjes, J. J., Eggen, B. J. L., van der Zee, E. A., and Henning, R. H. (2018). Brain inflammatory cytokines and microglia morphology changes throughout hibernation phases in Syrian hamster. *Brain Behav. Immun.* 68, 17–22. doi:10.1016/j.bbi.2017.10.009

Craddock, T. J., Tuszynski, J. A., Chopra, D., Casey, N., Goldstein, L. E., Hameroff, S. R., et al. (2012). The zinc dyshomeostasis hypothesis of Alzheimer's disease. *PLoS One* 7, e33552. doi:10.1371/journal.pone.0033552

Crary, J. F., Trojanowski, J. Q., Schneider, J. A., Abisambra, J. F., Abner, E. L., Alafuzoff, I., et al. (2014). Primary age-related tauopathy (PART): A common pathology associated with human aging. *Acta Neuropathol.* 128, 755–766. doi:10.1007/s00401-014-1349-0

Cross, D. A., Alessi, D. R., Cohen, P., Andjelkovich, M., and Hemmings, B. A. (1995). Inhibition of glycogen synthase kinase-3 by insulin mediated by protein kinase B. *Nature* 378, 785–789. doi:10.1038/378785a0

Davis, B. M., Salinas-Navarro, M., Cordeiro, M. F., Moons, L., and De Groef, L. (2017). Characterizing microglia activation: A spatial statistics approach to maximize information extraction. *Sci. Rep.* 7, 1576. doi:10.1038/s41598-017-01747-8

Esclaire, F., Lesort, M., Blanchard, C., and Hugon, J. (1997). Glutamate toxicity enhances Tau gene expression in neuronal cultures. *J. Neurosci. Res.* 49, 309–318. doi:10.1002/(sici)1097-4547(19970801)49:3<309::aid-jnr6>3.0.co;2-g

Fernandez-Valenzuela, J. J., Sanchez-Varo, R., Muñoz-Castro, C., De Castro, V., Sanchez-Mejias, E., Navarro, V., et al. (2020). Enhancing microtubule stabilization rescues cognitive deficits and ameliorates pathological phenotype in an amyloidogenic Alzheimer's disease model. *Sci. Rep.* 10, 14776. doi:10.1038/s41598-020-71767-4

Fricker, M., Tolkovsky, A. M., Borutaite, V., Coleman, M., and Brown, G. C. (2018). Neuronal cell death. *Physiol. Rev.* 98, 813–880. doi:10.1152/physrev.00011.2017

Gerson, J. E., Mudher, A., and Kayed, R. (2016). Potential mechanisms and implications for the formation of Tau oligomeric strains. *Crit. Rev. Biochem. Mol. Biol.* 51, 482–496. doi:10.1080/10409238.2016.1226251

Guerrero, A., De Strooper, B., and Arancibia-Cárcamo, I. L. (2021). Cellular senescence at the crossroads of inflammation and Alzheimer's disease. *Trends Neurosci.* 44, 714–727. doi:10.1016/j.tins.2021.06.007

Gutfreund, H. (1995). *Kinetics for the life Sciences: Receptors, transmitters and catalysts*. Cambridge (UK): Cambridge University Press. ISBN: 0-521-48027-2.

Herrera-Arozamena, C., Martí-Marí, O., Estrada, M., de la Fuente Revenga, M., and Rodríguez-Franco, M. I. (2016). Recent advances in neurogenic small molecules as innovative treatments for neurodegenerative diseases. *Molecules* 21, 1165. doi:10.3390/molecules21091165

Hitrec, T., Luppi, M., Bastianini, S., Squarcio, F., Berteotti, C., Lo Martire, V., et al. (2019). Neural control of fasting-induced torpor in mice. *Sci. Rep.* 9, 15462. doi:10.1038/s41598-019-51841-2

Hitrec, T., Squarcio, F., Cerri, M., Martelli, D., Occhinegro, A., Piscitiello, E., et al. (2021). Reversible tau phosphorylation induced by synthetic torpor in the spinal cord of the rat. *Front. Neuroanat.* 15, 592288. doi:10.3389/fnana.2021.592288

Holcik, M., and Korneluk, R. G. (2001). XIAP, the guardian angel. *Nat. Rev. Mol. Cell. Biol.* 2, 550–556. doi:10.1038/35080103

Hudson, J. W., and Scott, I. M. (1979). Daily torpor in the laboratory mouse, *Mus musculus* var. Albino. *Physiol. Zool.* 52, 205–218. doi:10.1086/physzool.52.2.30152564

Ibrahim, I. M., Abdelmalek, D. H., and Elfiky, A. A. (2019). GRP78: A cell's response to stress. *Life Sci.* 226, 156–163. doi:10.1016/j.lfs.2019.04.022

Ittner, A., Chua, S. W., Bertz, J., Volkerling, A., van der Hoven, J., Gladbach, A., et al. (2016). Site-specific phosphorylation of Tau inhibits amyloid-β toxicity in Alzheimer's mice. *Science* 354, 904–908. doi:10.1126/science.aah6205

Joseph, M., Anglada-Huguet, M., Paesler, K., Mandelkow, E., and Mandelkow, E. M. (2017). Anti-aggregant tau mutant promotes neurogenesis. *Mol. Neurodegener.* 12, 88. doi:10.1186/s13024-017-0230-8

Kovacs, G. G. (2017). *Tauopathies. Handb. Clin. Neurol.* 145, 355–368. doi:10.1016/B978-0-12-802395-2.00025-0

Lacoste, B., Angeloni, D., Dominguez-Lopez, S., Calderoni, S., Mauro, A., Fraschini, F., et al. (2015). Anatomical and cellular localization of melatonin MT1 and MT2 receptors in the adult rat brain. *J. Pineal Res.* 58, 397–417. doi:10.1111/jpi.12224

Lesort, M., Blanchard, C., Yardin, C., Esclaire, F., and Hugon, J. (1997). Cultured neurons expressing phosphorylated Tau are more resistant to apoptosis induced by NMDA or serum deprivation. *Brain Res. Mol. Brain Res.* 45, 127–132. doi:10.1016/s0169-328x(96)00284-7

Levenga, J., Wong, H., Milstead, R. A., Keller, B. N., LaPlante, L. E., and Hoeffer, C. A. (2017). AKT isoforms have distinct hippocampal expression and roles in synaptic plasticity. *Elife* 6, e30640. doi:10.7554/eLife.30640

Liu, D., Wei, N., Man, H. Y., Lu, Y., Zhu, L. Q., and Wang, J. Z. (2015). The MT2 receptor stimulates axonogenesis and enhances synaptic transmission by activating Akt signaling. *Cell Death Differ.* 22, 583–596. doi:10.1038/cdd.2014.195

Liu, L., Labani, N., Cecon, E., and Jockers, R. (2019). Melatonin target proteins: Too many or not enough? *Front. Endocrinol. (Lausanne)* 10, 791. doi:10.3389/fendo.2019.00791

Luppi, M., Hitrec, T., Di Cristoforo, A., Squarcio, F., Stanzani, A., Occhinegro, A., et al. (2019). Phosphorylation and dephosphorylation of tau protein during synthetic torpor. *Front. Neuroanat.* 13, 57. doi:10.3389/fnana.2019.00057

Majcher, U., Klejborowska, G., Moshari, M., Maj, E., Wietrzyk, J., Bartl, F., et al. (2018). Antiproliferative activity and molecular docking of novel double-modified colchicine derivatives. *Cells* 11, 192. doi:10.3390/cells7110192

Malia, T. J., Teplyakov, A., Ernst, R., Wu, S. J., Lacy, E. R., Liu, X., et al. (2016). Epitope mapping and structural basis for the recognition of phosphorylated tau by the anti-tau antibody AT8. *Proteins* 84, 427–434. doi:10.1002/prot.24988

Marshall, C. J. (1997). Cold-adapted enzymes. *Trends Biotechnol.* 15, 359–364. doi:10.1016/S0167-7799(97)01086-X

Morrison, S. F., and Nakamura, K. (2019). Central mechanisms for thermoregulation. *Annu. Rev. Physiol.* 81, 285–308. doi:10.1146/annurev-physiol-020518-114546

Nilson, A. N., English, K. C., Gerson, J. E., Barton Whittle, T., Nicolas Crain, C., Xue, J., et al. (2017). Tau oligomers associate with inflammation in the brain and retina of tauopathy mice and in neurodegenerative diseases. *J. Alzheimers Dis.* 55, 1083–1099. doi:10.3233/JAD-160912

Oelkrug, R., Heldmaier, G., and Meyer, C. W. (2011). Torpor patterns, arousal rates, and temporal organization of torpor entry in wildtype and UCP1-ablated mice. *J. Comp. Physiol. B* 181, 137–145. doi:10.1007/s00360-010-0503-9

Okawa, Y., Ishiguro, K., and Fujita, S. C. (2003). Stress-induced hyperphosphorylation of tau in the mouse brain. *FEBS Lett.* 535, 183–189. doi:10.1016/s0014-5793(02)03883-8

Padurariu, M., Ciobica, A., Mavroudis, I., Fotiou, D., and Baloyannis, S. (2012). Hippocampal neuronal loss in the CA1 and CA3 areas of Alzheimer's disease patients. *Psychiatr. Danub.* 24, 152–158. PMID: 22706413.

Paxinos, G., and Watson, C. (2007). *The rat brain in stereotaxic coordinates* 6th Edition. San Diego: Elsevier. ISBN–13: 978-0-12-547612-6.

Planel, E., Bretteville, A., Liu, L., Virag, L., Du, A. L., Yu, W. H., et al. (2009). Acceleration and persistence of neurofibrillary pathology in a mouse model of tauopathy following anesthesia. *FASEB J.* 23, 2595–2604. doi:10.1096/fj.08-122424

Planel, E., Miyasaka, T., Launey, T., Chui, D. H., Tanemura, K., Sato, S., et al. (2004). Alterations in glucose metabolism induce hypothermia leading to tau hyperphosphorylation through differential inhibition of kinase and phosphatase activities: Implications for alzheimer's disease. *J. Neurosci.* 24, 2401–2411. doi:10.1523/JNEUROSCI.5561-03.2004

Planel, E., Richter, K. E., Nolan, C. E., Finley, J. E., Liu, L., Wen, Y., et al. (2007). Anesthesia leads to tau hyperphosphorylation through inhibition of phosphatase activity by hypothermia. *J. Neurosci.* 27, 3090–3097. doi:10.1523/JNEUROSCI.4854-06.2007

Ransohoff, R. M. (2016). How neuroinflammation contributes to neurodegeneration. *Science* 353, 777–783. doi:10.1126/science.aag2590

Risso, G., Blaustein, M., Pozzi, B., Mammi, P., and Srebrow, A. (2015). Akt/PKB: One kinase, many modifications. *Biochem. J.* 468, 203–214. doi:10.1042/BJ20150041

Saaresranta, T., and Polo, O. (2003). Sleep-disordered breathing and hormones. *Eur. Respir. J.* 22, 161–172. doi:10.1183/09031936.03.00062403

Sanchez-Barcelo, E. J., Rueda, N., Mediavilla, M. D., Martinez-Cue, C., and Reiter, R. J. (2017). Clinical uses of melatonin in neurological diseases and mental and behavioural disorders. *Curr. Med. Chem.* 24, 3851–3878. doi:10.2174/0929867324666170718105557

Shukla, M., Govitrapong, P., Boontem, P., Reiter, R. J., and Satayavivad, J. (2017). Mechanisms of melatonin in alleviating alzheimer's disease. *Curr. Neuropharmacol.* 15, 1010–1031. doi:10.2174/1570159X15666170313123454

Snigdha, S., Smith, E. D., Prieto, G. A., and Cotman, C. W. (2012). Caspase-3 activation as a bifurcation point between plasticity and cell death. *Neurosci. Bull.* 28, 14–24. doi:10.1007/s12264-012-1057-5

Stanton, T. L., Craft, C. M., and Reiter, R. J. (1986). Pineal melatonin: Circadian rhythm and variations during the hibernation cycle in the ground squirrel, *Spermophilus lateralis*. *J. Exp. Zool.* 239, 247–254. doi:10.1002/jez.1402390212

Su, B., Wang, X., Drew, K. L., Perry, G., Smith, M. A., and Zhu, X. (2008). Physiological regulation of Tau phosphorylation during hibernation. *J. Neurochem.* 105, 2098–2108. doi:10.1111/j.1471-4159.2008.05294.x

Tinganelli, W., Hitrec, T., Romani, F., Simoniello, P., Squarcio, F., Stanzani, A., et al. (2019). Hibernation and radioprotection: Gene expression in the liver and testicle of rats irradiated under synthetic torpor. *Int. J. Mol. Sci.* 20, 352. doi:10.3390/ijms20020352

Ugolini, F., Lana, D., Nardiello, P., Nosi, D., Pantano, D., Casamenti, F., et al. (2018). Different patterns of neurodegeneration and glia activation in CA1 and CA3 hippocampal regions of TgCRND8 mice. *Front. Aging. Neurosci.* 10, 372. doi:10.3389/fnagi.2018.00372

Wang, Y., and Mandelkow, E. (2016). Tau in physiology and pathology. *Nat. Rev. Neurosci.* 17, 5–21. doi:10.1038/nrn.2015.1

Webers, A., Heneka, M. T., and Gleeson, P. A. (2020). The role of innate immune responses and neuroinflammation in amyloid accumulation and progression of Alzheimer's disease. *Immunol. Cell Biol.* 98, 28–41. doi:10.1111/imcb.12301

Weingarten, M. D., Lockwood, A. H., Hwo, S. Y., and Kirschner, W. (1975). A protein factor essential for microtubule assembly. *Proc. Nat. Acad. Sci. U. S. A.* 72, 1858–1862. doi:10.1073/pnas.72.5.1858

Whittington, R. A., Bretteville, A., Dickler, M. F., and Planel, E. (2013). Anesthesia and tau pathology. *Prog. Neuropsychopharmacol. Biol. Psychiatry* 47, 147–155. doi:10.1016/j.pnpbp.2013.03.004

Willis, C. K., and Wilcox, A. (2014). Hormones and hibernation: Possible links between hormone systems, winter energy balance and white-nose syndrome in bats. *Horm. Behav.* 66, 66–73. doi:10.1016/j.yhbeh.2014.04.009

Yu, Z., Jiang, N., Su, W., and Zhuo, Y. (2021). Necroptosis: A novel pathway in neuroinflammation. *Front. Pharmacol.* 12, 701564. doi:10.3389/fphar.2021.701564

frontiers | Frontiers in Physiology

TYPE Correction
PUBLISHED 25 July 2023
DOI 10.3389/fphys.2023.1256251

OPEN ACCESS

EDITED AND REVIEWED BY
Jérémy Terrien,
Muséum National d'Histoire Naturelle, France

*CORRESPONDENCE
Marco Luppi,
marco.luppi@unibo.it

†These authors have contributed equally to this work and share first authorship

RECEIVED 10 July 2023
ACCEPTED 13 July 2023
PUBLISHED 25 July 2023

CITATION
Squarcio F, Hitrec T, Piscitiello E, Cerri M, Giovannini C, Martelli D, Occhinegro A, Taddei L, Tupone D, Amici R and Luppi M (2023), Corrigendum: Synthetic torpor triggers a regulated mechanism in the rat brain, favoring the reversibility of Tau protein hyperphosphorylation. *Front. Physiol.* 14:1256251. doi: 10.3389/fphys.2023.1256251

Corrigendum: Synthetic torpor triggers a regulated mechanism in the rat brain, favoring the reversibility of Tau protein hyperphosphorylation

Fabio Squarcio[1†], Timna Hitrec[1†], Emiliana Piscitiello[1,2], Matteo Cerri[1], Catia Giovannini[2,3], Davide Martelli[1], Alessandra Occhinegro[1,2], Ludovico Taddei[1], Domenico Tupone[1,4], Roberto Amici[1] and Marco Luppi[1,2]*

[1]Department of Biomedical and Neuromotor Sciences, University of Bologna, Bologna, Italy, [2]Centre for Applied Biomedical Research—CRBA, St. Orsola Hospital, University of Bologna, Bologna, Italy, [3]Department of Experimental, Diagnostic and Specialty Medicines, University of Bologna, Bologna, Italy, [4]Department of Neurological Surgery, Oregon Health and Science University, Portland, OR, United States

KEYWORDS

deep hypothermia, microtubules, melatonin, glycogen synthase kinase 3β, hippocampus, parietal cortex

A Corrigendum on
Synthetic torpor triggers a regulated mechanism in the rat brain, favoring the reversibility of Tau protein hyperphosphorylation

by Squarcio F, Hitrec T, Piscitiello E, Cerri M, Giovannini C, Martelli D, Occhinegro A, Taddei L, Tupone D, Amici R and Luppi M (2023). Front. Physiol. 14:1129278. doi: 10.3389/fphys.2023.1129278

In the published article, there was an error in Figure 4E as published. The only **histogram bars** represented in **Panel E left side** (referred to P-Cx [i.e., Parietal cortex]) are wrong, together with the relative "y" scale. However, the representative Western blot bands depicted at the bottom of the histograms are correct, as described in the original caption that is also reported below. The corrected Figure 4 and its correct original caption appear below.

The authors apologize for these errors and state that this does not change the scientific conclusions of the article in any way. The original article has been updated.

10.3389/fphys.2023.1256251

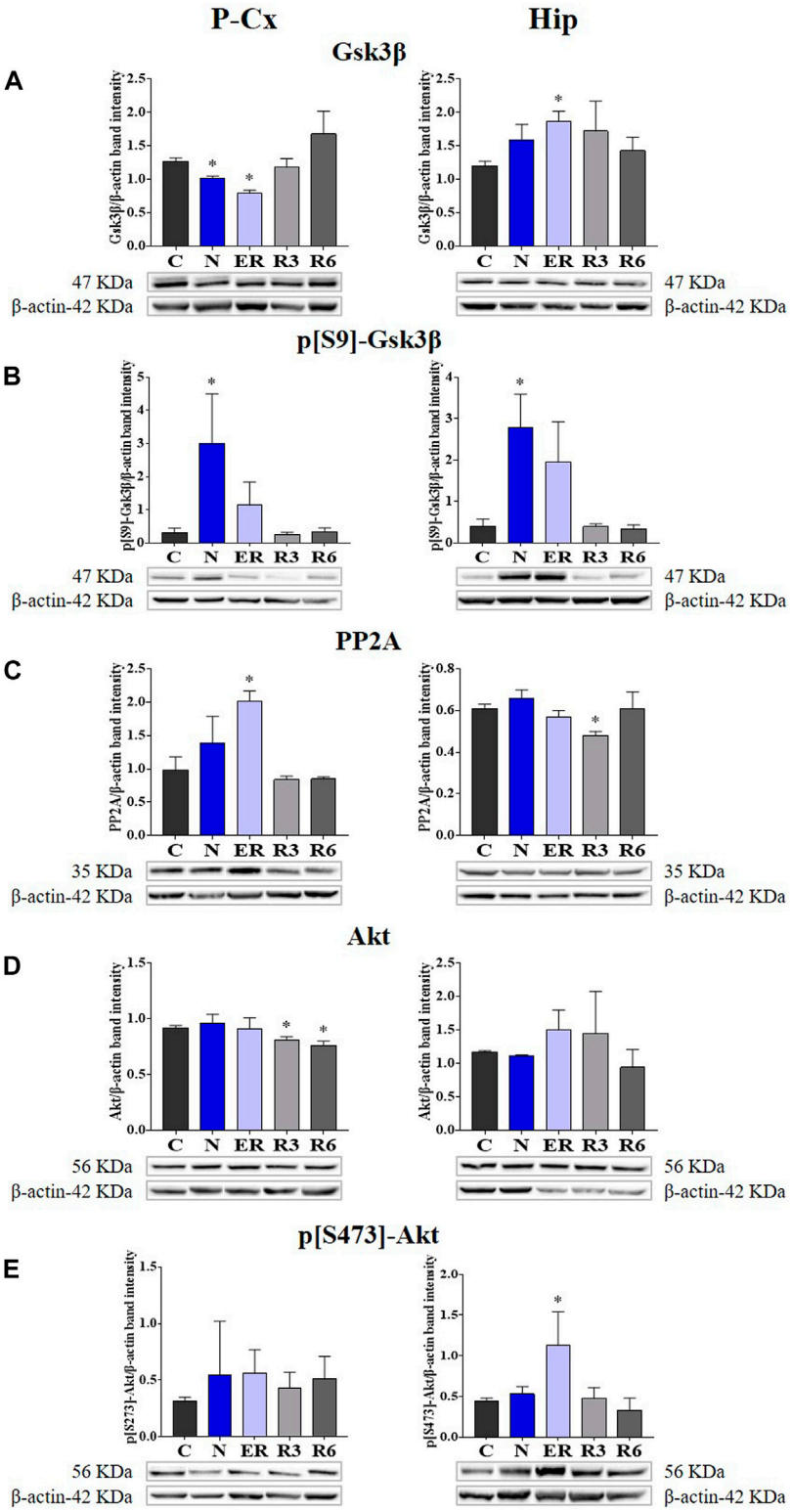

FIGURE 4
Western blot detection of the main enzymes involved in phosphorylation and dephosphorylation of Tau, determined in brain extracts of the parietal cortex (P-Cx) and hippocampus (Hip). Below each histogram, WB representative samples are shown for each experimental condition. **(A)** glycogen-synthase kinase-3β (GSK3β), the main kinase targeting Tau; **(B)** p[S9]-GSK3β (inactive form of GSK3β, phosphorylated at Ser9); **(C)** protein phosphatase-2A (PP2A), the main phosphatase targeting Tau; **(D)** different isoforms of Akt (protein kinase-B; Akt 1/2/3), kinases targeting GSK3β at Ser9 and antiapoptotic factors; **(E)** p[S473] Akt, the active form of Akt 1/2/3, phosphorylated at Ser473. Data are normalized by β-actin and expressed as means ± S.E.M., $n = 3$. *: $p < 0.05$ vs. C. Experimental groups (see **Figure 1**): C, control; N, samples taken at nadir of hypothermia, during ST; ER, early recovery, samples taken when Tb reached 35.5°C following ST; R3, samples taken 3 h after ER; R6, samples taken 6 h after ER.

Publisher's note

frontiers | Frontiers in Physiology

TYPE Review
PUBLISHED 26 June 2023
DOI 10.3389/fphys.2023.1207003

OPEN ACCESS

EDITED BY
Alex Rafacho,
Federal University of Santa Catarina, Brazil

REVIEWED BY
Mustafa Oztop,
Mehmet Akif Ersoy University, Türkiye
Shannon Noella Tessier,
Massachusetts General Hospital and Harvard Medical School, United States

*CORRESPONDENCE
Scott T. Cooper,
scooper@uwlax.edu

RECEIVED 16 April 2023
ACCEPTED 12 June 2023
PUBLISHED 26 June 2023

CITATION
De Vrij EL, Bouma HR, Henning RH and Cooper ST (2023), Hibernation and hemostasis.
Front. Physiol. 14:1207003.
doi: 10.3389/fphys.2023.1207003

Hibernation and hemostasis

Edwin L. De Vrij[1,2], Hjalmar R. Bouma[2,3], Robert H. Henning[2] and Scott T. Cooper[4]*

[1]Department of Plastic Surgery, University Medical Center Groningen, University of Groningen, Groningen, Netherlands, [2]Department of Clinical Pharmacy and Pharmacology, University Medical Center Groningen, Groningen, Netherlands, [3]Department of Internal Medicine, University Medical Center Groningen, University of Groningen, Groningen, Netherlands, [4]Biology Department, University of Wisconsin-La Crosse, La Crosse, WI, United States

Hibernating mammals have developed many physiological adaptations to accommodate their decreased metabolism, body temperature, heart rate and prolonged immobility without suffering organ injury. During hibernation, the animals must suppress blood clotting to survive prolonged periods of immobility and decreased blood flow that could otherwise lead to the formation of potentially lethal clots. Conversely, upon arousal hibernators must be able to quickly restore normal clotting activity to avoid bleeding. Studies in multiple species of hibernating mammals have shown reversible decreases in circulating platelets, cells involved in hemostasis, as well as in protein coagulation factors during torpor. Hibernator platelets themselves also have adaptations that allow them to survive in the cold, while those from non-hibernating mammals undergo lesions during cold exposure that lead to their rapid clearance from circulation when re-transfused. While platelets lack a nucleus with DNA, they contain RNA and other organelles including mitochondria, in which metabolic adaptations may play a role in hibernator's platelet resistance to cold induced lesions. Finally, the breakdown of clots, fibrinolysis, is accelerated during torpor. Collectively, these reversible physiological and metabolic adaptations allow hibernating mammals to survive low blood flow, low body temperature, and immobility without the formation of clots during torpor, yet have normal hemostasis when not hibernating. In this review we summarize blood clotting changes and the underlying mechanisms in multiple species of hibernating mammals. We also discuss possible medical applications to improve cold preservation of platelets and antithrombotic therapy.

KEYWORDS

hibernation, torpor, hemostasis, platelet, coagulation, metabolism, hypothermia

Overview of hemostasis

Blood plays an essential role in vertebrates by circulating oxygen and nutrients and removing wastes from all tissues. This requires an extensive network of vessels that contain fluid blood, yet can form solid clots if vessels are damaged to prevent the organism from bleeding to death. Spontaneous blot clot formation is counterbalanced by anticoagulant mechanisms that can become overwhelmed at the site of a wound leading to hemostasis. The word hemostasis is derived from the Greek αίμα/hema (=blood) and στάσις/stasis (=halt), literally the stopping of blood. Hemostasis is generally divided into three phases, primary hemostasis involving anucleated cells called platelets, secondary hemostasis triggered by a cascade of serine proteases to form a fibrin clot, and fibrinolysis, which breaks down the clot (Figure 1). There are multiple ways to activate hemostasis including endothelial cell injury, clotting factors or platelet alterations, and abnormal blood flow. During torpor, heart rate

and blood flow are reduced to levels that would lead to the formation of potentially lethal blood clots in most non-hibernating mammals. Hypothermia also affects both procoagulant and anticoagulant aspects of hemostasis. Hibernating mammals thus need multiple adaptations to reversibly suppress blood clotting during torpor, which will be discussed in this review.

Hibernating mammalian models

Hibernators encounter several risk factors for thrombosis including low body temperature, stasis of blood, hypercoagulability, and endothelial activation. During torpor a ground squirrel's body temperature drops from 35°C–38°C to 4°C–8°C (Lechler and Penick, 1963; Reddick et al., 1973), the heart rate is reduced from its normal 200–300 to three to five beats/min (Zatzman, 1984), and respiration is reduced from 100 to 200 to four to six breaths/min (McArthur and Milsom, 1991). As expected, blood pressure also drops from 140/100 mmHg to 60/30 mmHg, with values as low as 10 mmHg reported (Lyman and O'brien 1960). Thus hibernation entails periods of prolonged immobility (Carey et al., 2003; Utz et al., 2009) with low blood flow (stasis) in veins and atria (Horwitz et al., 2013), increased blood viscosity (Kirkebo, 1968; Halikas and Bowers, 1973; Arinell et al., 2018), cycles of hypoxia-reoxygenation, and cooling-rewarming with signs of endothelial activation (Carey et al., 2003; Talaei et al., 2012). Additionally, at entrance of the hibernation season, hibernators are generally grossly overweight (Martin, 2008). Remarkably, despite this multitude of risk factors for thromboembolism, hibernators do not demonstrate signs of organ damage due to thromboembolic complications during hibernation or upon arousal in spring (Cooper et al., 2012; Bonis et al., 2019).

A reversible decrease in hemostasis has been demonstrated during torpor in diverse hibernating animals. In small mammalian deep hibernators body temperature can drop to 2°C–4°C as found in ground squirrels (Svihla et al., 1951; Lechler and Penick, 1963; Reddick et al., 1973; Pivorun and Sinnamon, 1981; Bouma et al., 2010; Cooper et al., 2012; Hu et al., 2017; Öztop et al., 2019), hamsters (Denyes and Carter, 1961; Deveci et al., 2001; de Vrij et al., 2014), hedgehogs (Biorck et al., 1962; De Wit et al., 1985), and bats (Rashid et al., 2016). In contrast, large mammals like bears show more moderate body temperatures during hibernation by only dropping from 37°C to 32°C coupled with prolonged immobility (Fröbert et al., 2010; Welinder et al., 2016; Iles et al., 2017; Arinell et al., 2018; Thienel et al., 2023). Decreased hemostasis in

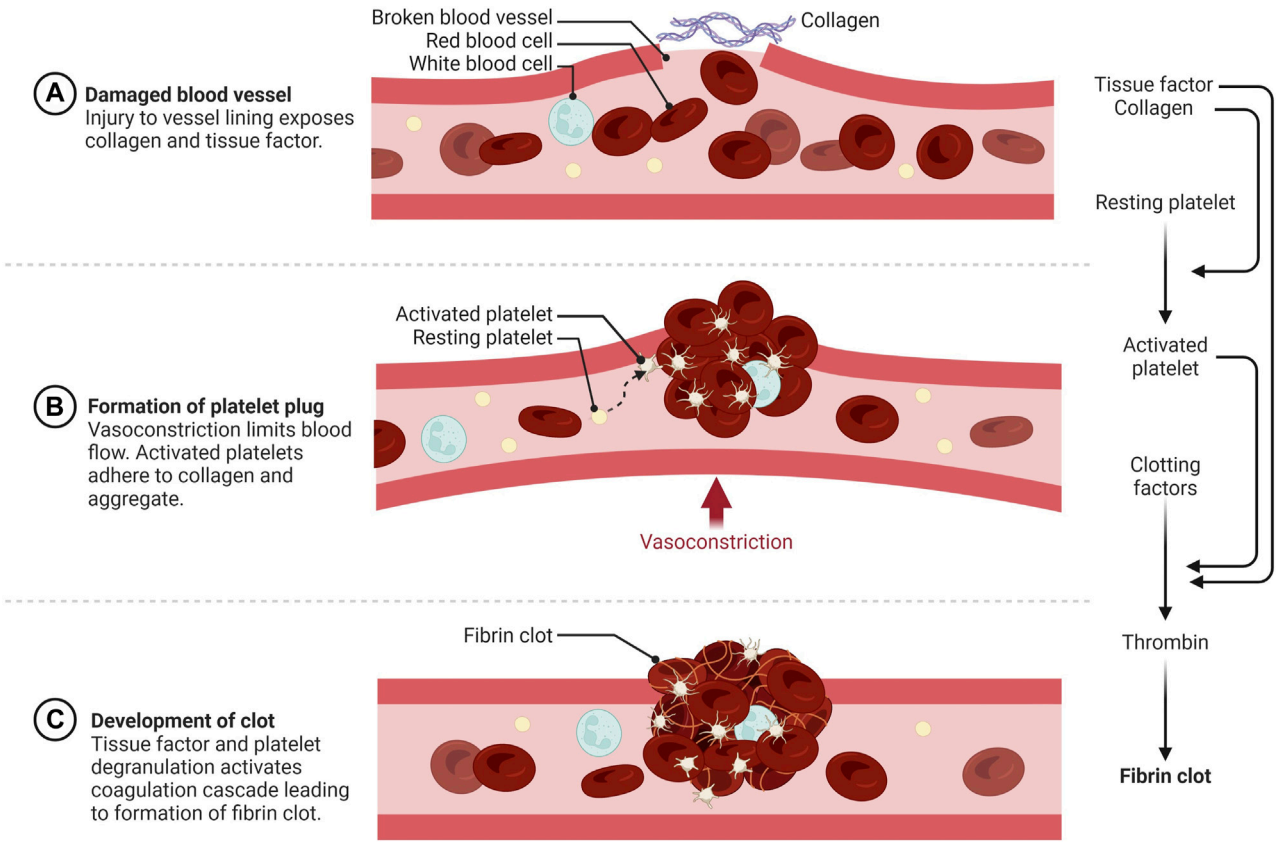

FIGURE 1
Schematic overview of hemostasis. **(A)** Primary hemostasis is initiated by vessel wall injury exposing the extracellular matrix (ECM) to blood. **(B)** Activated and degranulated platelets initiate platelet and white blood cell recruitment to form a platelet plug. This accelerates platelet aggregation, vasoconstriction, wound regeneration, and activation of secondary hemostasis. **(C)** Secondary hemostasis occurs via activation of the plasma coagulation system due to exposure of plasma zymogens to tissue factor (TF) and platelet activation products, forming a fibrin rich network that traps red and white blood cells and further strengthens the hemostatic plug https://biorender.com/.

10.3389/fphys.2023.1207003

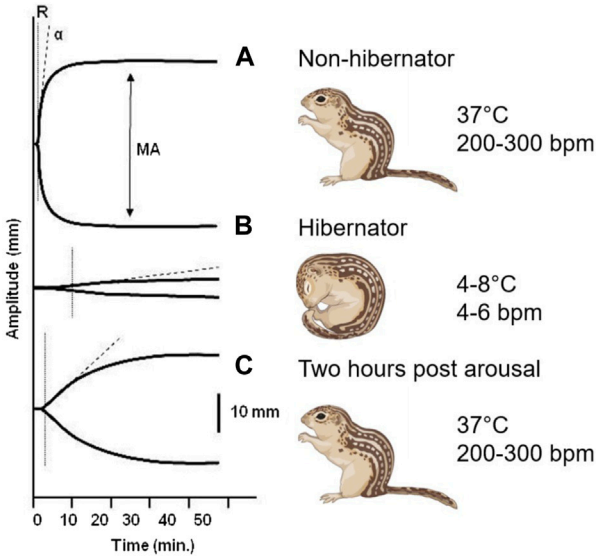

FIGURE 2
Thromboelastogram of 13-lined ground squirrel blood collected at different hibernation phases. **(A)** During summer, the rate of formation (R) and strength of the clot (MA, maximum amplitude) reflect fully functional primary and secondary hemostasis. **(B)** The time needed to form a clot increases and the strength of the clot dramatically decreases during the torpor phase of hibernation. **(C)** Within 2 hours of arousal both primary and secondary hemostasis are restored to functional levels (Cooper et al., 2012).

hibernators may partly be explained by the decrease in body temperature, as forced hypothermia also lowers platelet counts in hamsters, and even suppresses hemostasis in non-hibernating species like rats and mice (de Vrij et al., 2014). Finally, ectothermic vertebrates also reduce hemostasis during hibernation as seen in turtles (Barone and Jacques, 1975) and frogs (Ahmad et al., 1979). Given that a wide range of hibernating species suppress their hemostasis during torpor through multiple mechanisms, it is likely that this represents a vital physiological adaptation to multiple risk factors during torpor. The rapid restoration of hemostasis after arousal indicates that being able to form clots soon after arousal is also imperative. Changes in blot clot formation throughout hibernation is illustrated graphically by thromboelastograms where whole blood is treated with an activator of coagulation and the speed and strength of clot formation is measured (Figure 2). Because both primary and secondary hemostasis are regulated by proteins in circulation and platelets which lack a nucleus, the adaptations to rapid changes in temperature and blood flow must be inherent in these proteins and cells, and not rely on new synthesis as seen in other organs.

Effect of hypothermia on hemostasis

While clot formation may prevent bleeding after tissue damage and initiate wound healing, inadvertent generation of a thrombus can be detrimental for any organism. Virchow's Triad was first described in 1856 and identified venous stasis, vascular injury, and hypercoagulability as risk factors for thrombosis. The ensuing disseminated intravascular coagulation (DIC) of hypothermic patients may result in consumption of clotting factors, ischemia, and necrosis of organs and eventually result in death (Duguid et al., 1961; Stine, 1977; Mahajan et al., 1981). Besides provoking prothrombotic effects, decreased body temperature slows the enzymatic reactions in secondary hemostasis (Rohrer and Natale, 1992; DeLong et al., 2017), prolonging bleeding time in cold skin, and diminishing thromboxane A release from platelets (Valeri et al., 1995; Michelson et al., 1999). Consequently, hypothermia is associated with a secondary hypocoagulation state with prolonged time to clot formation in tests such as PT and APTT when temperatures drop below 35°C (Rohrer and Natale, 1992; Polderman, 2009). Low temperature *in vivo* increases activation, aggregation, and reversible storage of platelets in the liver or spleen (Van Poucke et al., 2014). Low temperatures of the extremities have been implicated to 'prime' platelets for activation at these sites most susceptible to bleeding throughout evolutionary history, which also leads to increased clearance of these platelets from circulation (Hoffmeister et al., 2003). Furthermore, both accidental and therapeutic hypothermia are associated with a reduction in platelet count known as thrombocytopenia (Vella et al., 1988; Chan and Beard, 1993; Mikhailidis and Barradas, 1993; Mallet, 2002; Morrell et al., 2008; Jacobs et al., 2013; Wang et al., 2015). Whether this thrombocytopenia in patients can be reversed quickly by rewarming—or whether thrombocytopenia recovers due to *de novo* production and release of platelets from the bone marrow—is still not clear.

Ex vivo cooling of platelets from non-hibernating mammals induces platelet shape changes similar to activation of platelets (White and Krivit, 1967; Winokur and Hartwig, 1995; Peerschke et al., 2008; Egidi et al., 2010), while low temperature also increases degranulation of activated platelets and plasma levels of activation products of platelets (Hoffmeister, 2011; Van Poucke et al., 2014). Cooled platelets demonstrate an increased tendency to aggregate (Xavier et al., 2007) and are rapidly cleared from circulation after transfusion (Becker et al., 1973; Berger et al., 1998; Van Poucke et al., 2014). Currently, human platelets are stored at 22°C–24°C room temperature before transfusion which increases risk of bacterial contamination and thus limits shelf-life to only 5–7 days, compared to 40 days for cold stored red blood cells (D'Alessandro et al., 2010). However, even if low body temperature leads to a 10-fold decrease in enzymatic activity and slowing down of clot formation, the prolonged time in torpor would be sufficient for clots to form during torpor. For example, to produce serum in the lab, blood is collected in the absence of an anticoagulant and stored in a refrigerator where it will still form a fibrin clot at 4°C if given enough time. Further unraveling the temperature effects on hemostasis may yield improved understanding of its role in hypothermic patients and in hibernating mammals and potentially disclose new pathways for drug development focused on novel antithrombotic strategies.

Primary hemostasis involves adherence of circulating platelets to damaged endothelium or subendothelial collagen and aggregation between platelets (Figure 1A). Platelets, which bud off from large multinuclear bone marrow cells called megakaryocytes, are 2–5 µm anucleated blood cells that play a major role in hemostasis,

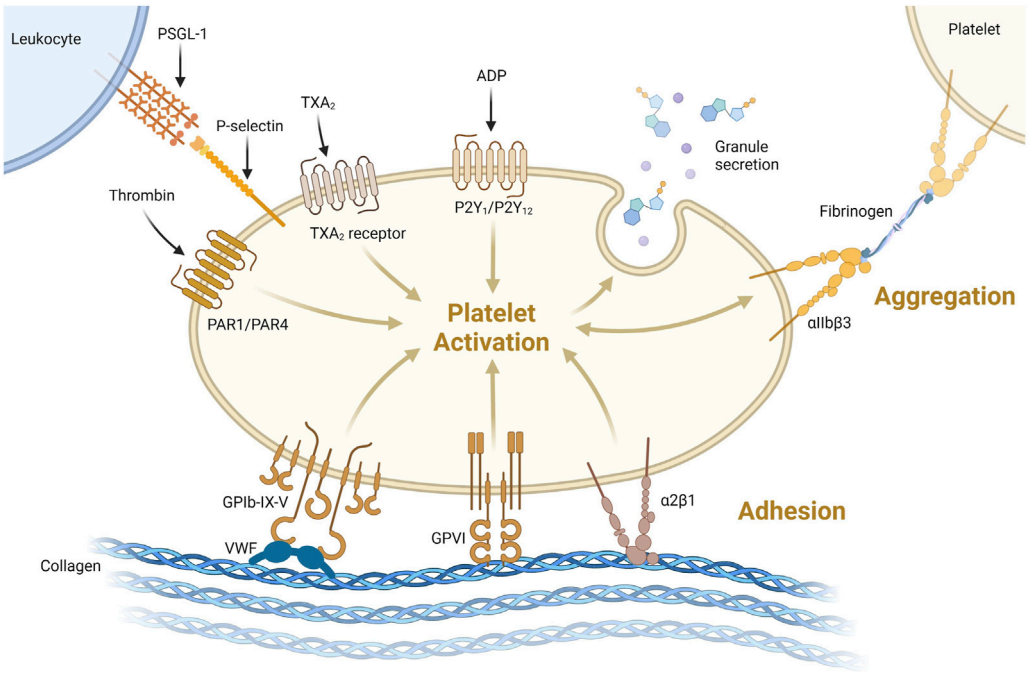

FIGURE 3
Platelets can be activated through one or more pathways. Illustrated here are activation via thrombin binding PAR1/PAR4, thromboxane 2 (TXA_2) binding TXA_2receptor or ADP binding P_2Y_1/P_2Y_{12} receptor. Platelets can be activated and bind collagen via VWF binding GPIb-IX-V or directly via GPVI or α2β1 receptors binding collagen. Activation leads to degranulation, secreting its granule content. Platelet-platelet aggregation is supported via αIIbβ3 binding via fibrinogen as shown on the top right. Platelet-leukocyte interaction acts via P-selectin binding to P-selectin glycoprotein 1 (PSGL-1, top left) https://biorender.com/.

inflammation, bacterial defense and wound regeneration and are even involved in cancer metastasis (Semple et al., 2011; Ware et al., 2013; Leblanc and Peyruchaud, 2016; Fernandez-Moure et al., 2017). Platelets are activated by many molecules including Von Willebrand Factor (VWF), collagen, thrombin, adenosine diphosphate (ADP) and adrenaline (Nieswandt et al., 2011; Versteeg et al., 2013). Activated platelets express membrane proteins including glycoprotein Ib-IX-V (GPIb-IX-V) and P-selectin that bind to activated endothelium or subendothelial collagen through VWF (Nieswandt et al., 2011) (Figure 3). Platelets degranulate upon activation, releasing molecules that stimulate further platelet activation, the coagulation cascade, inflammation, tissue regeneration and bacterial killing (Semple et al., 2011; Fernandez-Moure et al., 2017). More platelets are then recruited to the site of injury (Figure 1B). Platelets adhere to the subendothelial extracellular matrix (ECM) and forma hemostatic plug by aggregating with each other.

Primary hemostasis adaptations during torpor

Circulating platelet levels decrease about 10-fold in multiple hibernating species during torpor, with a return to normal levels as the animals rewarm during arousals (Figure 4). These dynamics could decrease the risk of a large intravascular clot forming during torpor, while restoring normal clotting activity upon arousal. The thrombocytopenia is temperature dependent and can be induced in hamsters, rats, and mice with forced chilling (de Vrij et al., 2014). Cold acclimation of rats and hamsters also reduced circulating platelet levels even though the animal's body temperatures did not decrease (Deveci et al., 2001). The rapid return of platelets in circulation after arousal, in the absence of large numbers of circulating immature platelets, suggests that hibernator platelets are stored during the cold and released into circulation during rewarming. Removal of the spleens of Syrian hamsters and 13-lined ground squirrels before or during torpor did not affect the platelet storage and release indicating that spleen is not required for storage as originally proposed (Reddick et al., 1973; Cooper et al., 2012; Cooper et al., 2016; de Vrij et al., 2021). Rather, platelet storage during torpor occurs in the sinusoids of the liver, consistent with this organ being responsible for storing platelets (Cooper et al., 2017; de Vrij et al., 2021). The mechanism of hepatic storage of platelets during torpor is currently unknown, potentially platelet margination may underlie the reversible storage and release in liver (de Vrij et al., 2021). Although platelets cluster together in liver sinusoids during torpor, they do not form irreversible thrombi. Several adaptations may prevent platelet activation during their slumber in cold liver sinusoids. Platelet GpIbα receptors can bind to VWF, but the plasma concentration of VWF decreases during torpor in bears, ground squirrels and hamsters, with a selective loss of the thrombogenic high molecular weight multimers (Cooper et al., 2016; Friedrich et al., 2017). Additionally, platelets from torpid ground squirrels bind less VWF and collagen, consistent with decreased GpIbα

10.3389/fphys.2023.1207003

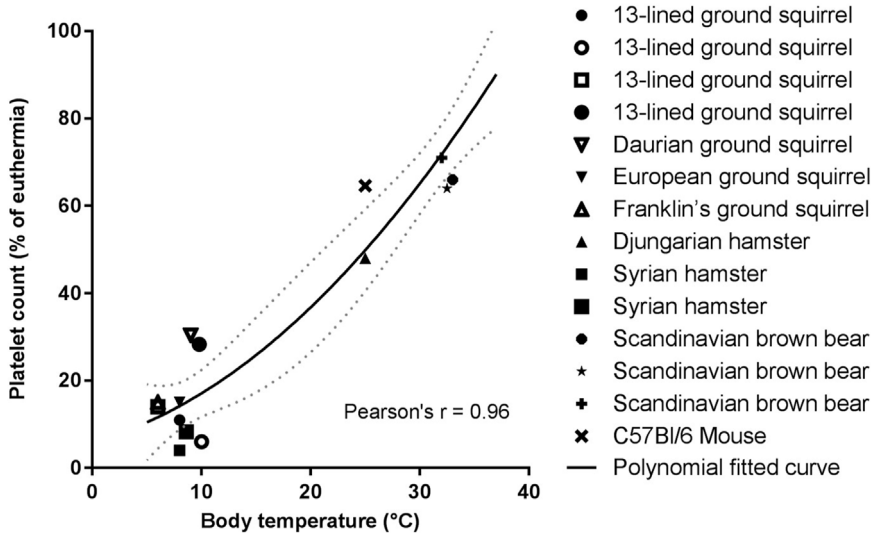

FIGURE 4
Temperature association with platelet count reduction is consistent for all hibernating mammals studied so far. Platelet count in torpor as percentage of euthermia platelet count was calculated from values of studies summarized in Table 1. If a study did not report euthermic platelet count, literature data were used. Fitted polynomial quadratic curve (black line) with 95% confidence interval (dotted gray line). Pearson's r = 0.96, $p < 0.05$ (Lechler and Penick, 1963; Reddick et al., 1973; Pivorun and Sinnamon, 1981; Bouma et al., 2010; Fröbert et al., 2010; Cooper et al., 2012; de Vrij et al., 2014; Welinder et al., 2016; Cooper et al., 2017; Hu et al., 2017; Arinell et al., 2018; de Vrij et al., 2021).

activity on their surface. Upon arousal, VWF levels return to normal rapidly, possibly by release of stores in platelets or endothelial cells (Cooper et al., 2016). The combination of decreased platelet and VWF levels along with decreased binding of platelets to VWF would all help to suppress activation of primary hemostasis during torpor-induced stasis.

Shape change is another prominent feature of cooled and hibernating platelets. Under normal conditions, platelets have a circumferential microtubule ring that keeps them in a disc conformation. In non-hibernating mammals, chilling platelets leads to depolymerization of their microtubules and the platelets become spherical and do not repolymerize upon warming (White and Krivit, 1967; Winokur and Hartwig, 1995). In contrast, ground squirrels and Syrian hamster platelet microtubules form rods when chilled and can reconstitute the circumferential ring upon rewarming (Cooper et al., 2017; de Vrij et al., 2021). This allows ground squirrel platelets to retain their overall shape after chilling. It is unclear if this rod shape has any physiological or adaptive significance, but it may protect platelets from damage caused by cold storage.

Cold storage of human and mouse platelets damages platelets in several ways, collectively termed cold storage lesions. Sialic acid residues on surface glycoproteins are cleaved leading to the rapid clearance of chilled platelets from circulation by the liver (Hoffmeister et al., 2003; Hoffmeister, 2011). Cold storage also induces intrinsic mitochondrial activated apoptosis in human and mouse platelets (Van Der Wal et al., 2010; Lebois and Josefsson, 2016; Stolla et al., 2020). In contrast, ground squirrel platelets stored *in vitro* in the cold are not cleared rapidly upon re-transfusion (Cooper et al., 2012). Ground squirrel platelets stored in the cold show decreased desialylation of surface glycoproteins and decreased phagocytosis by hepatocytes. They also appear to be resistant to induction of apoptosis as measured by caspase activation and surface phosphatidylserine on platelet membranes (Splinter et al., 2023). These adaptations of hibernator platelets to cold storage are consistent with their storage and release after weeks of cold storage during torpor and likely add to the rapid restoration of a hibernator's ability to form clots upon arousal.

Platelets are anucleate cells and their protein content is determined primarily by progenitor megakaryocytes in the bone marrow. Surprisingly, a bone marrow transcriptome of samples collected in the fall, winter, and summer from 13-lined ground squirrels revealed no significant differences in any platelet protein transcripts, including P-selectin, membrane receptors, and integrins (Cooper et al., 2016). The platelet proteome collected in the same species and at the same times of the year, also displayed no differences in integrins and signaling proteins, but did reveal significant seasonal differences in other proteins (Cooper et al., 2021). In the summer, platelets have increased heat shock proteins which could help with proper protein folding at warm temperatures. In the fall, as animals are going through short bouts of shallow torpor, pro-inflammatory and clotting proteins become less abundant in platelets. During torpor, more plasma-derived proteins such as albumin and lipoproteins are present in platelets which are known to inhibit apoptosis and thrombosis (Cooper et al., 2021). A very recent platelet proteome study on brown bears showed a 55-fold decrease in the heat shock protein HSP47 (SerpinH1) during hibernation (Thienel et al., 2023). This decrease correlated with a decline in DVT formation during prolonged immobilization, and was also demonstrated in humans, pigs, and knock-out mice. Interestingly, and in sharp contrast, a previous study of 13-lined ground squirrel platelet proteome documented unchanged HSP47 abundance across various phases of hibernation (Cooper et al., 2021). This marked difference in Hsp47 regulation could be due to bears being shallow hibernators and also of greater body mass compared to ground

TABLE 1 Primary hemostasis in hibernation.

Measurement	Euthermia	Torpor	Arousal	Species	References
Whole-blood clotting time					
(sec)	210 ± 76	315 ± 66*		13-lined ground squirrel	Lechler and Penick (1963)
(min)	2.2 ± 0.3	48.0 ± 5.4*	11.5 ± 1.5*,#	Franklin's ground squirrel	Pivorun and Sinnamon (1981)
(min)	4	11	5	Hedgehog	Biorck et al. (1962)
(sec)	81 ± 12	217 ± 30	164 ± 33	American black bear	Iles et al. (2017)
Thromboelastography					
R (min)	1.6 ± 0.4	16.2 ± 12.3*	4.7 ± 1.2*,#	13-lined ground squirrel	Cooper et al. (2012)
Alpha (°)	58.8 ± 11.3	6.6 ± 6.2*	17.1 ± 7.4*,#	13-lined ground squirrel	Cooper et al. (2012)
Maximum amplitude (mm)	47.2 ± 5.2	6.0 ± 6.8*	17.2 ± 10.4*,#	13-lined ground squirrel	Cooper et al. (2012)
G (dynes/cm^2)	4.6 ± 1.0	0.3 ± 0.4*	1.1 ± 0.8*,#	13-lined ground squirrel	Cooper et al. (2012)
Platelet aggregation (arbitrary units)					
ADP	70.0 ± 26.6	29.2 ± 8*		Scandinavian brown bear	Arinell et al. (2018)
	66 ± 23	33 ± 10*		Scandinavian brown bear	Arinell et al. (2018)
Arachidonic acid	73 ± 16	28 ± 9*		Scandinavian brown bear	Arinell et al. (2018)
	68 ± 20	33 ± 10*		Scandinavian brown bear	Arinell et al. (2018)
Collagen	68.3 ± 17	30.7 ± 10		Scandinavian brown bear	Arinell et al. (2018)
	63 ± 22	30 ± 7*		Scandinavian brown bear	Arinell et al. (2018)
TRAP	18.5 ± 10.0	9.2 ± 6.9*		Scandinavian brown bear	Arinell et al. (2018)
PAR-4	22.5 ± 7.1	12.7 ± 7.1*		Scandinavian brown bear	Arinell et al. (2018)
Platelet count					
(x 10^9/L)	445.2 ± 123.4 36.3°C	47.9 ± 22.3* 7.9°C		13-lined ground squirrel	Lechler and Penick (1963)
	303.6 ± 10.6 37°C	45 ± 3.4* 6°C	232.4 ± 19.7*,# 37°C	Franklin's ground squirrel	Pivorun and Sinnamon (1981)
	375.3 ± 40.8 37°C	114.2 ± 36.0* 9°C	217.0 ± 35.9*,# 37°C	Daurian ground squirrel	Hu et al. (2017)
	293 ± 81 36°C	44 ± 30.9* 8°C	194 ± 5*,# 35°C	European ground squirrel	Bouma et al. (2010)
		23.3 ± 1.3* 9.8°C	410.9 ± 59.2 36°C	13-lined ground squirrel	Cooper et al. (2012)
	394 ± 157	55 ± 30*		13-lined ground squirrel	Reddick et al. (1973)
	451 ± 87 35.5°C	128 ± 81 9.8°C	498 ± 144 36.4°C	13-lined ground squirrel	Cooper et al. (2017)
	797 ± 124 35°C	381 ± 239* 25°C	739 ± 253# 35°C	Djungarian hamster	de Vrij et al. (2014)
	198 ± 6 35°C	8 * 8°C	187# 35°C	Syrian hamster	de Vrij et al. (2014)
	430 ± 82 35.7°C	36 ± 17* 8.2°C	468 ± 100 35.4°C	Syrian hamster	de Vrij et al. (2021)
	207 ± 24			Scandinavian brown bear	Fröbert et al. (2010)
	262 ± 61 40°C	174 ± 51* 33°C	262 ± 61	Scandinavian brown bear	Arinell et al. (2018)
	229 ± 39	146 ± 47*		Scandinavian brown bear	Arinell et al. (2018)
	228 ± 36 37°C	149 ± 43* 32°C		Scandinavian brown bear	Welinder et al. (2016)

(Continued on following page)

TABLE 1 (*Continued*) **Primary hemostasis in hibernation.**

Measurement	Euthermia	Torpor	Arousal	Species	References
(%EU)	100% ± 31% (n = 19) 34°C	65% ± 29% * (n = 12) 26°C	111% ± 26% (n = 13) 33°C	Daily torpor C57Bl/6 Mouse	(De Vrij et al. unpublished)
(10^2/mm^3 Mean ± SE)	5.6 ± 0.6		6.0 ± 1.1	Common yellow bat	Rashid et al. (2016)
(10^2/mm^3 Mean ± SE)	7.5 ± 1.0		7.4 ± 1.2	Common pipistrelle bat	(Rashid et al., 2016)
P-selectin expressing platelets (%)	8 ± 7	0	7 ± 6	Syrian hamster	de Vrij et al. (2014)
	3 ± 1	11 ± 7	10 ± 3	Syrian hamster	de Vrij et al. (2021)
Platelets activated by ADP (%)	16 ± 14	16 ± 6	29 ± 6	Syrian hamster	de Vrij et al. (2014)
	22 ± 8	16 ± 2	47 ± 11*,#	Syrian hamster	de Vrij et al. (2021)
VWF (% relative to human plasma)	24.9 ± 3.7	2.4 ± 0.01*		13-lined ground squirrel	Cooper et al. (2016)
(%EU)	100% ± 10.5% (n = 10)	7.3% ± 3.2%* (n = 4)	8.4% ± 11.5%* (n = 4)	Syrian hamster	(De Vrij et al. unpublished)
(IU/mL)	1.7 ± 0.2	1.3 ± 0.2*		Scandinavian brown bear	Welinder et al. (2016)
VWF:collagen binding activity (%EU)	100% ± 10% (n = 7)	35% ± 15% (n = 4)	25% ± 33%* (n = 4)	Syrian hamster	(De Vrij et al. unpublished)

squirrel, so the immobilization puts bears at greater risk of DVT. Moreover, torpid bears have a modest drop in circulating platelets compared to deep hibernators (Figure 4), possibly warranting additional protection against DVT. It would be interesting to look more closely at the inhibition of HSP47 in deep hibernators other than 13 lined ground squirrel to appreciate its role in hibernation. In addition to the decrease in circulating platelet numbers, these proteomic changes could prevent unwanted activation of platelets during stasis or during their storage in liver. While there were no significant differences in the amounts of surface receptors or proteins in signaling pathways at the proteome level, it is possible that the activities of these pathways are altered. Alternatively, some of the proteins may be sequestered in the cytoplasm or secretory granules which could be resolved by immunohistochemical analysis. Studying the phosphoproteome and metabolome of platelets in torpor would help to resolve which pathways are affected.

In recent years, cultured cells from hibernators have demonstrated to hold specific adaptations that confer protection from cooling in a cell-autonomous way (Talaei et al., 2011; Ou et al., 2018; Hendriks et al., 2020). Mechanistically, these studies in hamster cell lines and ground squirrel pluripotent stem cells derived neurons indicate that adaptations in mitochondrial function, allowing cooled cells to maintain ATP production and lower reactive oxygen species production, constitute a key element of cell protection. Given that platelets contain mitochondria, we re-analyzed aforementioned ground squirrel platelet proteome data (Cooper et al., 2021) by separating out mitochondrial proteins. Analysis of the platelet proteins involved in metabolism revealed an increase in 79 proteins with clusters in lipoprotein metabolism, cholesterol esterification, and lipase activity during the winter. With respect to mitochondrial proteins, 24 were increased during the winter relative to summer and fall, with clusters in fatty acid beta-oxidation, the electron transport chain, and protein targeting to the mitochondria (Figure 5). These proteome changes correspond well with changes in most other tissues of hibernators, principally denoting the shift to lipid metabolism during hibernation as animals rely on fat stores for energy. As platelets appear to be no exception, it is conceivable that they hold similar cell autonomous protection from cooling damage as found in hamster and ground squirrel smooth muscle cells, kidney cells and neurons. Interestingly, ground squirrel neurons maintain their tubulin network during cooling by limitation of the production of reactive oxygen species (Ou et al., 2018). Such mechanism may also support tubulin stability and possibly underlie the difference in cooling induced platelet shape change between hibernators (reversible rod formation) and non-hibernators (irreversible sphere formation). Given this clearcut difference in response to cooling and the ease of obtaining primary cells, platelets constitute an important platform for the future study of cell-autonomous adaptations in hibernators.

Secondary hemostasis occurs simultaneously with primary hemostasis forming a fibrin network to trap red and white blood cells and further strengthen the hemostatic platelet plug (Figure 6). Secondary hemostasis occurs via a plasma coagulation cascade divided into the intrinsic and extrinsic pathways. Most clotting factors are serine proteases that are always present in plasma as inactive zymogens (identified by Roman numerals II, VII, IX, X, XI, and XII) and are activated by proteolysis (addition of an "a"). Factors V and VIII are non-enzymatic cofactors also activated by proteolysis. The extrinsic pathway starts with exposure and binding of tissue factor (TF) to plasma coagulation factor VII, which forms a TF/VIIa complex. The TF/VIIa complex proteolytically activates factors IX and X, commencing the common pathway, creating a prothrombinase complex with Va that converts prothrombin (factor II) into thrombin (IIa) (Versteeg et al., 2013). Thrombin slowly accumulates during the amplification phase, activating platelets and platelet derived factor V, amplifying the prothrombinase activity. In a positive feedback loop, thrombin activates factor XI and VIII, generating more factor Xa. Hemophilia A and B are defined by deficiencies in factors VIII and IX, respectively, which is associated with spontaneous and prolonged bleeding. The extrinsic pathway can be assayed *in vitro* by measuring the prothrombin time (PT). The intrinsic pathway of coagulation can be triggered independently by collagen, polyphosphates secreted by platelets, neutrophil extracellular

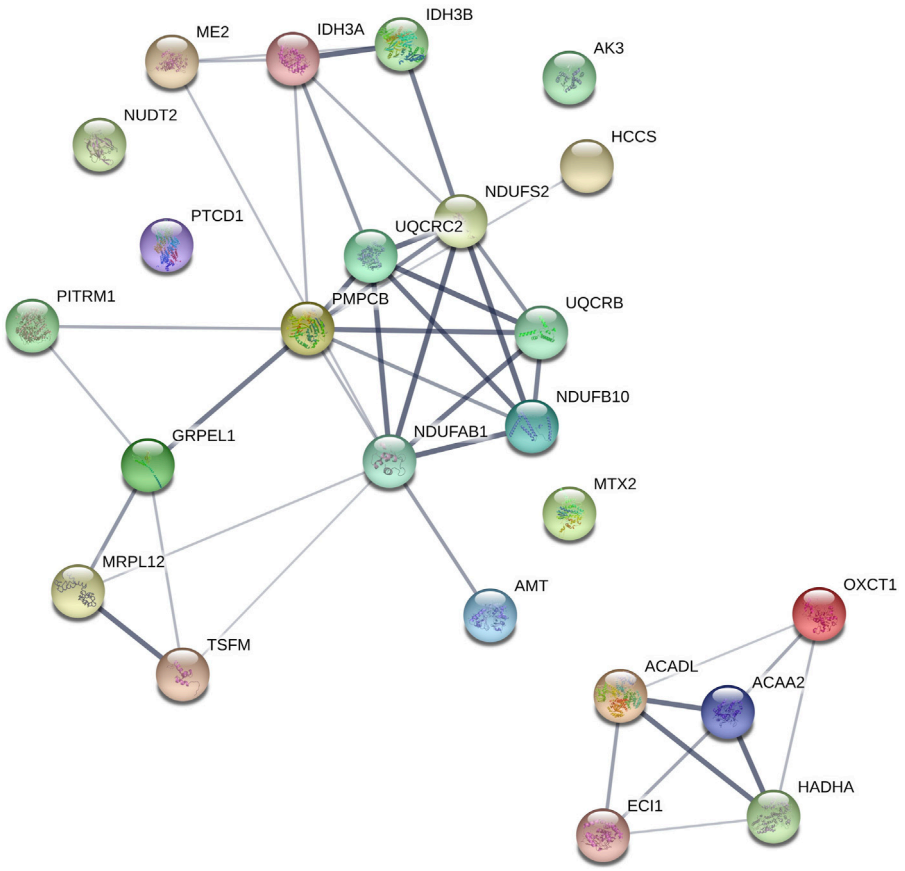

FIGURE 5
Mitochondrial proteins upregulated during winter clustered using STRING. OXCT1 (Succinyl-CoA-3-ketoacid coenzyme A transferase 1), ACADL (Long-chain specific acyl-CoA dehydrogenase), PMPCB (Mitochondrial-processing peptidase subunit beta), MTX2 (Metaxin-2); GRPEL1 (GrpE protein homolog 1), UQCRC2 (Cytochrome b-c1 complex subunit 2), NDUFB10 (NADH dehydrogenase [ubiquinone] 1 beta subcomplex subunit 10), AMT (Aminomethyltransferase), ACAA2 (3-ketoacyl-CoA thiolase), PTCD1 (Pentatricopeptide repeat-containing protein 1), IDH3 (Alsocitrate dehydrogenase [NAD] subunit alpha), ECI1 (Enoyl-CoA delta isomerase 1), TSFM (Elongation factor Ts), ME2 (NAD-dependent malic enzyme), HCCS (Cytochrome c-type heme lyase), MRPL12 (39S ribosomal protein L12), NDUFS2 (NADH dehydrogenase [ubiquinone] iron-sulfur protein 2), NUDT2 (Bis(5′-nucleosyl)-tetraphosphatase), HADHA (Trifunctional enzyme subunit alpha), IDH3B (Isocitrate dehydrogenase [NAD] subunit beta), PITRM1 (Presequence protease), AK3 (GTP-AMP phosphotransferase AK3), UQCRB (Cytochrome b-c1 complex subunit 7), NDUFAB1 (Acyl carrier protein).

traps (NETs), and artificial material such as glass, leading to activation of factors XII, XI, kallikrein and the subsequent downstream coagulation factors (Muller et al., 2009; Versteeg et al., 2013). The intrinsic pathway can be assessed *in vitro* by measuring the activated partial thromboplastin time (APTT).

Secondary hemostasis adaptations during torpor

Secondary hemostasis is reduced during torpor in ground squirrels, bears, hedgehogs, and hamsters. In general, hibernating animals in torpor reduce the level of coagulation factors VIII, IX and XI resembling mild hemophilia A, B and C respectively (Denyes and Carter, 1961; Biorck et al., 1962; Lechler and Penick, 1963; Cooper et al., 2016; Welinder et al., 2016). The decreases in factor VIII, IX and XI during torpor in examined hibernating species are on average 78%, 61% and 51%, respectively, compared to euthermic non-hibernating values (Figure 7). Interestingly, the extrinsic pathway of the coagulation cascade remains fairly unaltered during hibernation. A logical explanation could be that thrombosis due to stasis of blood should be prevented, but blood clotting due to tissue damage by an intruder or predator (activating the extrinsic pathway) may still be vital. An alternative explanation is that during torpor, damage to blood vessels is unlikely, so suppressing the extrinsic pathway is not necessary and protection against stasis-induced clots is more important. Remarkably, one clotting factor consistently showed an increase in protein levels during torpor: prothrombin. Possibly, this is caused by a decrease in its normal baseline formation resulting from inhibition of spontaneous, low-level activation of the clotting cascade, thus diminishing the conversion of prothrombin into thrombin (Lechler and Penick, 1963; Welinder et al., 2016). Prothrombin mRNA levels were slightly decreased in the livers of hibernating 13-lined ground squirrels, consistent with this explanation (Gillen et al., 2021). To assess the overall level of activation of clotting, levels of the irreversible complex between thrombin and its inhibitor antithrombin may be used. Thrombin-antithrombin complexes were decreased during hibernation in 13-lined ground squirrels, consistent with suppression of secondary hemostasis (Bonis et al., 2019). An alternative to reducing clotting

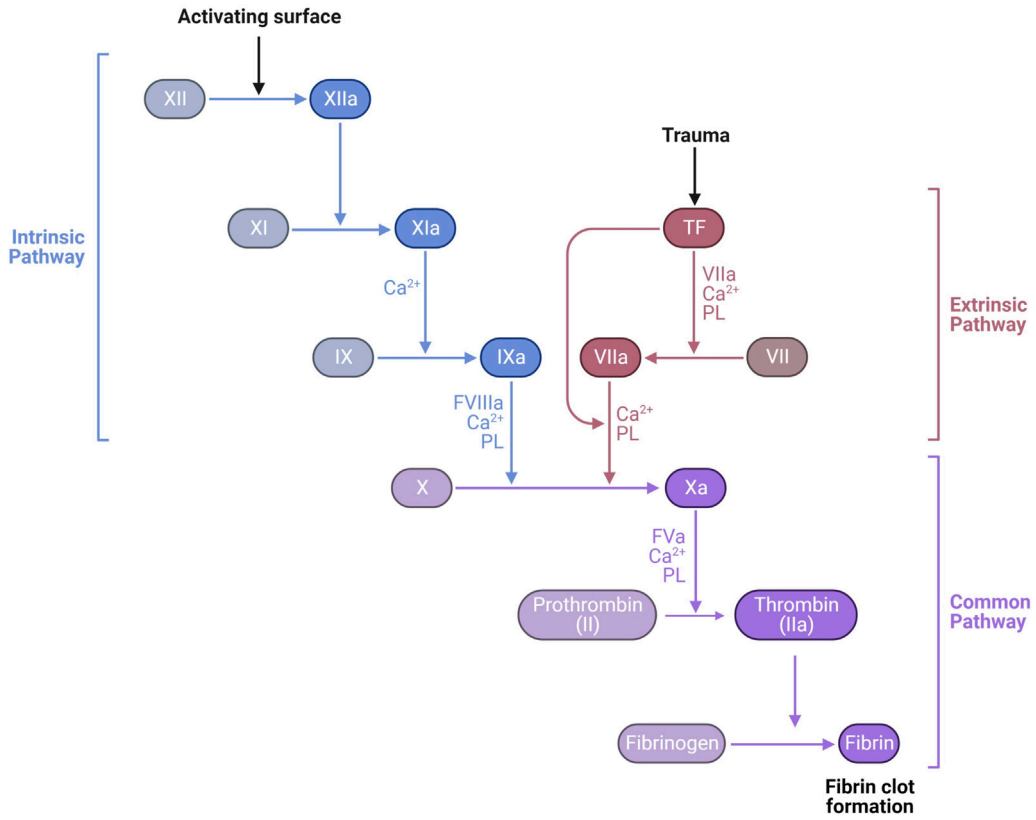

FIGURE 6
Laboratory measurement of the coagulation cascade is divided into the intrinsic pathway, measured by activated partial thromboplastin time (APTT) dependent on factors XII, XI, IX, and VIII, and the extrinsic pathway, measured by prothrombin time (PT) dependent on factor VII. Both APTT and PT also depend on the common pathway factors II (prothrombin), V, X, and fibrinogen. The final product of the common pathway is activation of thrombin (IIa) which cleaves fibrinogen (I) into fibrin (1a) forming a clot https://biorender.com/.

factors would be to increase anticoagulants. Yet, the anticoagulant proteins antithrombin and protein C are not reduced in torpid hamsters and ground squirrels (Bonis et al., 2019). However, in hibernating bears antithrombin levels are reduced, but it is not known if this is due to decreased production of antithrombin or increased consumption (Welinder et al., 2016). Collectively, torpor features the suppression of both the intrinsic and extrinsic arms of the coagulation cascade leading to prolonged APTT times and a mild extension of PT times (Biorck et al., 1962; Lechler and Penick, 1963; Pivorun and Sinnamon, 1981; De Wit et al., 1985; Iles et al., 2017). Diverse hibernators including shallow hibernators (bears), facultative hibernators (hamsters), and deep seasonal hibernators (ground squirrels and bats) use similar adaptations. These common strategies reduce both primary and secondary hemostasis leading to prolonged APTT (Figure 7).

The decreased activities of clotting factors in the blood correlate well with the changes in APTT and PT, however, the differences in protein levels could be due to decreased synthesis or increased consumption during torpor. Many of the blood proteins involved in secondary hemostasis are produced in liver, and a few are released from platelets and endothelial cells. In addition to traditional activity assays, transcriptome, proteome, and metabolomes are being analyzed in liver and plasma to identify changes in hemostatic regulators. The livers of torpid 13-lined ground squirrels revealed decreases in prothrombin, factor V, factor IX, tissue factor, and heparin cofactor II mRNA while VWF mRNA was decreased in bone marrow (Cooper et al., 2016; Gillen et al., 2021). There was also an increase in α2 macroglobulin mRNA in liver during hibernation, a serine protease inhibitor that can inhibit a broad range of clotting factors and its protein level has been previously shown to increase during torpor (Srere et al., 1995), potentially contributing to the suppressed state of hemostasis in torpor. Although these findings are in line with a suppression of hemostasis in torpor, some other studies demonstrate changes that are less unidirectional or involve both procoagulant and anticoagulant factors. For example, clotting factor mRNA expression was unexpectedly decreased in the brains of hibernating Himalayan marmots, but not in their livers (Bai et al., 2019). Another marmot transcriptome study compared two species, but did not look into seasonal variation in expression (Liu et al., 2016). While transcriptomes are useful in measuring new synthesis of proteins, activity in plasma is ultimately estimated by measuring levels of circulating protein which can be detected using proteomics. The bear plasma proteome revealed decreases in clotting factors similar to that reported for individual factor assays with winter increases in α2 macroglobulin, potentially inhibiting thrombin, whereas thrombin itself and fibrinogen were also increased. In contrast, factors VIII and IX and VWF decreased in winter, in line with a suppression of hemostasis, but also the anticoagulant

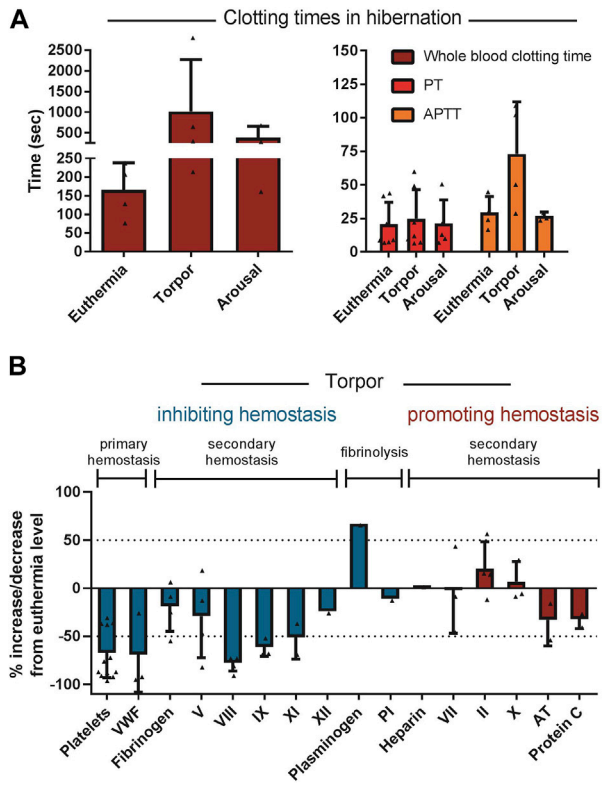

FIGURE 7
Regulation of components of primary hemostasis, secondary hemostasis, and fibrinolysis tilts towards inhibition of hemostasis during torpor. **(A)** Whole blood clotting time and APTT are prolonged during torpor in several species and return to normal during arousal. In contrast, PT is not consistently prolonged. **(B)** All factor levels are normalized as percentage of euthermia level. If a study did not report euthermic level, literature data was used. Data is represented as mean and standard deviation, with each triangle representing the data from an individual study listed in Table 2.

factors antithrombin and protein C decreased (Welinder et al., 2016). An arctic ground squirrel liver proteome also revealed increased α2 macroglobulin but a decrease in antithrombin during torpor (Shao et al., 2010). Finally, a liver proteome of 13-lined ground squirrels showed no seasonal differential expression of proteins involved in hemostasis (Rose et al., 2011). Although all analyzed hibernating mammals demonstrated some suppression within the hemostatic system, there remains some variation between species regarding which factors are involved and whether some procoagulant factors are increased. For the most part proteomic studies seem to align better with assays of individual proteins than do transcriptomic studies. This suggests that protein levels may be regulated more by consumption than transcriptionally. Further analysis of the plasma and liver proteomes may reveal other adaptations that regulate hemostasis.

Fibrinolysis adaptations during torpor

Proteins released from endothelial cells after clot formation initiate fibrinolysis. The cross-linked fibrin network is enzymatically degraded by plasmin, which is formed from plasminogen by tissue plasminogen activator (t-PA). t-PA is slowly released by damaged endothelium enabling a gradual degradation of fibrin after the bleeding has stopped and tissue regeneration has started (Gonias, 2021). A marker of fibrinolysis activation is the level of circulating complexes between tPA and its inhibitor plasminogen activator inhibitor 1 (PAI-1). In ground squirrel torpor, PAI-1 levels are decreased along with tPA-PAI-1 complexes consistent with a hyperfibrinolytic state (Bonis et al., 2019). In ground squirrels, plasminogen levels drop two-fold while in bears and hamsters an increase is seen during torpor. Upon fibrinolysis, fibrin in a clot is cleaved into fibrin degradation products, of which D-dimers can be detected in plasma and is commonly used in the diagnosis of venous or arterial thrombosis. In bears, hamsters, and ground squirrels no increases in D-dimers are seen during hibernation, consistent with low levels of clot formation and fibrinolysis (Iles et al., 2017; Bonis et al., 2019). The lack of D-dimers is consistent with suppression of secondary hemostasis and absence of actual clot fibrinolysis during torpor, while the hyperfibrinolytic state reflected by increased tPA and PAI-1 may be an added layer of protection in the event that a clot does form (Figure 7).

Medical applications

The pathways that prevent activation and clearance of circulating platelets throughout hibernation, key receptors and ligands for platelet margination, and suppression of activation and apoptosis in the cold remain to be determined. Yet, unraveling these pathways could have direct applications in the storage of human platelets. Mimicking the hibernator's platelet resilience to extended cold storage by unlocking their cell-autonomous adaptations might allow long-term cold storage for human platelet transfusion, thus improving transfusion availability and reducing costs. Human red blood cells can be stored in the cold, and research on arctic ground squirrel red blood cells stored in the cold revealed novel protective mechanisms that may be applicable to human red blood cells, but is beyond the scope of this review on hemostasis and hibernation (Gehrke et al., 2019). Additionally, expanding our knowledge about the effects of lower temperature on hemostasis may help understand its role in patients with accidental hypothermia, e.g., near drowning, or those undergoing therapeutic hypothermia. Advancement of these insights will help physicians to better evaluate advantages and disadvantages of therapeutic hypothermia. More applications for therapeutic hypothermia may arise, as mild intraoperative hypothermia may for instance be beneficial in cardiac surgery (Hendriks et al., 2022) and plastic surgery by reducing thrombosis in free tissue transfer, hence improving free flap survival (Liu et al., 2011).

Understanding the mechanisms that hibernators use to prevent activation and clearance of platelets, and prevent thromboembolic complications, may be relevant for other medical applications other than surgery. Pulmonary embolism arising from DVT is a serious medical condition caused by immobilization leading to activation of blood clotting. A study in bears revealed the role of decreased platelet HSP47 in preventing clot formation (Thienel et al., 2023), and this could be translated to humans and other

10.3389/fphys.2023.1207003

TABLE 2 Secondary hemostasis in hibernation.

Measurement	Euthermia (EU)	Torpor	Arousal	Species	References
Thrombin time (sec)	13.2 ± 0.7	15.8 ± 0.7*	14.7 ± 1.3	Franklin's ground squirrel	Pivorun and Sinnamon (1981)
	37°C	6°C	37°C		
PT (sec)	9.8 ± 1.6	10.6 ± 1.5		13-lined ground squirrel	Lechler and Penick (1963)
	36.3°C	7.9°C			
	8.1 ± 0.3	8.3 ± 0.2	14.0 ± 2.1 *,#	Franklin's ground squirrel	Pivorun and Sinnamon (1981)
	37°C	6°C	37°C		
	42.6	60.5	51.2	European Hedgehog	De Wit et al. (1985)
	8.75 ± 0.5			Golden hamster	Deveci et al. (2001)
	41–48	38–62		Red-eared slider (turtle); Painted turtle	Barone and Jacques (1975)
	8.6 ± 0.3	7.6 ± 1.5	8.1 ± 2.2	American black bear	Iles et al. (2017)
	22	23	22	Hedgehog	Biorck et al. (1962)
(%EU)	100% ± 3% (n = 5) 37°C	129% ± 16% * (n = 5) 20°C	110% ± 4%# (n = 5) 35°C	C57Bl/6 pharmacological torpor	(De Vrij et al. unpublished)
(%EU)	100% ± 9% (n = 10)	184% ± 82% (n = 3)	84% ± 6%# (n = 4)	Syrian hamster	(De Vrij et al. unpublished)
	36°C	9°C	37°C		
APTT (sec)	45.5 ± 8.7	109.3 ± 42*		13-lined ground squirrel	Lechler and Penick (1963)
	36°C	8°C			
	25.0 ± 1.0	51.0 ± 2.4*	30.1 ± 1.4#	Franklin's ground squirrel	Pivorun and Sinnamon (1981)
	36°C	6°C	37°C		
	29.8 ± 0.27			Golden hamster	Deveci et al. (2001)
	17.6 ± 0.8	29.7 ± 7.9*	24.5 ± 2.1*	American black bear	Iles et al. (2017)
(%EU)	100% ± 22% (n = 10)	339% ± 88% (n = 3)	86% ± 12%# (n = 4)	Syrian hamster	(De Vrij et al. unpublished)
	36°C	9°C	37°C		
Thrombin generation (%EU)	100% ± 23% (n = 3) 36°C	8% ± 19%* (n = 7) 9°C	61% ± 58% (n = 5) 37°C	Syrian hamster	(De Vrij et al. unpublished)
Prothrombin (U/mL)	443 ± 132 36.3°C	698 ± 143* 7.9°C		13-lined ground squirrel	Lechler and Penick (1963)
(IU/mL)	1.10 ± 0.19	1.29 ± 0.31*		Scandinavian brown bear	Welinder et al. (2016)
(Sec)	11.5 ± 0.3 37°C	11.9 ± 0.3 6°C	10.5 ± 0.3*,# 37°C	Franklin's ground squirrel	Pivorun and Sinnamon (1981)
(U/mL)	20	55	90	Hedgehog	Biorck et al. (1962)
(%EU)	100% ± 10% 36°C	116% ± 20% 9°C	184% ± 15% * 37°C	Syrian hamster	(De Vrij et al. unpublished)
Residual prothrombin in serum (U/mL)	27 ± 38 36°C	449 ± 157* 8°C		13-lined ground squirrel	Lechler and Penick (1963)
Factor II, VII, X combined assay (sec)	12.8 ± 0.4 37°C	14.3 ± 0.6 6°C		Franklin's ground squirrel	Pivorun and Sinnamon (1981)
Factor V	639% ± 212% 36°C	570% ± 143%		13-lined ground squirrel	Lechler and Penick (1963)
		7.9°C			
(Sec)	16.2 ± 0.3	20.1 ± 0.3*	17.8 ± 0.4*,# 37°C	Franklin's ground squirrel	Pivorun and Sinnamon (1981)
	37°C	6°C			

(Continued on following page)

TABLE 2 (*Continued*) Secondary hemostasis in hibernation.

Measurement	Euthermia (EU)	Torpor	Arousal	Species	References
(% human plasma)	450	542	354	Hedgehog	Biorck et al. (1962)
(%EU)	100% ± 44%	20% ± 5% *	72% ± 26%	Syrian hamster	(De Vrij et al. unpublished)
	36°C	9°C	37°C		
Factor VII	369% ± 138% 36°C	536%		13-lined ground squirrel	Lechler and Penick (1963)
		8°C			
	1.01 ± 0.6	0.57 ± 0.14		Scandinavian brown bear	Welinder et al. (2016)
(%EU)	100% ± 15%	93% ± 22%	133% ± 11%	Syrian hamster	(De Vrij et al. unpublished)
	36°C	9°C	37°C		
Factor VIII	165% ± 73% 36°C	35% ± 11%*		13-lined ground squirrel	Lechler and Penick (1963)
		8°C			
(% relative to human plasma)	232 ± 2.0	68 ± 0.1*	230%	13-lined ground squirrel	Cooper et al. (2016)
(IU/mL)	2.92 ± 1.03	0.86 ± 0.35 *		Scandinavian brown bear	Welinder et al. (2016)
(%EU)	100% ± 15%	11% ± 5% *	52% ± 37%	Syrian hamster	(De Vrij et al. unpublished)
	36°C	9°C	37°C		
Factor IX (% human plasma)	378 ± 157	188 ± 65*		13-lined ground squirrel	Lechler and Penick (1963)
	36°C	8°C			
	425 ± 20	140 ± 4.0*	380%	13-lined ground squirrel	Cooper et al. (2016)
(%EU)	100% ± 13%	34% ± 10%	150% ± 23%#	Syrian hamster	(De Vrij et al. unpublished)
	36°C	9°C	37°C		
Factor X	867% ± 126% 36°C	805% ± 269% 8°C		13-lined ground squirrel	Lechler and Penick (1963)
(Sec)	18.9 ± 0.4	18.7 ± 0.7	19.4 ± 0.3	Franklin's ground squirrel	Pivorun and Sinnamon (1981)
	37°C	6°C	37°C		
(%EU)	100% ± 16%	131% ± 30%	138% ± 13%	Syrian hamster	(De Vrij et al. unpublished)
	36°C	9°C	37°C		
Factor XI (%)	111	72		13-lined ground squirrel	Lechler and Penick (1963)
	36°C	8°C			
(%EU)	100% ± 22%	34% ± 14% *	92% ± 31%#	Syrian hamster	(De Vrij et al. unpublished)
	36°C	9°C	37°C		
Factor XII	291% ± 71% 36°C	222% ± 70%		13-lined ground squirrel	Lechler and Penick (1963)
		8°C			
Fibrinogen (mg%)	189 ± 49	145 ± 34		13-lined ground squirrel	Lechler and Penick (1963)
	36°C	8°C			
(g/L)	2.09 ± 0.94	2.26 ± 0.46		Scandinavian brown bear	Welinder et al. (2016)
(%)	0.54	0.5	0.29	Hedgehog	Biorck et al. (1962)
(%EU)	100% ± 20%	45% ± 20%	130% ± 65%#	Syrian hamster	(De Vrij et al. unpublished)
	36°C	9°C	37°C		
Plasminogen (%EU)	100% ± 31% (n = 10)	168% ± 51% (n = 5)	249% ± 51% (n = 5) *		(De Vrij et al. unpublished)

(Continued on following page)

TABLE 2 (*Continued*) **Secondary hemostasis in hibernation.**

Measurement	Euthermia (EU)	Torpor	Arousal	Species	References
(% relative to human plasma)	37.6% ± 9.2%	19.7% ± 12.3%		13-lined ground squirrel	Bonis et al. (2019)
PAI-1 (ng/mL)	2.15 ± 1.04	0.45 ± 0.35		13-lined ground squirrel	Bonis et al. (2019)
Plasmin inhibitor (%EU)	100% ± 5%	89% ± 18%	109% ± 24%	Syrian hamster	(De Vrij et al. unpublished)
	36°C	9°C	37°C		
Protein C (IU/mL)	0.44 ± 0.08	0.33 ± 0.08*		Scandinavian brown bear	Welinder et al. (2016)
(%EU)	100% ± 12%	61% ± 9%	112% ± 14%#	Syrian hamster	(De Vrij et al. unpublished)
	36°C	9°C	37°C		
Antithrombin (IU/mL)	0.98 ± 0.09	0.47 ± 0.04*		Scandinavian brown bear	Welinder et al. (2016)
(%EU)	100% ± 6%	86% ± 11%	104% ± 7.2%	Syrian hamster	(De Vrij et al. unpublished)
	36°C	9°C	37°C		
Heparin (sec)	36.6 ± 0.3 37°C	37.7 ± 0.4		Franklin's ground squirrel	Pivorun and Sinnamon (1981)
		6°C			
D-dimer (ug/L)		152	124	American black bear	Iles et al. (2017)
	15 ± 13	28 ± 32	10 ± 17	Syrian hamster	de Vrij et al. (2021)
	36.3°C ± 0.9°C	8.8°C ± 0.7°C	36.7°C ± 1.1°C		
(%EU)	100% ± 55%	76% ± 22%	80% ± 26%	13-lined ground squirrel	Bonis et al. (2019)

mammals under immobilization. This research could have direct applications in screening patients at risk of DVT with elevated HSP47 and also by developing therapeutic treatments to block HSP47 in immobilized patients. Diffuse intravascular coagulation (DIC) is a severe complication that can arise in critically ill patients. Sepsis, a syndrome of organ failure due to a dysregulated host response to infection, is a common cause of critical illness and DIC. DIC is associated with thromboembolic complications on the one hand and bleeding complications due to consumption of platelets and coagulation factors on the other hand. Therapeutic hypothermia may improve the coagulopathy as measured by thromboelastography in patients with sepsis or septic shock (Johansen et al., 2015), and even decrease mortality and end-organ damage in sepsis as demonstrated experimentally (Acosta-Lara and Varon, 2013). Preventing fever and maintaining normothermia (37°C) by cooling volunteers upon injection of endotoxin, decreases markers of DIC that were induced by endotoxin challenge (Harmon et al., 2021). Yet, therapeutic hypothermia did not lower mortality in sepsis (Itenov et al., 2018).

The use of anticoagulant drugs to prevent thromboembolic complications in high-risk situations after major surgery, in patients with atrial fibrillation, or after a previous unproven thromboembolic event, is associated with bleeding complications as major side effect. Moreover, bleeding is the most common adverse drug event bringing patients to emergency wards (Leendertse et al., 2008; Budnitz et al., 2011) and the newest class of anticoagulants, direct oral anticoagulants (DOAC), are associated with fatal bleeding on 0.16 per 100 patient-years (Chai-Adisaksopha et al., 2015). Therefore bleeding requires correction of anticoagulation as quickly as possible. If a pharmacological tool becomes available to mimic the torpor induced suppression of thrombosis, it may add the benefit of a rapid reversal strategy, since arousal rapidly reverses antithrombotic effects within minutes to hours. However, most reversal techniques require several hours to reverse anticoagulation, i.e., by administering fresh frozen plasma, Vitamin K or prothrombin complex concentrate (Fredriksson et al., 1992; Hanley, 2004). To date, only two registered monoclonal antibody fragments against DOAC are faster and reverse anticoagulation within minutes (White et al., 2022), but are highly expensive. Therefore, the development of new treatment and reversal strategies may help physicians to effectively manage the life-threatening emergency of bleeding in anticoagulated patients (Christos and Naples, 2016). Unraveling the mechanisms driving the hemostatic adaptations in hibernators might contribute to the development of these novel, reversible and safer anticoagulants with lower risk on coagulation abnormalities—even at euthermia—in patients with critical illnesses like sepsis, trauma and after major surgery.

Summary and future research

In spite of the expected risk of thrombosis during hibernation due to prolonged immobility with reduced blood flow and increased blood viscosity, hibernating mammals do not show signs of thrombotic complications during or after hibernation (Figure 8). During torpor in diverse hibernating species of mammals, there is a rapid and reversible anti-thrombotic shift by the reduction in circulating platelets, VWF, and coagulation factors. This results in a mixed phenotype resembling

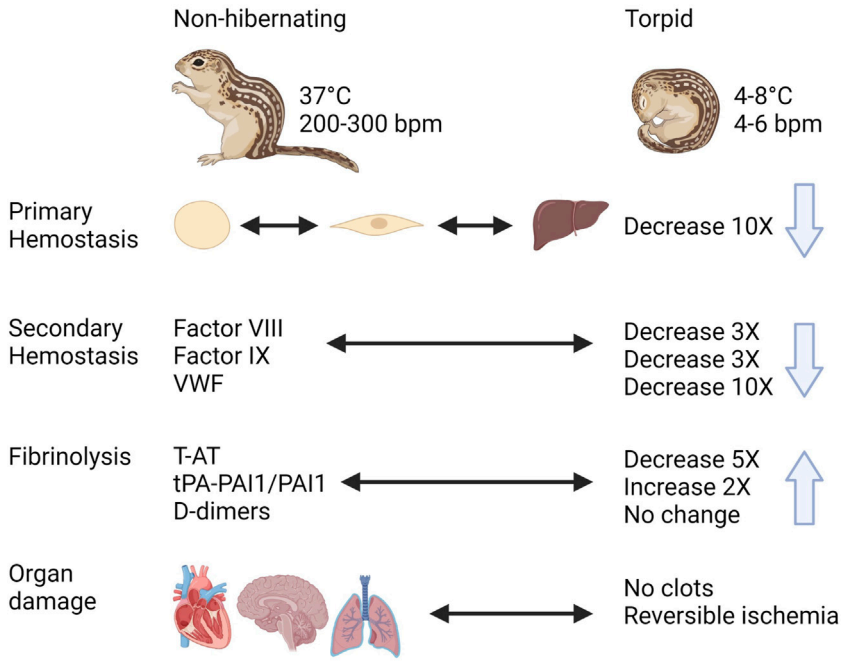

FIGURE 8
Graphical summary of trends in regulation of hemostasis in a hibernating mammal https://biorender.com/.

thrombocytopenia, Von Willebrand Disease, and Hemophilia A, B and C. At the same time, torpid animals maintain factors required for fibrinolysis. One of the most remarkable adaptations is the ability to store platelets in the liver sinusoids during torpor, releasing them intact after prolonged periods of storage in the cold. Future research should use phosphoproteome and metabolomics studies to identify seasonal differences in signaling pathways and molecules released by platelets, in addition to characterizing mitochondrial function. Many common adaptations protect hibernating mammals from unwanted activation of hemostasis during torpor and yet allow for a quick reversal of this state to restore proper hemostasis during arousal. The mechanisms behind these reversible adaptations remain to be discovered and may open doors for novel therapies and improved treatments.

Author contributions

All authors listed have made a substantial, direct, and intellectual contribution to the work and approved it for publication.

Funding

S.T.C. received funding from the National Institutes of Health, USA.

Acknowledgments

We would like to thank T. Lisman and J. Adelmeijer from the Surgical Research Laboratory, Department of Surgery, University of Groningen, University Medical Center Groningen, Groningen, the Netherlands, as well as M. Lukens and R. Mulder from the Department of Laboratory Medicine, University Medical Center Groningen, Groningen, the Netherlands, for their help in measurements from hibernating Syrian hamster and interpretation of these data.

Conflict of interest

The authors declare that the research was conducted in the absence of any commercial or financial relationships that could be construed as a potential conflict of interest.

Publisher's note

References

Acosta-Lara, P., and Varon, J. (2013). Therapeutic hypothermia in sepsis: To use or not to use? *Am. J. Emerg. Med.* 31, 381–382. doi:10.1016/j.ajem.2012.09.017

Ahmad, N., Dube, B., Agarwal, G. P., and Dube, R. K. (1979). Comparative studies of blood coagulation in hibernating and non-hibernating frogs (Rana tigrina). *Thromb. Haemost.* 42, 959–964. doi:10.1055/s-0038-1656986

Arinell, K., Blanc, S., Welinder, K. G., Støen, O. G., Evans, A. L., and Fröbert, O. (2018). Physical inactivity and platelet function in humans and Brown bears: A comparative study. *Platelets* 29, 87–90. doi:10.1080/09537104.2017.1336530

Bai, L., Liu, B., Ji, C., Zhao, S., Liu, S., Wang, R., et al. (2019). Hypoxic and cold adaptation insights from the himalayan marmot genome. *iScience* 11, 519–530. doi:10.1016/j.isci.2018.11.034

Barone, M. C., and Jacques, F. A. (1975). The effects of induced cold torpor and time of year on blood coagulation in Pseudemys scripta elegans and *Chrysemys picta* belli. *Comp. Biochem. Physiol. A Comp. Physiol.* 50, 717–721. doi:10.1016/0300-9629(75)90134-6

Becker, G. A., Tuccelli, M., Kunicki, T., Chalos, M. K., and Aster, R. H. (1973). Studies of platelet concentrates stored at 22 C nad 4 C. *Transfusion* 13, 61–68. doi:10.1111/j.1537-2995.1973.tb05442.x

Berger, G., Hartwell, D. W., and Wagner, D. D. (1998). P-Selectin and platelet clearance. *Blood* 92, 4446–4452. doi:10.1182/blood.v92.11.4446

Biorck, G., Johansson, B. W., and Nilsson, I. M. (1962). Blood coagulation studies in hedgehogs, in a hibernating and a non-hibernating state, and in dogs, hypothermic and normothermic. *Acta Physiol. Scand.* 56, 334–348. doi:10.1111/j.1748-1716.1962.tb02510.x

Bonis, A., Anderson, L., Talhouarne, G., Schueller, E., Unke, J., Krus, C., et al. (2019). Cardiovascular resistance to thrombosis in 13-lined ground squirrels. *J. Comp. Physiology B* 189, 167–177. doi:10.1007/s00360-018-1186-x

Bouma, H. R., Strijkstra, A. M., Boerema, A. S., Deelman, L. E., Epema, A. H., Hut, R. A., et al. (2010). Blood cell dynamics during hibernation in the European Ground Squirrel. *Vet. Immunol. Immunopathol.* 136, 319–323. doi:10.1016/j.vetimm.2010.03.016

Budnitz, D. S., Lovegrove, M. C., Shehab, N., and Richards, C. L. (2011). Emergency hospitalizations for adverse drug events in older Americans. *N. Engl. J. Med.* 365, 2002–2012. doi:10.1056/NEJMsa1103053

Carey, H. V., Andrews, M. T., and Martin, S. L. (2003). Mammalian hibernation: Cellular and molecular responses to depressed metabolism and low temperature. *Physiol. Rev.* 83, 1153–1181. doi:10.1152/physrev.00008.2003

Chai-Adisaksopha, C., Hillis, C., Isayama, T., Lim, W., Iorio, A., and Crowther, M. (2015). Mortality outcomes in patients receiving direct oral anticoagulants: A systematic review and meta-analysis of randomized controlled trials. *J. Thromb. Haemost.* 13, 2012–2020. doi:10.1111/jth.13139

Chan, K. M., and Beard, K. (1993). A patient with recurrent hypothermia associated with thrombocytopenia. *Postgrad. Med. J.* 69, 227–229. doi:10.1136/pgmj.69.809.227

Christos, S., and Naples, R. (2016). Anticoagulation reversal and treatment strategies in major bleeding: Update 2016. *West J. Emerg. Med.* 17, 264–270. doi:10.5811/westjem.2016.3.29294

Cooper, S., Lloyd, S., Koch, A., Lin, X., Dobbs, K., Theisen, T., et al. (2017). Temperature effects on the activity, shape, and storage of platelets from 13-lined ground squirrels. *J. Comp. Physiology B* 187, 815–825. doi:10.1007/s00360-017-1081-x

Cooper, S., Sell, S., Nelson, L., Hawes, J., Benrud, J. A., Kohlnhofer, B. M., et al. (2016). Von Willebrand factor is reversibly decreased during torpor in 13-lined ground squirrels. *J. Comp. Physiol. B* 186, 131–139. doi:10.1007/s00360-015-0941-5

Cooper, S., Wilmarth, P. A., Cunliffe, J. M., Klimek, J., Pang, J., Tassi Yunga, S., et al. (2021). Platelet proteome dynamics in hibernating 13-lined ground squirrels. *Physiol. Genomics* 53, 473–485. doi:10.1152/physiolgenomics.00078.2021

Cooper, S. T., Richters, K. E., Melin, T. E., Liu, Z. J., Hordyk, P. J., Benrud, R. R., et al. (2012). The hibernating 13-lined ground squirrel as a model organism for potential cold storage of platelets. *Am. J. Physiol. Regul. Integr. Comp. Physiol.* 302, R1202–R1208. doi:10.1152/ajpregu.00018.2012

Cooper, S. T., Sell, S. S., Fahrenkrog, M., Wilkinson, K., Howard, D. R., Bergen, H., et al. (2016). Effects of hibernation on bone marrow transcriptome in thirteen-lined ground squirrels. *Physiol. Genomicsphysiolgenomics* 48, 513–525. doi:10.1152/physiolgenomics.00120.2015

D'Alessandro, A., Liumbruno, G., Grazzini, G., and Zolla, L. (2010). Red blood cell storage: The story so far. *Blood Transfus.* 8, 82–88. doi:10.2450/2009.0122-09

de Vrij, E. L., Bouma, H. R., Goris, M., Weerman, U., de Groot, A. P., Kuipers, J., et al. (2021). Reversible thrombocytopenia during hibernation originates from storage and release of platelets in liver sinusoids. *J. Comp. Physiol. B* 191, 603–615. doi:10.1007/s00360-021-01351-3

de Vrij, E. L., Vogelaar, P. C., Goris, M., Houwertjes, M. C., Herwig, A., Dugbartey, G. J., et al. (2014). Platelet dynamics during natural and pharmacologically induced torpor and forced hypothermia. *PLoS One* 9, e93218. doi:10.1371/journal.pone.0093218

De Wit, C. A., Persson, G., Nilsson, I. M., and Johansson, B. W. (1985). Circannual changes in blood coagulation factors and the effect of warfarin on the hedgehog *Erinaceus europaeus*. *Comp. Biochem. Physiol. A* 80, 43–47. doi:10.1016/0300-9629(85)90675-9

DeLong, J. P., Gibert, J. P., Luhring, T. M., Bachman, G., Reed, B., Neyer, A., et al. (2017). The combined effects of reactant kinetics and enzyme stability explain the temperature dependence of metabolic rates. *Ecol. Evol.* 7, 3940–3950. doi:10.1002/ece3.2955

Denyes, A., and Carter, J. D. (1961). Clotting-time of cold-exposed and hibernating hamsters. *Nature* 190, 450–451. doi:10.1038/190450a0

Deveci, D., Stone, P. C., and Egginton, S. (2001). Differential effect of cold acclimation on blood composition in rats and hamsters. *J. Comp. Physiol. B* 171, 135–143. doi:10.1007/s003600000156

Duguid, H., Simpson, R. G., and Stowers, J. M. (1961). Accidental hypothermia. *Lancet* 2, 1213–1219. doi:10.1016/s0140-6736(61)92588-0

Egidi, M. G., D'Alessandro, A., Mandarello, G., and Zolla, L. (2010). Troubleshooting in platelet storage temperature and new perspectives through proteomics. *Blood Transfus.* 8 (3), s73–s81. doi:10.2450/2010.012S

Fernandez-Moure, J. S., Van Eps, J. L., Cabrera, F. J., Barbosa, Z., Medrano Del Rosal, G., Weiner, B. K., et al. (2017). Platelet-rich plasma: A biomimetic approach to enhancement of surgical wound healing. *J. Surg. Res.* 207, 33–44. doi:10.1016/j.jss.2016.08.063

Fredriksson, K., Norrving, B., and Strömblad, L. G. (1992). Emergency reversal of anticoagulation after intracerebral hemorrhage. *Stroke* 23, 972–977. doi:10.1161/01.str.23.7.972

Friedrich, A. U., Kakuturu, J., Schnorr, P. J., Beyer, D. E., Jr., Palesty, J. A., Dickson, E. W., et al. (2017). Comparative coagulation studies in hibernating and summer-active black bears (*Ursus americanus*). *Thromb. Res.* 158, 16–18. doi:10.1016/j.thromres.2017.07.034

Fröbert, O., Christensen, K., Fahlman, A., Brunberg, S., Josefsson, J., Särndahl, E., et al. (2010). Platelet function in Brown bear (*Ursus arctos*) compared to man. *Thromb. J.* 8, 11. doi:10.1186/1477-9560-8-11

Gehrke, S., Rice, S., Stefanoni, D., Wilkerson, R. B., Nemkov, T., Reisz, J. A., et al. (2019). Red blood cell metabolic responses to torpor and arousal in the hibernator arctic ground squirrel. *J. Proteome Res.* 18, 1827–1841. doi:10.1021/acs.jproteome.9b00018

Gillen, A. E., Fu, R., Riemondy, K. A., Jager, J., Fang, B., Lazar, M. A., et al. (2021). Liver transcriptome dynamics during hibernation are shaped by a shifting balance between transcription and RNA stability. *Front. Physiology* 12, 662132. doi:10.3389/fphys.2021.662132

Gonias, S. L. (2021). Plasminogen activator receptor assemblies in cell signaling, innate immunity, and inflammation. *Am. J. Physiol. Cell Physiol.* 321, C721–c734. doi:10.1152/ajpcell.00269.2021

Halikas, G., and Bowers, K. (1973). Seasonal variation in blood viscosity of the hibernating arctic ground squirrel (Spermophilus undulatus plesius). *Comp. Biochem. Physiol. A Comp. Physiol.* 44, 677–681. doi:10.1016/0300-9629(73)90522-7

Hanley, J. P. (2004). Warfarin reversal. *J. Clin. Pathol.* 57, 1132–1139. doi:10.1136/jcp.2003.008904

Harmon, M. B. A., Heijnen, N. F. L., de Bruin, S., Sperna Weiland, N. H., Meijers, J. C. M., de Boer, A. M., et al. (2021). Induced normothermia ameliorates the procoagulant host response in human endotoxaemia. *Br. J. Anaesth.* 126, 1111–1118. doi:10.1016/j.bja.2021.02.033

Hendriks, K. D. W., Castela Forte, J. N., Kok, W. F., Mungroop, H. E., Bouma, H. R., Scheeren, T. W. L., et al. (2022). Mild hypothermia during cardiopulmonary bypass assisted CABG is associated with improved short- and long-term survival, a 18-year cohort study. *PLOS ONE* 17, e0273370. doi:10.1371/journal.pone.0273370

Hendriks, K. D. W., Joschko, C. P., Hoogstra-Berends, F., Heegsma, J., Faber, K. N., and Henning, R. H. (2020). Hibernator-derived cells show superior protection and survival in hypothermia compared to non-hibernator cells. *Int. J. Mol. Sci.* 21, 1864. doi:10.3390/ijms21051864

Hoffmeister, K. M., Felbinger, T. W., Falet, H., Denis, C. V., Bergmeier, W., Mayadas, T. N., et al. (2003). The clearance mechanism of chilled blood platelets. *Cell* 112, 87–97. doi:10.1016/s0092-8674(02)01253-9

Hoffmeister, K. M. (2011). The role of lectins and glycans in platelet clearance. *J. Thromb. Haemost.* 9 (1), 35–43. doi:10.1111/j.1538-7836.2011.04276.x

Horwitz, B. A., Chau, S. M., Hamilton, J. S., Song, C., Gorgone, J., Saenz, M., et al. (2013). Temporal relationships of blood pressure, heart rate, baroreflex function, and body temperature change over a hibernation bout in Syrian hamsters. *Am. J. Physiol. Regul. Integr. Comp. Physiol.* 305, R759–R768. doi:10.1152/ajpregu.00450.2012

Hu, H. X., Du, F. Y., Fu, W. W., Jiang, S. F., Cao, J., Xu, S. H., et al. (2017). A dramatic blood plasticity in hibernating and 14-day hindlimb unloading Daurian ground squirrels (Spermophilus dauricus). *J. Comp. Physiol. B* 187, 869–879. doi:10.1007/s00360-017-1092-7

Iles, T. L., Laske, T. G., Garshelis, D. L., and Iaizzo, P. A. (2017). Blood clotting behavior is innately modulated in *Ursus americanus* during early and late denning relative to summer months. *J. Exp. Biol.* 220, 455–459. doi:10.1242/jeb.141549

Itenov, T. S., Johansen, M. E., Bestle, M., Thormar, K., Hein, L., Gyldensted, L., et al. (2018). Induced hypothermia in patients with septic shock and respiratory failure (CASS): A randomised, controlled, open-label trial. *Lancet Respir. Med.* 6, 183–192. doi:10.1016/S2213-2600(18)30004-3

Jacobs, S. E., Berg, M., Hunt, R., Tarnow-Mordi, W. O., Inder, T. E., and Davis, P. G. (2013). Cooling for newborns with hypoxic ischaemic encephalopathy. *Cochrane Database Syst. Rev.* 2013, CD003311. doi:10.1002/14651858.CD003311

Johansen, M. E., Jensen, J. U., Bestle, M. H., Ostrowski, S. R., Thormar, K., Christensen, H., et al. (2015). Mild induced hypothermia: Effects on sepsis-related coagulopathy--results from a randomized controlled trial. *Thromb. Res.* 135, 175–182. doi:10.1016/j.thromres.2014.10.028

Kirkebo, A. (1968). Temperature effects on the viscosity of blood and the aorta distension from a hibernator, *Erinaceus europaeus* L. *Acta Physiol. Scand.* 73, 385–393. doi:10.1111/j.1365-201x.1968.tb10877.x

Leblanc, R., and Peyruchaud, O. (2016). Metastasis: New functional implications of platelets and megakaryocytes. *Blood* 128, 24–31. doi:10.1182/blood-2016-01-636399

Lebois, M., and Josefsson, E. C. (2016). Regulation of platelet lifespan by apoptosis. *Platelets* 27, 497–504. doi:10.3109/09537104.2016.1161739

Lechler, E., and Penick, G. D. (1963). Blood clotting defect in hibernating ground squirrels (Citellus tridecemlineatus). *Am. J. Physiol.* 205, 985–988. doi:10.1152/ajplegacy.1963.205.5.985

Leendertse, A. J., Egberts, A. C., Stoker, L. J., and van den Bemt, P. M.HARM Study Group (2008). Frequency of and risk factors for preventable medication-related hospital admissions in The Netherlands. *Arch. Intern Med.* 168, 1890–1896. doi:10.1001/archinternmed.2008.3

Liu, Y., Wang, B., Wang, L., Vikash, V., Wang, Q., Roggendorf, M., et al. (2016). Transcriptome analysis and comparison of *Marmota monax* and Marmota himalayana. *PLoS One* 11, e0165875. doi:10.1371/journal.pone.0165875

Liu, Y. J., Hirsch, B. P., Shah, A. A., Reid, M. A., and Thomson, J. G. (2011). Mild intraoperative hypothermia reduces free tissue transfer thrombosis. *J. Reconstr. Microsurg* 27, 121–126. doi:10.1055/s-0030-1268211

Lyman, C. P., and O'brien, R. C. (1960). Circulatory changes in the thirteen-lined ground squirrel during the hibernation cycle. *Bull. Mus. Comp. Zoology* 124, 353–372.

Mahajan, S. L., Myers, T. J., and Baldini, M. G. (1981). Disseminated intravascular coagulation during rewarming following hypothermia. *JAMA* 245, 2517–2518. doi:10.1001/jama.1981.03310490035022

Mallet, M. L. (2002). Pathophysiology of accidental hypothermia. *QJM* 95, 775–785. doi:10.1093/qjmed/95.12.775

Martin, S. L. (2008). Mammalian hibernation: A naturally reversible model for insulin resistance in man? *Diab Vasc. Dis. Res.* 5, 76–81. doi:10.3132/dvdr.2008.013

McArthur, M. D., and Milsom, W. K. (1991). Changes in ventilation and respiratory sensitivity associated with hibernation in columbian (*Spermophilus columbianus*) and golden-mantled (*Spermophilus lateralis*) ground squirrels. *Physiol. Zool.* 64, 940–959. doi:10.1086/physzool.64.4.30157950

Michelson, A. D., Barnard, M. R., Khuri, S. F., Rohrer, M. J., MacGregor, H., and Valeri, C. R. (1999). The effects of aspirin and hypothermia on platelet function *in vivo*. *Br. J. Haematol.* 104, 64–68. doi:10.1046/j.1365-2141.1999.01146.x

Mikhailidis, D. P., and Barradas, M. A. (1993). A patient with recurrent hypothermia associated with thrombocytopenia. *Postgrad. Med. J.* 69, 752. doi:10.1136/pgmj.69.815.752

Morrell, C. N., Murata, K., Swaim, A. M., Mason, E., Martin, T. V., Thompson, L. E., et al. (2008). *In vivo* platelet-endothelial cell interactions in response to major histocompatibility complex alloantibody. *Circ. Res.* 102, 777–785. doi:10.1161/CIRCRESAHA.107.170332

Muller, F., Mutch, N. J., Schenk, W. A., Smith, S. A., Esterl, L., Spronk, H. M., et al. (2009). Platelet polyphosphates are proinflammatory and procoagulant mediators *in vivo*. *Cell* 139, 1143–1156. doi:10.1016/j.cell.2009.11.001

Nieswandt, B., Pleines, I., and Bender, M. (2011). Platelet adhesion and activation mechanisms in arterial thrombosis and ischaemic stroke. *J. Thromb. Haemost.* 9 (1), 92–104. doi:10.1111/j.1538-7836.2011.04361.x

Ou, J., Ball, J. M., Luan, Y., Zhao, T., Miyagishima, K. J., Xu, Y., et al. (2018). iPSCs from a hibernator provide a platform for studying cold adaptation and its potential medical applications. *Cell* 173, 851–863. doi:10.1016/j.cell.2018.03.010

Öztop, M., Özbek, M., Liman, N., Beyaz, F., Ergün, E., and Ergün, L. (2019). Localization profiles of natriuretic peptides in hearts of pre-hibernating and hibernating Anatolian ground squirrels (Spermophilus xanthoprymnus). *Vet. Res. Commun.* 43, 45–65. doi:10.1007/s11259-019-9745-5

Peerschke, E. I., Yin, W., and Ghebrehiwet, B. (2008). Platelet mediated complement activation. *Adv. Exp. Med. Biol.* 632, 81–91. doi:10.1007/978-0-387-78952-1_7

Pivorun, E. B., and Sinnamon, W. B. (1981). Blood coagulation studies in normothermic, hibernating, and aroused Spermophilus franklini. *Cryobiology* 18, 515–520. doi:10.1016/0011-2240(81)90212-1

Polderman, K. H. (2009). Mechanisms of action, physiological effects, and complications of hypothermia. *Crit. Care Med.* 37, S186–S202. doi:10.1097/CCM.0b013e3181aa5241

Rashid, N., Irfan, M., Nadeem, M. S., and Shabbir, A. (2016). Comparative seasonal haematology of two bat species, scotophilus heathii and Pipistrellus pipistrellus, in a subtropical area of Pakistan. *Pak. J. Zoology* 48, 1503.

Reddick, R. L., Poole, B. L., and Penick, G. D. (1973). Thrombocytopenia of hibernation. Mechanism of induction and recovery. *Lab. Invest.* 28, 270–278.

Rohrer, M. J., and Natale, A. M. (1992). Effect of hypothermia on the coagulation cascade. *Crit. Care Med.* 20, 1402–1405. doi:10.1097/00003246-199210000-00007

Rose, J. C., Epperson, L. E., Carey, H. V., and Martin, S. L. (2011). Seasonal liver protein differences in a hibernator revealed by quantitative proteomics using whole animal isotopic labeling. *Comp. Biochem. Physiol. Part D. Genomics Proteomics* 6, 163–170. doi:10.1016/j.cbd.2011.02.003

Semple, J. W., Italiano, J. E., Jr., and Freedman, J. (2011). Platelets and the immune continuum. *Nat. Rev. Immunol.* 11, 264–274. doi:10.1038/nri2956

Shao, C., Liu, Y., Ruan, H., Li, Y., Wang, H., Kohl, F., et al. (2010). Shotgun proteomics analysis of hibernating arctic ground squirrels. *Mol. Cell. proteomics MCP* 9, 313–326. doi:10.1074/mcp.M900260-MCP200

Splinter, N., Mancosky, A., Laffin, C., Clement, M., Nisius, M., Arbs, B., et al. (2023). Platelets from 13lined ground squirrels are resistant to cold storage lesions. *J Comp Physiol B.* 193 (1), 125–134. doi:10.1007/s00360-022-01469-y

Srere, H. K., Belke, D., Wang, L. C., and Martin, S. L. (1995). Alpha 2-Macroglobulin gene expression during hibernation in ground squirrels is independent of acute phase response. *Am. J. Physiol.* 268, R1507–R1512. doi:10.1152/ajpregu.1995.268.6.R1507

Stine, R. J. (1977). Accidental hypothermia. *JACEP* 6, 413–416. doi:10.1016/s0361-1124(77)80007-5

Stolla, M., Bailey, S. L., Fang, L., Fitzpatrick, L., Gettinger, I., Pellham, E., et al. (2020). Effects of storage time prolongation on *in vivo* and *in vitro* characteristics of 4°C-stored platelets. *Transfusion* 60, 613–621. doi:10.1111/trf.15669

Svihla, A., Bowman, H. R., and Ritenour, R. (1951). Prolongation of clotting time in dormant estivating mammals. *Science* 114, 298–299. doi:10.1126/science.114.2960.298

Talaei, F., Bouma, H. R., Hylkema, M. N., Strijkstra, A. M., Boerema, A. S., Schmidt, M., et al. (2012). The role of endogenous H2S formation in reversible remodeling of lung tissue during hibernation in the Syrian hamster. *J. Exp. Biol.* 215, 2912–2919. doi:10.1242/jeb.067363

Talaei, F., Bouma, H. R., Van der Graaf, A. C., Strijkstra, A. M., Schmidt, M., and Henning, R. H. (2011). Serotonin and dopamine protect from hypothermia/rewarming damage through the CBS/H2S pathway. *PLoS One* 6, e22568. doi:10.1371/journal.pone.0022568

Thienel, M., Müller-Reif, J. B., Zhang, Z., Ehreiser, V., Huth, J., Shchurovska, K., et al. (2023). Immobility-associated thromboprotection is conserved across mammalian species from bear to human. *Science* 380, 178–187. doi:10.1126/science.abo5044

Utz, J. C., Nelson, S., O'Toole, B. J., and van Breukelen, F. (2009). Bone strength is maintained after 8 months of inactivity in hibernating golden-mantled ground squirrels, *Spermophilus lateralis*. *J. Exp. Biol.* 212, 2746–2752. doi:10.1242/jeb.032854

Valeri, C. R., MacGregor, H., Cassidy, G., Tinney, R., and Pompei, F. (1995). Effects of temperature on bleeding time and clotting time in normal male and female volunteers. *Crit. Care Med.* 23, 698–704. doi:10.1097/00003246-199504000-00019

Van Der Wal, D. E., Du, V. X., Lo, K. S. L., Rasmussen, J. T., Verhoef, S., and Akkerman, J. W. N. (2010). Platelet apoptosis by cold-induced glycoprotein Ibα clustering. *J. Thrombosis Haemostasis* 8, 2554–2562. doi:10.1111/j.1538-7836.2010.04043.x

Van Poucke, S., Stevens, K., Marcus, A. E., and Lance, M. (2014). Hypothermia: Effects on platelet function and hemostasis. *Thromb. J.* 12, 31. doi:10.1186/s12959-014-0031-z

Vella, M. A., Jenner, C., Betteridge, D. J., and Jowett, N. I. (1988). Hypothermia-induced thrombocytopenia. *J. R. Soc. Med.* 81, 228–229. doi:10.1177/014107688808100414

Versteeg, H. H., Heemskerk, J. W., Levi, M., and Reitsma, P. H. (2013). New fundamentals in hemostasis. *Physiol. Rev.* 93, 327–358. doi:10.1152/physrev.00016.2011

Wang, C. H., Chen, N. C., Tsai, M. S., Yu, P. H., Wang, A. Y., Chang, W. T., et al. (2015). Therapeutic hypothermia and the risk of hemorrhage: A systematic review and meta-analysis of randomized controlled trials. *Med. Baltim.* 94, e2152. doi:10.1097/MD.0000000000002152

Ware, J., Corken, A., and Khetpal, R. (2013). Platelet function beyond hemostasis and thrombosis. *Curr. Opin. Hematol.* 20, 451–456. doi:10.1097/MOH.0b013e32836344d3

Welinder, K. G., Hansen, R., Overgaard, M. T., Brohus, M., Sønderkær, M., von Bergen, M., et al. (2016). Biochemical foundations of health and energy conservation in hibernating free-ranging subadult Brown bear *Ursus arctos*. *J. Biol. Chem.* 291, 22509–22523. doi:10.1074/jbc.M116.742916

White, J. G., and Krivit, W. (1967). An ultrastructural basis for the shape changes induced in platelets by chilling. *Blood* 30, 625–635. doi:10.1182/blood.v30.5.625.625

White, K., Faruqi, U., and Cohen, A. A. T. (2022). New agents for DOAC reversal: A practical management review. *Br. J. Cardiol.* 29, 1. doi:10.5837/bjc.2022.001

Winokur, R., and Hartwig, J. H. (1995). Mechanism of shape change in chilled human platelets. *Blood* 85, 1796–1804. doi:10.1182/blood.v85.7.1796.bloodjournal8571796

Xavier, R. G., White, A. E., Fox, S. C., Wilcox, R. G., and Heptinstall, S. (2007). Enhanced platelet aggregation and activation under conditions of hypothermia. *Thromb. Haemost.* 98, 1266–1275. doi:10.1160/th07-03-0189

Zatzman, M. L. (1984). Renal and cardiovascular effects of hibernation and hypothermia. *Cryobiology* 21, 593–614. doi:10.1016/0011-2240(84)90220-7

frontiers | Frontiers in Physiology

TYPE Original Research
PUBLISHED 28 June 2023
DOI 10.3389/fphys.2023.1214087

OPEN ACCESS

EDITED BY
Jérémy Terrien,
Muséum National d'Histoire Naturelle, France

REVIEWED BY
Fabrice Bertile,
UMR7178 Institut Pluridisciplinaire Hubert Curien (IPHC), France
Sarah Rice,
University of Alaska Fairbanks, United States

*CORRESPONDENCE
Matthew T. Andrews,
matt.andrews@nebraska.edu

RECEIVED 28 April 2023
ACCEPTED 15 June 2023
PUBLISHED 28 June 2023

CITATION
Heinis FI, Alvarez S and Andrews MT (2023), Mass spectrometry of the white adipose metabolome in a hibernating mammal reveals seasonal changes in alternate fuels and carnitine derivatives. *Front. Physiol.* 14:1214087. doi: 10.3389/fphys.2023.1214087

Mass spectrometry of the white adipose metabolome in a hibernating mammal reveals seasonal changes in alternate fuels and carnitine derivatives

Frazer I. Heinis[1], Sophie Alvarez[2] and Matthew T. Andrews[1]*

[1]School of Natural Resources, University of Nebraska-Lincoln, Lincoln, NE, United States, [2]Proteomics and Metabolomics Facility, Nebraska Center for Biotechnology, University of Nebraska-Lincoln, Lincoln, NE, United States

Mammalian hibernators undergo substantial changes in metabolic function throughout the seasonal hibernation cycle. We report here the polar metabolomic profile of white adipose tissue isolated from active and hibernating thirteen-lined ground squirrels (*Ictidomys tridecemlineatus*). Polar compounds in white adipose tissue were extracted from five groups representing different timepoints throughout the seasonal activity-torpor cycle and analyzed using hydrophilic interaction liquid chromatography-mass spectrometry in both the positive and negative ion modes. A total of 224 compounds out of 660 features detected after curation were annotated. Unsupervised clustering using principal component analysis revealed discrete clusters representing the different seasonal timepoints throughout hibernation. One-way analysis of variance and feature intensity heatmaps revealed metabolites that varied in abundance between active and torpid timepoints. Pathway analysis compared against the KEGG database demonstrated enrichment of amino acid metabolism, purine metabolism, glycerophospholipid metabolism, and coenzyme A biosynthetic pathways among our identified compounds. Numerous carnitine derivatives and a ketone that serves as an alternate fuel source, beta-hydroxybutyrate (BHB), were among molecules found to be elevated during torpor. Elevated levels of the BHB-carnitine conjugate during torpor suggests the synthesis of beta-hydroxybutyrate in white adipose mitochondria, which may contribute directly to elevated levels of circulating BHB during hibernation.

KEYWORDS

hibernation, polar metabolites, hypothermia, white adipose, metabolomics, HILIC-MS, ground squirrels

1 Introduction

As an adaptation to inhospitable environmental conditions, mammalian hibernators undergo seasonal heterothermy. Throughout this process, hibernating mammals enter multi-day bouts of torpor (TOR), during which their core body temperature drops to near ambient temperatures, which can be as low as −3°C for Arctic ground squirrels (Barnes, 1989). Hibernating mammals have adapted to survive severe environmental and physiological stresses that would be lethal to individuals not adapted for hibernation, such as the lack of food for up to 5–6 months, prolonged hypothermia, decreases in

metabolic rate, and substantial decreases in heart and respiratory rate (reviewed in Carey et al., 2003; Geiser, 2004). The molecular and physiological adaptations that allow deep hibernators to survive such stresses are of significant biomedical interest (reviewed in Andrews, 2019).

The thirteen-lined ground squirrel (*Ictidomys tridecemlineatus*) is a deep hibernator that does not feed during hibernation and therefore relies on stored calorie reserves. White adipose tissue (WAT) serves as a crucial calorie depot throughout the hibernation season. During the active summer months, ground squirrels gain weight as they store dietary energy as lipids in WAT. WAT mass increases during late summer and early fall when hibernators are near their peak body weight (Schwartz et al., 2015). After the onset of torpor in mid to late fall, WAT mass and adipocyte size progressively decrease as stored triglycerides are mobilized (Florant et al., 2004). During torpor, ground squirrels undergo a shift in metabolism away from the utilization of circulating glucose towards the catabolism of stored fat (Bauer et al., 2001; Buck et al., 2002).

Torpor bouts are interrupted by brief periods of rewarming and activity, termed interbout arousals (IBAs), in which a hibernator warms from near-freezing hypothermia to approximately 37°C for 12–24 h before returning to torpor (Hampton et al., 2010). Although the function of IBAs has not been definitively identified, these regular periods of elevated body temperature and activity may serve several key functions including new mRNA and protein synthesis and turnover; facilitating mobilization of metabolites from tissues into circulation; allow for the conversion of toxic metabolites that accumulated during torpor; and permit chemical reactions to occur that cannot proceed at low temperature (Galster and Morrison, 1975; van Breukelen and Martin, 2001; van Breukelen and Martin, 2002; Prendergast et al., 2002; Epperson et al., 2011; D'Alessandro et al., 2017; Wiersma et al., 2018; Rice et al., 2020).

The circannual cycle of adiposity in hibernating animals, and the role of hibernator WAT in supporting the survival of animals during prolonged starvation, are potentially significant for improving human health and biomedical science. The transcriptome profile of hibernator tissues has been comprehensively studied throughout the seasonal hibernation cycle (Hampton et al., 2011; Hampton et al., 2013; Schwartz et al., 2013; Cooper et al., 2016; Luan et al., 2018). Several groups have previously investigated the metabolome of the hibernator brain (Henry et al., 2007), plasma (Epperson et al., 2011; D'Alessandro et al., 2017), erythrocyte (Gehrke et al., 2019), and liver (Serkova et al., 2007; Nelson et al., 2009) at different times throughout the circannual hibernation cycle. Understanding the ways in which different hibernator organ systems produce, utilize, release, and take up metabolites, and the ways that those processes are influenced by the hibernation cycle, are crucial for understanding hibernator physiology and using that knowledge to improve non-hibernator health, such as a hibernation-based treatment for hemorrhagic shock (Klein et al., 2010; Perez de Lara Rodriguez et al., 2017).

In this study we interrogated the white adipose polar metabolome to evaluate the contribution of this tissue to torpor-associated metabolic changes, and to determine adipose tissue-specific adaptations during hibernation. Rather than a lipidomic study that would focus on hydrophobic calorie-storage molecules such as triacylglycerols, we sought to determine the identity of polar metabolites and their possible role in fuel mobilization throughout the hibernation season. We collected abdominal white adipose tissue at different times during the seasonal hibernation cycle, performed liquid-liquid extraction of WAT samples to enrich for polar compounds, and evaluated those extracts by hydrophilic interaction chromatography-tandem mass spectrometry (HILIC-MS) in both the positive and negative ion modes.

2 Materials and methods

2.1 Animal care and handling

All animal use in this study was approved by the Institutional Animal Care and Use Committee at the University of Nebraska-Lincoln (UNL Project #1927).

Thirteen-lined ground squirrels were trapped near Lincoln, Nebraska during June, July, and August. Ground squirrels were housed at UNL veterinary facilities under the care of UNL Institutional Animal Care Program veterinary staff. Squirrels were singly housed at 21°C–22°C and 12h–12h light-dark cycle with chow (Envigo #2016) and sunflower seeds available *ad libitum*.

On October 1, room temperature was decreased to 12°C to facilitate the entry to torpor. On November 1, ground squirrels were transferred to new cages with extra bedding material and no food and moved to a 24 h dark environmental chamber at 5°C to facilitate deep torpor. Ground squirrels were housed in this environmental chamber until early March, when they were transferred to new cages at 21°C–22°C with chow and sunflower seeds available *ad libitum* and a 12h–12h light-dark cycle. Water remained available *ad libitum* at all times.

At different times throughout the hibernation season (Table 1; Supplementary Table S1), ground squirrels were transferred to a decapicone restraint and euthanized by rapid decapitation via guillotine for tissue collection. Collection timepoints represented the following points in the hibernation season: September Active (1_SEPT), in mid-September; Fall Torpor (2_OCT), in mid-October; Winter Torpor (3_TOR), in December and January; Interbout Arousal (4_IBA), in December, January, and February; and March Active (5_MAR), in late March. Rectal body temperatures were taken at the time of sacrifice during OCT, TOR, and IBA timepoints from October to February (Table 1). IBA status was determined after animals were placed in torpor conditions by investigator assessment of animal activity and body temperature at the time of sacrifice. In particular, IBA animals display movement not seen in torpid animals. This includes shivering, heavy breathing, body extension, and movement of limbs. These various behaviors can occur at a wide range of body temperatures that were recorded at the time of sacrifice. We cannot determine whether these animals are arousing or entering torpor because they are not telemetered. Ground squirrel tissues were surgically collected after euthanasia and snap-frozen using liquid nitrogen, then stored at −80°C until use. White adipose tissues used in this study were taken from the abdomen. Aliquots of WAT from each animal (N = 47 biological replicates, 87% female, distributed amongst five timepoints, Table 1) were weighed using a chilled aluminum block and transferred to the UNL Proteomics and Metabolomics Facility on dry ice for metabolomics analysis.

TABLE 1 Animal characteristics summary.

Group	1_SEPT	2_OCT	3_TOR	4_IBA	5_MAR	Total
N total	9	9	13	8	8	47
(N male)	1	0	3	2	0	6
Average Body Temp at Sacrifice (T_b, °C)	N/A (Active)	14.3 ± 3.4	5.7 ± 0.3	26.2 ± 13.8	N/A (Active)	N/A
Average Weight at Capture (W_i, g)	144.6 ± 31.4	111.6 ± 21.3	161.0 ± 51.4	117.4 ± 38.6	165.3 ± 11.9	151.9 ± 41.0
Average Weight at Sacrifice (W_f, g)	232.2 ± 42.7	213.6 ± 32.0	176.2 ± 16.5	187.8 ± 33.6	179.4 ± 25.8	196.6 ± 36.4
Average Weight in Late October (W_{oct}, g)	N/A	N/A	199.1 ± 22.5	246.8 ± 48.8	269.4 ± 32.0	231.6 ± 45.1

Summary of ground squirrel characteristics. Detailed information on group assignment, body weight, sex, body temperature, date of collection, and date of sacrifice for all 47 ground squirrels used in this study is located in Supplementary Table S1. Values indicate group mean ± standard deviation for all rows except N total and N male.

2.2 Untargeted metabolomics using liquid chromatography—tandem mass spectrometry (LC-MS/MS) and data analysis

For each animal an aliquot of 150 mg of white adipose tissue was extracted using a chilled solution of water:chloroform:methanol (3:5:12) spiked with 10 µL of 100 µM of CUDA (12-[(cyclohexylcarbamoyl)amino]dodecanoic acid) as internal standard. The samples were disrupted and homogenized by adding two stainless steel beads (SSB 32) using the TissueLyserII (Qiagen, Germantown, MD, United States) at 25 Hz for 8 min. After centrifugation at 16,000 g for 5 min at 4°C, the supernatants were collected and transferred to a new tube. The samples were back extracted using the same solution and the supernatant collected after centrifugation was combined to the first one. To separate the water/methanol phase from the chloroform, a chilled solution of water:chloroform (3:4.5) was added to the supernatant, vortexed and centrifuged for 5 min at 16,000 g at 4°C. The upper phase was transferred to a new tube and dried down using a speed-vac. The pellets were re-dissolved in 15% methanol. Blank tubes were extracted alongside the samples to remove contaminant background from the data analysis. In addition, an aliquot of the samples was pooled to make a quality control (QC) sample which was run every 10 samples and samples were run using a randomized sequence order (Supplementary Table S4) to correct for batch effect.

A HILIC (Hydrophilic Interaction Liquid Chromatography)-MS/MS workflow running on a Vanquish LC system interfaced with a QE-HF mass spectrometer was used to profile the metabolites in negative and positive ion mode, as previously described in (Grzybowski et al., 2022). Data from LC-MS/MS analysis were processed with Compound Discoverer software v3.1 (ThermoFisher Scientific, Waltham, MA, United States) for peak detection, deconvolution, alignment, quantification, normalization, and identification/annotation. The annotation was done using several mass spectral libraries; the Thermo mzCloud library (20,905 entries), the MoNA (MassBank of North America) LC-MS/MS library for positive (98,154 entries) and MS/MS negative (43,457 entries), and in house library created using authentic standards run with the same conditions as the samples. The annotated peaks were manually reviewed for peak shape, chromatogram alignment integrity and MS/MS match. The annotated metabolites (Supplementary Table S2) were classified according to (Schymanski et al., 2014) in accordance with the Metabolomics Standards Initiative guidelines (Sumner et al., 2007). After processing the data as described in the next section, some unknown features (including MS/MS data) with interesting abundance pattern between the different groups were further analyzed using MS-Finder v 3.5 (Tsugawa et al., 2016; Lai et al., 2018), a software for structure elucidation using MS and MS/MS spectra of unknown compounds, and SIRIUS 4 (Dührkop et al., 2019) which integrates CSI:FingerID for searching molecular structure databases.

2.3 Statistical analysis

Feature intensity tables for all compounds were analyzed using MetaboAnalyst 5.0 (https://www.metaboanalyst.ca/). Feature intensity tables were $\log_{10}$ transformed and auto scaled (mean-centered and divided by the standard deviation of each variable). Boxplot representations of annotated feature intensities display group mean (yellow pip), group median (horizontal line), 25th-75th percentiles (box), and 95% confidence interval of the median (whiskers). Boxplots displayed in Figure 3 display $\log_{10}$-transformed and auto scaled feature peak intensity values, and boxplots in the Supplementary Data (Supplementary Figures S2, S3) display both the input feature intensities (original) and normalized intensity values as described for Figure 3. Annotated feature names were trimmed of any notation indicating chirality. Metabolite names were searched using the Human Metabolome Database (https://hmdb.ca/), PubChem (https://pubchem.ncbi.nlm.nih.gov/), and ChemSpider (Royal Society of Chemistry, http://www.chemspider.com/) to identify chemical synonyms of annotated features.

One-way analysis of variance and principal component analysis were calculated separately for features in the positive and negative ion modes. Tukey's HSD test was used to identify between-timepoint differences. One-way ANOVA and Tukey's HSD results were considered significant for $p < 0.05$ after Benjamini–Hochberg FDR correction. A hierarchical clustering heatmap (Figure 2) was generated using a list of annotated metabolites merged from both ion modes. Subgroup analysis for pairwise volcano plots was conducted separately for each ion mode (Figure 5), with a *t*-test threshold for significance of $p < 0.01$ after B-H FDR correction. Pathway and enrichment analysis were conducted using a unified list of annotated compounds corrected for features found in both ion modes and compared against RefMet

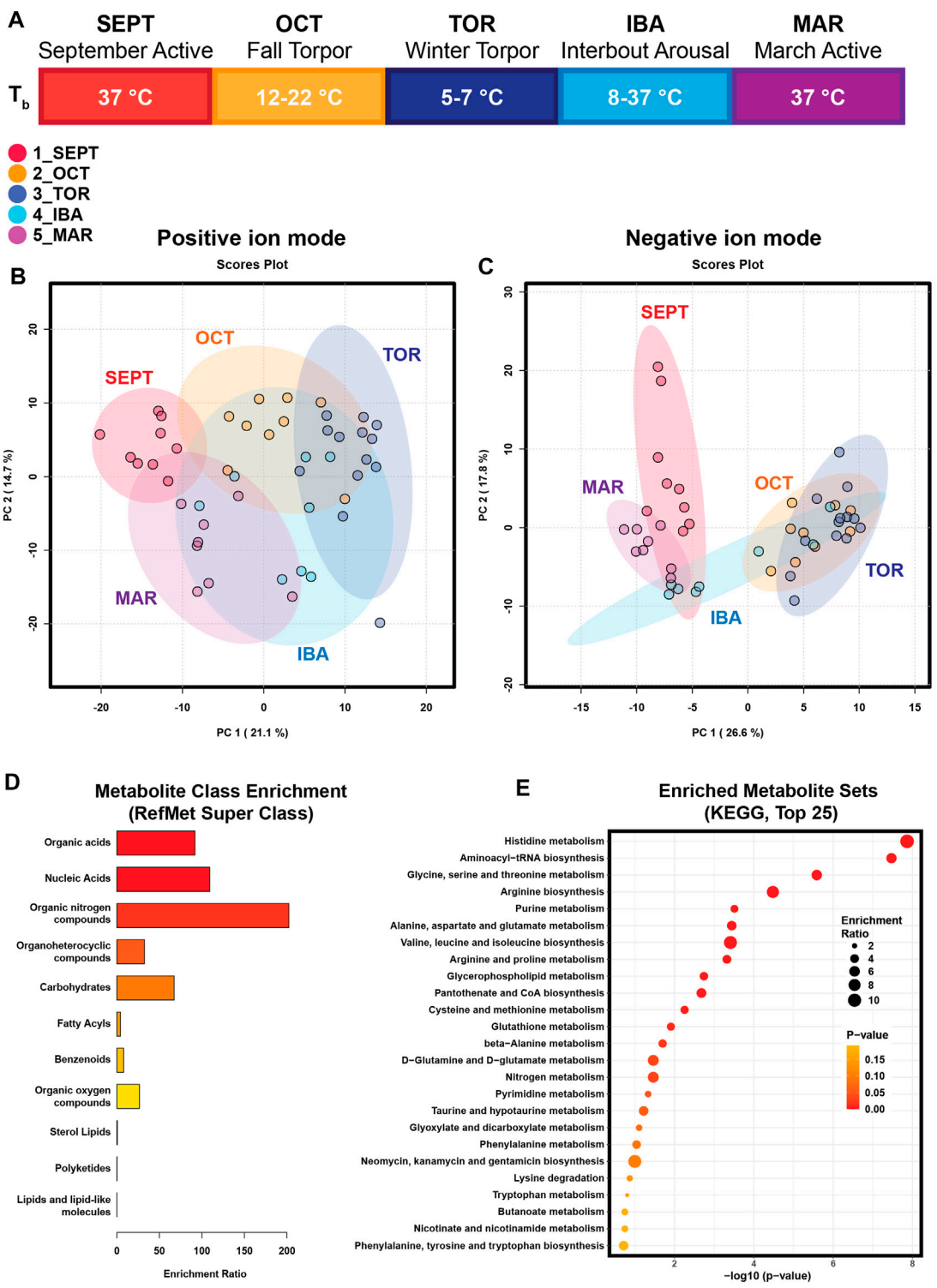

FIGURE 1
Principal Component Analysis and Enrichment Summaries. **(A)** Schematic of the hibernation season and study timepoints. SEPT (September Active); OCT (October, Fall Torpor); TOR (December-February, Winter Torpor); IBA (December-February, Interbout Arousal); MAR (March Active). Body temperatures (Tb) for ground squirrels at these timepoints are indicated. **(B)** Principal Component Analysis of annotated features from positive-mode HILIC MS. **(C)** Principal Component Analysis of annotated features from negative-mode HILIC MS. **(D)** Enrichment analysis output for chemical super-class. Annotated metabolite lists from positive and negative ion modes were combined and submitted to MetaboAnalyst for metabolite class enrichment analysis, compared against Metabolomics Workbench RefMet for chemical Super Class. Enrichment Ratio indicates the ratio of annotated features found to expected. **(E)** Enrichment analysis output for KEGG pathways enriched in annotated white adipose polar metabolites. Annotated metabolite lists were unified and submitted to MetaboAnalyst 5.0 for metabolite pathway enrichment analysis, compared against KEGG metabolic pathways. Enrichment ratio represents the ratio of observed metabolites in a given KEGG pathway to an expected number of observations.

chemical super class (Metabolomics Workbench, https://www.metabolomicsworkbench.org) and KEGG metabolite pathways (https://www.genome.jp/kegg/). Figures were assembled using Illustrator (Adobe) and Prism 9 (GraphPad).

3 Results

To evaluate the WAT metabolome throughout the hibernation season, animals from timepoints corresponding to five conditions in the seasonal progression of hibernation were euthanized for tissue collection (Figure 1A; Table 1; Supplementary Table S1). September Active (1_SEPT) animals were sacrificed in September, during euthermic weight gain. Body temperatures in the Fall Torpor (2_OCT) group ranged from 12°C to 22°C (OCT T_b mean and SD 14.3°C ± 3.4°C), indicating that these animals were entering shallow bouts of torpor in preparation for deep winter torpor. Winter Torpor (3_TOR) body temperatures at sacrifice ranged from 5.2°C to 6.3°C (TOR T_b 5.7°C ± 0.3°C). Interbout arousal (4_IBA) animals had highly variable body temperatures ranging from 8.2°C to 37°C (IBA T_b 26.2°C ± 13.8°C). IBA status was differentiated from TOR at the time of sacrifice by investigators' judgment of body temperature and activity level (see Section 2). March Active (5_MAR) ground squirrels were sacrificed in mid-late March after being returned to normal housing conditions and provided food *ad libitum*.

Body weight at the time of capture for all ground squirrels in this study was 151.9 ± 41.0 g (mean ± SD). Ground squirrels sacrificed in September and October gained an average of 87.7 ± 56.0 g and 102.0 ± 40.8 g total body weight, respectively, from capture to sacrifice. Animals weighed in late October (those in the Torpor, IBA, and March Active groups) weighed 231.6 ± 45.1 g, having gained an average of 64.9 ± 58.8 g after capture. Hibernating ground squirrels progressively lost body mass somewhat proportionate to the time spent in hibernation: ground squirrels sacrificed in December and January (3_TOR) were 22.9 ± 21.5 g lighter at sacrifice than in October; IBA animals sacrificed in December, January, and February were 59.0 ± 34.3 g lighter at sacrifice than October; and March active ground squirrels sacrificed in March were 90.0 ± 38.5 g lighter at sacrifice than in October (Table 1; Supplementary Table S1). High variance in individual weight gain in this cohort may reflect differences in animal age, total time of housing, or animals' acclimation to housing.

WAT samples were extracted via liquid-liquid extraction using chilled water: chloroform: methanol for untargeted profiling of polar metabolites using hydrophilic interaction liquid chromatography-mass spectrometry (HILIC-MS).

A total of 454 features were detected in positive ion mode and 206 in negative ion mode using untargeted HILIC-MS, after manual curation of the data. The log of octanol-water partition coefficient, log K_{ow}, showed a negative correlation when plotted against the retention time of the HILIC-MS metabolites (Supplementary Figure S1) as expected according to (Theodoridis et al., 2023). Amongst the features detected, 166 compounds were annotated in positive-mode analysis and 79 in negative-mode analysis. A total of 21 annotated compounds overlapped between both modes. MS peak intensity lists from positive and negative modes were analyzed separately for ANOVA and principal component analysis rather than being summed or averaged. Compounds annotated in both ion modes were separately included in statistical analysis of both positive and negative ion mode feature lists. Most of the features annotated in both ion modes were either concordant or partially concordant in seasonal intensity profile (Supplementary Figure S5). Only two annotated features, serine and 2-aminonicotinic acid, were non-concordant in seasonal feature intensity profile.

Principal component analysis (PCA) revealed clustering of samples in accordance with seasonal timepoints in both the positive and negative ion modes (Figures 1B, C). In both ion modes, timepoint groups were clustered and adjacent or overlapping with groups of similar activity status: SEPT and MAR active timepoints were adjacent in both ion modes, OCT and TOR groups were adjacent or clustered together, and IBA groups were dispersed relative to the other groups, possibly reflecting a brief normothermic phenotype flanked by multi-day hypothermic torpor bouts. Annotated feature lists from both ion modes were unified and submitted to MetaboAnalyst for chemical class and metabolic pathway enrichment analysis. Metabolite class analysis compared against the Metabolomics Workbench RefMet utility for chemical super class demonstrated enrichment of organic acids, nucleic acids, organic nitrogen compounds, carbohydrates, and organoheterocyclic compounds (Figure 1D). Notably, lipids were mostly absent from the annotated features, suggesting that liquid-liquid extraction and hydrophilic interaction chromatography successfully enriched WAT extracts for polar compounds. Pathway analysis comparing the unified annotated feature list against KEGG metabolic pathways demonstrated enrichment of amino acid metabolism, purine metabolism, phospholipid synthesis, and pantothenate-coenzyme A biosynthetic pathways (Figure 1E).

Amongst annotated features, one-way analysis of variance identified 118 significant features from positive mode and 56 significant features from negative mode. A heatmap representing the hierarchical clustering of the top 100 annotated features from a merged list of both ion modes (as assessed by ANOVA *p*-value) is shown in Figure 2. Boxplots for every annotated feature in this study are separated by ion mode and shown in Supplementary Figures S2, S3. Statistical summary tables including all annotated and unknown HILIC-MS features, separated in tabs by ion mode and analysis type, are located in Supplementary Table S3.

We identified carnitine and twelve acylcarnitine derivatives from positive-mode analysis of the ground squirrel WAT metabolome. Of these, the majority were elevated during torpor and torpor-associated timepoints (Figures 3A–D). Free carnitine remained at consistent levels throughout the seasonal timepoints. Acetylcarnitine, hydroxybutyrylcarnitine, and all medium- and long-chain acylcarnitines were found to be elevated during OCT, TOR, and IBA relative to active timepoints. Only propionylcarnitine and 2-methylbutyrylcarnitine, both short-chain odd-numbered acylcarnitines, were higher during active timepoints relative to OCT and TOR. The coenzyme A precursor, pantothenic acid (vitamin B5) increased in abundance during TOR relative to SEPT and IBA timepoints (Figure 3E).

Alternative fuels such as ketones beta-hydroxybutyrate (BHB) and 2-oxobutyrate, as well as the ketogenic amino acids leucine and isoleucine, were elevated during torpor relative to active timepoints. An increase in 5-hydroxycaproic acid, a medium-chain fatty acid,

10.3389/fphys.2023.1214087

FIGURE 2
Hierarchical Clustering Heatmaps for Top 100 Features. Hierarchical clustering of the top 100 annotated metabolites from a merged list of both positive and negative ion modes, as assessed by one-way ANOVA *p*-value. Groups were not reordered to preserve the seasonal progression of timepoints through hibernation. All biological replicates are shown (sample IDs are displayed at the bottom of each column). Normalized, $\log_{10}$ transformed, and auto scaled feature intensity values ranged from −3 to 3.

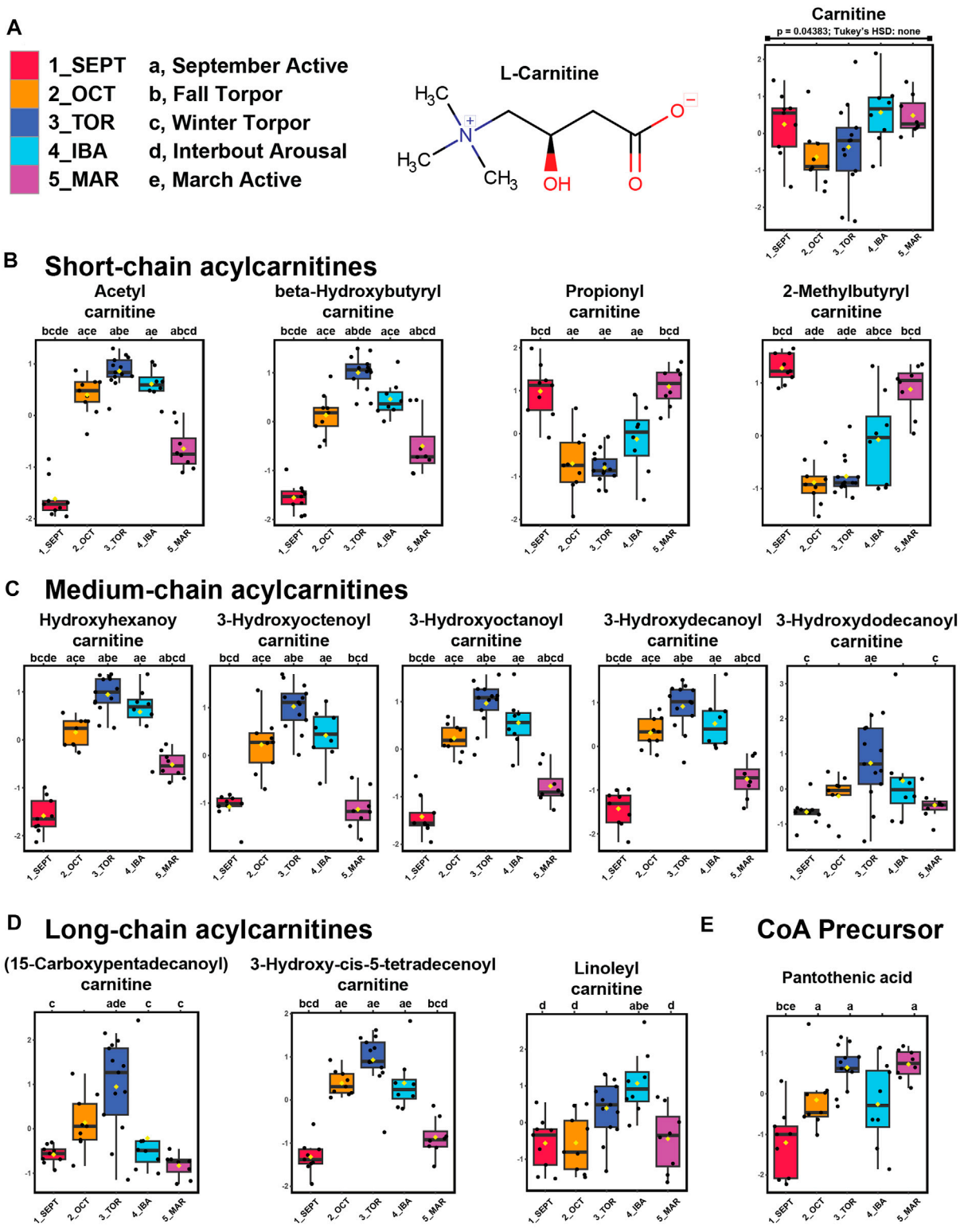

FIGURE 3
Acylcarnitines and pantothenic acid are elevated in WAT during torpor. Feature intensity boxplots of carnitine, short-chain acylcarnitines, medium-chain acylcarnitines, long-chain acylcarnitines, and pantothenic acid throughout the hibernation season. Panels: boxplot representations of feature intensity. Normalized feature intensities were $\log_{10}$ transformed and auto scaled (mean-centered and divided by the standard deviation of each variable). Yellow pip: mean; horizontal central line: median; boxes: 25th-75th percentiles; whiskers: 95% confidence interval of the median. Boxplot Y-axes represent the fold change of feature intensity after $\log_{10}$ transformation and auto scaling. Statistical marks: each timepoint is assigned a letter from a through e in seasonal order: SEPT = a; OCT = b; TOR = c; IBA = d; MAR = e (Figure 3A). Significant Tukey's HSD results ($p < 0.05$) between groups are indicated by the presence of the opposing group letter(s) over each boxplot position. Supplementary Table S3 contains comprehensive ANOVA and
(*Continued*)

FIGURE 3 (Continued)
Tukey's results for all features. **(A–D)** Most acylcarnitines except propionyl- and 2-methylbutyrylcarnitine increased in abundance during October fall torpor, winter torpor, and interbout arousal timepoints. **(E)** The coenzyme A precursor, pantothenic acid, was elevated during OCT, TOR, and MAR relative to SEPT.

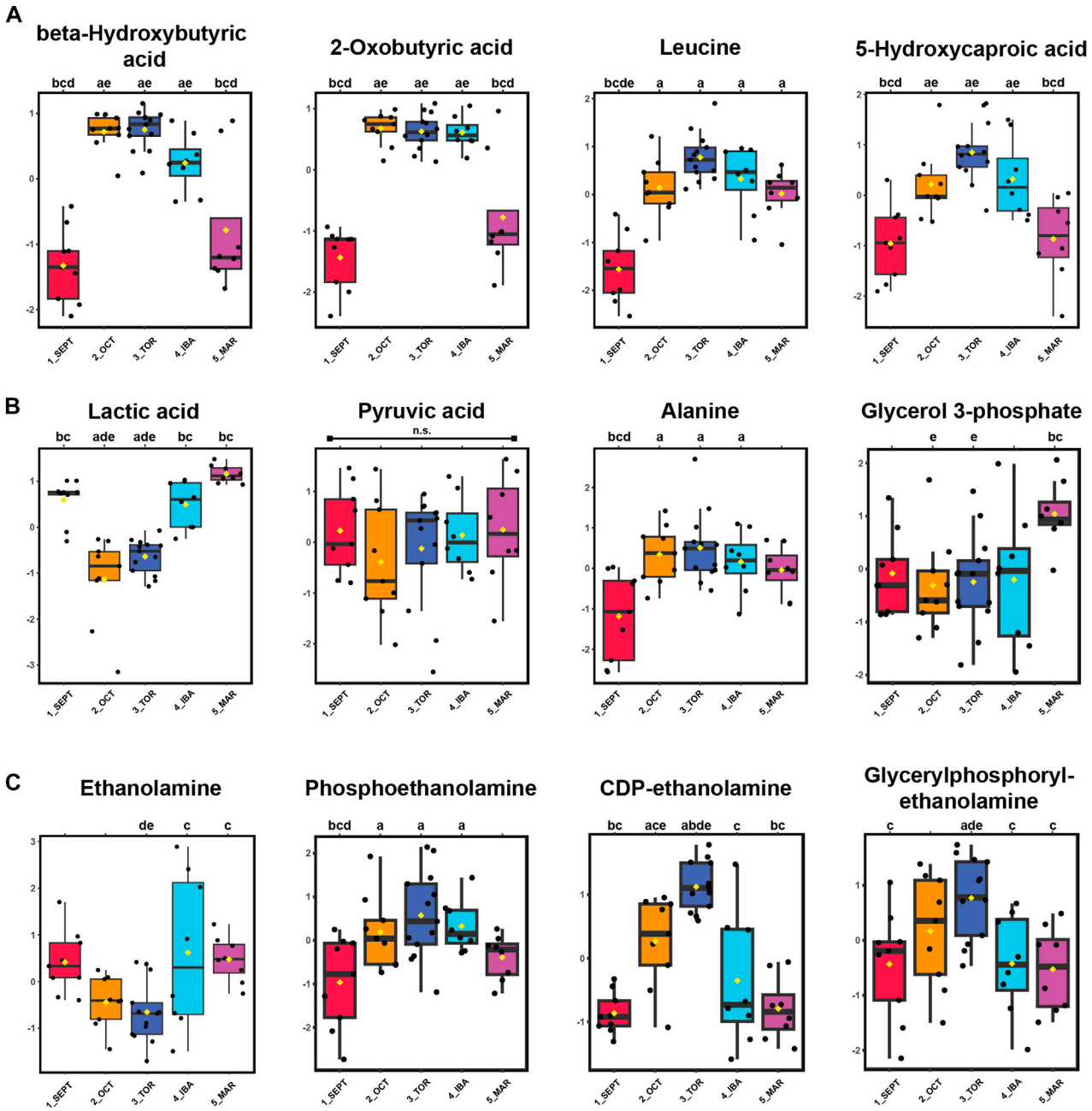

FIGURE 4
Ketones, Ketogenic Amino Acids, and Glycerophospholipid Precursors are Elevated in WAT During Torpor. Panels: $\log_{10}$ transformed and auto-scaled boxplot representations of feature intensity, as in Figure 3. Statistical marks: each timepoint is assigned a letter from a through e in seasonal order: SEPT = a; OCT = b; TOR = c; IBA = d; MAR = e. Significant Tukey's HSD results ($p < 0.05$) between groups are indicated by the presence of the opposing group letter(s) over each boxplot position. Supplementary Table S3 contains comprehensive ANOVA and Tukey's results for all features. **(A)** Feature intensity boxplots of ketones, ketogenic metabolites, and medium-chain fatty acids. **(B)** Glycolytic by-products and transamination pathway metabolites. **(C)** Glycerophospholipid precursors.

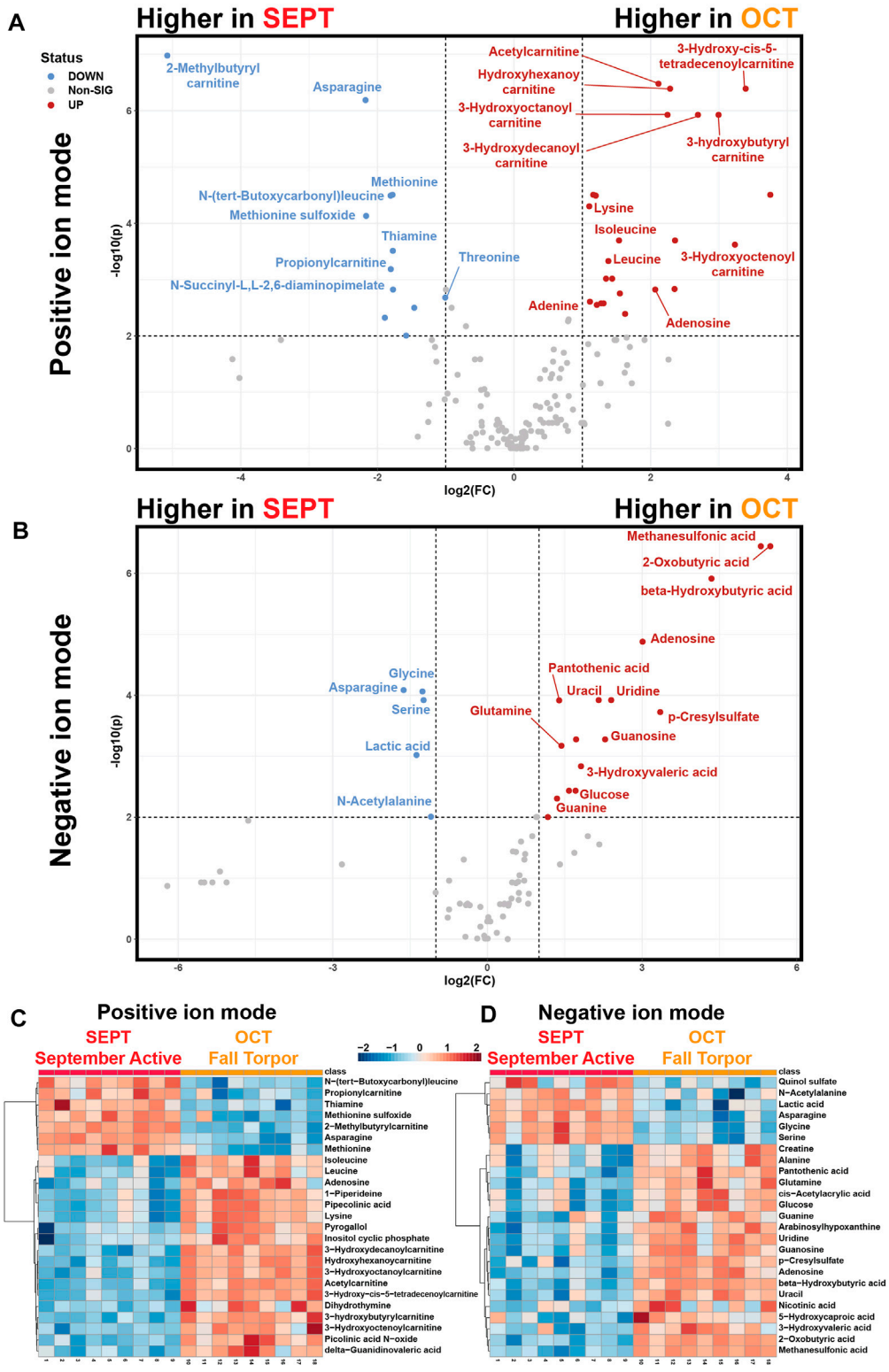

FIGURE 5
Pairwise Comparisons between September Active and Fall Torpor WAT. Pairwise comparison between feature intensities from the September active (SEPT) and fall torpor (OCT) timepoints. **(A)** Positive-mode volcano plot for SEPT vs. OCT. *x*-axis: log2 fold change (FC) of normalized feature intensity. *y*-axis: $-\log_{10}(p)$ from pairwise *t*-test. Significance threshold was set to $p < 0.01$ for pairwise subgroup comparisons. Statistical tables for Figure 5 are included in Supplementary Table S5. Volcano plot is arranged so that features with higher intensity in SEPT are to the left side and features higher in OCT are to the right. **(B)** Negative-mode volcano plot for SEPT vs. OCT, as in 5A. **(C)** Positive ion mode heatmap for the pairwise comparison between SEPT and OCT. All biological replicates (1–18) from 1_SEPT and 2_OCT groups are shown. Normalized feature intensity values ranged from −2 to +2. Top 25 features as assessed by *t*-test are shown. **(D)** Negative ion mode heatmap for the pairwise comparison between SEPT and OCT, as in 5C.

during torpor-associated timepoints suggests increased mobilization of intracellular lipids during that time (Figure 4A). Pyruvate abundance remained consistent throughout the hibernation season, whereas its corresponding transamination metabolite, alanine, became elevated during torpor. Lactic acid levels decreased substantially during OCT and TOR timepoints (Figure 4B) and show the opposite profile of BHB and 2-oxobutyrate for those timepoints, indicating decreased glucose utilization and elevated ketone synthesis and/or uptake in WAT during torpor.

Phospholipid precursors ethanolamine, phosphoethanolamine, and CDP-ethanolamine were annotated. CDP-ethanolamine and the phospholipid breakdown product, glycerylphosphorylethanolamine, were elevated during torpor relative to active and IBA states (Figure 4C). For the fifteen alpha-amino acids identified in this study, most were elevated during torpor-associated timepoints except for glutamic acid, aspartic acid, asparagine, and methionine, which decreased in abundance during torpor to varying degrees (Supplementary Figures S2, S3). Valine, histidine, arginine, tyrosine, and cysteine were not annotated here, although 1-methylhistidine was found in positive-mode analysis.

Pairwise analysis of neighboring active timepoints (Figure 5, SEPT vs. OCT) showed that short- and medium-chain acylcarnitines, purines, and ketones were elevated during fall torpor relative to late summer active timepoints (Figures 5A, B). Asparagine, glycine, serine, lactic acid, and odd-numbered short-chain acylcarnitines were less abundant in OCT relative to SEPT. Glucose was more abundant in OCT WAT samples, coinciding with the shift away from circulating glucose utilization in torpor (Buck et al., 2002). Heatmaps representing the top 25 annotated metabolites assessed by *t*-test for each MS ion mode are shown in Figures 5C, D. Volcano plot tables including both annotated and unknown features are located in Supplementary Table S3.

4 Discussion

As the main fat storage depot, white adipose tissue (WAT) provides hibernating mammals with a reliable source of energy to survive prolonged periods of starvation and near-freezing body temperatures (Florant et al., 1990; Florant et al., 2004; Dark, 2005). Energy is stored in WAT as triacylglycerol molecules that contain three fatty acid chains. Several hibernating species rely on these lipid stores to meet their energy needs in the absence of feeding over a span of several months. This exclusive reliance on WAT over a 4–5-month period demands a tissue that has the versatility to release carbon compounds that can be used as fuel in multiple organs over a wide range of body temperatures.

To identify molecules that facilitate WAT function and serve as part of the supply chain from triacylglycerol stores to a mobilized fuel source, we used a metabolomic approach to identify polar metabolites in ground squirrels at five points throughout the hibernation season. Our findings show that ground squirrel WAT is an active metabolic organ that may contribute to whole-body metabolism in addition to serving as a source of circulating glycerol and non-esterified fatty acids. We found that fatty acid beta-oxidation precursors, in the form of varying acylcarnitines and coenzyme A precursors, were nearly uniformly elevated during fall and winter torpor timepoints.

Conversion of triacylglycerols to non-esterified fatty acids requires the activity of various lipases. To help with this process during torpor, WAT in the thirteen-lined ground squirrel expresses pancreatic triacylglycerol lipase which can liberate fatty acids at temperatures as low as 0°C (Andrews et al., 1998; Bauer et al., 2001; Squire et al., 2003). The unexpected finding of a pancreatic lipase in white adipose over 20 years ago underscores the versatility of ground squirrel WAT and suggests that there could be other novel mechanisms at play. This includes the generation of numerous carnitine derivatives found in this study that can be transported in or out of the mitochondria as fuel for adipocytes, as well as the generation of smaller carbon compounds that be transported and metabolized in other tissues.

We show that alternative fuels such as ketones beta-hydroxybutyrate (BHB) and 2-oxobutyrate, as well as the ketogenic amino acids leucine and isoleucine, were elevated in WAT during torpor relative to active timepoints. Unlike the larger fatty acids from which it is derived, BHB is a 4-carbon carboxylic acid that passes through the blood and provides an alternative fuel to various organs throughout the body (Cuenoud et al., 2020). The D-stereoisomer of BHB is elevated in ground squirrel blood during torpor and is the preferred fuel over glucose in both the brain and heart during hibernation (Andrews et al., 2009). We previously used a proteomic approach (Russeth et al., 2006) to show that the ground squirrel heart increases its capacity to use ketones during hibernation by up-regulating Succinyl CoA transferase (SCOT). SCOT is an important enzyme because it catalyzes the rate-limiting step in ketone metabolism by producing acetoacetyl-CoA, which is further metabolized to form two molecules of acetyl-CoA that enter the TCA cycle and lead to the production of ATP. SCOT mRNA (encoded by the OXCT1 gene) is present in WAT and other ground squirrel tissues throughout the year (Hampton et al., 2013; https://www.d.umn.edu/~mhampton/GB18.html).

The formation of ketones such as BHB was originally thought to occur exclusively in the liver of mammals. However, it was recently shown in mice that WAT can directly produce and secrete BHB (Nishitani et al., 2022). Our finding that BHB, BHB-carnitine, and ketogenic amino acids are elevated in the WAT metabolome during torpor suggests an alternate mechanism to produce BHB and support whole-body organ function in the absence of feeding during hibernation (Figure 6). The direct formation of BHB in WAT dispenses with a sole reliance on liver ketogenesis and provides an alternative source of this important 4-carbon fuel that can cross the blood-brain barrier and support brain function when brain glycolytic activity has been halted and circulating glucose levels are low (Andrews et al., 2009).

We selected a pairwise comparison between the September Active (SEPT) and Fall Torpor (OCT) timepoints for subgroup analysis (Figure 5). The comparison between these timepoints was particularly interesting, because the timepoints under comparison occurred before and during ground squirrel preparation for deep torpor. SEPT animals were housed at 21°C–22°C room air with food and 12h–12 h light-dark, whereas OCT animals received the same food and light-dark timing, but room air had been decreased to 12°C prior to OCT sacrifice. Throughout the mid-to-late fall season, hibernators are undergoing shallow torpor bouts (Russell et al., 2010), and are approaching or have reached their maximal body weight (Schwartz et al., 2015).

We found that OCT ground squirrel WAT, relative to SEPT, had numerous signs of torpor preparation. Elevated OCT levels of BHB and decreased lactate indicate that torpor-associated metabolic

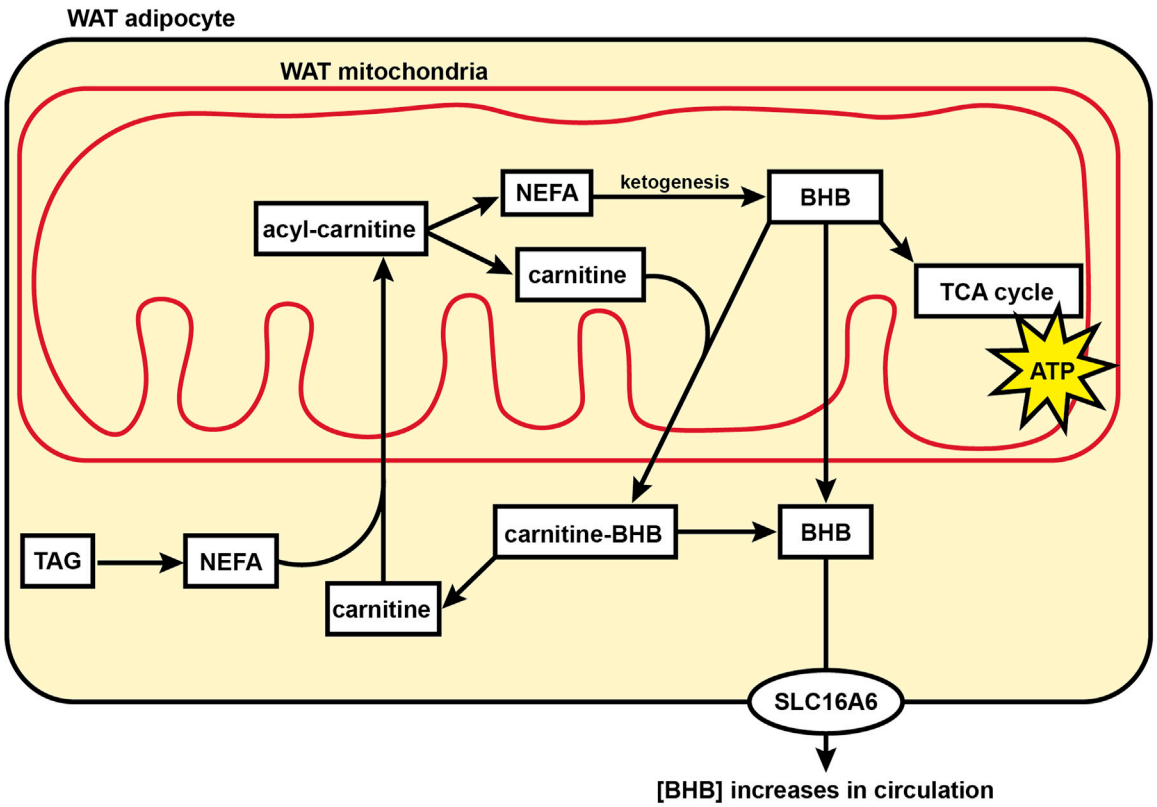

FIGURE 6
Model showing fuel utilization and transport in the mitochondria of hibernator WAT during torpor. During torpor, acylcarnitine content substantially increases for many acyl carbon chain lengths including NEFAs, indicating an increase in mitochondrial acyl carbon import and supporting a transition to fatty acid oxidation for cellular energy supply relative to glucose utilization. BHB levels in WAT increase substantially during torpor, supporting the hypothesis that WAT may be utilized by WAT mitochondria or directly contribute to circulating ketones during torpor. Abbreviations: ATP, adenosine triphosphate; BHB, beta-hydroxybutyrate; NEFA, non-esterified fatty acid; SLC16A6, solute carrier family 16 member 6; TAG, triacylglycerol; TCA cycle, tricarboxylic acid cycle; WAT, white adipose tissue.

changes have been initiated, and we likewise observed an increase in OCT acylcarnitine abundance. Adenosine, also elevated in OCT, is closely associated with the onset of torpor (Jinka et al., 2011). Significant decreases in methionine, methionine sulfoxide, asparagine, and the dietary supplement thiamine may indicate ground squirrel metabolism has shifted towards torpor conditions (D'Alessandro et al., 2017) or that feeding has ceased following the OCT room temperature shift to 12°C.

It is worth noting that the CoA precursor, pantothenate, is generally thought of as a dietary-derived metabolite not synthesized directly in animal tissues (Depeint et al., 2006), yet we observed it to increase during torpor (Figure 3E) when ground squirrels are no longer feeding. Previous metabolomic investigations of ground squirrel plasma likewise found circulating pantothenic acid to be elevated during torpor relative to active timepoints (Nelson et al., 2010; Epperson et al., 2011). Although the precise cause cannot be determined from this study, this may result from pantothenate redistribution from other tissues during torpor. Alternatively, this may reflect activity of the ground squirrel gut microbiome, which has recently been shown to be important for other functions during torpor, including nitrogen recycling (Regan et al., 2022).

Phospholipids and phospholipid precursors were increased in pre-torpor active and winter torpor states (certain ethanolamines, particularly phosphoethanolamine and CDP-ethanolamine, see Figure 4). We hypothesize that these metabolites are incorporated into the growing lipid droplet during summer activity and feeding, and as lipids become mobilized from the WAT lipid droplet during winter torpor, these membrane components become newly available and thus increase in abundance. CDP-ethanolamine and glycerylphosphorylethanolamine levels decreased from TOR to IBA (Figure 4C), which may indicate the consumption and incorporation of these metabolites into new membrane synthesis or other recycling pathways during IBAs. Interestingly, previous liver metabolomics found ethanolamines as well as phosphocholine and phosphatidylcholine to be elevated late in IBAs ("entry to torpor" timepoints in Serkova et al., 2007), which could reflect tissue differences or could be attributable to differences in the specificity with which torpor-arousal timepoints were collected.

We profiled the abundance of fifteen alpha-amino acids (AAs) throughout the hibernation season in WAT (Supplementary Figures S2, S3; Supplementary Tables S2, S3). These AAs followed a variety of abundance patterns throughout hibernation. AAs that increased in abundance from SEPT through OCT into TOR, followed by a decrease in IBA and MAR included glutamine, proline, lysine, leucine, and isoleucine. Asparagine and methionine abundance dropped sharply from SEPT to OCT and TOR, increasing in IBA and MAR. Glycine and threonine abundance decreased from SEPT to OCT, but increased again

in TOR, IBA, and MAR. Other alpha-AAs were found to be present in WAT but had less variation throughout their seasonal abundance profiles. In general, these findings concur with metabolomics analysis from other hibernator tissues including plasma (Epperson et al., 2011; D'Alessandro et al., 2017) and liver (Serkova et al., 2007). The branched-chain amino acids leucine and isoleucine were elevated in OCT, TOR, and IBA relative to SEPT in WAT, which differed from previous findings in liver where these were highest in summer timepoints (Serkova et al., 2007), possibly reflecting tissue differences in branched chain aminotransferase enzyme expression (Gillen et al., 2021).

Several modified amino acids were elevated in TOR relative to other timepoints, including acetylproline and acetylarginine. Previous work on hibernator plasma metabolomics (Epperson et al., 2011) identified acetylated amino acids as elevated in late torpor and the arousal from torpor to activity, followed by decreased abundance in IBAs, and suggested that these metabolites may be selectively salvaged during torpor in order to facilitate their reuse during interbout arousals. Although our annotated acetyl-AAs are distinct from those found in that previous study, they have a comparable abundance pattern and may reflect a similar mechanism in hibernator adipose tissue. This result therefore supports a role for interbout arousals in cellular maintenance during hibernation, as a necessary euthermic period where essential reactions can occur at a permissive temperature.

Further supporting the hypothesis that IBAs support hibernation by enabling cellular maintenance, we annotated several uremic toxins in the hibernator WAT metabolome (e.g., p-Cresylsulfate and N3,N4-dimethylarginine, see Figure 2 and Supplementary Material). These features became strongly elevated during TOR timepoints, with diminished abundance during IBAs. Although these steady-state measurements represent a snapshot in time and do not allow us to define the source and destination for these metabolites, this TOR-IBA abundance pattern suggests that IBAs are important for the clearance or recycling of metabolic by-products. Supporting the findings of Rice et al. (2020), we found urea to be relatively unchanged throughout the hibernation cycle which may indicate either the suppression of the urea cycle during torpor or relative balance in its steady-state inputs and outputs.

Environmental conditions impose extreme demands on the physiology of hibernating animals throughout the circannual hibernation cycle. To survive, hibernators must enact a whole-body hibernation phenotype in which every organ system must adapt and coordinate with the rest of the body. White adipose tissue undergoes some of the most striking changes in its configuration throughout the season, representing the majority of a hibernator's summer weight gain and subsequent winter weight loss. WAT serves a crucial role as a major calorie depot for hibernating animals. Our findings demonstrate that WAT is a highly dynamic organ throughout the hibernation cycle that may contribute more directly to whole-body metabolic regulation than previously recognized.

Data availability statement

The original contributions presented in the study are included in the article/Supplementary Material, further inquiries can be directed to the corresponding author.

Ethics statement

The animal study was reviewed and approved by the Institutional Animal Care and Use Committee at the University of Nebraska-Lincoln.

Author contributions

FH and MA contributed to study conception and design. SA contributed to the sample preparation and acquisition design, data collection and data analysis. FH contributed to data analysis and designed the figures. MA provided funding. All authors contributed to the article and approved the submitted version.

Funding

This project was supported by the University of Nebraska Office of the President and Institute of Agriculture and Natural Resources. The Proteomics and Metabolomics Facility (RRID:SCR_021314), Nebraska Center for Biotechnology at the University of Nebraska-Lincoln and instrumentation are supported by the Nebraska Research Initiative.

Acknowledgments

The authors wish to thank the Institutional Animal Care Program at the University of Nebraska-Lincoln for invaluable veterinary support. We also wish to thank Ashley McMurchie, Kevin Rugira, Eric Tom, and Olivia Schuster. Ashley McMurchie contributed to the model in Figure 6.

Conflict of interest

MA is a co-inventor of technology derived from Klein et al. (2010), and is an advisor for Fauna Bio Inc.

The remaining authors declare that the research was conducted in the absence of any commercial or financial relationships that could be construed as a potential conflict of interest.

Publisher's note

Supplementary material

The Supplementary Material for this article can be found online at: https://www.frontiersin.org/articles/10.3389/fphys.2023.1214087/full#supplementary-material

References

Andrews, M. T. (2019). Molecular interactions underpinning the phenotype of hibernation in mammals. *J. Exp. Biol.* 222, jeb160606. doi:10.1242/jeb.160606

Andrews, M. T., Russeth, K. P., Drewes, L. R., and Henry, P.-G. (2009). Adaptive mechanisms regulate preferred utilization of ketones in the heart and brain of a hibernating mammal during arousal from torpor. *Am. J. Physiol. Regul. Integr. Comp. Physiol.* 296, R383–R393. doi:10.1152/ajpregu.90795.2008

Andrews, M. T., Squire, T. L., Bowen, C. M., and Rollins, M. B. (1998). Low-temperature carbon utilization is regulated by novel gene activity in the heart of a hibernating mammal. *Proc. Natl. Acad. Sci. U. S. A.* 95, 8392–8397. doi:10.1073/pnas.95.14.8392

Barnes, B. M. (1989). Freeze avoidance in a mammal: Body temperatures below 0 degree C in an arctic hibernator. *Science* 244, 1593–1595. doi:10.1126/science.2740905

Bauer, V. W., Squire, T. L., Lowe, M. E., and Andrews, M. T. (2001). Expression of a chimeric retroviral-lipase mRNA confers enhanced lipolysis in a hibernating mammal. *Am. J. Physiology-Regulatory, Integr. Comp. Physiology* 281, R1186–R1192. doi:10.1152/ajpregu.2001.281.4.R1186

Buck, M. J., Squire, T. L., and Andrews, M. T. (2002). Coordinate expression of the PDK4 gene: A means of regulating fuel selection in a hibernating mammal. *Physiol. Genomics* 8, 5–13. doi:10.1152/physiolgenomics.00076.2001

Carey, H. V., Andrews, M. T., and Martin, S. L. (2003). Mammalian hibernation: Cellular and molecular responses to depressed metabolism and low temperature. *Physiol. Rev.* 83, 1153–1181. doi:10.1152/physrev.00008.2003

Cooper, S. T., Sell, S. S., Fahrenkrog, M., Wilkinson, K., Howard, D. R., Bergen, H., et al. (2016). Effects of hibernation on bone marrow transcriptome in thirteen-lined ground squirrels. *Physiol. Genomics* 48, 513–525. doi:10.1152/physiolgenomics.00120.2015

Cuenoud, B., Hartweg, M., Godin, J.-P., Croteau, E., Maltais, M., Castellano, C.-A., et al. (2020). Metabolism of exogenous D-beta-hydroxybutyrate, an energy substrate avidly consumed by the heart and kidney. *Front. Nutr.* 7, 13. doi:10.3389/fnut.2020.00013

D'Alessandro, A., Nemkov, T., Bogren, L. K., Martin, S. L., and Hansen, K. C. (2017). Comfortably numb and back: Plasma metabolomics reveals biochemical adaptations in the hibernating 13-lined ground squirrel. *J. Proteome Res.* 16, 958–969. doi:10.1021/acs.jproteome.6b00884

Dark, J. (2005). Annual lipid cycles in hibernators: Integration of physiology and behavior. *Annu. Rev. Nutr.* 25, 469–497. doi:10.1146/annurev.nutr.25.050304.092514

Depeint, F., Bruce, W. R., Shangari, N., Mehta, R., and O'Brien, P. J. (2006). Mitochondrial function and toxicity: Role of the B vitamin family on mitochondrial energy metabolism. *Chemico-Biological Interact.* 163, 94–112. doi:10.1016/j.cbi.2006.04.014

Dührkop, K., Fleischauer, M., Ludwig, M., Aksenov, A. A., Melnik, A. V., Meusel, M., et al. (2019). Sirius 4: A rapid tool for turning tandem mass spectra into metabolite structure information. *Nat. Methods* 16, 299–302. doi:10.1038/s41592-019-0344-8

Epperson, L. E., Karimpour-Fard, A., Hunter, L. E., and Martin, S. L. (2011). Metabolic cycles in a circannual hibernator. *Physiol. Genomics* 43, 799–807. doi:10.1152/physiolgenomics.00028.2011

Florant, G. L., Nuttle, L. C., Mullinex, D. E., and Rintoul, D. A. (1990). Plasma and white adipose tissue lipid composition in marmots. *Am. J. Physiology-Regulatory, Integr. Comp. Physiology* 258, R1123–R1131. doi:10.1152/ajpregu.1990.258.5.R1123

Florant, G. L., Porst, H., Peiffer, A., Hudachek, S. F., Pittman, C., Summers, A. S., et al. (2004). Fat-cell mass, serum leptin and adiponectin changes during weight gain and loss in yellow-bellied marmots (*Marmota flaviventris*). *J. Comp. Physiol. B* 174, 633–639. doi:10.1007/s00360-004-0454-0

Galster, W., and Morrison, P. R. (1975). Gluconeogenesis in arctic ground squirrels between periods of hibernation. *Am. J. Physiol.* 228, 325–330. doi:10.1152/ajplegacy.1975.228.1.325

Gehrke, S., Rice, S., Stefanoni, D., Wilkerson, R. B., Nemkov, T., Reisz, J. A., et al. (2019). Red blood cell metabolic responses to torpor and arousal in the hibernator arctic ground squirrel. *J. Proteome Res.* 18, 1827–1841. doi:10.1021/acs.jproteome.9b00018

Geiser, F. (2004). Metabolic rate and body temperature reduction during hibernation and daily torpor. *Annu. Rev. Physiol.* 66, 239–274. doi:10.1146/annurev.physiol.66.032102.115105

Gillen, A. E., Fu, R., Riemondy, K. A., Jager, J., Fang, B., Lazar, M. A., et al. (2021). Liver transcriptome dynamics during hibernation are shaped by a shifting balance between transcription and RNA stability. Frontiers in Physiology 12. Available at: https://www.frontiersin.org/articles/10.3389/fphys.2021.662132 (Accessed May 28, 2023).

Grzybowski, M. W., Zwiener, M., Jin, H., Wijewardane, N. K., Atefi, A., Naldrett, M. J., et al. (2022). Variation in morpho-physiological and metabolic responses to low nitrogen stress across the sorghum association panel. *BMC Plant Biol.* 22, 433. doi:10.1186/s12870-022-03823-2

Hampton, M., Melvin, R. G., and Andrews, M. T. (2013). Transcriptomic analysis of Brown adipose tissue across the physiological extremes of natural hibernation. *PLoS One* 8, e85157. doi:10.1371/journal.pone.0085157

Hampton, M., Melvin, R. G., Kendall, A. H., Kirkpatrick, B. R., Peterson, N., and Andrews, M. T. (2011). Deep sequencing the transcriptome reveals seasonal adaptive mechanisms in a hibernating mammal. *PLoS One* 6, e27021. doi:10.1371/journal.pone.0027021

Hampton, M., Nelson, B. T., and Andrews, M. T. (2010). Circulation and metabolic rates in a natural hibernator: An integrative physiological model. *Am. J. Physiol. Regul. Integr. Comp. Physiol.* 299, R1478–R1488. doi:10.1152/ajpregu.00273.2010

Henry, P.-G., Russeth, K. P., Tkac, I., Drewes, L. R., Andrews, M. T., and Gruetter, R. (2007). Brain energy metabolism and neurotransmission at near-freezing temperatures: *In vivo* (1)H MRS study of a hibernating mammal. *J. Neurochem.* 101, 1505–1515. doi:10.1111/j.1471-4159.2007.04514.x

Jinka, T. R., Tøien, Ø., and Drew, K. L. (2011). Season primes the brain in an arctic hibernator to facilitate entrance into torpor mediated by adenosine A(1) receptors. *J. Neurosci.* 31, 10752–10758. doi:10.1523/JNEUROSCI.1240-11.2011

Klein, A. H., Wendroth, S. M., Drewes, L. R., and Andrews, M. T. (2010). Small-volume d-β-hydroxybutyrate solution infusion increases survivability of lethal hemorrhagic shock in rats. *Shock* 34, 565–572. doi:10.1097/SHK.0b013e3181e15063

Lai, Z., Tsugawa, H., Wohlgemuth, G., Mehta, S., Mueller, M., Zheng, Y., et al. (2018). Identifying metabolites by integrating metabolome databases with mass spectrometry cheminformatics. *Nat. Methods* 15, 53–56. doi:10.1038/nmeth.4512

Luan, Y., Ou, J., Kunze, V. P., Qiao, F., Wang, Y., Wei, L., et al. (2018). Integrated transcriptomic and metabolomic analysis reveals adaptive changes of hibernating retinas. *J. Cell. Physiology* 233, 1434–1445. doi:10.1002/jcp.26030

Nelson, C. J., Otis, J. P., and Carey, H. V. (2010). Global analysis of circulating metabolites in hibernating ground squirrels. *Comp. Biochem. Physiology Part D Genomics Proteomics* 5, 265–273. doi:10.1016/j.cbd.2010.07.002

Nelson, C. J., Otis, J. P., Martin, S. L., and Carey, H. V. (2009). Analysis of the hibernation cycle using LC-MS-based metabolomics in ground squirrel liver. *Physiol. Genomics* 37, 43–51. doi:10.1152/physiolgenomics.90323.2008

Nishitani, S., Fukuhara, A., Tomita, I., Kume, S., Shin, J., Okuno, Y., et al. (2022). Ketone body 3-hydroxybutyrate enhances adipocyte function. *Sci. Rep.* 12, 10080. doi:10.1038/s41598-022-14268-w

Perez de Lara Rodriguez, C. E., Drewes, L. R., and Andrews, M. T. (2017). Hibernation-based blood loss therapy increases survivability of lethal hemorrhagic shock in rats. *J. Comp. Physiol. B* 187, 769–778. doi:10.1007/s00360-017-1076-7

Prendergast, B. J., Freeman, D. A., Zucker, I., and Nelson, R. J. (2002). Periodic arousal from hibernation is necessary for initiation of immune responses in ground squirrels. *Am. J. Physiol. Regul. Integr. Comp. Physiol.* 282, R1054–R1062. doi:10.1152/ajpregu.00562.2001

Regan, M. D., Chiang, E., Liu, Y., Tonelli, M., Verdoorn, K. M., Gugel, S. R., et al. (2022). Nitrogen recycling via gut symbionts increases in ground squirrels over the hibernation season. *Science* 375, 460–463. doi:10.1126/science.abh2950

Rice, S. A., ten Have, G. A. M., Reisz, J. A., Gehrke, S., Stefanoni, D., Frare, C., et al. (2020). Nitrogen recycling buffers against ammonia toxicity from skeletal muscle breakdown in hibernating arctic ground squirrels. *Nat. Metab.* 2, 1459–1471. doi:10.1038/s42255-020-00312-4

Russell, R. L., O'Neill, P. H., Epperson, L. E., and Martin, S. L. (2010). Extensive use of torpor in 13-lined ground squirrels in the fall prior to cold exposure. *J. Comp. Physiol. B* 180, 1165–1172. doi:10.1007/s00360-010-0484-8

Russeth, K. P., Higgins, L., and Andrews, M. T. (2006). Identification of proteins from non-model organisms using mass spectrometry: Application to a hibernating mammal. *J. Proteome Res.* 5, 829–839. doi:10.1021/pr050306a

Schwartz, C., Hampton, M., and Andrews, M. T. (2015). Hypothalamic gene expression underlying pre-hibernation satiety. *Genes Brain Behav.* 14, 310–318. doi:10.1111/gbb.12199

Schwartz, C., Hampton, M., and Andrews, M. T. (2013). Seasonal and regional differences in gene expression in the brain of a hibernating mammal. *PLoS One* 8, e58427. doi:10.1371/journal.pone.0058427

Schymanski, E. L., Jeon, J., Gulde, R., Fenner, K., Ruff, M., Singer, H. P., et al. (2014). Identifying small molecules via high resolution mass spectrometry:

Communicating confidence. *Environ. Sci. Technol.* 48, 2097–2098. doi:10.1021/es5002105

Serkova, N. J., Rose, J. C., Epperson, L. E., Carey, H. V., and Martin, S. L. (2007). Quantitative analysis of liver metabolites in three stages of the circannual hibernation cycle in 13-lined ground squirrels by NMR. *Physiol. Genomics* 31, 15–24. doi:10.1152/physiolgenomics.00028.2007

Squire, T. L., Lowe, M. E., Bauer, V. W., and Andrews, M. T. (2003). Pancreatic triacylglycerol lipase in a hibernating mammal. II. Cold-adapted function and differential expression. *Physiol. Genomics* 16, 131–140. doi:10.1152/physiolgenomics.00168.2002

Sumner, L. W., Amberg, A., Barrett, D., Beale, M. H., Beger, R., Daykin, C. A., et al. (2007). Proposed minimum reporting standards for chemical analysis chemical analysis working group (CAWG) metabolomics standards initiative (MSI). *Metabolomics* 3, 211–221. doi:10.1007/s11306-007-0082-2

Theodoridis, G., Gika, H., Raftery, D., Goodacre, R., Plumb, R. S., and Wilson, I. D. (2023). Ensuring fact-based metabolite identification in liquid chromatography–mass spectrometry-based metabolomics. *Anal. Chem.* 95, 3909–3916. doi:10.1021/acs.analchem.2c05192

Tsugawa, H., Kind, T., Nakabayashi, R., Yukihira, D., Tanaka, W., Cajka, T., et al. (2016). Hydrogen rearrangement rules: Computational MS/MS fragmentation and structure elucidation using MS-FINDER software. *Anal. Chem.* 88, 7946–7958. doi:10.1021/acs.analchem.6b00770

van Breukelen, F., and Martin, S. L. (2002). Reversible depression of transcription during hibernation. *J. Comp. Physiol. B* 172, 355–361. doi:10.1007/s00360-002-0256-1

van Breukelen, F., and Martin, S. L. (2001). Translational initiation is uncoupled from elongation at 18 degrees C during mammalian hibernation. *Am. J. Physiol. Regul. Integr. Comp. Physiol.* 281, R1374–R1379. doi:10.1152/ajpregu.2001.281.5.R1374

Wiersma, M., Beuren, T. M. A., de Vrij, E. L., Reitsema, V. A., Bruintjes, J. J., Bouma, H. R., et al. (2018). Torpor-arousal cycles in Syrian hamster heart are associated with transient activation of the protein quality control system. *Comp. Biochem. Physiol. B Biochem. Mol. Biol.* 223, 23–28. doi:10.1016/j.cbpb.2018.06.001

frontiers | Frontiers in Physiology

TYPE Original Research
PUBLISHED 13 July 2023
DOI 10.3389/fphys.2023.1207529

OPEN ACCESS

EDITED BY
Sylvain Giroud,
University of Veterinary Medicine Vienna, Austria

REVIEWED BY
Victoria Diedrich,
University of Ulm, Germany
Naresh Chandra Bal,
KIIT University, India

*CORRESPONDENCE
S. Ryan Oliver,
sryan.oliver@gmail.com

RECEIVED 17 April 2023
ACCEPTED 22 June 2023
PUBLISHED 13 July 2023

CITATION
Hunstiger M, Johannsen MM and Oliver SR (2023), Non-shivering thermogenesis is differentially regulated during the hibernation season in Arctic ground squirrels.
Front. Physiol. 14:1207529.
doi: 10.3389/fphys.2023.1207529

Non-shivering thermogenesis is differentially regulated during the hibernation season in Arctic ground squirrels

Moriah Hunstiger[1], Michelle Marie Johannsen[1,2] and S. Ryan Oliver[1]*

[1]Department of Chemistry and Biochemistry, University of Alaska Fairbanks, Fairbanks, AK, United States, [2]Institute of Arctic Biology, University of Alaska Fairbanks, Fairbanks, AK, United States

Arctic ground squirrels are small mammals that experience physiological extremes during the hibernation season. Body temperature rises from 1°C to 40°C during interbout arousal and requires tight thermoregulation to maintain rheostasis. Tissues from wild-caught Arctic ground squirrels were sampled over 9 months to assess the expression of proteins key to thermogenic regulation. Animals were sacrificed while aroused, and the extensor digitorum longus, diaphragm, brown adipose tissue, and white adipose tissue were probed using Western blots to assess protein expression and blood was sampled for metabolite analysis. Significant seasonal expression patterns emerged showing differential regulation. Contrary to our prediction, white adipose tissue showed no expression of uncoupling protein 1, but utilization of uncoupling protein 1 peaked in brown adipose tissue during the winter months and began to taper after terminal arousal in the spring. The opposite was true for muscular non-shivering thermogenesis. Sarco/endoplasmic reticulum calcium ATPase 1a and 2a expressions were depressed during the late hibernation season and rebounded after terminal arousal in diaphragm tissues, but only SERCA2a was differentially expressed in the extensor digitorum longus. The uncoupler, sarcolipin, was only detected in diaphragm samples and had a decreased expression during hibernation. The differential timing of these non-shivering pathways indicated distinct functions in maintaining thermogenesis which may depend on burrow temperature, availability of endogenous resources, and other seasonal activity demands on these tissues. These results could be impacted by fiber type makeup of the muscles collected, the body weight of the animal, and the date of entrance or exit from hibernation.

KEYWORDS

hibernation, sarcolipin, ground squirrel, non-shivering thermogenesis, metabolism

Introduction

Among mammals, there are many strategies to overcome the environmental challenges of food scarcity and harsh thermal conditions. One of these strategies is hibernation, a physiological phenomenon whereby an animal deviates from the mammalian pattern of homeothermy to that of heterothermy (Heldmaier et al., 2004). A distinct hallmark of homeothermy is a consistently high body temperature, in the range between 34 and 42°C for most mammals (Ivanov, 2006; Porter & Kearney, 2009). The heterothermy phenotype is characterized by periods of suppressed metabolism, which consequently reduces metabolic heat production and can present widely from

short daily variations to seasonal multiday decreases in body temperature depending on the species (Grigg et al., 2004). Mammals that experience heterothermy include members from all three subclasses of mammals, namely, monotremes, marsupials, and eutherians. Among the eutherians are bears, bats, hedgehogs, hamsters, tenrecs, and ground squirrels (Grabek et al., 2015). An extreme example of heterothermy is the hibernation phenotype expressed by the Arctic ground squirrel (AGS), *Urocitellus parryii*.

Hibernation in AGS is characterized by periods of torpor during the fall and winter months and a return to homeothermy during spring and summer (Buck & Barnes, 1999; Barnes & Ritter, 2019). Torpid AGSs undergo significantly reduced metabolic rates and concomitant reduction in body temperature (Buck & Barnes, 1999; Barnes & Ritter, 2019). However, torpor is not a physiological state that remains constant across the hibernation season but occurs in 2- to 3-week bouts interrupted by interbout arousals (IBAs)—discrete intervals when the metabolic rate and body temperature return to euthermic levels (Buck et al., 2008; Karpovich et al., 2009). During an IBA, AGSs revert from a state of low metabolism to a state of high-energy expenditure in a relatively short period of time, between 10 and 20 h for a typical mid-winter IBA (Buck et al., 2008). Rewarming, during an IBA, can cause metabolic rates that are six times greater than the resting metabolic rate and has two distinct phases with the first phase initiated by non-shivering thermogenesis (NST) in brown adipose tissue (BAT) until the body temperature is approximately 16°C (Tøien et al., 2001; Karpovich et al., 2009; Williams et al., 2011). Shivering is recruited during the second phase of an IBA to increase the body temperature until euthermic levels are reached (Tøien et al., 2001; Cannon & Nedergaard, 2004; Williams et al., 2011). During the initial rewarming phase of an IBA, the AGS's body temperature increases from a torpid body temperature of approximately 1°C to approximately 40°C (Buck & Barnes, 1999; Barnes & Ritter, 2019). This discrepancy in the body temperature results in IBAs being energetically expensive, and it is estimated that arousals account for up to 86% of energy expenditure during a complete torpor–arousal cycle in the AGS hibernating at an environmental temperature of 2°C (Karpovich et al., 2009). Because rewarming and cooling during a full IBA cycle is so energetically costly, it requires tight regulation to rapidly increase and decrease the body temperature to ensure metabolic rheostasis.

The use of uncoupling protein 1 (UCP1) in BAT is a well-documented mechanism for heat production (NST) in small eutherians (Cannon & Nedergaard, 2004). Heat is generated when UCP1 allows protons to leak back across the mitochondrial inner membrane, dissipating the proton motive force created by the electron transport chain (Cannon & Nedergaard, 2004). The presence of UCP1 uncoupling is thought to increase the capacity by 20% to generate heat in BAT (Cannon & Nedergaard, 2004). By comparison, beige or brite adipocytes are induced thermogenic cells in white adipose tissue (WAT) that can be adapted by chronic cold exposure or other environmental factors to mimic the properties of brown adipocytes and utilize UCP1 (Cannon & Nedergaard, 2004; Wu et al., 2012; Ikeda & Yamada, 2020). Brite cells can contribute to NST using UCP1 and can also use calcium-cycling via sarco/endoplasmic reticulum calcium ATPase 2b (SERCA2b) to facilitate rewarming mechanisms (Cannon & Nedergaard, 2004; Wu et al., 2012; Ikeda & Yamada, 2020). By increasing the amount of cold-induced thermogenic tissue or the concentration of thermogenic proteins, an animal can greatly increase the capacity for NST, metabolism, and temperature regulation (Cannon & Nedergaard, 2004; Wu et al., 2012; Ikeda & Yamada, 2020).

Recently, a new mechanism of NST has been proposed in which sarcolipin (SLN), and possibly phospholamban (PLB), uncouples SERCA1a/2a ATP hydrolysis in skeletal muscle tissues. The proposed mechanism, similar to UCP1 in fat tissues, suggests that heat is produced when SLN uncouples the hydrolysis of ATP from the calcium pumping action of SERCA (Pant et al., 2016). SLN is widely expressed in neonatal mouse skeletal muscle but that expression decreases in fast-twitch muscles like the extensor digitorum longus (EDL) as development progresses but the expression of SLN remains high in fast-oxidative and slow-twitch muscles like the diaphragm (DIA) (Rowland, Bal, & Periasamy, 2015a; Pant et al., 2015; Sopariwala et al., 2015; Bal et al., 2021). However, the expression of SLN in neonatal mice in cold acclimatized conditions increases in fast-twitch muscles (Pant et al., 2015; Bal et al., 2021). This indicates that depending on the fiber type composition, muscles will express SLN in response to cold stress supporting the postulation that the induction of SLN uncoupling may be involved in thermogenic regulation (Bal et al., 2021). This mechanism is additionally supported when mice with reduced BAT thermogenesis capabilities can maintain the core body temperature in the presence of cold challenge, indicating some sort of compensatory metabolic process (Bal et al., 2012; 2017). In a partner study, when $SLN^{-/-}$ mice were exposed to severe cold (4°C), there was a drastic decrease in the core body temperature from 37°C to 32.2°C ± 1.4°C after 4 h and a precipitous drop to 26.9°C ± 1.9°C after 6 h (Bal et al., 2012; 2017), indicating that SLN uncoupling could be a contributor to the overall metabolism and heat production. This mechanism has demonstrated capabilities to potentially compensate for the lack of UCP1 thermogenesis when mice with ablated interscapular BAT defended their body temperature, 35.8°C ± 0.4°C, similar to their counterparts with intact BAT, 36.3°C ± 0.2°C (Bal et al., 2012). Additionally, when UCP1:SLN double knockout mice or $SLN^{-/-}$ mice with downregulated activity of BAT were challenged with acute cold, hypothermia was induced, and in gradual cold conditions, mice could not maintain adequate fat stores (Rowland et al., 2015a; Bal et al., 2017). Taken together, these studies indicate that both UCP1 and SLN are essential for optimal thermogenesis in mice and other small mammals.

The most studied animal models are currently eutherian homeotherms that maintain a relatively stable body temperature when compared to their heterothermic counterparts. We propose that NST in the skeletal muscles via SLN/SERCA uncoupling could be a mechanism employed by AGSs, in conjunction with thermogenic adipose tissue and shivering, to assist both in metabolism and large temperature ranges experienced by AGSs across the hibernation season as well as in acute conditions of an IBA. This project provides a valuable comparison between homeotherms and heterotherms to better understand the capacity of these uncouplers contributing to thermogenesis during times of increased metabolic stress. This research seeks to identify if these proteins are expressed in AGS, they vary by muscle group based on the fiber type makeup or muscle activity, and how the expression patterns of these proteins during hibernation can give insight into how these thermogenic mechanisms contribute to energy utilization

and metabolic regulation in this novel hibernator model. It was hypothesized that SLN/SERCA uncoupling and UCP1 uncoupling would follow similar increased expression patterns within their respective tissues—muscle and adipose—during early and late hibernation IBAs when compared to pre- and post-hibernation samples, with the muscle groups likely varying in expression patterns. Specifically, EDL and DIA in AGSs will both express proteins that are involved in muscular NST, but they may show varied expressions based on the fiber type makeup.

Methods

Animals

AGSs (*U. parryii*) were wild caught in the Brooks Range near Toolik Field Station of the University of Alaska Fairbanks (UAF) during July 2016 under a permit from the Alaska Department of Fish and Game. Upon being taken to the UAF animal facility, the animals were moved to single metal cages and screened for *Salmonella*, and they underwent a 2-week-long quarantine. The animals were initially housed under simulated summer conditions of 20°C with a 12 h:12 h light:dark cycle. During the transition out of the summer active season, August and early September, the animals were moved to a cold chamber at 2°C with a 4 h:20 h light:dark cycle to simulate winter conditions. The animals were daily checked, and water bottles were filled to provide water *ad libitum*. A total of 10 pellets of Mazuri rodent chow were provided daily to the animals until signs of hibernation were observed. Hibernating animals were visually assessed for respiration, body posture, and behavior parameters for indications of hibernation status. Hibernating AGSs typically adopt a curled position within the nest with their backs oriented upward and tails tucked under their abdomen and chest. Breathing decreases to 1–2 shallow breaths per minute, and they have a depressed body temperature of 0–2°C. Hibernation was communicated to the staff and researchers by placing wood shavings on the animal's back, and if the shavings were undisturbed for 24 h, then the animal was determined to be hibernating.

All animal procedures were reviewed and approved by the Animal Care and Use Committee of the University of Alaska Fairbanks (IACUC #864841) and were consistent with the guidelines established by the veterinary staff and the UAF animal facility.

Tissue collection and processing

Euthanasia and opportunistic tissue sample collection occurred at six distinct time points, namely, cold exposed summer active, early hibernation season, late hibernation season, 3 days post arousal, 8 days post terminal arousal, 15 days post terminal arousal, and cold exposed summer active with all groups having n = 4 based on an *a priori* power analysis with a power of 0.9, error of 0.05, and hibernation rate of 100% (Figure 1). Summer active samples were collected in early June after terminal arousal in April and May when the animals stopped expressing torpor and returned to normothermic body temperatures (Figure 1). All animals had their rectal body temperature measured prior to tissue collection. Only tissues from animals with a body temperature greater than 34°C were used in this study. AGSs in the summer cohort were still housed at winter temperatures, 2°C, but had transitioned to summer light conditions. During early and late hibernation, samples were collected during an IBA when thermogenic proteins were predicted to be highly expressed based on the assertion that slow loss of protein integrity during torpor and the resultant need for replenishment may provide the impetus for arousal episodes (Epperson et al., 2004; Martin et al., 2008). Five tissues were collected from each animal, namely, blood, DIA, EDL, WAT, and BAT. The muscles were chosen based on fiber type specificity in other rodents. The DIA is constitutively active during torpor, and in other rodent species has been shown to have a mixed fiber type makeup (Eddinger et al., 1985). The EDL in mice and rats is dominant in Type II muscle fibers (Eddinger et al., 1985; Soukup et al., 2002; Schiaffino & Reggiani, 2011). The blood was centrifuged (chilled) at 3,000 *g* for 10 min and plasma was removed and frozen in liquid nitrogen. The muscle tissues were flash-frozen, in foil packets, using liquid nitrogen, and placed in a −80°C freezer for later analysis.

The whole frozen muscle tissue was placed in a falcon tube with 2–5 mL homogenizing buffer (10 mM sodium bicarbonate, 2 mM sodium azide, 10 mM tris-Cl, and pH 7.5) in a volume relative to tissue mass (range: 0.2–0.79 g in 2 mL, 0.8–1.59 g in 3 mL, 1.6–2.39 g in 4 mL, and 2.4 or greater in 5 mL). The tissue was finely minced with scissors and subjected to three rounds of 15 s homogenization using a Tekmar Tissuemizer, resting on ice between rounds. The homogenate was filtered through two layers of gauze to remove fascia, tendons, or large unhomogenized tissue pieces. The homogenizing tube was rinsed onto a gauze with 1 mL homogenizing buffer to minimize the loss of sample. The filtered homogenate was centrifuged at 2,000 *g* for 10 min. The supernatant was removed and centrifuged at 10,000 *g* for 5 min (Fisher Scientific accuSpin Micro 17R). Then, the supernatant was gently agitated on a refrigerated shaker with KCl to solubilize myosin globules for 30 min. The samples were then centrifuged at 40,000 *g* for 15 min (Beckman Coulter Allegra 64R Centrifuge). The supernatant was removed and sarcoplasmic reticulum pellets were suspended in 200 µL lysis buffer (150 mM sodium chloride, 5 mM EDTA, 50 mM Tris, 1.0% Triton-X, 10% sodium deoxycholate, 10% SDS, and pH 8) and mixed using repeated pipetting. Protein quantification was performed using the Modified Lowry Protein Assay Kit (Thermo Scientific 23240), and the samples were stored at −80°C until later analysis.

Adipose tissue was extracted using the Minute Total Protein Extraction Kit for adipose tissue/cultured adipocytes (Invent Biotechnologies AT-022) where 50–80 mg portions of tissues were homogenized with extraction powder and buffer A via mortar and pestle. Slurry was then centrifuged, frozen to solidify excess adipose residues, and then centrifuged again. The resultant supernatants received approximately 20 µL of buffer B, with brown adipose extracts being additionally diluted up to 1 mL with DI water. The total protein concentration was calculated using the filter paper assay method by blotting 1 µL of BAT extract or 3 µL of WAT extract and BSA standards (0–8 µg) on a filter paper, and proteins were stained using Coomassie brilliant blue G stain (Minamide & Bamburg, 1990). Dye was extracted and absorbance was measured at

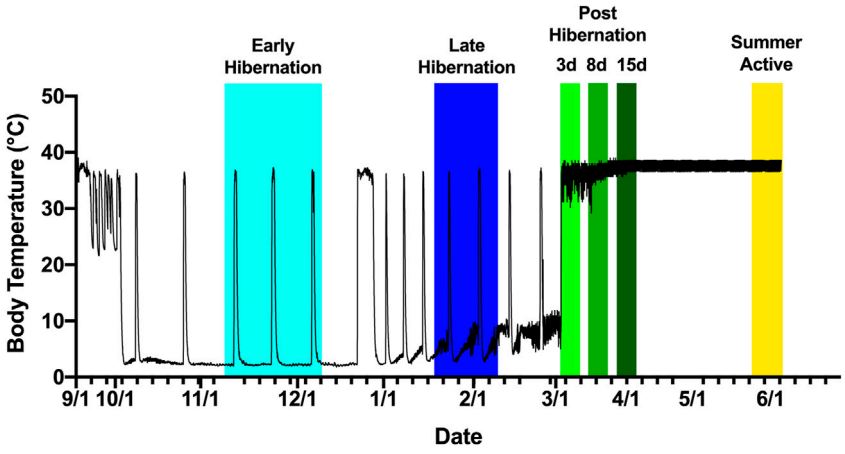

FIGURE 1
Tissue collection scheme based on body temperature of an Arctic ground squirrel during hibernation. Internal body temperature during hibernation season is shown as a solid black line. Animals were sampled aroused or active from November 2016 to June 2017. Early hibernation was defined as undergoing at least 2–3 full torpor bouts shown in light blue ranging from 15 November to 8 December. Late hibernation was defined as continued regular torpor bouts after the turn of the new year, with IBAs shown in dark blue ranging from 22 January to 18 February. Post hibernation (days 3,8, and 15) defined as arousal from torpor without re-entrance into torpor shown in shades of green ranging from 28 February to 3 April. Summer active defined as a return to euthermic phenotype but still exposed to cold shown in yellow ranging from 3 June to 13 June.

600 nm in a 96-well plate, and the protein concentration was calculated based on absorbance values from the bovine serum albumin (BSA) standard curve with resulting concentrations falling between 1.5 and 10 µ/µL (Minamide & Bamburg, 1990). The samples were then stored at −80°C.

Western blots

The Western blot analysis was performed to determine the expression levels of SLN, PLB, UCP1, SERCA1a, and SERCA2a in samples. Proteins from tissue homogenates were separated in tricine-based SDS-PAGE for small proteins with 10 µg protein loaded (4% stacking and 16% resolving for PLB and SLN) and were run at 20 V for 45 min and then 90 V until the dye front had migrated 75% of the way down the gel. Standard tris-glycine SDS-PAGE was used for larger proteins with 5 µg protein loaded (4% stacking and 12% resolving for SERCA1a, SERCA2a, and UCP1) and was run at 190 V until the dye front reached near the bottom of the gel. Separated proteins were transferred onto 0.2 µm nitrocellulose at 75 V for 3 h using a wet transfer method. After transfer, the membranes were rinsed for 5 min using a Ponceau stain to visualize total protein loading and use for protein normalization. Images were captured using a standard camera phone and membranes were rinsed with DI water until the liquid ran clear. The membranes were blocked with 5% BSA in TBS for 2 h before being probed with primary antibody at a 1:1,000 dilution in 5% BSA in TBS overnight, rinsed with 1% BSA in TBST, and then immunoprobed with horseradish peroxidase–conjugated secondary antibody at a 1: 10,000 dilution in 1% BSA in TBST. Antibodies used for probing the proteins of interest were SLN (Millipore, ABT13), PLB (SAB4502212), SERCA1a (Abcam, ab105172), SERCA2a (Abcam, ab2861), UCP1 (Sigma, U6382), and secondary (Thermo Fisher 32460). Protein–antibody complexes were detected using SuperSignal West Pico PLUS Chemiluminescence Substrate (Thermo Fisher 34579). Blots were reused for probing with SERCA1a and SERCA2a and SLN and PLB being probed on the same blot following the Abcam mild stripping protocol. Blots were incubated with two rounds of mild stripping buffer (15 g glycine, 1 g SDS, 10 mL Tween 20, and pH 2.2 in 1 L) for 10 min, followed by two 10 min washes with PBS (1 L of 10× 80 g sodium chloride, 36.3 g sodium phosphate dibasic, 2.4 g potassium phosphate, adjust to 7.4 pH), 2–5 min washes with TBST, followed by blocking in 5% BSA and probed as described previously. Protein bands were visualized by exposing for 2–5 min using an Amersham Imager (AI680UV). Whole blot images are presented in Supporting Material.

Blood analysis

High-throughput metabolomics analysis was performed at the University of Colorado School of Medicine Metabolomics Facility. AGS plasma samples were thawed on ice and metabolites were extracted by adding chilled 5:3:2 methanol:acetonitrile:water (v/v/v) to each tube, 1:24 plasma:buffer (v/v), followed by subsequent vortexing and centrifugation both at 4°C as described by Nemkov et al. (2019). All supernatants were analyzed twice (20 µL injections) by ultra-high performance liquid chromatography using a Thermo Vanquish UHPLC coupled with a Thermo Q Exactive mass spectrometer in positive and negative polarity modes. For each method, the UHPLC utilized a C18 column at a flow rate of 0.45 mL/min for 5 min.

Data were analyzed using Maven (1.4.20-dev-772), and quality controls were maintained as described by Nemkov et al. (2017).

Statistical analysis

Quantification of band density in Western blots was analyzed using ImageJ (FIJI). All values were normalized to the densitometric

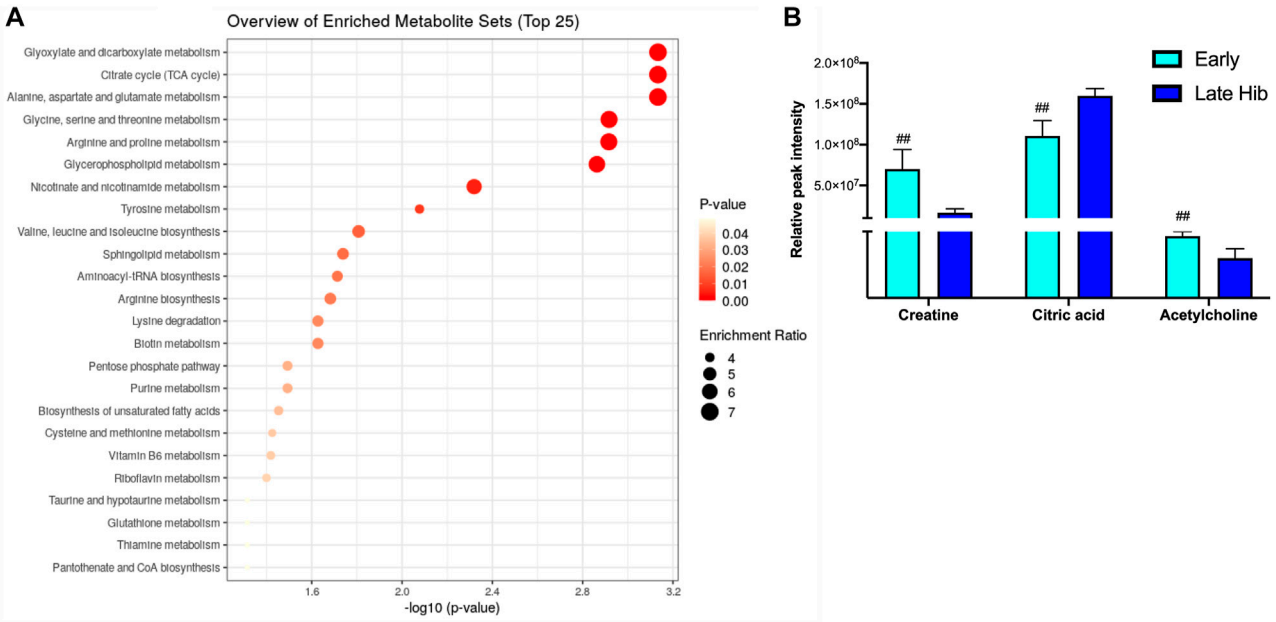

FIGURE 2
Enrichment analysis of metabolites at two time points during hibernation. **(A)** Late hibernation had energy pathways linked to glyoxylate and citric acid cycles enriched when compared to early ($p < 0.05$). **(B)** Creatine, citric acid, and acetylcholine were three metabolites that were identified as key metabolites influencing the enrichment of pathways between early and late hibernation ($p < 0.05$). Values assessed with MetaboAnalyst enrichment analysis with KEGG 2019 (Kanehisa, 2000; 2019; Kanehisa et al., 2023) as the comparative library and significance threshold of Holms' p-value < 0.05.

sum of bands visualized through Ponceau staining. The values are presented as box and whiskers. Significance was set at $p \leq 0.05$ and all densitometry comparisons were performed using a one-way ANOVA with a Tukey's *post hoc* analysis in the Prism software. When analyzing the blood metabolites, early hibernation was used as the reference time point to normalize and determine fold change and p-value. Raw metabolites were filtered by p-value ($p < 0.05$), and this subset of data was analyzed for pathway enrichment using the MetaboAnalyst software and the KEGG 2019 database (Kanehisa, 2000; 2019; Kanehisa et al., 2023). All enrichment data are presented using Holms' p-value < 0.05 and representative plots of key significant metabolites.

Results

Changes in metabolic indicators

The blood metabolite analysis was done on the plasma of AGSs as indicators of full-body metabolic processes and tissue crosstalk. Early/late hibernation and 15 days post hibernation were chosen for enrichment analysis as these were the main inflection points in the protein data. As expected, there were distinct changes in the metabolic pathways related to fatty acid metabolism and usage such as the biosynthesis of fatty acids, elongation, degradation, and linoleic acid metabolism all being enriched during early hibernation as compared to 15 days post hibernation (Figure 2A). The one non-fatty acid pathway enriched in the 15 days post hibernation group when compared to the early hibernation group was glycine/serine/threonine metabolism. Two metabolites with an altered expression between early and 15 days post hibernation and implicated in multiple pathways were palmitic acid and linoleic acid ($p < 0.05$, Figure 2B). The comparison between early and late hibernation had two pathways of enrichment, namely, the citrate cycle and glyoxylate/dicarboxylate that were increased during late hibernation (Figure 3A). The key metabolites involved in these processes, which had significant changes, were creatine, citric acid, and acetylcholine (Figure 3B).

Fluctuations of UCP1 expression and beiging of white adipose tissue

To determine whether UCP1 expression fluctuated across the hibernation season and if beiging is naturally induced to increase thermogenic capacity, 5 µg of BAT and WAT protein extracts were analyzed. We observed the upregulation of UCP1 in BAT during early, late, and 3 days post hibernation when compared to 8 days and 15 days post hibernation with a pattern of gradual decrease in expression after terminal arousal (Figure 4). Specifically, the 8 days post arousal UCP1 expression was downregulated fourfold when compared to hibernation, and 15 days post downregulation reached a 10-fold decrease (Figure 4). However, there was no difference in the expression of UCP1 in WAT across all time points as it appears that AGSs hibernating at 2°C do not express UCP1 in WAT during natural hibernation (Supplementary Figure S3).

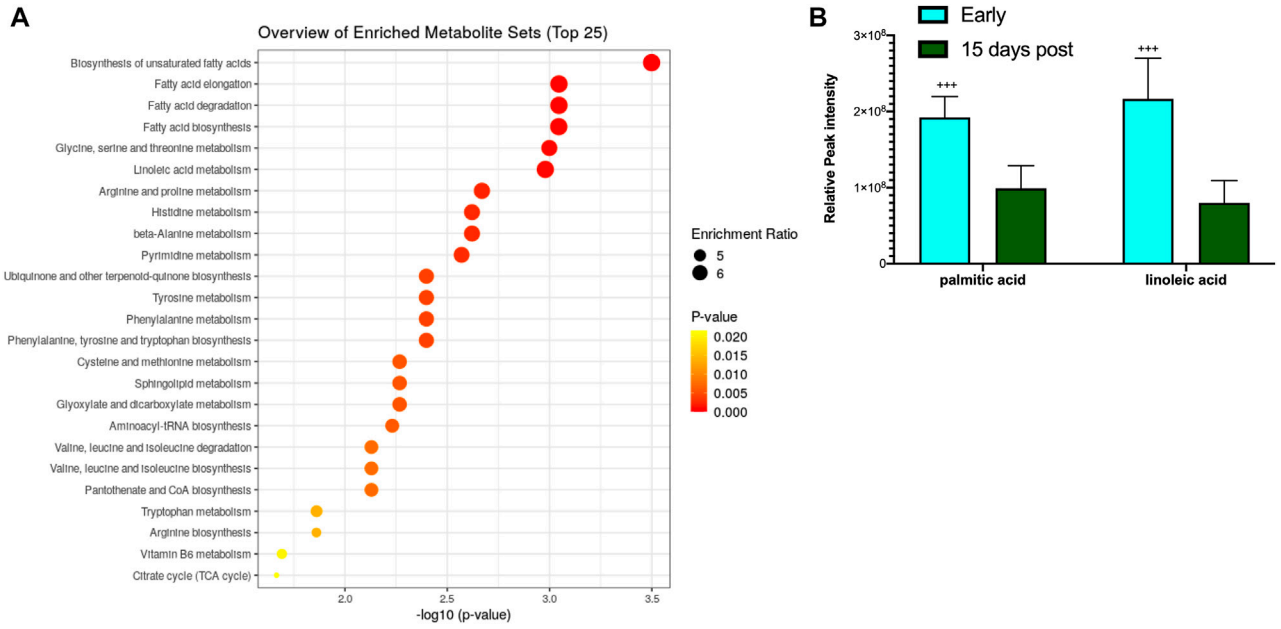

FIGURE 3
Enrichment analysis of metabolites during hibernation *vs.* terminal arousal. **(A)** Early hibernation compared to 15 days post hibernation showing fatty acid pathways linked to biosynthesis (saturated and unsaturated), elongation, degradation, and linoleic acid metabolism to be enriched during early hibernation ($p < 0.05$). **(B)** Palmitic and linoleic acids are two metabolites that were significantly increased for multiple fatty acid utilization pathways during early hibernation ($p < 0.05$). Values assessed with MetaboAnalyst enrichment analysis with KEGG 2019 (Kanehisa, 2000; 2019; Kanehisa et al., 2023) as the comparative library and significance threshold of Holms' *p*-value <0.05.

Expression of SERCA regulators: SLN

As expected, based on the literature of SLN expression in other species and muscles predominant in fiber type 1, EDL neither showed any levels of SLN expression at any of the time points collected nor were there detectable levels of monomeric or pentameric PLB at any of our collection time points for the EDL muscles (Supplementary Figure S6). However, the DIA, a mixed fiber type constitutively active muscle, showed detectable levels of both proteins. SLN showed a decrease in expression during early hibernation when compared to 8 and 15 days post hibernation with a fold change between 2 and 3 ($p < 0.05$, Figure 3A). Only the monomeric form of PLB was detectable in the DIA but was not analyzable (Supplementary Figure S5).

SERCA1a and 2a expression in skeletal muscle

To analyze SERCA1a and SERCA2a expressions in AGS, 5 µg of DIA and EDL tissue homogenate was analyzed. SERCA1a showed a depressed expression in AGS diaphragm during late hibernation when compared to summer active, 3 days post, and 8 days post arousal (Figure 6A). Summer active had a twofold increase in the expression compared to late hibernation ($p < 0.05$) and the 3 and 8 days post samples had approximately 2.5-fold increase compared to the late hibernation time point ($p < 0.01$). SERCA2a had a decreased expression at the following time points: summer active, early, late, and 3 days when compared to 8 days post hibernation with the greatest depression in expression during early hibernation (Figure 6C). Summer active, late, and 3 days post hibernation had between 1.6- and 2-fold decrease when compared to 8 days post hibernation ($p < 0.05$). Although early hibernation had a 2.7-fold decrease in expression when compared to 8 days post ($p < 0.01$), both SERCA1a and SERCA2a had similar patterns of expression in DIA with downregulation occurring during early and late hibernation and upregulation after terminal arousal.

The assessment of SERCA1a in EDL did not reveal any significant differences in expression across hibernation at any time point (Figure 6B). However, the expression of SERCA2a did increase in summer active when compared to late hibernation and all post-arousal sample sets (Figure 6D). Summer active had twofold upregulation when compared to the late hibernation time point ($p < 0.001$) and between a 2.3- and 2.6-fold increase in expression over the post hibernation time points ($p < 0.001$). Early hibernation had a similar pattern of expression when compared to that of summer active but the comparison to late, 3 days, and 8 days post hibernation did not reveal any results of statistical significance. However, when compared to 15 days post hibernation, early hibernation had a twofold increase in SERCA2a expression ($p < 0.05$).

Discussion

It has been well established that the protein–protein interaction between SLN and SERCA1a/2a lowers Ca^{2+} reuptake (v_{max}) of SERCA for calcium transport and PLB alters the calcium-binding affinity to SERCA (Bhupathy et al., 2007; Sahoo et al., 2013). It has

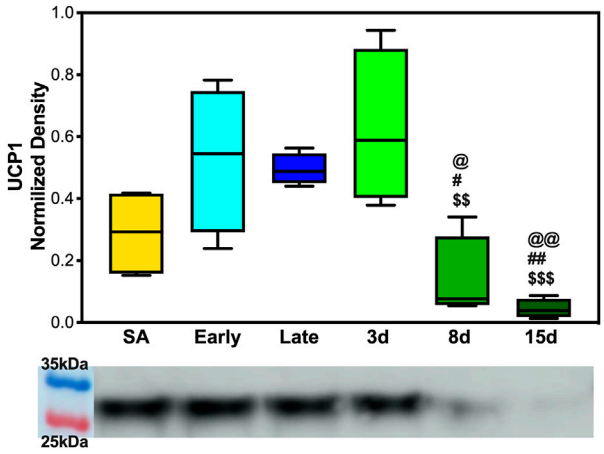

FIGURE 4
UCP1 expression in brown adipose tissue. (A) Early, late, and 3 days post hibernation had an increased UCP1 expression when compared to 15 days post hibernation ($p < 0.001$, $p < 0.01$, $p < 0.001$) and early, late, and 3 days post hibernation had greater expression than 8 days post hibernation ($p < 0.05$, $p < 0.05$, and $p < 0.01$). Symbols indicate a significant difference based on a one-way ANOVA with Tukey's *post hoc* analysis, with significance set at $p \leq 0.05$. Symbols indicate significance as follows: &, SA; @, early; #, late; $, 3 days; *, 8 days; +, 15 days. All values are represented as box and whiskers.

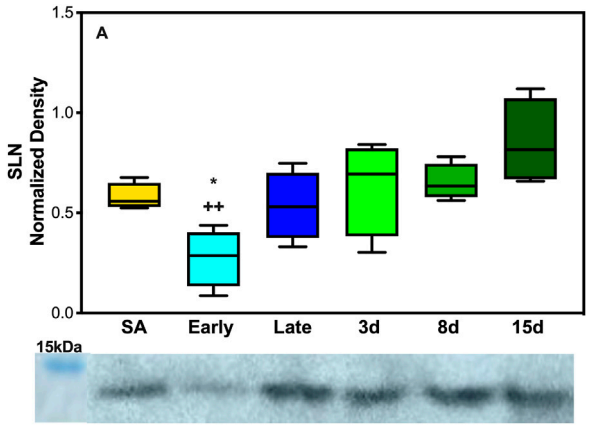

FIGURE 5
Expression of SERCA regulator SLN in AGS skeletal muscle. **(A)** Expression of SLN in AGS diaphragm shows a decrease in expression during early hibernation when compared to 8 ($p < 0.05$) and 15 days post hibernation ($p < 0.01$). Symbols indicate a significant difference based on a one-way ANOVA with Tukey's *post hoc* analysis, with significance set at $p \leq 0.05$. Symbols are as follows: *, 8 days; and +, 15 days. All values are represented as box and whiskers.

been demonstrated in model species (mice and rats) that when challenged with cold, SLN and UCP1 both contribute to maintain metabolism and appropriate body composition when functioning alone (Bal et al., 2012; 2017). Studies have shown that in modified mouse models, interruption of both SLN and UCP1 utilization at the same time can be detrimental to defending body temperature and maintaining fat stores (Rowland et al., 2015b; Pant et al., 2016; Bal et al., 2017). Analyzing these proteins in a novel unmodified model that is naturally adapted to both defending and suppressing thermogenic pathways can provide a new insight into their metabolic capabilities; in particular, how the expression of these proteins during periods of metabolic intensity can indicate the use of SERCA uncoupling to regulate thermogenesis and provide an insight into its thermoregulatory relationship and interplay with other heat production pathways. In this study, we set out to examine the expression of proteins key to non-shivering thermogenesis in both muscle and adipose tissues in AGSs after experiencing an IBA. We hypothesized that during the late and early hibernation season, our proteins of interest, namely, SERCA1a/2a, SLN, PLB, and UCP1, would be upregulated in AGS as this would coincide with the largest temperature fluctuations, and thus the metabolic demands would be the greatest. We also hypothesized that the expression of proteins affiliated with muscle uncoupling would have distinct expression patterns based on the muscle sampled.

WAT did not show any expression of UCP1 in contrast to what we hypothesized based on cold exposure studies in other rodent species (Supplementary Figure S3). Beiging of WAT and the accompanying expression of UCP1 in mice were observed during extreme cold and, in some cases, taking as little as 4 h at 4°C to become detectable in the transcriptome (Liang et al., 2019). For AGS, wild burrow temperature can range from 4 to 26°C with the average burrow temperature during the hibernation season being −8°C (Barnes & Buck, 2000). Animals in this project were housed at a constant 2°C, and while this is in the range of the natural burrow temperature, it is well above the average seen in the wild. This may indicate that the standard laboratory hibernaculum temperature was insufficient to induce WAT beiging in AGS. In line with our hypothesis, UCP1 in BAT experienced the largest degree of fold change in expression during early, late, and 3 days post hibernation with downregulation occurring after terminal arousal at 8 and 15 days post hibernation (Figure 4). This is consistent with research in another small mammalian hibernator, the 13-lined ground squirrel, which shows utilization of UCP1 uncoupling is the greatest during torpor and IBA in the hibernation season, when thermogenic stress is at its peak, and lowest during the spring season (Ballinger et al., 2016). This is also supported in Djungarian hamsters where BAT depots are at the greatest size—up to 5% of their body mass—at the end of the summer season and smallest during terminal arousal in spring with BAT atrophy showing a decrease in mitochondrial abundance (Rafael et al., 1985; Hindle & Martin, 2014). Increased UCP1 expression during hibernation is also supported by our metabolomics data that show increased fatty acid metabolism and transport during early hibernation and a decrease during 15 days post hibernation (Figure 5A). UCP1 mitochondrial metabolism is dependent on ß-oxidation, which relies on the metabolism of fatty acids and it is likely that UCP1 expression would be high in conjunction with fatty acid metabolism and utilization (Hankir, 2018). However, the two fatty acids most differentiated between these two time points were linoleic and palmitic acid (Figure 5B). Palmitic acid is not an ideal fuel source in mouse models and has been shown to not feed directly into ß-oxidation in brown adipocytes (Vergnes et al., 2011; Hankir, 2018). Although linoleic and palmitic acids are not optimal fuel sources, they may be recruited into the lipid membrane allowing for

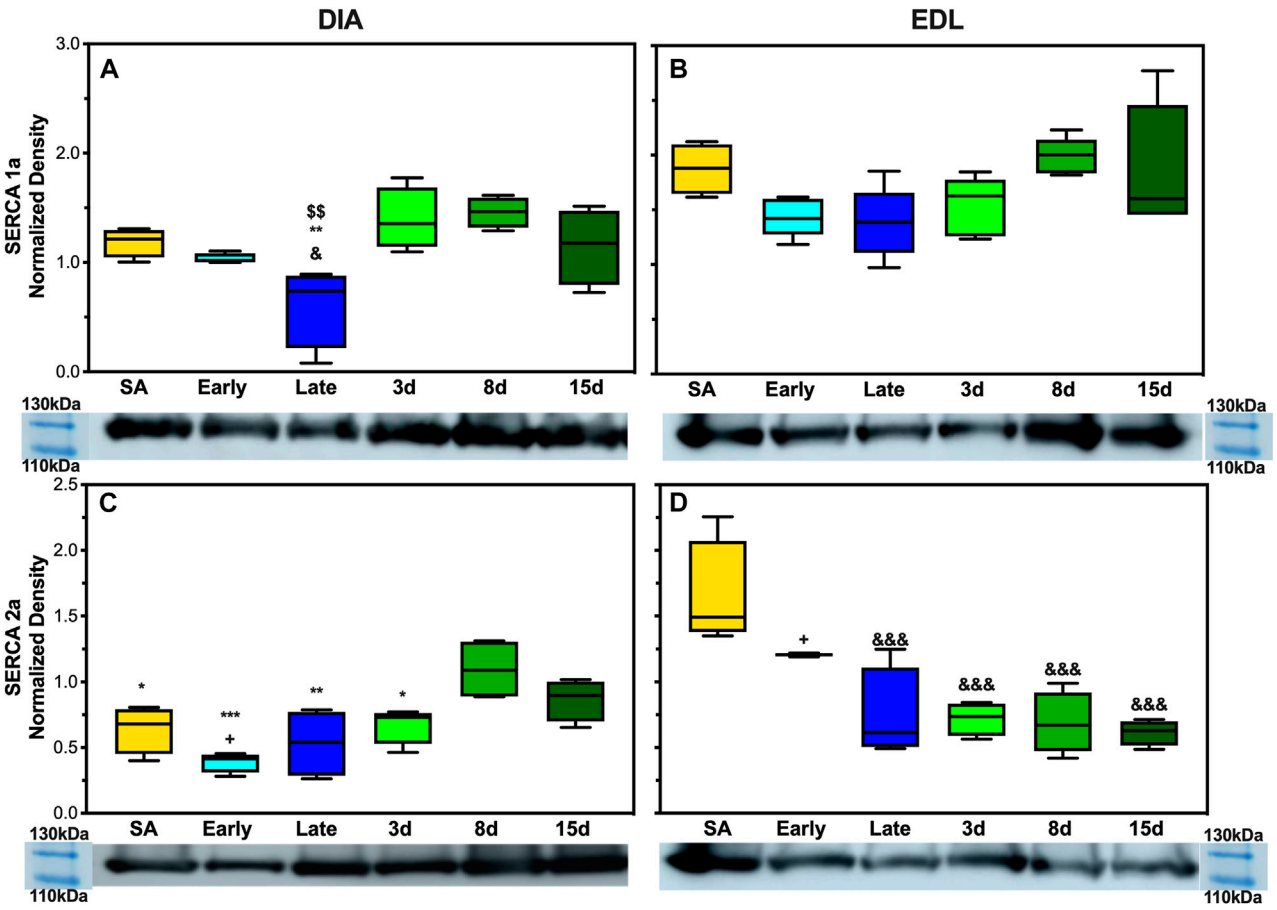

FIGURE 6
Expression of SERCA1a and SERCA2a in AGS skeletal muscle. **(A)** Expression of SERCA1a in AGS diaphragm shows a decrease in expression during late hibernation when compared to SA ($p < 0.05$), 3 days post hibernation ($p < 0.01$), and 8 days post hibernation ($p < 0.01$) **(B)** SERCA1a was not detectably different at any time point in EDL. **(C)** SERCA2a shows an increased expression in the diaphragm during 8 days post hibernation when compared to summer active ($p < 0.05$), early ($p < 0.001$), late ($p < 0.01$), and 3 days post hibernation ($p < 0.05$). 15 days post hibernation was increased when compared to early hibernation ($p < 0.05$). **(D)** SERCA2a in EDL had a decrease in expression at late hibernation ($p < 0.001$), 3 days post hibernation ($p < 0.001$), 8 days post hibernation ($p < 0.001$), and 15 days post hibernation ($p < 0.001$) when compared to SA. 15 days post hibernation had decreased when compared to early hibernation ($p < 0.05$). Symbols indicate a significant difference based on a one-way ANOVA with Tukey's *post hoc* analysis, with significance set at $p \leq 0.05$. Symbols are as follows: &, SA; @, early; #, late; $, 3 days; *, 8 days; +, 15 days. All values are represented as box and whiskers.

modification in the conformation of membrane-bound proteins (Beck et al., 2006; 2007). UCP1 is an integral membrane protein and has been shown to activate exclusively in the presence of long-chain fatty acids, with palmitic acid and linoleic acid enrichment in lipid bilayers increasing UCP1 activation and conductance (Beck et al., 2006; 2007). Therefore, it is likely that enrichment of these fatty acids may indicate possible mediation of bilayer conformation changes in UCP1 in hibernating AGS allowing for increased UCP1 functionality and overall heat production during periods of increased metabolism rather than increases in ß-oxidation. This could also affect the function of SERCA, another integral membrane protein that depends heavily on bilayer composition for functionality. It has been shown that in the hearts of hibernating Syrian hamsters that increased linoleic acid in the sarcoplasmic reticulum membrane allowed animals to reach a lower body temperature and increase SERCA activity during entrance into and during torpor (Giroud et al., 2013). This is supported by our results of linoleic acid being lower during periods of low metabolic demand when compared to the hibernation season when SERCA activity may be more heavily relied on to maintain thermoregulation in AGS.

In EDL, there was no observed difference in SERCA1a expression at any point during the hibernation season but the alternative isoform, SERCA2a, had observed changes in expression. SERCA2a protein increased during the active season when compared to the collection points during hibernation (Figures 2B,D). Additionally, the uncoupler SLN showed no expression in EDL at any of the time points in this study. This was not in line with our hypothesis, but a possible explanation could be the fiber type specificity and preferential fuel utilization during hibernation. In rats, EDL is a type II dominant muscle with 95–98% type II and 2–5% type I muscle fibres (Eddinger et al., 1985; Soukup et al., 2002; Schiaffino & Reggiani, 2011). Type I muscle fibers are characterized by using fatty acid fuel sources, resistance to fatigue (long-duration activity), recruitment for shivering, SLN expression, and SERCA2a expression. By contrast, type II muscle fibers are known for

glycolytic fuel utilization, fast twitch (utilized for strong fast movements), less efficient shivering, lack of SLN content, and SERCA1a expression (Close, 1967; Minamisawa et al., 2003; Babu et al., 2005; Babu et al., 2007). However, type II fibers can be subdivided into A, B, and X with type IIa being similar to I, resistant to fatigue and more oxidative, whereas type IIx fibers have moderate oxidative and glycolytic capacity, and type IIb fibers have a high glycolytic capacity and high fatigability (Schiaffino & Reggiani, 2011).

In rodents, fiber type switching during certain environmental stressors is possible. For example, a predominant type II fiber type muscle such as EDL could start to express alternative fibers, potentially due to the demand or available fuel sources. During hibernation, fatty acid oxidation and utilization are the main sources of thermogenic fuel which may encourage fiber type switching to type IIa predominance during the hibernation season. The downregulation of SERCA2a during late and post hibernation runs counter to this postulation. However, this could be due to the hybridization of type I fibers with type IIa fibers and a reliance on isoform switching to type IIa fibers in EDL to balance two functions during hibernation and post hibernation: one is to utilize fatty acid metabolism more efficiently during times of resource scarcity in early and late hibernation (Figure 5A) and the other is to prepare for the rigors of the active season upon emergence in the spring when animals are grazing, mating, evading predators, and in general having higher activity levels that may require fast explosive movements that are dependent on type II fibers. The expression of SERCA1a and SERCA2a likely provides limited information on fiber type predominance and switching in EDL during hibernation, and future fiber typing in AGS could add greatly to these results.

In contrast to EDL, DIA had decreased expression levels of SERCA1a and SERCA2a during late and early hibernation and similar patterns of expression in SLN during early hibernation (Figures 2A,C, 3). DIA in rodents is a mixed fiber type muscle with approximately 50:50 fiber type makeup (Eddinger et al., 1985). During torpor, respiratory frequency is between 2–6 breaths/min and increases to 160–180 breaths/min during an IBA (Tøien et al., 2001; Christian et al., 2014). Both SERCA1a and SERCA2a in DIA had similar decreased expression patterns during early and late time points which can be explained by 1) more efficient utilization of fuel resources and 2) the activity level of the diaphragm being greatly decreased during torpor when compared to an IBA or during terminal arousal. All samples were collected during arousal, and it is possible that SERCA1a and SERCA2a can have further depressed expressions during torpor *vs.* IBA, and these results can be impacted by the sampling method employed in this study.

The response of SLN was the opposite of what was initially hypothesized with the lowest levels of expression in the DIA occurring during early hibernation and was not detectable in the EDL (Figure 3, Supplementary Figure S6). SLN uncoupling may not be required in early hibernation as UCP1 uncoupling in BAT may be sufficient in maintaining body temperature, and the addition of shivering provides a sufficient thermogenic resource for successful IBAs. By contrast, after terminal arousal when fat stores have been depleted, fatty acid utilization is decreased and UCP1 expression lowers (Figure 4). SLN uncoupling may be required to defend body temperature until animals can roam free of burrows and use ambulatory movements for heat production. In theory, AGSs utilize SLN uncoupling during periods of peak metabolic activity and thermogenic stress. For an AGS, this would be during the process of arousal when body temperature rises from −2.9°C to 40°C (Barnes & Ritter, 2019). Our animals were sampled while fully aroused, when peak metabolic activity had elapsed, and normothermic temperature had been achieved, which could be masking some of the occurring muscle NST. Alternatively, these results can indicate that SLN may be performing a role outside uncoupling during the terminal arousal. In mouse SLN overexpression models, SLN has been shown to increase the endurance of muscles, increase resistance to fatigue, and prime the muscles in response to metabolic demand without switching fiber types (Sopariwala et al., 2015). Increased levels of SLN expression in AGS 8 and 15 days post hibernation(Figure 3A) can be explained by this phenomenon and supports our results as DIA activity greatly increases during terminal arousal and SLN can provide a stop-gap measure to reduce the fatigability of the muscle until fiber type dominance can compensate for increased activity going into the active spring and summer months.

Taken together, these results are in line with previous data that muscle groups show specificity in the expression of SLN and SERCA isoforms (Eddinger et al., 1985; Bal et al., 2021). Both EDL and DIA show distinct patterns of expression in SLN, SERCA1a, and SERCA2a in AGSs (Figure 5; Figure 6, and Supplementary Figure S6). This could allow AGS to recruit specific muscles for thermogenic maintenance and that fiber type makeup may determine the contribution of a singular muscle group to total NST. These data are also supported by the literature in mice with SLN expression occurring only in slow-twitch muscles and negligible in fast-twitch muscles in non-cold acclimated mice (Pant et al., 2015). This indicates that the cold conditions of a standard hibernaculum may not be sufficient in this cold-acclimated species to induce SLN expression in EDL, as seen in neonatal mice, or to induce UCP1 expression in WAT (Pant et al., 2015). Additionally, the results of this study highlight the interplay between BAT and muscle NST. With the interesting phenomenon of decreases in UCP1 expression coinciding with the increases in SLN expression during terminal arousal at 8 and 15 days post hibernation (Figures 4, 5). This is aligned with data that show that when BAT thermogenesis is impaired either by ablation in mice or UCP1$^{-/-}$ rats, reliance on muscle-based thermogenesis is increased (Bal et al., 2016; Warfel et al., 2023). In addition, both of these studies present limitations to muscle NST that can explain our results: one is that animals relying solely on NST cannot maintain body temperature during prolonged periods of cold exposure (Warfel et al., 2023) and the other is that muscle NST is more energetically expensive than BAT and would require exogenous food sources (Bal et al., 2016). Both of these postulations are in line with our results as SLN expression peaks after terminal arousal in AGSs when spring temperatures increase and food sources become more plentiful. This could indicate a more complex synergy between BAT and muscle thermogenesis in AGSs during hibernation and throughout the year as a whole.

Conclusion

Although this study had a limited sample size, we could show that AGSs differentially express proteins involved in muscle NST based on the muscle group. Specifically, AGSs express the recently discovered SERCA uncoupler SLN, although it still remains unknown to what extent is this pathway recruited. Our data suggest that brown adipose

NST is a strongly upregulated process in AGS during hibernation and that SLN is reduced, which could be a mechanism for allowing shivering mechanisms in muscles or to utilize endogenous fuel sources more efficiently. AGSs may utilize SLN uncoupling in the DIA and other tissues not analyzed in this study to maintain thermogenic rheostasis during hibernation. Furthermore, a similar pattern has been shown in 13 lined ground squirrels (Oliver et al., 2019) and the ability to control NST has been suggested to have great evolutionary implications in other species (Grigg et al., 2022). With many pathways involved in hibernation being conserved across mammalian species, understanding the extent of SLN uncoupling and its role in metabolism, energy expenditure, and fuel utilization during hibernation could provide insight into the ability of this conserved pathway to affect energy expenditure in other species, such as humans.

To further define the utilization of SLN uncoupling and expression of patterns of proteins linked to NST in both muscle and adipose, a broader range of skeletal muscle groups with a variety of fiber type makeup can be collected from both aroused and torpid animals and analyzed for the uncoupling pathway expression. Animals can also be housed at lower temperatures to mimic the wild environment to induce more differentiated expression patterns particularly to see if UCP1 expression in WAT and SLN expression in EDL can be induced. Additionally, full-scale fiber typing of the AGS muscle tissue can be done to see if 1) it is consistent with other rodent models and 2) the extent to which fiber type switching is prevalent across the hibernation season and how that incorporates into muscle group contribution to non-shivering muscle thermogenesis and fuel utilization during periods of thermogenic stress (Heinis et al., 2015, Shaikh et al., 2016).

Data availability statement

The raw data supporting the conclusions of this article will be made available by the authors, without undue reservation.

Ethics statement

The animal study was reviewed and approved by University of Alaska IACUC.

Author contributions

MH is the primary scientist who conducted the experiments, analyzed the data, and wrote the main text of the manuscript. MJ aided in sample preparation and analysis. SO is the PI for the project, oversaw the experimental parameters, aided in figure preparation, and edited the text and figures. All authors contributed to the article and approved the submitted version.

Funding

Research reported in this publication was supported by the Institutional Development Award (IDeA) from the National Institute of General Medical Sciences of the National Institutes of Health under grant number P20GM103395. The content is solely the responsibility of the authors and does not necessarily reflect the official views of the NIH.

Acknowledgments

The authors thank Brian Barnes and Jeannette Moore for their invaluable assistance and opportunistic harvesting of samples. The authors would like to recognize all members of the Oliver lab staff, with special recognition going to Jace Rogers. The authors would also like to thank the UAF BiRD staff for their dedication to this project and their work in the field.

Conflict of interest

The authors declare that the research was conducted in the absence of any commercial or financial relationships that could be construed as a potential conflict of interest.

Publisher's note

Supplementary material

The Supplementary Material for this article can be found online at: https://www.frontiersin.org/articles/10.3389/fphys.2023.1207529/full#supplementary-material

References

Babu, G. J., Bhupathy, P., Carnes, C. A., Billman, G. E., and Periasamy, M. (2007). Differential expression of sarcolipin protein during muscle development and cardiac pathophysiology. *J. Mol. Cell. Cardiol.* 43 (2), 215–222. doi:10.1016/j.yjmcc.2007.05.009

Babu, G., Zheng, Z., Natarajan, P., Wheeler, D., Janssen, P., and Periasamy, M. (2005). Overexpression of sarcolipin decreases myocyte contractility and calcium transient. *Cardiovasc. Res.* 65 (1), 177–186. doi:10.1016/j.cardiores.2004.08.012

Bal, N. C., Gupta, S. C., Pant, M., Sopariwala, D. H., Gonzalez-Escobedo, G., Turner, J., et al. (2021). Is upregulation of sarcolipin beneficial or detrimental to muscle function? *Front. Physiology* 12, 633058. doi:10.3389/fphys.2021.633058

Bal, N. C., Maurya, S. K., Singh, S., Wehrens, X. H. T., and Periasamy, M. (2016). Increased reliance on muscle-based thermogenesis upon acute minimization of Brown adipose tissue function. *J. Biol. Chem.* 291 (33), 17247–17257. doi:10.1074/jbc.M116.728188

Bal, N. C., Maurya, S. K., Sopariwala, D. H., Sahoo, S. K., Gupta, S. C., Shaikh, S. A., et al. (2012). Sarcolipin is a newly identified regulator of muscle-based thermogenesis in mammals. *Nat. Med.* 18 (10), 1575–1579. doi:10.1038/nm.2897

Bal, N. C., Singh, S., Reis, F. C. G., Maurya, S. K., Pani, S., Rowland, L. A., et al. (2017). Both Brown adipose tissue and skeletal muscle thermogenesis processes are activated

during mild to severe cold adaptation in mice. *J. Biol. Chem.* 292 (40), 16616–16625. doi:10.1074/jbc.M117.790451

Ballinger, M. A., Hess, C., Napolitano, M. W., Bjork, J. A., and Andrews, M. T. (2016). Seasonal changes in Brown adipose tissue mitochondria in a mammalian hibernator: From gene expression to function. *Am. J. Physiology-Regulatory, Integr. Comp. Physiology* 311 (2), R325–R336. doi:10.1152/ajpregu.00463.2015

Barnes, B. M., and Buck, C. L. (2000). "Hibernation in the extreme: Burrow and body temperatures, metabolism, and limits to torpor bout length in arctic ground squirrels," in *Life in the cold* (Berlin, Germany: Springer). doi:10.1007/978-3-662-04162-8_7

Barnes, B. M., and Ritter, D. (2019). "Patterns of body temperature change in hibernating arctic ground squirrels," in *Life in the cold* (Boca Raton, Florida, United States: CRC Press). doi:10.1201/9780429040931-12

Beck, V., Jabůrek, M., Breen, E. P., Porter, R. K., Ježek, P., and Pohl, E. E. (2006). A new automated technique for the reconstitution of hydrophobic proteins into planar bilayer membranes. Studies of human recombinant uncoupling protein 1. *Biochimica Biophysica Acta (BBA) - Bioenergetics* 1757 (5–6), 474–479. doi:10.1016/j.bbabio.2006.03.006

Beck, V., Jaburek, M., Demina, T., Rupprecht, A., Porter, R. K., Jezek, P., et al. (2007). Polyunsaturated fatty acids activate human uncoupling proteins 1 and 2 in planar lipid bilayers. *FASEB J.* 21 (4), 1137–1144. doi:10.1096/fj.06-7489com

Bhupathy, P., Babu, G. J., and Periasamy, M. (2007). Sarcolipin and phospholamban as regulators of cardiac sarcoplasmic reticulum Ca2+ ATPase. *J. Mol. Cell. Cardiol.* 42 (5), 903–911. doi:10.1016/j.yjmcc.2007.03.738

Buck, C. L., and Barnes, B. M. (1999). Annual cycle of body composition and hibernation in free-living arctic ground squirrels. *J. Mammal.* 80 (2), 430–442. doi:10.2307/1383291

Buck, C. L., Breton, A., Kohl, F., Tøien, Ø., and Barnes, B. (2008). "Overwinter body temperature patterns in free-living Arctic Ground Squirrels (*Spermophilus parryii*)," in *Hypometabolism in animals: Torpor, hibernation and cryobiology* (KwaZulu-Natal, South Africa: University of KwaZulu-Natal), 317–326.

Cannon, B., and Nedergaard, J. (2004). Brown adipose tissue: Function and physiological significance. *Physiol. Rev.* 84 (1), 277–359. doi:10.1152/physrev.00015.2003

Christian, S. L., Roe, T., Rasley, B. T., Moore, J. T., Harris, M. B., and Drew, K. L. (2014). Habituation of Arctic ground squirrels (Urocitellus parryii) to handling and movement during torpor to prevent artificial arousal. *Front. Physiology* 5, 174. doi:10.3389/fphys.2014.00174

Close, R. (1967). Properties of motor units in fast and slow skeletal muscles of the rat. *J. Physiology* 193 (1), 45–55. doi:10.1113/jphysiol.1967.sp008342

Eddinger, T. J., Moss, R. L., and Cassens, R. G. (1985). Fiber number and type composition in extensor digitorum longus, soleus, and diaphragm muscles with aging in Fisher 344 rats. *J. Histochem. Cytochem.* 33 (10), 1033–1041. doi:10.1177/33.10.2931475

Epperson, L. E., Dahl, T. A., and Martin, S. L. (2004). Quantitative analysis of liver protein expression during hibernation in the golden-mantled ground squirrel. *Mol. Cell. Proteomics* 3 (9), 920–933. doi:10.1074/mcp.M400042-MCP200

Giroud, S., Frare, C., Strijkstra, A., Boerema, A., Arnold, W., and Ruf, T. (2013). Membrane phospholipid fatty acid composition regulates cardiac SERCA activity in a hibernator, the Syrian hamster (*Mesocricetus auratus*). *PLoS ONE* 8 (5), e63111. doi:10.1371/journal.pone.0063111

Grabek, K. R., Martin, S. L., and Hindle, A. G. (2015). Proteomics approaches shed new light on hibernation physiology. *J. Comp. Physiology B* 185 (6), 607–627. doi:10.1007/s00360-015-0905-9

Grigg, G. C., Beard, L. A., and Augee, M. L. (2004). The evolution of endothermy and its diversity in mammals and birds. *Physiological Biochem. Zoology* 77 (6), 982–997. doi:10.1086/425188

Grigg, G., Nowack, J., Bicudo, J. E. P. W., Bal, N. C., Woodward, H. N., and Seymour, R. S. (2022). Whole-body endothermy: Ancient, homologous and widespread among the ancestors of mammals, birds and crocodylians. *Biol. Rev.* 97, 766–801. doi:10.1111/brv.12822

Hankir, M. K. (2018). Loading and firing the Brown adipocyte. *Adipocyte* 7 (1), 4–11. doi:10.1080/21623945.2017.1405879

Heinis, F. I., Vermillion, K. L., Andrews, M. T., and Metzger, J. M. (2015). Myocardial performance and adaptive energy pathways in a torpid mammalian hibernator. *Am. J. Physiology-Regulatory, Integr. Comp. Physiology* 309 (4), R368–R377. doi:10.1152/ajpregu.00365.2014

Heldmaier, G., Ortmann, S., and Elvert, R. (2004). Natural hypometabolism during hibernation and daily torpor in mammals. *Respir. Physiology Neurobiol.* 141 (3), 317–329. doi:10.1016/j.resp.2004.03.014

Hindle, A. G., and Martin, S. L. (2014). Intrinsic circannual regulation of Brown adipose tissue form and function in tune with hibernation. *Am. J. Physiology-Endocrinology Metabolism* 306 (3), E284–E299. doi:10.1152/ajpendo.00431.2013

Ikeda, K., and Yamada, T. (2020). UCP1 dependent and independent thermogenesis in Brown and beige adipocytes. *Front. Endocrinol.* 11, 498. doi:10.3389/fendo.2020.00498

Ivanov, K. P. (2006). The development of the concepts of homeothermy and thermoregulation. *J. Therm. Biol.* 31 (1–2), 24–29. doi:10.1016/j.jtherbio.2005.12.005

Kanehisa, M., Furumichi, M., Sato, Y., Kawashima, M., and Ishiguro-Watanabe, M. (2023). KEGG for taxonomy-based analysis of pathways and genomes. *Nucleic Acids Res.* 51 (D1), D587–D592. doi:10.1093/nar/gkac963

Kanehisa, M., and Goto, S. (2000). Kegg: Kyoto encyclopedia of genes and genomes. *Nucleic Acids Res.* 28 (1), 27–30. doi:10.1093/nar/28.1.27

Kanehisa, M. (2019). Toward understanding the origin and evolution of cellular organisms. *Protein Sci.* 28 (11), 1947–1951. doi:10.1002/pro.3715

Karpovich, S. A., Tøien, Ø., Buck, C. L., and Barnes, B. M. (2009). Energetics of arousal episodes in hibernating arctic ground squirrels. *J. Comp. Physiology B* 179 (6), 691–700. doi:10.1007/s00360-009-0350-8

Liang, X., Pan, J., Cao, C., Zhang, L., Zhao, Y., Fan, Y., et al. (2019). Transcriptional response of subcutaneous white adipose tissue to acute cold exposure in mice. *Int. J. Mol. Sci.* 20 (16), 3968. doi:10.3390/ijms20163968

Martin, S. L., Epperson, L. E., Rose, J. C., Kurtz, C. C., Ané, C., and Carey, H. V. (2008). Proteomic analysis of the winter-protected phenotype of hibernating ground squirrel intestine. *Am. J. Physiology-Regulatory, Integr. Comp. Physiology* 295 (1), R316–R328. doi:10.1152/ajpregu.00418.2007

Minamide, L. S., and Bamburg, J. R. (1990). A filter paper dye-binding assay for quantitative determination of protein without interference from reducing agents or detergents. *Anal. Biochem.* 190 (1), 66–70. doi:10.1016/0003-2697(90)90134-U

Minamisawa, S., Wang, Y., Chen, J., Ishikawa, Y., Chien, K. R., and Matsuoka, R. (2003). Atrial chamber-specific expression of sarcolipin is regulated during development and hypertrophic remodeling. *J. Biol. Chem.* 278 (11), 9570–9575. doi:10.1074/jbc.M213132200

Nemkov, T., Hansen, K. C., and D'Alessandro, A. (2017). A three-minute method for high-throughput quantitative metabolomics and quantitative tracing experiments of central carbon and nitrogen pathways. *Rapid Commun. Mass Spectrom.* 31 (8), 663–673. doi:10.1002/rcm.7834

Nemkov, T., Reisz, J. A., Gehrke, S., Hansen, K. C., and D'Alessandro, A. (2019). High-throughput metabolomics: Isocratic and gradient mass spectrometry-based methods. *Methods Mol. Biol.* 1978, 13–26. doi:10.1007/978-1-4939-9236-2_2

Oliver, S. R., Anderson, K. J., Hunstiger, M. M., and Andrews, M. T. (2019). Turning down the heat: Down-regulation of sarcolipin in a hibernating mammal. *Neurosci. Lett.* 696, 13–19. doi:10.1016/j.neulet.2018.11.059

Pant, M., Bal, Naresh. C., and Periasamy, M. (2016). Sarcolipin: A key thermogenic and metabolic regulator in skeletal muscle. *Trends Endocrinol. Metabolism* 27 (12), 881–892. doi:10.1016/j.tem.2016.08.006

Pant, M., Bal, N. C., and Periasamy, M. (2015). Cold adaptation overrides developmental regulation of sarcolipin expression in mice skeletal muscle: SOS for muscle-based thermogenesis? *J. Exp. Biol.* 218, 2321–2325. doi:10.1242/jeb.119164

Porter, W. P., and Kearney, M. (2009). Size, shape, and the thermal niche of endotherms. *Proc. Natl. Acad. Sci.* 106, 19666–19672. doi:10.1073/pnas.0907321106

Rafael, J., Vsiansky, P., and Heldmaier, G. (1985). Seasonal adaptation of Brown adipose tissue in the Djungarian hamster. *J. Comp. Physiology B* 155 (4), 521–528. doi:10.1007/BF00684683

Rowland, L. A., Bal, N. C., Kozak, L. P., and Periasamy, M. (2015a). Uncoupling protein 1 and sarcolipin are required to maintain optimal thermogenesis, and loss of both systems compromises survival of mice under cold stress. *J. Biol. Chem.* 290 (19), 12282–12289. doi:10.1074/jbc.M115.637603

Rowland, L. A., Bal, N. C., and Periasamy, M. (2015b). The role of skeletal-muscle-based thermogenic mechanisms in vertebrate endothermy. *Biol. Rev.* 90 (4), 1279–1297. doi:10.1111/brv.12157

Sahoo, S. K., Shaikh, S. A., Sopariwala, D. H., Bal, N. C., and Periasamy, M. (2013). Sarcolipin protein interaction with sarco(endo)plasmic reticulum Ca2+ATPase (SERCA) is distinct from phospholamban protein, and only sarcolipin can promote uncoupling of the SERCA pump. *J. Biol. Chem.* 288 (10), 6881–6889. doi:10.1074/jbc.M112.436915

Schiaffino, S., and Reggiani, C. (2011). Fiber types in mammalian skeletal muscles. *Physiol. Rev.* 91 (4), 1447–1531. doi:10.1152/physrev.00031.2010

Shaikh, S. A., Sahoo, S. K., and Periasamy, M. (2016). Phospholamban and sarcolipin: Are they functionally redundant or distinct regulators of the sarco(Endo)Plasmic reticulum calcium ATPase? *J. Mol. Cell. Cardiol.* 91, 81–91. doi:10.1016/j.yjmcc.2015.12.030

Sopariwala, D. H., Pant, M., Shaikh, S. A., Goonasekera, S. A., Molkentin, J. D., Weisleder, N., et al. (2015). Sarcolipin overexpression improves muscle energetics and reduces fatigue. *J. Appl. Physiology* 118 (8), 1050–1058. doi:10.1152/japplphysiol.01066.2014

Soukup, T., Zachařová, G., and Smerdu, V. (2002). Fibre type composition of soleus and extensor digitorum longus muscles in normal female inbred Lewis rats. *Acta Histochem.* 104 (4), 399–405. doi:10.1078/0065-1281-00660

Tøien, Ø., Drew, K. L., Chao, M. L., and Rice, M. E. (2001). Ascorbate dynamics and oxygen consumption during arousal from hibernation in Arctic ground squirrels. *Am. J. Physiology-Regulatory, Integr. Comp. Physiology* 281 (2), R572–R583. doi:10.1152/ajpregu.2001.281.2.R572

Vergnes, L., Chin, R., Young, S. G., and Reue, K. (2011). Heart-type fatty acid-binding protein is essential for efficient Brown adipose tissue fatty acid oxidation and cold tolerance. *J. Biol. Chem.* 286 (1), 380–390. doi:10.1074/jbc.M110.184754

Warfel, J. D., Elks, C. M., Bayless, D. S., Vandanmagsar, B., Stone, A. C., Velasquez, S. E., et al. (2023). Rats lacking *Ucp1* present a novel translational tool for the investigation of thermogenic adaptation during cold challenge. *Acta Physiol.* 238 (1), e13935. doi:10.1111/apha.13935

Williams, C. T., Goropashnaya, A. V., Buck, C. L., Fedorov, V. B., Kohl, F., Lee, T. N., et al. (2011). Hibernating above the permafrost: Effects of ambient temperature and season on expression of metabolic genes in liver and Brown adipose tissue of arctic ground squirrels. *J. Exp. Biol.* 214 (8), 1300–1306. doi:10.1242/jeb.052159

Wu, J., Boström, P., Sparks, L. M., Ye, L., Choi, J. H., Giang, A.-H., et al. (2012). Beige adipocytes are a distinct type of thermogenic fat cell in mouse and human. *Cell* 150 (2), 366–376. doi:10.1016/j.cell.2012.05.016

frontiers | Frontiers in Physiology

TYPE Original Research
PUBLISHED 16 August 2023
DOI 10.3389/fphys.2023.1220058

OPEN ACCESS

EDITED BY
Yoshifumi Yamaguchi,
Hokkaido University, Japan

REVIEWED BY
Caroline Habold,
UMR7178 Institut pluridisciplinaire Hubert Curien (IPHC), France
Lara Amaral-Silva,
University of Missouri, United States

*CORRESPONDENCE
Taito Kamata,
kamata@agr.niigata-u.ac.jp

†These authors have contributed equally to this work and share last authorship

RECEIVED 10 May 2023
ACCEPTED 07 August 2023
PUBLISHED 16 August 2023

CITATION
Kamata T, Yamada S and Sekijima T (2023), Differential AMPK-mediated metabolic regulation observed in hibernation-style polymorphisms in Siberian chipmunks.
Front. Physiol. 14:1220058.
doi: 10.3389/fphys.2023.1220058

Differential AMPK-mediated metabolic regulation observed in hibernation-style polymorphisms in Siberian chipmunks

Taito Kamata[1,2*†], Shintaro Yamada[1,3†] and Tsuneo Sekijima[2]

[1]Graduate School of Science and Technology, Niigata University, Niigata, Japan, [2]Faculty of Agriculture, Niigata University, Niigata, Japan, [3]Institute of Biomedical Science, Kansai Medical University, Osaka, Japan

Hibernation is a unique physiological phenomenon allowing extreme hypothermia in endothermic mammals. Hypometabolism and hypothermia tolerance in hibernating animals have been investigated with particular interest; recently, studies of cultured cells and manipulation of the nervous system have made it possible to reproduce physiological states related to hypothermia induction. However, much remains unknown about the periodic regulation of hibernation. In particular, the physiological mechanisms facilitating the switch from an active state to a hibernation period, including behavioral changes and the acquisition of hypothermia tolerance remain to be elucidated. AMPK is a protein known to play a central role not only in feeding behavior but also in metabolic regulation in response to starvation. Our previous research has revealed that chipmunks activate AMPK in the brain during hibernation. However, whether AMPK is activated during winter in non-hibernating animals is unknown. Previous comparative studies between hibernating and non-hibernating animals have often been conducted between different species, consequently it has been impossible to account for the effects of phylogenetic differences. Our long-term monitoring of siberian chipmunks, has revealed intraspecific variation between those individuals that hibernate annually and those that never become hypothermic. Apparent differences were found between hibernating and non-hibernating types with seasonal changes in lifespan and blood HP levels. By comparing seasonal changes in AMPK activity between these polymorphisms, we clarified the relationship between hibernation and AMPK regulation. In hibernating types, phosphorylation of p-AMPK and p-ACC was enhanced throughout the brain during hibernation, indicating that AMPK-mediated metabolic regulation is activated. In non-hibernating types, AMPK and ACC were not seasonally activated. In addition, AMPK activation in the hypothalamus had already begun during high Tb before hibernation. Changes in AMPK activity in the brain during hibernation may be driven by circannual rhythms, suggesting a hibernation-regulatory mechanism involving AMPK activation independent of Tb. The differences in brain AMPK regulation between hibernators and non-hibernators revealed in this study were based on a single species thus did not involve phylogenetic differences, thereby supporting

Abbreviations: AMPK, AMP-activated protein kinase; ACC, Acetyl-CoA carboxylase; eEF2, eukaryotic elongation factor 2HP hibernation-specific protein; mTOR, mammalian target of rapamycin; p-AMPK, phosphorylated AMPK; p-ACC, phosphorylated ACC; Tb, body temperature.

the importance of brain temperature-independent AMPK activation in regulating seasonal metabolism in hibernating animals.

KEYWORDS

Acc, AMPK, brain, chipmunk, circannual rhythm, hibernation, hypothalamus, Polymorphisms

Introduction

Hibernation is a unique physiological phenomenon allowing extreme hypothermia in certain endothermic animals. Hibernating individuals switch behaviors and physiological states beyond Tb between active and hibernation phases (Geiser, 2013). Hibernating animals maintain hypothermia for days to weeks (Geiser and Ruf, 1995). In daily torpor, which is often compared to hibernation, the Tb drop is less than 12 h (Geiser and Ruf, 1995). Furthermore, hibernation is generally more seasonal than daily torpor, with hibernation occurring from fall to winter in many hibernating species (Geiser, 2020). The essential factor distinguishing the two is that the circadian clock does not control hibernation, unlike daily torpor (Ruf and Geiser, 2015). Mammalian hibernators are often typed by feeding strategies and driving mechanisms of hibernation onset. Regarding the driving mechanism, obligate hibernators (e.g., ground squirrels Spermophilus, marmots Marmotini, and bears Ursus), which are triggered by an endogenous factor such as circannual rhythm, and facultative hibernators (e.g., hamsters Mesocricetus), which are triggered by changes in environmental conditions such as food and day length (Jansky et al., 1984; Kortner and Geiser, 2000; Schwartz and Andrews, 2013; Chayama et al., 2016). The chipmunks Tamias generally belongs to the obligate hibernators; however, eastern chipmunk T. striatus has a variable depth of torpor under food conditions (Munro et al., 2005), and siberian chipmunk T. sibiricus has a daily torpor type as a regional variation (Masaki, 2005) and non-hibernating individuals (Kondo et al., 2006). Regarding feeding strategy, chipmunks and hamsters are food-storing, whereas ground squirrels, marmots and bears are fat accumulating (Vander wall, 1990; Humphries et al., 2003). Besides the physiology and behavioral ecology of hibernation, for example, resistance to adverse factors including fungi, viruses and radiation have been well-studied (Torke and Twente, 1977; Sharapov, 1984; Schwartz et al., 2015; Puspitasari et al., 2021). Understanding the systems that regulate seasonal switching is very interesting and has long been the subject of research on hibernating animals (for example, ground squirrel: Yurisova and Polenov (1979); Ren et al. (2022), hamster; Bartness and Wade (1985); Garidou et al. (2003), bear; Fedrov et al. (2014), bat; Callard et al. (1983). Until the 1980s, the approach was mainly based on humoral factors and anatomy (Dawe and Spurrier, 1972; Oeltgen et al., 1978; Hudson and Wang, 1979). Since the 1990s, advancements in molecular biology techniques have allowed for the investigation of various genes that undergo changes in relation to the hypothermic state of hibernation in tissues such as the brain and liver (Takamatsu et al., 1993; Srere et al., 1995; O'Hara et al., 1999). From the 2000s onwards, omics analyses have made it possible to comprehensively profile the physiological states of hibernating animals, revealing the expression of genes and proteins involved in low-temperature tolerance and energy metabolism during hibernation (Williams et al., 2006; Shao et al., 2010; Schwartz et al., 2013; Xu et al., 2013). Recently, there has been increased interest in hibernation and daily torpor state, which is a period of reduced metabolism shorter than hibernation, in the fields of medicine and drug discovery. Approaches such as cell culture studies and manipulation of the nervous system have been utilized to analyze the intrinsic characteristics of hibernating cells and the mechanisms of low-temperature induction *in vivo* (Ou et al., 2018; Hrvatin et al., 2020).

Whether physiological and biomolecular changes during hibernation are the driving factors for hibernation or not, require careful discussion. Extreme hypothermia alters hundreds of gene expressions (Williams et al., 2006; Shao et al., 2010; Schwartz et al., 2013; Xu et al., 2013), and it is unlikely that all of the change factors are hibernation drivers. Therefore, simple comparisons of the changes in physiological states that occur with hibernation are likely to detect noise in elucidating the driving mechanisms of hibernation. Studies incorporating several perspectives can effectively test whether target factors are associated with hibernation drive. For example, Grabek et al. (2015) focused their validation on the phase immediately before the transition to hypothermia, in addition to the active and hibernating phases, to extract genetic changes independent of hypothermia. In addition, attempts have been made to consider the significance of their physiological mechanisms by comparing hibernating and non-hibernating animals (Caprette and Senturia, 1984; Matos-Cruz et al., 2017). However, for the former, there is the problem that the hibernation transition period is difficult to define, while for the latter, phylogenetic differences between different species are inevitably included. It is essential to consider physiological and phylogenetic differences when making comparisons to determine whether changes in specific factors are involved in driving hibernation.

We have previously focused on the metabolic regulator protein AMPK to elucidate the mechanism of metabolic regulation of hibernation during fluctuations in Tb. AMPK is an intracellular, trimeric protein kinase of α, β, and γ subunits (Kahn et al., 2005). This kinase is phosphorylated and activated when intracellular AMP/ATP increases. It maintains constant intracellular energy homeostasis by activating the catabolic pathway and inhibiting the anabolic pathway. Activated AMPK increases ATP synthesis by phosphorylating ACC, which is involved in fatty acid synthesis (Dyck et al., 1999). Furthermore, activated AMPK is known to suppress protein synthesis via phosphorylation of eEF2, which is involved in the translation process of protein synthesis (Browne et al., 2004). AMPK has also been reported to have cytoprotective effects via energy saving, such as ischemia tolerance and cancer suppression. More recently, it has become clear that changes in AMPK activity in the brain's nerves also regulate systemic metabolisms, such as feeding and heat production, via the

autonomic nervous system (López et al., 2016). We hypothesized that AMPK as a metabolic sensor may be involved in metabolic regulation of hypothermia tolerance in hibernation and in nervous system-mediated systemic metabolic inhibition, and we have conducted research on AMPK function during hibernation. We compared the expression levels of p-AMPK and p-ACC in different tissues of hibernating and active siberian chipmunks (Yamada et al., 2019). As a result, we have shown that p-AMPK and p-ACC are enhanced during hibernation, particularly in the brain, and may inhibit protein synthesis in brain cells via downstream factors such as eEF2. On the other hand, phosphorylation of AMPK was not observed in most of the peripheral tissues. In marmot, some studies have reported changes in p-AMPK in the hypothalamus during hibernation and while awakening from hibernation by administration of an AMPK agonist to the third ventricle (Florant et al., 2010). These results suggest that modulation of AMPK activity in the brain may be involved in the metabolic regulation of hibernation and hypothermia tolerance. However, it is not known whether these changes in AMPK activity are specific to hibernating animals and related to the driving of hibernation, or are linked to a further hypothermia-dependent response.

In this study, we approached the position of AMPK in the hibernation regulation of chipmunks from two perspectives. First, we examined whether the seasonal activation of AMPK was hibernation specific. A non-hibernating type of siberian chipmunk has been confirmed, which does not exhibit hibernation throughout its life span (Kondo et al., 2006). We focused on the polymorphisms of their hibernation style, expecting to be able to minimize phylogeny-dependent physiological differences. Criteria for classifying hibernation styles were established by long-term Tb monitoring. We tested whether hypothermia is induced by day length changes and stress, in order to prove that the non-hibernating type is not a reversible phenotype. We clarified whether the non-hibernating type activates AMPK seasonally, using the hibernating type as a control group. Second, we investigated whether changes in AMPK precede the induction of hibernation. To precisely define the hibernation transition phase, we prepared natural day length conditions and monitored blood HP levels known to induce hibernation in chipmunks (Kondo et al., 2006). By comparing the three phases of active, pre-hibernation, and hibernation, we clarified whether AMPK activation was a factor that was altered prior to the induction of hypothermia.

Materials and methods

Animals

Male siberian chipmunks less than 1 year of age were purchased from Arcland Sakamoto Co. The animals were housed individually at 23°C under 12 h-light/dark cycle conditions and provided a standard mouse diet and water *ad libitum*. The animals were maintained under these conditions for at least 6 months to acclimate to laboratory conditions. After checking their general health conditions, they were used in the experiments described below.

All experiments involving the animals complied with protocols that were reviewed by the Institutional Animal Care and Use Committee and approved by the President of Niigata University (Permit Number: Niigata Univ. Res. 13–2, 258–1, 399–1, 530, SA00106, SA00107, SA00228, and SA00738). All protocols performed followed the Guiding Principles for Care and Use of Laboratory Animals (NIH, United States).

Determination of hibernation state by measuring surface Tb

Temperature logger measurements are common in hibernation studies; however, the effects of invasive procedures on the maintenance of a non-hibernating state in chipmunks remains unknown. Therefore, we investigated the relationship between surface and core Tb to establish a non-invasive method of determining hibernation state.

Paraffin-coated (Eto et al., 2018) temperature loggers (Thermochron G, KN Laboratories) were implanted in the abdominal cavity of anaesthetized animals. Five animals were kept at 23°C for 2 weeks after implantation, then transferred to conditions of constant 5°C and darkness and monitored for 30 days. We measured core Tb every 30 min, and measured surface Tb (using an infrared irradiation thermometer; IT-540N, HORIBA) 21 times per animal throughout the study period, matching the timing of core Tb measurements.

Establishment of criteria for classifying hibernation style

To create typological criteria for hibernation styles (hibernating and non-hibernating types), we kept 324 animals under conditions of constant 5°C and darkness. We measured the surface Tb once daily (17:00–20:00). We placed wood chips on the body surface of hibernating animals to confirm whether they were still hibernating the next day. Food and water were provided *ad libitum*. Through lifelong monitoring, the number of days of cold exposure required to induce hibernation was determined.

Hibernation induction under semi-natural conditions

To support that hibernating and non-hibernating types are not differences in animal decision-making but phenotypic irreversibility, we considered that validation under conditions other than 5°C and constant darkness be necessary. Therefore, we conducted a hibernation induction experiment by semi-natural conditions. Furthermore, this experiment will allow us to make seasonal comparisons of Tb for chipmunks whose life cycles are free-running under constant conditions such as 5°C and constant darkness (Kondo et al., 2006).

Initially, 11 animals were kept under 5°C and darkness for 190 days and Tb monitoring was performed to classify hibernating (n = 5) and non-hibernating types (n = 6). We moved the animals to semi-natural condition in April. The environment in this room is controlled by natural light and outside temperature. Day length and outside temperature changes

during the experiment are shown in Supporting Information S1. In Niigata Prefecture, Japan, where the experiments were conducted, day length was approximately 10–15 h, and the range of temperature was −1.7°C–30.8°C (JMA, 2023; NAOJ, 2023) during the experiment. Room temperature was controlled not to exceed 25°C.

We set up three treatments: hibernating type (CT, n = 5) and non-hibernating type (NH, n = 3) with food and water provided *ad libitum*, and non-hibernating type with bi-daily water deprivation (NHW, n = 3). We conducted water deprivation from 21-September to 20-March under short-day conditions (12 h or less). Water deprivation has long been considered one of the external factors involved in the occurrence or non-occurrence of hibernation onset (Ibuka and Fukumura, 1997). Core Tb was measured with implanted loggers from September to May.

Measurement of blood HP concentration

For comparison of HP regulation (as described by Kondo et al., 2006), we kept hibernating (n = 11) and non-hibernating types (n = 5) under 5°C and darkness for 24 months. We collected blood samples from the lateral tarsal vein of experimental animals once a month. Samples of approximately 400 µl of blood were collected, and plasma was separated using a centrifuge. To prevent clotting during blood collection, 10 µl of heparin was mixed with the blood. The separated plasma was stored at −80°C until the concentration was measured. The Western blot method was used to measure the concentration of HPs (HP-20, HP-25, and HP-27) in the blood.

Tissue sampling

As the non-hibernating type does not exhibit hypothermia, it is difficult to identify the phases corresponding to the transition from the active season to the hibernating season in this type. Tissue sampling was therefore conducted under semi-natural conditions. We sampled hibernating types in three phases: active, pre-hibernation, and hibernation. The timing of sample-taking was guided by Tb and blood HP levels (Supporting Information S2). HP is a factor related to hibernation regulation in chipmunks and is known to decrease blood levels prior to hibernation (Kondo and Kondo, 1992). For the non-hibernating type, only the month was used as a guide, as neither Tb nor blood HP changes. Therefore, we sampled active hibernating and non-hibernating types in summer, hibernating type during the pre-hibernation state in autumn, and both hibernating and non-hibernating types in winter.

We anaesthetized the animals using CO_2 then euthanized them by decapitation. After craniotomy, the brain was divided on ice into the cerebral cortex, hippocampus, cerebellum, diencephalon, and hypothalamus regions. The heart, liver, kidneys, and skeletal muscle were sampled for peripheral tissues after opening the abdomen. Each tissue sample was frozen on dry ice and stored at −80°C.

Materials

Anti-phospho-AMPKα (Thr172), anti-phospho-ACC (Ser79), were purchased from Cell Signaling Technology. Validation of their antibody specificity to chipmunk proteins has been confirmed in a previous study (Yamada et al., 2019). The amino acid sequence of AMPKα1, the phosphorylation site of AMPK, the target molecule in this study, has also been shown to be well conserved among species (Yamada et al., 2019). We used the same antibodies that were used by Kondo et al. (2006), having received them from Dr. Kondo. HP is a protein that forms a complex of three types: −20, −25, and −27. As previous studies (Kondo and Kondo, 1992; Takamatsu et al., 1993) have shown that the blood cycles of any HP are synchronized, in this study we used the HP-20 antibody to measure the hibernation cycle of chipmunks.

Western blotting

Tissue extracts and Western blotting were performed as described previously by Yamada et al. (2019). Frozen tissue samples were weighed and homogenized in ten volumes of lysis buffer (62.5 mM Tris-HCl (pH 6.8), 2% SDS, Complete protease inhibitor cocktail (Roche Applied Science Ltd.), and PhosStop (Roche Applied Science). After centrifugation (15,000 rpm × 60 min), supernatants were collected. The protein concentration of each sample was determined by Lowry (BIO-RAD). For plasma samples, a 100-fold volume of lysis buffer (62.5 mM Tris-HCl (pH 6.8), 2% SDS, Complete protease inhibitor cocktail (Roche Applied Science) was used.

Equal amounts of protein (30–50 µg per lane for indicated molecules) were subjected to sodium dodecyl sulfate-polyacrylamide gel electrophoresis (7.5%–15% acrylamide) and transferred to polyvinylidene fluoride membranes. Plasma samples were loaded to 10 nl per lane and electrophoresed in the same manner as tissue samples. Membranes were cropped around the appropriate molecular size to save the amount of antibodies. The membranes were blocked in TNT (150 mM NaCl, 10 nM Tris-HCl (pH 7.4), and 0.05% tween-20) containing 10% BSA and then incubated with the indicated primary antibody overnight. After washing with TNT, blotted membranes were incubated with horseradish-peroxidase (HRP)-conjugated anti-rabbit IgG (1: 10000 dilution; Dako Cytomation) or HRP-conjugated anti-mouse IgG (1:10000 dilution; Jackson Immune Research) for 1 h. After washing, peroxidase activity was detected by chemiluminescence reagents (Western Lightning, PerkinElmer Life Science) and visualized on X-ray film (Fujifilm Medical). The quantity of protein expressed was quantified by ImageJ software and standardized by β-actin.

Statistical analysis

We used R ver. 4.2.1 for all statistical analyses (R Core Team, 2023). Log-Rank tests were used to compare survival rates between hibernating and non-hibernating types, and T-tests were used for all two-group comparisons. For all multi-group comparisons we used analysis of variance (ANOVA) and Tukey HSD test. To demonstrate circannual rhythmicity, we Fourier transformed blood HP levels for 24 months and calculated frequencies (month) and amplitudes. We showed the mean ± SE in results.

10.3389/fphys.2023.1220058

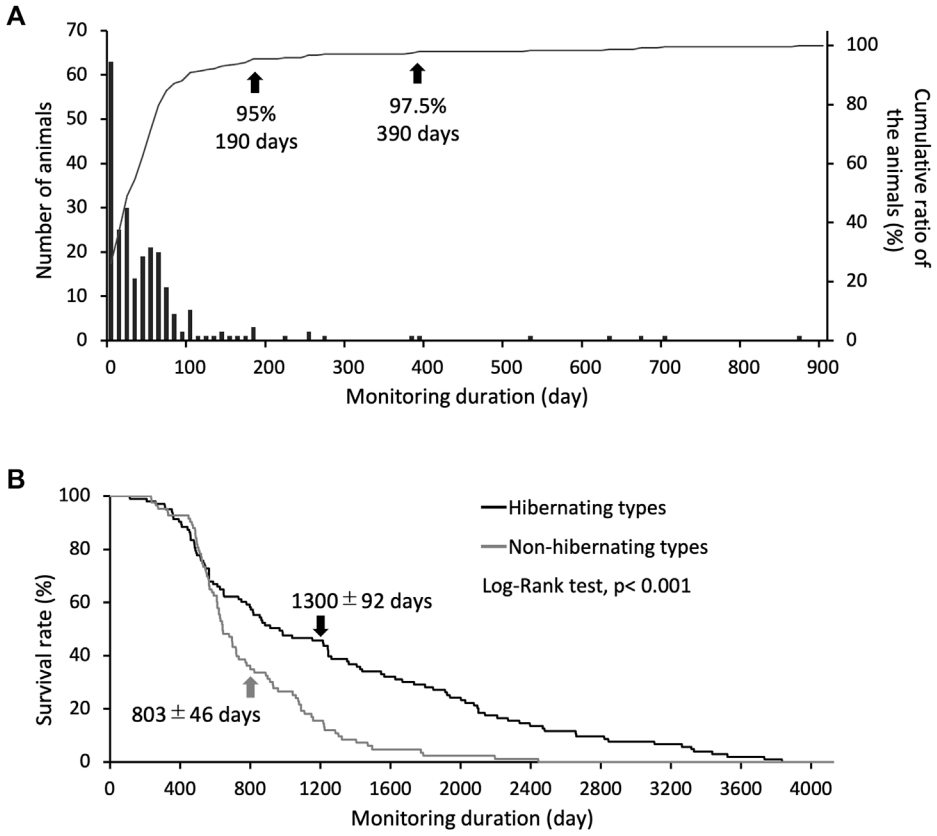

FIGURE 1
Criteria for identifying hibernation styles through long-term hibernation monitoring. **(A)** bars show the number of animals for each day required to reach hibernation induction, and the line shows the cumulative ratio of the animals hibernated (only use hibernating types, n = 241). Arrows indicate the number of days for the classification accuracy of hibernating and non-hibernating types. **(B)** Shows the difference in survival rates between individual hibernating (n = 103) and non-hibernating chipmunks (n = 83), with a significant difference between them (Log-Rank test, $p < 0.001$). Arrows show mean ± SE.

Results

Relationship between core and surface Tb

Under conditions of 5°C and darkness, surface Tb during hibernation was in the range 3.7°C–7.9°C, and core Tb was in the range 4.5°C–8.0°C, whereas during arousal surface Tb was in the range 14.9°C–23.4°C and core Tb was in the range 36.0°C–38.5°C (Supporting Information S3A). Hibernating and arousal states could be clearly distinguished because Tb ranges did not overlap. Therefore, we defined hibernation state as surface Tb below 10°C and arousal state as above 11°C. This criterion allowed non-invasive monitoring of hibernating types that hibernate periodically and non-hibernating types that never hibernate (Supporting Informations S3B, C).

Criteria for classifying hibernation styles

Induction of hypothermia was identified in 241 of 324 study animals, of which 95% became hypothermic and hibernated after 190 days, and 97.5% became hypothermic and hibernated after 390 days (Figure 1A). Eighty-three non-hibernating animals were identified. The life span of the hibernating type (1,300 ± 92 days) was approximately 1.7 times that of the non-hibernating type (803 ± 46 days), indicating a significant difference in survival rates between the two types (Figure 1B). Individuals used for life-span analysis were kept at 5°C throughout their lives.

Variation of HP regulation between hibernation styles

HPs fluctuation patterns of hibernating and non-hibernating types under conditions of 5°C and darkness were studied for 2 years (see Figure 2A). Fourier transformation of the 24-month HPs levels showed that the most substantial amplitudes for the hibernating type were at frequencies of approximately 12 months. In contrast, the amplitudes were weaker for the non-hibernating type (Figure 2B). we focused on the standard deviations of HPs changes and found significant differences between hibernating and non-hibernating types (Figure 2C).

Non-hibernating type as an irreversible phenotype

The hibernating type showed seasonal hibernation induction, whereas the non-hibernating type did not become

10.3389/fphys.2023.1220058

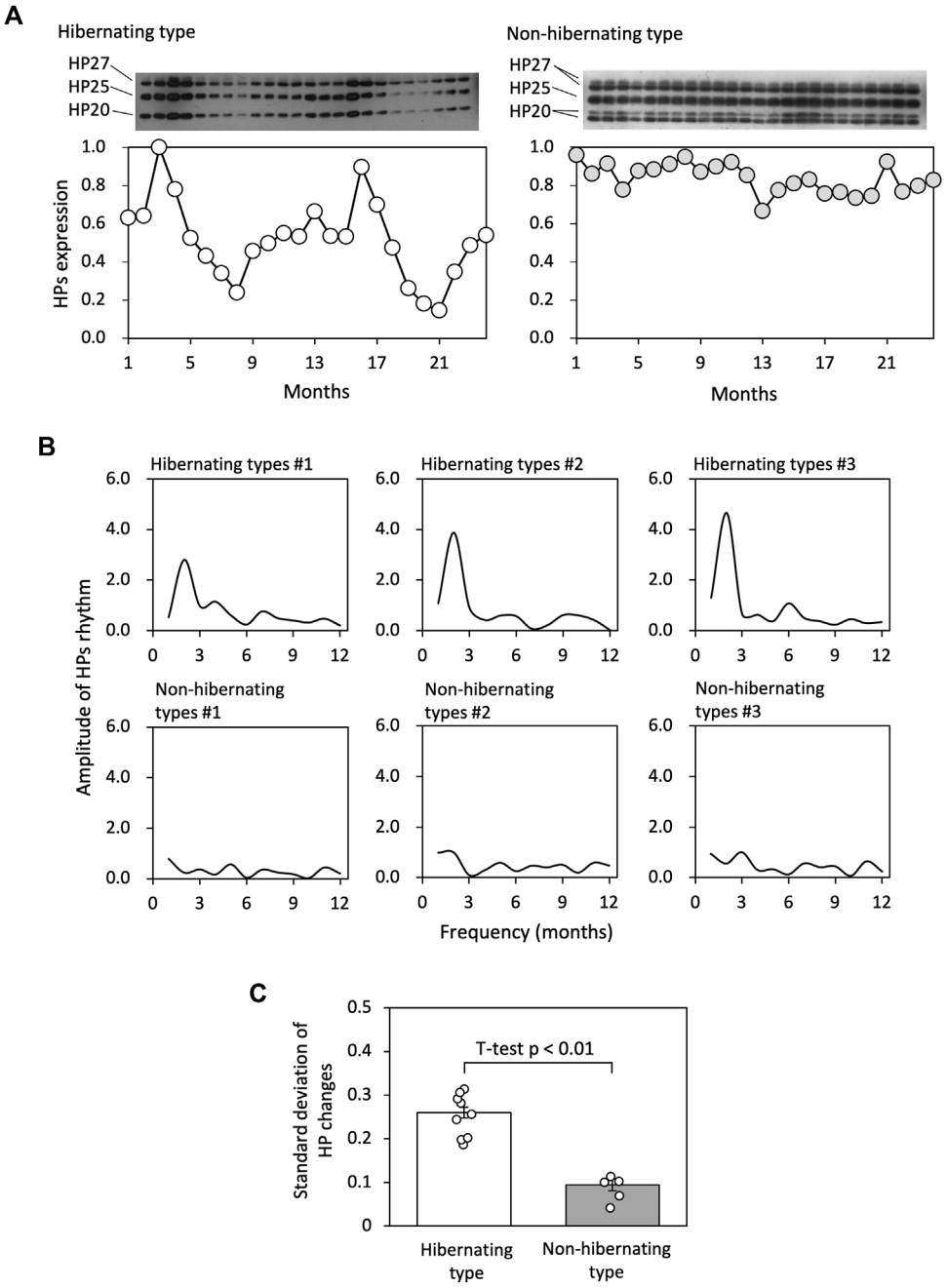

FIGURE 2
Comparison of HP regulation between hibernating and non-hibernating types. **(A)** Shows typical HPs (HP-20, HP-25, and HP-27) fluctuation patterns of hibernating and non-hibernating types under conditions of 5°C and constant darkness. **(B)** Shows the amplitude values for frequency (months) of the HPs rhythm for 24 months by Fourier transformation in hibernating and non-hibernating types. **(C)** Shows the standard deviation of HPs level for hibernating (n = 11) and non-hibernating types (n = 5).

hypothermic, even under water stress (Figure 3). Mean value ± SE of minimum Tb measurements throughout the experimental period were 8.6°C ± 0.1°C for CT, 35.8°C ± 0.4°C for NH, and 33.3°C ± 0.7°C for NHW. The mean value of parameters on hibernation (only CT) were as follows: hibernation began on 2 November ± 5.1 days and ended on 15 April ± 2.5 days; 54.6 ± 4.4 times of bout were recorded with a maximum hibernation bout of 94.4 ± 2.7 h; mean hibernation duration was 164 ± 6.2 days.

We focused on Tb during the arousal state, so as to allow for comparisons between hibernating and non-hibernating types (Figure 4). Significant differences between treatments were found between September (before hibernation) and April (after hibernation ended). No significant differences

10.3389/fphys.2023.1220058

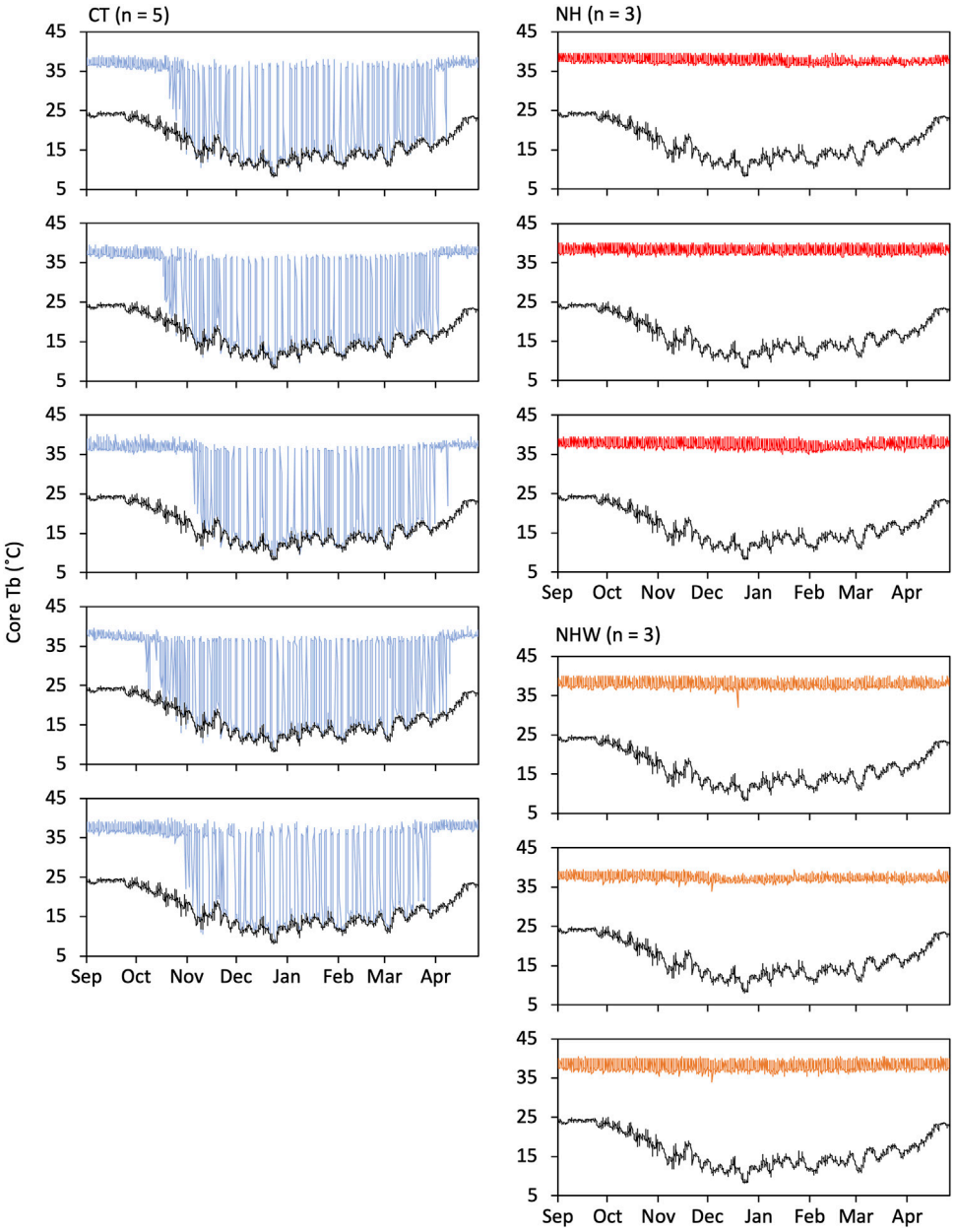

FIGURE 3
Hibernation induction under semi-natural conditions. Hibernating and non-hibernating types classified by monitoring under conditions of 5°C and darkness after being moved to semi-natural conditions. We investigated whether non-hibernating types hibernate under natural environmental conditions (temperature and day length changes) and bi-daily water deprivation (from 23 September to 21 March). Tb changes of all animals used in the experiment are shown in figure. Specify colored line indicates Tb and black line indicate the ambient temperature. CT (hibernation type, blue), NH (non-hibernating type, red), and NHW (non-hibernating type with water deprivation, orange).

were found in May, the active season. The most significant divergence in arousal temperature between hibernating and non-hibernating types (a difference of approximately 2.5°C) was during the mid-hibernation period, in December. All groups showed diurnal synchronized changes in Tb, which increased during the day and decreased at night, with the differences between groups being greater during the day (08:00–16:00) than at night (16:00–08:00).

Comparison of AMPK activation between hibernation style polymorphisms

p-AMPK and p-ACC were enhanced in all brain regions during hibernation, and significant differences were found between summer and winter in the hibernating type (Figure 5A). For p-AMPK and p-ACC of the non-hibernating type, significant differences were found between summer and winter only in the hippocampus, which was enhanced in winter (Figure 5B).

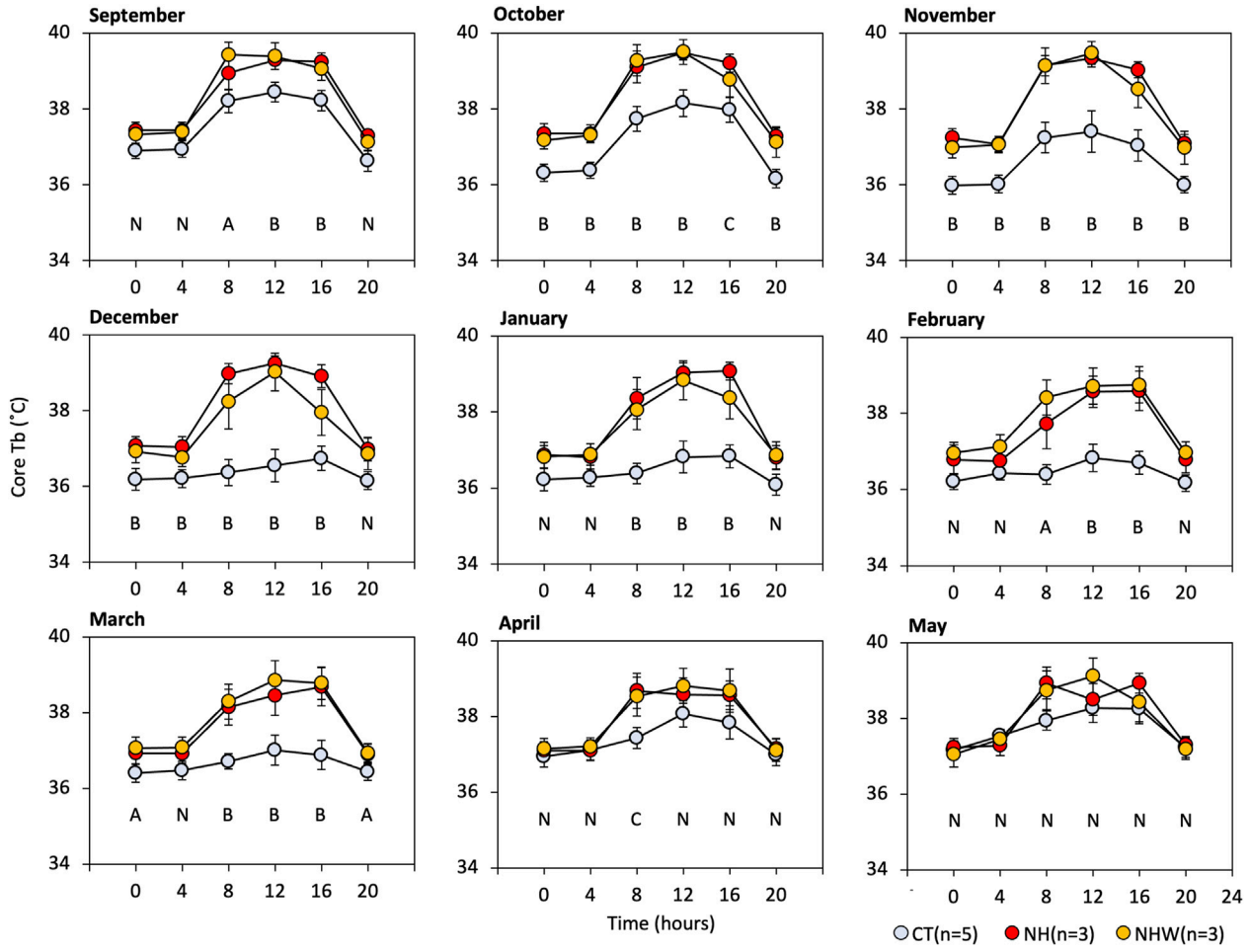

FIGURE 4
Monthly arousal Tb under semi-natural conditions. We extracted core Tb every 4 hours while subjects were awake (≥35°C). Specify colored circle indicates arousal Tb. CT (hibernation type, blue), NH (non-hibernating type, red), and NHW (non-hibernating type with water deprivation, orange). Letters indicate multiple comparisons with statistical significance (N, no significance in all combinations; A, CT-NHW; B, CT-NH, and–NHW; C, CT-NH), $p < 0.05$ Tukey HSD after ANOVA). Error bars indicate SE.

For peripheral tissues during hibernation, no significant differences in p-AMPK were found between summer and winter for almost all tissues (Figure 6A). p-AMPK expression was decreased only in the liver. For p-ACC, significant differences between summer and winter were found only in the liver and kidney, with a decrease in the liver and an increase in the kidney during winter (Figure 6A). For the non-hibernating type, a significant difference between winter and summer was found only in p-AMPK in the kidneys (Figure 6B).

AMPK activation in the pre-hibernation period

Significant differences between summer and autumn were found for p-AMPK in the cerebral cortex and diencephalon and for p-ACC in the hypothalamus (Figure 7). Significant differences between autumn and winter were found for p-AMPK in the diencephalon and p-ACC in the hypothalamus. Although no significant differences were found, p-AMPK levels in the hypothalamus and p-ACC levels in the cortex and hippocampus tended to be greater in autumn than in summer.

Discussion

Hibernation style polymorphisms

Several studies of intraspecific variation in hibernation have been conducted on Sciuridae. Among ground squirrel species, hibernation periods have been reported to vary regionally (Zervanos et al., 2010; Sheriff et al., 2011; Grabek et al., 2019). Variation among individuals within the same population has been reported in the eastern chipmunk, the Tb of the hibernating state and energy reserves determine the torpor frequency and depth (Munro et al., 2005; Levesque and Tattersall, 2010). Siberian chipmunks from the Korean (T. s. barberi) and Japanese populations (T. *s. lineatus*) have different hibernation patterns under the same keeping conditions, with shorter bouts in the former and longer ones in the latter (Masaki, 2005). The

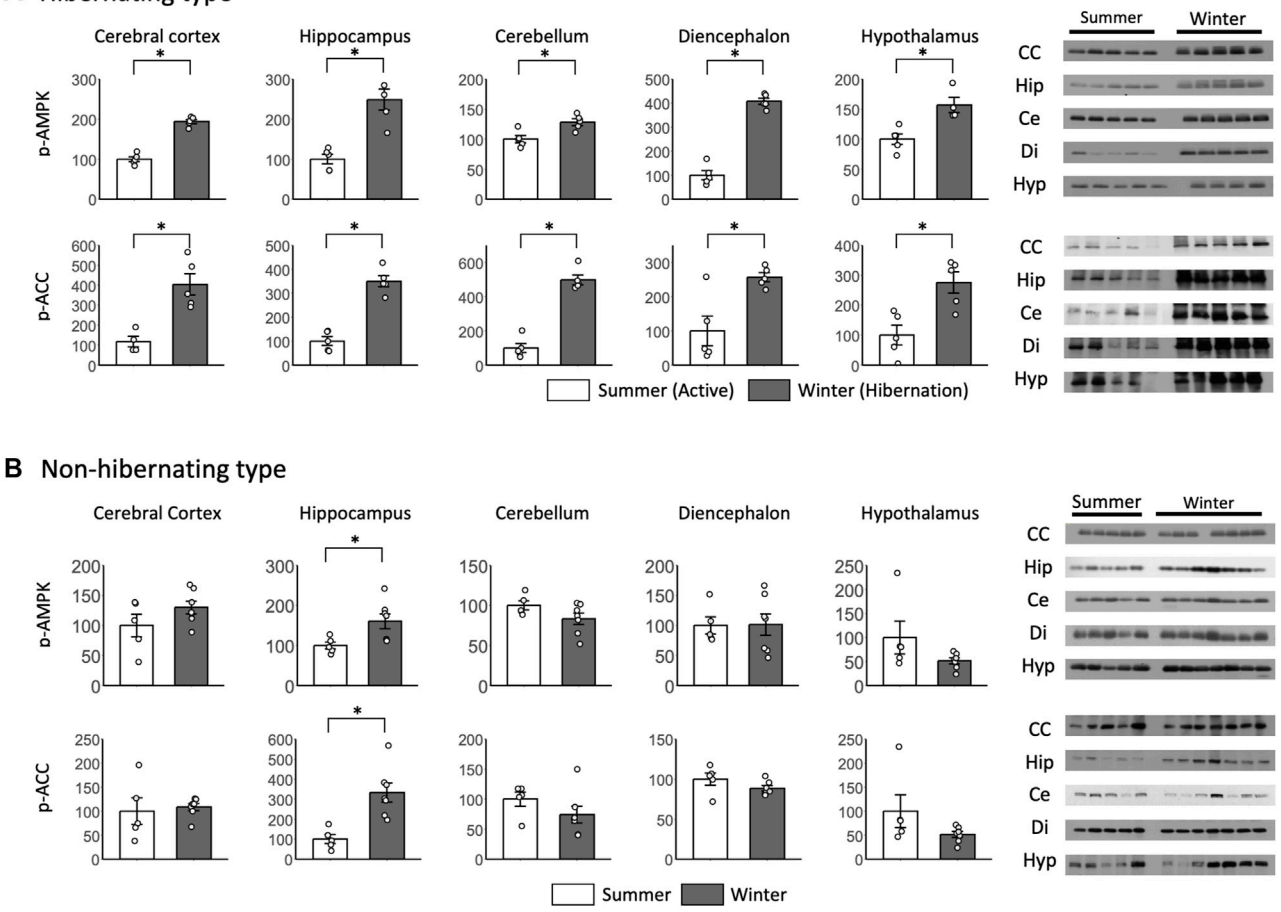

FIGURE 5
Comparison of phosphorylated AMPK and ACC expression in the brain between hibernating and non-hibernating types. Expression levels of phosphorylated AMPK and ACC (p-AMPK and p-ACC) in brain tissues (cerebral cortex, hippocampus, cerebellum, diencephalon, and hypothalamus) of hibernating **(A)** and non-hibernating types **(B)**. Error bar means SE. Hibernating type: active n = 5 (hypothalamus only n = 4), Hibernating n = 5, non-hibernating type summer n = 5, winter n = 7. CC: Cerebral Cortex; Hip: Hippocampus; Ce: Cerebellum; Di: Diencephalon; Hyp: Hypothalamus. *$p < 0.05$ student' t-test. Internal control see Supporting Information S4A.

clear emergence of hibernating and non-hibernating types, even in the same keeping condition as in our study, is extremely rare in hibernation studies to date. Whether non-hibernating types behave in the field has not been confirmed, however, Turbill and Prior (2016) estimate that survival rates for non-hibernating rodents are higher and hibernating rodents lower in warmer environments. Siberian chipmunk, which has a wide range in Eurasia (Lissovsky et al., 2017), may be regionally adapted by having a polymorphism of various hibernation styles. Investigating the distribution, abundance ratios, and phylogeny of the polymorphisms in the field are future works.

We found the lack of a blood HP rhythm in non-hibernating types to be evident, as did Kondo et al. (2006) in a previous study, and it seems likely that there are mutations in the integrative regulatory systems involved in HP transport to the brain. Pseudogenization of HP in the family Sciuridae results in a lack of hibernation ability (Takamatsu et al., 1993; Kojima et al., 2001; Ono et al., 2003; Tsukamoto et al., 2007), indicating that HP regulation is involved in the mechanisms that determine hibernation style. The presence or absence of HP brain transport in the non-hibernating type is a target for future research.

In syrian golden hamsters *Mesocricetus auratus* and arctic ground squirrels Urocitellus parryii, it has been reported that decreased arousal Tb is related to the hibernation cycle (Olson et al., 2013; Chayama et al., 2016). The relationship between hypometabolism on arousal and extreme hypothermia, such as in hibernation and daily torpor, has been tested by administering N6-Cyclohexyladenosine (CHA) to starved rats and ground squirrels (Jinka et al., 2010; Jinka et al., 2011; Olson et al., 2013). Sensitivity to CHA is increased at lower Tb levels, which has been shown to result in more significant temperature reductions than at high Tb levels. Mechanisms that allow hypothermia may be associated with reduced basal Tb. A lack of such a function may be inferred in the non-hibernating type.

Little is known about the genetic regulatory mechanisms involved in intraspecific variation in hibernation style. Grabek et al. (2019) recently showed that genetic factors are responsible for intraspecific variation in the hibernation period of thirteen-

10.3389/fphys.2023.1220058

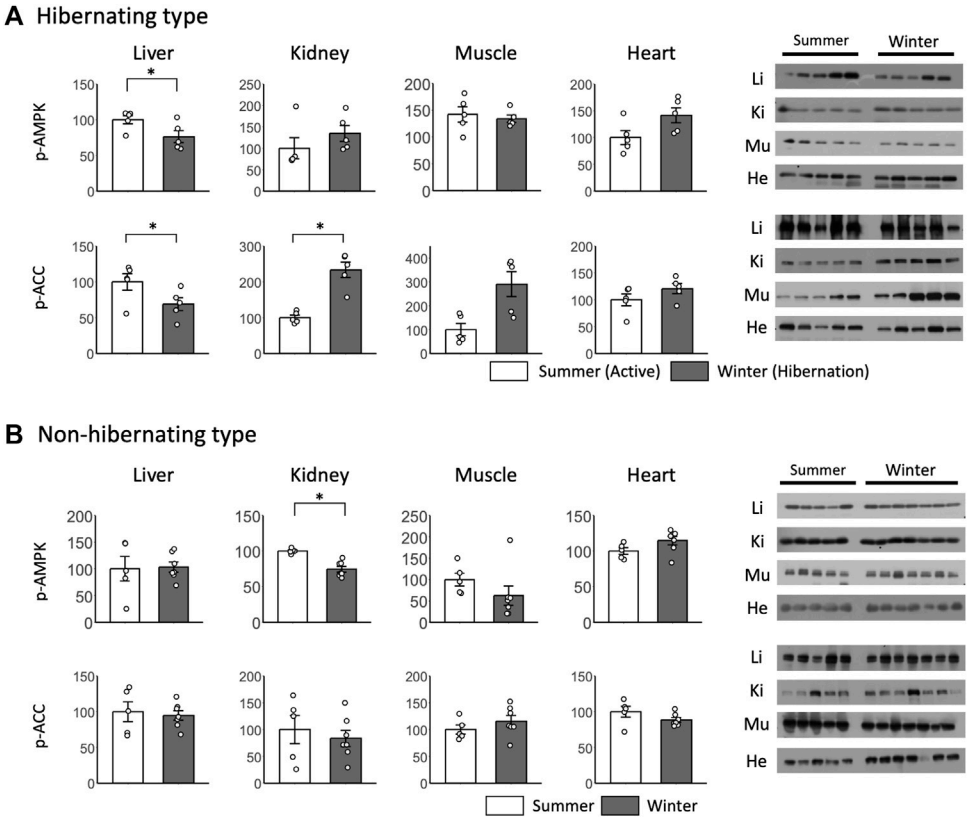

FIGURE 6
Comparison of phosphorylated AMPK and ACC expression in peripheral tissues between hibernating and non-hibernating types. Expression levels of phosphorylated AMPK and ACC (p-AMPK and p-ACC) in peripheral tissues (liver, kidney, muscle, heart) of hibernating **(A)** and non-hibernating types **(B)**. Error bar means SE. Hibernating type: summer n = 5, winter n = 5 (hypothalamus only n = 4), non-hibernating type summer n = 5, winter n = 7. Liv, Liver; Kid, Kidney; Mus, Muscle; Hea, Heart. *$p < 0.05$ student' t-test. Internal control see Supporting Information S4A.

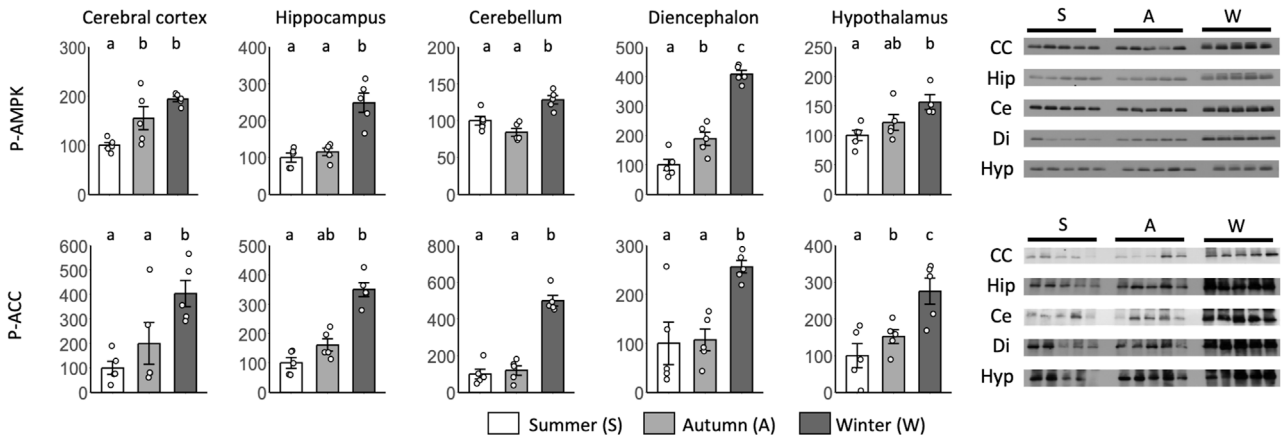

FIGURE 7
Seasonal AMPK and ACC expression in the brain during the hibernation transition. Expression levels of phosphorylated AMPK and ACC (p-AMPK and p-ACC) in brain tissues (cerebral cortex, hippocampus, cerebellum, diencephalon, and hypothalamus) during summer, autumn, and winter. Error bar means SE. Hibernation type: summer n = 5 (hypothalamus only n = 4), autumn n = 5, winter n = 5. Letters indicate significant differences, $p < 0.05$ Tukey HSD after ANOVA. CC, Cerebral Cortex; Hip, Hippocampus; Ce, Cerebellum; Di, Diencephalon; Hyp, Hypothalamus. Internal control see Supporting Information S4B.

lined ground squirrel Ictidomys tridecemlineatus. However, there have been no reports on the genetic factors determining hibernation or non-hibernation within the same species. To address this subject, we have established chipmunk breeding methods under laboratory conditions and have successfully carried out planned crosses (Kamata et al., 2020). In the future we aim to use breeding and positional cloning to elucidate the mode and rate of inheritance of hibernation-style polymorphisms, and search for the dominant genes involved in the hibernation drive.

Is AMPK activation related to a driving factor for hibernation?

AMPK activation in hibernating animals has been reported to be enhanced in the ground squirrel's adipocytes (Horman et al., 2005) and in the chipmunk brain's cerebral cortex and hypothalamus (Yamada et al., 2019). AMPK activation in the liver was inconsistent, with some enhanced and some suppressed (Yamada et al., 2019). Unlike Yamada et al. (2019), the present study found enhancement in the whole brain (cerebral cortex, hippocampus, cerebellum, diencephalon, and hypothalamus), and we consider that the inconsistency in responses is likely related to rearing conditions. In Yamada et al. (2019), study animals were maintained at 5°C and in constant darkness, while in this study, they were maintained at ambient temperature and natural day length. The hibernation cycle of chipmunks is free-running under constant-dark conditions (Kondo et al., 2006) and is adjusted by natural day length (Figure 3). The metabolic regulator Akt, which shares a downstream factor with AMPK, is known to change its phosphorylation state depending on the phase of hibernation regulation (Cai et al., 2004). The more pronounced phosphorylation of AMPK in this study may be because AMPK phosphorylation by the hibernation cycle was detected more accurately than by Yamada et al. (2019).

The seasonal activation of AMPK in the brain occurred according to circannual rhythms and disappeared with the lack of the rhythms, which strongly supports a relationship between AMPK and hibernation. AMPK activation in hibernation is not independently influenced by day length and would be regulated by endogenous mechanisms. As for the peripheral tissues, AMPK activation may not be essential for metabolic regulation in hibernation, as pointed out in a previous study (Horman et al., 2005). However, previous studies (Horman et al., 2005; Yamada et al., 2019) as well as the current study consistently observed the suppression of AMPK phosphorylation in the liver during hibernation. This suggests that AMPK may be suppressed by regulatory functions to strongly promote fatty acid synthesis as an energy storage source, as Horman et al. (2005). In the non-hibernating type, phosphorylation of AMPK and ACC was found during hibernation only in the hippocampus, despite the absence of AMPK phosphorylation in most tissues. It is well known that the hippocampus is the brain region primarily important for memory, and AMPK has been reported to have memory-related functions in the hippocampus (Zhou et al., 2023). Several studies on memory during hibernation have been reported. In particular, male chipmunks have been reported to memorize a female's den before hibernation for the early spring mating season and to be able to maintain this memory during hibernation (Kawamichi and Kawamichi, 1993). Thus, the phosphorylation of AMPK and ACC in the hippocampus of non-hibernating chipmunks as well as hibernating chipmunks may suggest that signaling systems related to neural energy utilization and seasonal regulation related to neural plasticity in relation to memory are driven by a different system than hibernation.

Since physiological changes that precede hibernation begin before hypothermia (Kondo, 1987; Grabek et al., 2015), the pre-hibernation state is considered an essential phase for elucidating the driving mechanisms. *In vitro* assays revealed that AMPK is activated at low temperatures (Knight et al., 2015); however, our study found a non-temperature dependence of seasonal AMPK activation in the hypothalamus and mesencephalon. AMPK functions in the brain include acting on downstream factors such as eEF2, mTOR, and ACC to inhibit protein and lipid synthesis and reduce wasteful energy consumption (Kahn et al., 2005). Furthermore, these functions are known to have protective effects on neurons, including ischemia tolerance, by suppressing reactive oxygen species and energy starvation and promoting autophagy. Since hypothermia is known to cause leakage of neurotransmitters and damage to mitochondria and cytoskeleton by reactive oxygen species (Schwartz et al., 2013; Ou et al., 2018), activation of AMPK during the hypothermic phase of hibernation may have a protective effect on neurons from low temperature and energy starvation. On the other hand, it has been noted that excessive AMPK activation can also cause excessive activation of autophagy and destroy neurons (Li et al., 2011), which will need to be verified in the future. AMPK has recently been shown to be involved in feeding and body thermoregulation, in addition to its function in neurons alone, by being activated in the diencephalon and hypothalamus (López et al., 2016). Activation of AMPK in the hypothalamus produces heat in brown adipose tissue and other tissues via sympathetic inhibition, and activation of AMPK in the Arcuate Nucleus enhances feeding (López et al., 2016). AMPK agonists induced feeding and inhibited hibernation in marmots, which fast during hibernation (Florant et al., 2010). In chipmunks, in contrast, known to feed during hibernation, activation of AMPK in the hypothalamus may be essential for maintaining feeding. AMPK is activated in the hypothalamus and mesencephalon before and during hibernation when basal body temperature decreases (Figure 4). Suppression of thermogenesis in brown adipose tissue via activation of AMPK (López et al., 2016) is associated with hibernation. It may contribute to increased brown adipose tissue before hibernation (MacCannell et al., 2017). Although it is not clear in this study whether AMPK affects the hypothermia induction of hibernation, in the future, intracerebroventricular administration experiments, as well as detailed behavioral and temperature monitoring, will clarify the relationship between AMPK activation and the function of hibernation.

AMPK activation during starvation is a passive response dependent on external factors (Kajita et al., 2008; Healy et al.,

2011). In contrast, AMPK activation associated with the hibernation cycle is an active regulatory system, that is, adjusted by external factors (day length and ambient temperature). The variation of AMPK seasonality and the lack of HP rhythm may be vital to revealing the driving mechanisms of hibernation. Adiponectin, which is homologous to HP (Fujita et al., 2013), is one of the top factors of AMPK (Scherer et al., 1995; Kubota et al., 2007). We may gain a deeper understanding of the role of AMPK in driving hibernation by looking at the response of AMPK and its downstream factors after intracerebroventricular administration of HP.

Conclusion

In this study, we developed classification criteria for hibernating and non-hibernating types of Siberian chipmunks and identified variations in the seasonality and HP rhythm of thermoregulation. Through comparisons among the revealed hibernation polymorphisms, it was shown that AMPK, a sensor of metabolic regulation, is likely to be involved in hibernation metabolism, especially in the brain. Furthermore, validation in the pre-hibernation period revealed that AMPK activation in the diencephalon and hypothalamus occurs prior to hibernation. Considering the seasonal trends in body temperature of chipmunks, the HP rhythm, and the function of AMPK, it is suggested through this study that AMPK is likely involved in systemic metabolic regulation important for hibernation via the autonomic nervous system and in hypothermia tolerance during hibernation.

Data availability statement

The original contributions presented in the study are included in the article/Supplementary Material, further inquiries can be directed to the corresponding author.

Ethics statement

The animal study was approved by the Institutional Animal Care and Use Committee and approved by the President of Niigata University. The study was conducted in accordance with the local legislation and institutional requirements.

Author contributions

TK, SY, and TS designed the study. TK and SY performed the experiments and wrote the manuscript. All authors contributed to the article and approved the submitted version.

Funding

This research was supported by the Japan Society for the Promotion of Science (16K15060 and 22K20700) and the Sasakawa Scientific Research Grant from the Japan Science Society (29-540).

Acknowledgments

We are grateful to Dr. Noriaki Kondo, for provision of HP antibodies, associate professor Nobuyuki Takei, for advice on protein experiments. Dr. Takeshi Eto, for instructions on logger coating, and Dr. Mark Brazil for carefully proofreading the manuscript.

Conflict of interest

The authors declare that the research was conducted in the absence of any commercial or financial relationships that could be construed as a potential conflict of interest.

Publisher's note

Supplementary material

The Supplementary Material for this article can be found online at: https://www.frontiersin.org/articles/10.3389/fphys.2023.1220058/full#supplementary-material

References

Bartness, T. J., and Wade, G. N. (1985). Photoperiodic control of seasonal body weight cycles in hamsters. *Neurosci. Biobehav. Rev.* 9 (4), 599–612. doi:10.1016/0149-7634(85)90006-5

Browne, G. J., Finn, S. G., and Proud, C. G. (2004). Stimulation of the amp-activated protein kinase leads to activation of eukaryotic elongation factor 2 kinase and to its phosphorylation at a novel site, serine 398. *J. Biol. Chem.* 279 (13), 12220–12231. doi:10.1074/jbc.M309773200

Cai, D., McCarron, R. M., Yu, E. Z., Li, Y., and Hallenbeck, J. (2004). Akt phosphorylation and kinase activity are down-regulated during hibernation in the 13-lined ground squirrel. *Brain Res.* 1014 (1–2), 14–21. doi:10.1016/j.brainres.2004.04.008

Callard, G. V., Kunz, T. H., and Petro, Z. (1983). Identification of androgen metabolic pathways in the brain of little brown bats (*Myotis lucifugus*): sex and seasonal differences. *Biol. Reproduction* 28 (5), 1155–1161. doi:10.1095/biolreprod28.5.1155

Caprette, D. R., and Senturia, J. B. (1984). Isovolumetric performance of isolated ground squirrel and rat hearts at low temperature. *Am. J. Physiology-Regulatory, Integr. Comp. Physiology* 247 (4), R722–R727. doi:10.1152/ajpregu.1984.247.4.R722

Chayama, Y., Ando, L., Tamura, Y., Miura, M., and Yamaguchi, Y. (2016). Decreases in body temperature and body mass constitute pre-hibernation remodelling in the Syrian golden hamster, a facultative mammalian hibernator. *R. Soc. Open Sci.* 3 (4), 160002. doi:10.1098/rsos.160002

Dawe, A. R., and Spurrier, W. A. (1972). The blood-borne "trigger" for natural mammalian hibernation in the 13-lined ground squirrel and the woodchuck. *Cryobiology* 9 (3), 163–172. doi:10.1016/0011-2240(72)90028-4

Dyck, J. R. B., Kudo, N., Barr, A. J., Davies, S. P., Hardie, D. G., and Lopaschuk, G. D. (1999). Phosphorylation control of cardiac acetyl-CoA carboxylase by cAMP-dependent protein kinase and 5'-AMP activated protein kinase. *Eur. J. Biochem.* 262 (1), 184–190. doi:10.1046/j.1432-1327.1999.00371.x

Eto, T., Sakamoto, S. H., Okubo, Y., Tsuzuki, Y., Koshimoto, C., and Morita, T. (2018). Individual variation of daily torpor and body mass change during winter in the large Japanese field mouse (Apodemus speciosus). *J. Comp. Physiology B* 188 (6), 1005–1014. doi:10.1007/s00360-018-1179-9

Fedorov, V. B., Goropashnaya, A. V., Stewart, N. C., Tøien, Ø., Chang, C., Wang, H., et al. (2014). Comparative functional genomics of adaptation to muscular disuse in hibernating mammals. *Mol. Ecol.* 23 (22), 5524–5537. doi:10.1111/mec.12963

Florant, G. L., Fenn, A. M., Healy, J. E., Wilkerson, G. K., and Handa, R. J. (2010). To eat or not to eat: the effect of AICAR on food intake regulation in yellow-bellied marmots (*Marmota flaviventris*). *J. Exp. Biol.* 213 (12), 2031–2037. doi:10.1242/jeb.039131

Fujita, S., Okamoto, R., Taniguchi, M., Ban-Tokuda, T., Konishi, K., Goto, I., et al. (2013). Identification of bovine hibernation-specific protein complex and evidence of its regulation in fasting and aging. *J. Biochem.* 153 (5), 453–461. doi:10.1093/jb/mvt008

Grabek, K. R., Cooke, T. F., Epperson, L. E., Spees, K. K., Cabral, G. F., Sutton, S. C., et al. (2019). Genetic variation drives seasonal onset of hibernation in the 13-lined ground squirrel. *Commun. Biol.* 2 (1), 478. doi:10.1038/s42003-019-0719-5

Garidou, M.-L., Vivien-Roels, B., Pévet, P., Miguez, J., and Simonneaux, V. (2003). Mechanisms regulating the marked seasonal variation in melatonin synthesis in the European hamster pineal gland. *Am. J. Physiology-Regulatory, Integr. Comp. Physiology* 284 (4), R1043–R1052. doi:10.1152/ajpregu.00457.2002

Geiser, F. (2013). Hibernation. *Curr. Biol.* 23 (5), R188–R193. doi:10.1016/j.cub.2013.01.062

Geiser, F., and Ruf, T. (1995). Hibernation versus daily torpor in mammals and birds: physiological variables and classification of torpor patterns. *Physiol. Zool.* 68 (6), 935–966. doi:10.1086/physzool.68.6.30163788

Geiser, F. (2020). Seasonal expression of avian and mammalian daily torpor and hibernation: not a simple summer-winter affair. *Front. Physiology* 11, 436. doi:10.3389/fphys.2020.00436

Grabek, K. R., Martin, S. L., and Hindle, A. G. (2015). Proteomics approaches shed new light on hibernation physiology. *J. Comp. Physiology B* 185 (6), 607–627. doi:10.1007/s00360-015-0905-9

Healy, J. E., Gearhart, C. N., Bateman, J. L., Handa, R. J., and Florant, G. L. (2011). AMPK and ACCchange with fasting and physiological condition in euthermic and hibernating golden-mantled ground squirrels (Callospermophilus lateralis). *Comp. Biochem. Physiology Part A Mol. Integr. Physiology* 159 (3), 322–331. doi:10.1016/j.cbpa.2011.03.026

Horman, S., Hussain, N., Dilworth, S. M., Storey, K. B., and Rider, M. H. (2005). Evaluation of the role of AMP-activated protein kinase and its downstream targets in mammalian hibernation. *Comp. Biochem. Physiology Part B Biochem. Mol. Biol.* 142 (4), 374–382. doi:10.1016/j.cbpb.2005.08.010

Hrvatin, S., Sun, S., Wilcox, O. F., Yao, H., Lavin-Peter, A. J., Cicconet, M., et al. (2020). Neurons that regulate mouse torpor. *Nature* 583 (7814), 115–121. doi:10.1038/s41586-020-2387-5

Hudson, J. W., and Wang, L. C. H. (1979). Hibernation: endocrinologic aspects. *Annu. Rev. Physiology* 41 (1), 287–303. doi:10.1146/annurev.ph.41.030179.001443

Humphries, M. M., Thomas, D. W., and Kramer, D. L. (2003). The role of energy availability in mammalian hibernation: a cost-benefit approach. *Physiological Biochem. Zoology* 76 (2), 165–179. doi:10.1086/367950

Ibuka, N., and Fukumura, K. (1997). Unpredictable deprivation of water increases the probability of torpor in the syrian hamster. *Physiology Behav.* 62 (3), 551–556. doi:10.1016/S0031-9384(97)00017-6

Jansky, L., Haddad, G., Kahlerovy, Z., and Nedoma, J. (1984). Effect of external factors on hibernation of golden hamsters. *J. Comp. Physiology B* 154 (4), 427–433. doi:10.1007/BF00684450

Jinka, T. R., Carlson, Z. A., Moore, J. T., and Drew, K. L. (2010). Altered thermoregulation via sensitization of A1 adenosine receptors in dietary-restricted rats. *Psychopharmacology* 209 (3), 217–224. doi:10.1007/s00213-010-1778-y

Jinka, T. R., Toien, O., and Drew, K. L. (2011). Season primes the brain in an arctic hibernator to facilitate entrance into torpor mediated by adenosine a1 receptors. *J. Neurosci.* 31 (30), 10752–10758. doi:10.1523/JNEUROSCI.1240-11.2011

JMA (2023). Japan Meteorological Agency. historical weather data. Available at: https://www.data.jma.go.jp/obd/stats/etrn/.

Kahn, B. B., Alquier, T., Carling, D., and Hardie, D. G. (2005). AMP-activated protein kinase: ancient energy gauge provides clues to modern understanding of metabolism. *Cell. Metab.* 1 (1), 15–25. doi:10.1016/j.cmet.2004.12.003

Kajita, K., Mune, T., Ikeda, T., Matsumoto, M., Uno, Y., Sugiyama, C., et al. (2008). Effect of fasting on PPARgamma and AMPK activity in adipocytes. *Diabetes Res. Clin. Pract.* 81 (2), 144–149. doi:10.1016/j.diabres.2008.05.003

Kamata, T., Sakamoto, A., Yamada, S., and Sekijima, T. (2020). Estrus characteristics of female Siberian chipmunk (Tamias sibiricus) under laboratory condition. *Mammalian Sci.* 60 (1), 3–13. doi:10.11238/mammalianscience.60.3

Kawamichi, M., and Kawamichi, T. (1993). "Factors affecting hibernation commencement and spring emergence in Siberian chipmunks (Eutamias sibiricus)," in *Life in the cold: Ecological, physiological, and molecular mechanisms*. Editors C. Carey, G. L. Florant, B. A. Wunder, and B. Horwitz (Boulder, Colorado: Westview Press), 81–89.

Knight, J. R. P., Bastide, A., Roobol, A., Roobol, J., Jackson, T. J., Utami, W., et al. (2015). Eukaryotic elongation factor 2 kinase regulates the cold stress response by slowing translation elongation. *Biochem. J.* 465 (2), 227–238. doi:10.1042/BJ20141014

Kojima, M., Shiba, T., Kondo, N., and Takamatsu, N. (2001). The tree squirrel HP-25 gene is a pseudogene: analysis of tree squirrel HP-25 gene. *Eur. J. Biochem.* 268 (22), 5997–6002. doi:10.1046/j.0014-2956.2001.02572.x

Kondo, N. (1987). Identification of a pre-hibernating state in myocardium from nonhibernating chipmunks. *Experientia* 43 (8), 873–875. doi:10.1007/BF01951645

Kondo, N., and Kondo, J. (1992). Identification of novel blood proteins specific for mammalian hibernation. *J. Biol. Chem.* 267 (1), 473–478. doi:10.1016/S0021-9258(18)48519-5

Kondo, N., Sekijima, T., Kondo, J., Takamatsu, N., Tohya, K., and Ohtsu, T. (2006). Circannual control of hibernation by hp complex in the brain. *Cell.* 125 (1), 161–172. doi:10.1016/j.cell.2006.03.017

Körtner, G., and Geiser, F. (2000). The temporal organization of daily torpor and hibernation: circadian and circannual rhythms. *Chronobiology Int.* 17 (2), 103–128. doi:10.1081/CBI-100101036

Kubota, N., Yano, W., Kubota, T., Yamauchi, T., Itoh, S., Kumagai, H., et al. (2007). Adiponectin stimulates AMP-activated protein kinase in the hypothalamus and increases food intake. *Cell. metab.* 6 (1), 55–68. doi:10.1016/j.cmet.2007.06.003

Levesque, D. L., and Tattersall, G. J. (2010). Seasonal torpor and normothermic energy metabolism in the Eastern chipmunk (Tamias striatus). *J. Comp. Physiology B* 180 (2), 279–292. doi:10.1007/s00360-009-0405-x

Li, J., Benashski, S., and McCullough, L. D. (2011). Post-stroke hypothermia provides neuroprotection through inhibition of amp-activated protein kinase. *J. Neurotrauma* 28 (7), 1281–1288. doi:10.1089/neu.2011.1751

Lissovsky, A. A., Obolenskaya, E. V., Ge, D., and Yang, Q. (2017). Phylogeny and distribution of palaearctic chipmunks Eutamias (rodentia: sciuridae). Hystrix it. *J. Mamm.* 28 (1), 107–109. doi:10.4404/hystrix–28.1-12172

López, M., Nogueiras, R., Tena-Sempere, M., and Diéguez, C. (2016). Hypothalamic AMPK: a canonical regulator of whole-body energy balance. *Nat. Rev. Endocrinol.* 12 (7), 421–432. doi:10.1038/nrendo.2016.67

MacCannell, A., Sinclair, K., Friesen-Waldner, L., McKenzie, C. A., and Staples, J. F. (2017). Water–fat MRI in a hibernator reveals seasonal growth of white and brown adipose tissue without cold exposure. *J. Comp. Physiology B* 187 (5–6), 759–767. doi:10.1007/s00360-017-1075-8

Masaki, M. (2005). Variation in torpor patterns of Tamias sibiricus. *Int. Mammal. Congr.* 9, S3004. Abstract.

Matos-Cruz, V., Schneider, E. R., Mastrotto, M., Merriman, D. K., Bagriantsev, S. N., and Gracheva, E. O. (2017). Molecular prerequisites for diminished cold sensitivity in ground squirrels and hamsters. *Cell. Rep.* 21 (12), 3329–3337. doi:10.1016/j.celrep.2017.11.083

Munro, D., Thomas, D. W., and Humphries, M. M. (2005). Torpor patterns of hibernating eastern chipmunks Tamias striatus vary in response to the size and fatty acid composition of food hoards. *J. Animal Ecol.* 74 (4), 692–700. doi:10.1111/j.1365-2656.2005.00968.x

NAOJ (2023). National astronomical observatory of Japan. Local calendar. Available at: https://eco.mtk.nao.ac.jp/koyomi/dni/.

Nedergaard, J., and Cannon, B. (1990). Mammalian hibernation. *Philosophical Trans. R. Soc. Lond. B, Biol. Sci.* 326 (1237), 669–685. doi:10.1098/rstb.1990.0038

Oeltgen, P. R., Bergmann, L. C., Spurrier, W. A., and Jones, S. B. (1978). Isolation of a hibernation inducing trigger(S) from the plasma of hibernating woodchucks. *Prep. Biochem.* 8 (2–3), 171–188. doi:10.1080/00327487808069058

O'Hara, B. F., Watson, F. L., Srere, H. K., Kumar, H., Wiler, S. W., Welch, S. K., et al. (1999). Gene expression in the brain across the hibernation cycle. *J. Neurosci.* 19 (10), 3781–3790. doi:10.1523/JNEUROSCI.19-10-03781.1999

Olson, J. M., Jinka, T. R., Larson, L. K., Danielson, J. J., Moore, J. T., Carpluck, J., et al. (2013). Circannual rhythm in body temperature, torpor, and sensitivity to A_1 adenosine receptor agonist in arctic ground squirrels. *J. Biol. Rhythms* 28 (3), 201–207. doi:10.1177/0748730413490667

Ono, M., Kojima-Kawagoe, M., Kondo, N., Shiba, T., and Takamatsu, N. (2003). Comparative study of HP-27 gene promoter activities between the chipmunk and tree squirrel. *Gene* 302 (1–2), 193–199. doi:10.1016/S0378-1119(02)01152-6

Ou, J., Ball, J. M., Luan, Y., Zhao, T., Miyagishima, K. J., Xu, Y., et al. (2018). Ipscs from a hibernator provide a platform for studying cold adaptation and its potential medical applications. *Cell.* 173 (4), 851–863. doi:10.1016/j.cell.2018.03.010

Puspitasari, A., Cerri, M., Takahashi, A., Yoshida, Y., Hanamura, K., and Tinganelli, W. (2021). Hibernation as a tool for radiation protection in space exploration. *Life* 11 (1), 54. doi:10.3390/life11010054

R Core Team (2023). *R: a language and environment for statistical computing*. China: R Foundation for Statistical Computing.

Ren, Y., Song, S., Liu, X., and Yang, M. (2022). Phenotypic changes in the metabolic profile and adiponectin activity during seasonal fattening and hibernation in female Daurian ground squirrels (Spermophilus dauricus). *Integr. Zool.* 17 (2), 297–310. doi:10.1111/1749-4877.12504

Ruf, T., and Geiser, F. (2015). Daily torpor and hibernation in birds and mammals. *Biol. Rev.* 90 (3), 891–926. doi:10.1111/brv.12137

Scherer, P. E., Williams, S., Fogliano, M., Baldini, G., and Lodish, H. F. (1995). A novel serum protein similar to c1q, produced exclusively in adipocytes. *J. Biol. Chem.* 270 (45), 26746–26749. doi:10.1074/jbc.270.45.26746

Schwartz, C., and Andrews, M. T. (2013). Circannual transitions in gene expression. *Curr. Top. Dev. Biol.* 105, 247–273. doi:10.1016/B978-0-12-396968-2.00009-9

Schwartz, C., Hampton, M., and Andrews, M. T. (2015). Hypothalamic gene expression underlying pre-hibernation satiety: gene expression in natural satiety. *Genes., Brain Behav.* 14 (3), 310–318. doi:10.1111/gbb.12199

Schwartz, C., Hampton, M., and Andrews, M. T. (2013). Seasonal and regional differences in gene expression in the brain of a hibernating mammal. *PLoS ONE* 8 (3), e58427. doi:10.1371/journal.pone.0058427

Shao, C., Liu, Y., Ruan, H., Li, Y., Wang, H., Kohl, F., et al. (2010). Shotgun proteomics analysis of hibernating arctic ground squirrels. *Mol. Cell. Proteomics* 9 (2), 313–326. doi:10.1074/mcp.M900260-MCP200

Sharapov, V. M. (1984). Influence of animal hibernation on the development of mycoses. *Mycopathologia* 84 (2–3), 77–80. doi:10.1007/BF00436516

Sheriff, M. J., Kenagy, G. J., Richter, M., Lee, T., Tøien, Ø., Kohl, F., et al. (2011). Phenological variation in annual timing of hibernation and breeding in nearby populations of Arctic ground squirrels. *Proc. R. Soc. B Biol. Sci.* 278 (1716), 2369–2375. doi:10.1098/rspb.2010.2482

Srere, H. K., Belke, D., Wang, L. C., and Martin, S. L. (1995). Alpha 2-macroglobulin gene expression during hibernation in ground squirrels is independent of acute phase response. *Am. J. Physiology-Regulatory, Integr. Comp. Physiology* 268 (6), R1507–R1512. doi:10.1152/ajpregu.1995.268.6.R1507

Takamatsu, N., Ohba, K.-I., Kondo, J., Kondo, N., and Shiba, T. (1993). Hibernation-associated gene regulation of plasma proteins with a collagen-like domain in mammalian hibernators. *Mol. Cell. Biol.* 13 (3), 1516–1521. doi:10.1128/mcb.13.3.1516

Torke, K. G., and Twente, J. W. (1977). Behavior of *Spermophilus lateralis* between periods of hibernation. *J. Mammal.* 58 (3), 385–390. doi:10.2307/1379337

Tsukamoto, D., Fujii, G., Kondo, N., Ito, M., Shiba, T., and Takamatsu, N. (2007). USF is involved in the transcriptional regulation of the chipmunk HP-25 gene. *Gene* 396 (2), 268–272. doi:10.1016/j.gene.2007.03.014

Turbill, C., and Prior, S. (2016). Thermal climate-linked variation in annual survival rate of hibernating rodents: shorter winter dormancy and lower survival in warmer climates. *Funct. Ecol.* 30 (8), 1366–1372. doi:10.1111/1365-2435.12620

Vander Wall, S. B. (1990). *Food hoarding in animals*. Chicago: University of Chicago Press.

Williams, D. R., Epperson, L. E., Li, W., Hughes, M. A., Taylor, R., Rogers, J., et al. (2006). Seasonally hibernating phenotype assessed through transcript screening. *Physiol. Genomics* 24 (1), 13–22. doi:10.1152/physiolgenomics.00301.2004

Willis, C. K. R. (2017). Trade-offs influencing the physiological ecology of hibernation in temperate-zone bats. *Integr. Comp. Biol.* 57 (6), 1214–1224. doi:10.1093/icb/icx087

Xu, Y., Shao, C., Fedorov, V. B., Goropashnaya, A. V., Barnes, B. M., and Yan, J. (2013). Molecular signatures of mammalian hibernation: comparisons with alternative phenotypes. *BMC Genomics* 14 (1), 567. doi:10.1186/1471-2164-14-567

Yamada, S., Kamata, T., Nawa, H., Sekijima, T., and Takei, N. (2019). AMPK activation, eEF2 inactivation, and reduced protein synthesis in the cerebral cortex of hibernating chipmunks. *Sci. Rep.* 9 (1), 11904. doi:10.1038/s41598-019-48172-7

Yurisova, M. N., and Polenov, A. L. (1979). The hypothalamo-hypophysial system in the ground squirrel, citellus erythrogenys brandt: II. Seasonal changes in the classical neurosecretory system of a hibernator. *Cell. Tissue Res.* 198 (3), 539–556. doi:10.1007/BF00234197

Zervanos, S. M., Maher, C. R., Waldvogel, J. A., and Florant, G. L. (2010). Latitudinal differences in the hibernation characteristics of woodchucks (*Marmota monax*). *Physiological Biochem. Zoology* 83 (1), 135–141. doi:10.1086/648736

Zhou, X., Yang, W., Wang, X., and Ma, T. (2023). Isoform-specific effects of neuronal repression of the AMPK catalytic subunit on cognitive function in aged mice. *Aging* 15, 932–946. doi:10.18632/aging.204554

frontiers | Frontiers in Physiology

TYPE Original Research
PUBLISHED 21 August 2023
DOI 10.3389/fphys.2023.1207620

OPEN ACCESS

EDITED BY
Sylvain Giroud,
University of Veterinary Medicine Vienna, Austria

REVIEWED BY
Carla Frare,
Syracuse University, United States
Frazer Heinis,
University of Nebraska-Lincoln, United States
Sarah Rice,
University of Alaska Fairbanks, United States

*CORRESPONDENCE
Sarah V. Emser,
sarah.emser@univie.ac.at

RECEIVED 17 April 2023
ACCEPTED 31 July 2023
PUBLISHED 21 August 2023

CITATION
Emser SV, Spielvogel CP, Millesi E and Steinborn R (2023), Mitochondrial polymorphism m.3017C>T of SHLP6 relates to heterothermy. *Front. Physiol.* 14:1207620. doi: 10.3389/fphys.2023.1207620

Mitochondrial polymorphism m.3017C>T of SHLP6 relates to heterothermy

Sarah V. Emser[1,2]*, Clemens P. Spielvogel[3], Eva Millesi[1] and Ralf Steinborn[2,4]

[1]Department of Behavioral and Cognitive Biology, University of Vienna, Vienna, Austria, [2]Genomics Core Facility, VetCore, University of Veterinary Medicine, Vienna, Austria, [3]Department of Biomedical Imaging and Image-Guided Therapy, Division of Nuclear Medicine, Medical University of Vienna, Vienna, Austria, [4]Department of Microbiology, Immunobiology and Genetics, University of Vienna, Vienna, Austria

Heterothermic thermoregulation requires intricate regulation of metabolic rate and activation of pro-survival factors. Eliciting these responses and coordinating the necessary energy shifts likely involves retrograde signalling by mitochondrial-derived peptides (MDPs). Members of the group were suggested before to play a role in heterothermic physiology, a key component of hibernation and daily torpor. Here we studied the mitochondrial single-nucleotide polymorphism (SNP) m.3017C>T that resides in the evolutionarily conserved gene *MT-SHLP6*. The substitution occurring in several mammalian orders causes truncation of SHLP6 peptide size from twenty to nine amino acids. Public mass spectrometric (MS) data of human SHLP6 indicated a canonical size of 20 amino acids, but not the use of alternative translation initiation codons that would expand the peptide. The shorter isoform of SHLP6 was found in heterothermic rodents at higher frequency compared to homeothermic rodents ($p < 0.001$). In heterothermic mammals it was associated with lower minimal body temperature (T_b, $p < 0.001$). In the thirteen-lined ground squirrel, brown adipose tissue—a key organ required for hibernation, showed dynamic changes of the steady-state transcript level of *mt-Shlp6*. The level was significantly higher before hibernation and during interbout arousal and lower during torpor and after hibernation. Our finding argues to further explore the mode of action of SHLP6 size isoforms with respect to mammalian thermoregulation and possibly mitochondrial retrograde signalling.

KEYWORDS

daily torpor, hibernation, mitogenomics, mitochondrial-derived peptide (MDP), micropeptide, SHLP6, rodents, extended vertebrate mitochondrial genetic code

1 Introduction

Mammalian species use heterothermy as a very effective energy-saving strategy to overcome harsh environmental conditions (Morales et al., 2021). In addition to maintaining a T_b of around 37°C during activity, heterothermic species are capable to enter controlled, hypometabolic phases of less or more than 24 h termed daily torpor or hibernation (multiday torpor), respectively (Barnes et al., 1986; Hume et al., 2002; Sheriff et al., 2013; Ruf and Geiser, 2015). Heterothermy often refers to a regular adaptation to seasonality over several months but can also be used as a response to unpredictable environmental conditions and emergency situations (Nowack et al., 2020). Despite stratification into the phenotypes of daily and multiday torpor, patterns of heterothermic responses are highly diverse (Ruf and

Geiser, 2015; Levesque et al., 2016; Nespolo et al., 2021). Currently, heterothermy is considered a preceding state of endothermy in early mammals, with mainly passive temperature regulation and short or longer-term metabolic upregulation. This view regards daily torpor and hibernation as derived states of early heterothermy (Nowack et al., 2020).

Torpor can be viewed as series of physiological adaptations including reduction of T_b and metabolic rate (*MR*) (Ruf and Geiser, 2015), electro-cerebral inactivity (Andrews, 2019) and others. While foraging is continued in species that employ daily torpor, hibernation requires preparation such as accumulation of body fat or food stores (Humphries et al., 2003; Siutz et al., 2016), modification of reproductive and digestive systems and reliably favourable conditions for quick recovery (Barnes et al., 1986; Hume et al., 2002; Sheriff et al., 2013). Hibernation is interspersed by short obligate euthermic phases termed interbout arousals whose duration is inversely related to torpid *MR* (Ruf et al., 2022). The phases are triggered by accumulation or depletion of metabolites to eliminate cellular damage (Galster and Morrison, 1975; van Breukelen and Martin, 2001; Wiersma et al., 2018). Although necessary, interbout arousal is energetically expensive (Carey et al., 2003; Karpovich et al., 2009) and associated with increased cellular damage and production of reactive oxygen species (Carey et al., 2000; Brown and Staples, 2011; Nowack et al., 2019).

The active metabolic suppression during torpor coincides with a reversible repression of mitochondrial respiration down to 30% (Staples and Brown, 2008; Brown et al., 2012; Mathers et al., 2017). Mitochondria are responsible for oxidative phosphorylation (OXPHOS) and ATP production. Nucleoids of this cellular organelle have a uniform size and frequently contain a single copy of a compact circular genome, for example, on average 1.4 copies of a 16.5 kb circular genome (mitogenome) in case of man (Kukat et al., 2011). The common mitogenome in Vertebrata encodes 13 essential protein subunits of the respiratory chain, two rRNAs, 22 tRNAs (Ren et al., 2023) and several small open-reading frame (sORF)-derived micropeptides, commonly defined as polypeptides with a relatively arbitrary length of less than 100 to 150 amino acids [references in (Sousa and Farkas, 2018)], that represent the low end of the canonical protein spectrum (Schlesinger and Elsasser, 2022). Currently, the latter subgroup of micropeptides termed MDPs, consists of Humanin (Hashimoto et al., 2001), Gau [gene antisense ubiquitous (Faure et al., 2011)], MOTS-c [mitochondrial ORF of the 12S rRNA type-c (Lee et al., 2015)], SHLP1-6 [small Humanin-like peptides 1 to 6 (Cobb et al., 2016)], SHMOOSE [Small Human Mitochondrial ORF Over SErine tRNA (Miller et al., 2022)] and MTALTND4 [mitochondrial alternative ND4 protein (Kienzle et al., 2023)]. At least for a species which does not have a nuclear insertion of mitochondrial origin [NUMT (Wei et al., 2022)], mtDNA is the exclusive source for MDP coding, as, for example, in the cases of rat Humanin and rat MOTS-c (Paharkova et al., 2015). Cytoplasmic tRNA import (Rubio et al., 2008; Jeandard et al., 2019; Kienzle et al., 2023) and the use of alternative start codons (compiled by NCBI at https://www.ncbi.nlm.nih.gov/Taxonomy/Utils/wprintgc.cgi) expand the coding capacity of the mitochondrial genetic code, with consequences for MDP size (see below, Figures 3, 4F) and also for fine-tuning of complex biological systems that would be highly likely given the uniquely suited small size of MDPs.

Physiological extremes of hypothermic torpor and rapid arousal requires tremendous resilience of the cardiovascular and nervous systems to counteract the reduction and resumption of blood flow (Dave et al., 2012; Andrews, 2019). Contribution to the heterothermic phenotype can involve alteration of transcriptional and/or posttranscriptional regulation, post-translational modification (PTM) that is subject of dynamic regulation during hibernation (Tessier et al., 2017; Mathers and Staples, 2019), and microproteins such as Humanin, MOTS-c and SHLP2 (Supplementary Table S1). MOTS-c was the first MDP identified as a regulator of thermal homeostasis (Lu et al., 2019). Administration of MOTS-c enhanced cold tolerance by boosting two mechanism that are needed for heterothermy, namely white fat browning and thermogenic gene expression in brown adipose tissue, a well-known organ for thermogenesis (Lu et al., 2019). It downregulates circulating metabolites that are associated with type-2 diabetes and obesity, enhances glucose tolerance and insulin sensitivity (Lee et al., 2015; Kim et al., 2018; Benayoun and Lee, 2019) and functions as a host-defence peptide according to a preprint (Rice, 2023). Mitochondrial retrograde signalling, a major form of mitochondria to nucleus crosstalk that is activated by altered mitochondrial function under normal or pathophysiological conditions and enables reprogramming of nuclear gene expression (Liu and Butow, 2006; Granat et al., 2020), is the likely route of MOTS-c-mediated metaboloprotection. Humanin, the MDP archetype, shows elevated transcript and peptide expression in the brain cortex during hibernation pointing to protection of delicate brain tissues and neuronal connections against hibernation-associated stresses (Szereszewski and Storey, 2019).

Involvement in modulating endothermic thermoregulation may also be assumed for SHLP6, another member of the MDP group that is inducible by high-intensity exercise (Woodhead et al., 2020); Supplementary Table S1). Exercise generates high levels of acute mechanical, metabolic and thermoregulatory stress (Holloszy and Coyle, 1984; Wagner, 1991; Hamilton and Booth, 2000) and causes an adaptive response that might explain the inverse relationship with conditions such as metabolic and cardiovascular disease (Wenger and Bell, 1986; Harber et al., 2017; Laukkanen and Kujala, 2018). A similar inverse relationship is encountered during hibernation when the organism adjusts to a drastic change in physiology (Kurtz et al., 2021). SHLP6 is one of the most widely distributed MDPs with predictions ranging from mammals (Emser et al., 2021) to other vertebrates and some spiders (Supplementary Table S2). Across tissues of the mouse it shows pronounced differences in expression ranging from high abundance in liver and kidney, over weak expression in heart, brain, spleen and prostate, down to a lack in testes and muscle (Cobb et al., 2016). Being an apoptosis enhancer (Cobb et al., 2016), SHLP6 could be involved in organ shrinkage, hence facilitate reduction of energy consumption during torpor or thermoregulation (Hume et al., 2002).

Other members of the SHLP family are antagonistic to the apoptosis inducer SHLP6. They promote cell proliferation [SHLP4 (Cobb et al., 2016)], improve cell viability, reduce cell apoptosis, and share protective effects with Humanin [SHLP2 and SHLP3 (Cobb et al., 2016)]. SHLP2, in addition, promotes thermogenesis in interscapular brown adipose tissue (Kim et al., 2023). SHMOOSE boosts mitochondrial oxygen consumption, modifies energy signalling and metabolism in the central nervous system as well

as reduces mitochondrial superoxide production (Miller et al., 2022). At least some of these functionalities would be essential for a torpid state that is accompanied by lower oxygen unloading to tissues. For example, attenuation of oxygen consumption mediated by MTALTND4 might be beneficial in this respect.

This study speculated on the role of SHLP6 in endothermic thermoregulation of rodents and added another MDP with a role in daily torpor and hibernation.

2 Materials and methods

2.1 Extraction and validation of mtDNA sequences from DNA- or RNA-seq data

DNA-, RNA- or exome sequencing data contained in the Sequence Read Archive (SRA) of NCBI were screened for the species with information on the use of endothermic heterothermy, but no information on the SHLP6-coding sequence. Sequence reads were downloaded to the Galaxy server [(Galaxy, 2022); https://usegalaxy.eu/], mapped to the closest mtDNA homologue available through BBmap (Bushnell, 2014) and aligned using rnaSPAdes [(Bushmanova et al., 2019); http://cab.spbu.ru/software/rnaspades/], respectively. For validation, we followed the proposed gold standard for mitogenome publishing and authentication (Sangster and Luksenburg, 2021). Phylogeny was reconstructed based on the mitochondrial mRNA-, rRNA- and tRNA-coding genes without partitioning using the maximum-likelihood approach performed in IQ-TREE [release 1.6.12 of 15 August 2019; (Nguyen et al., 2015; Kalyaanamoorthy et al., 2017; Hoang et al., 2018); http://iqtree.Cibiv.univie.ac.at/]. The sequences of mitogenomes were automatically annotated using the MITOchondrial genome annotation Server (MITOS) server [(Bernt et al., 2013); http://mitos.bioinf.uni-leipzig.de/index.py].

2.2 Amino acid sequences and phylogenetic reconstruction

Rodent orthologues of SHLP6 were identified using the sORF of human SHLP6 as query (GenBank accession number KX067784.1) for a Basic Local Alignment Search Tool (BLAST) search (target number: ≤5,000). Results were viewed in the Multiple Sequence Alignment Viewer of NCBI (https://www.ncbi.nlm.nih.gov/projects/msaviewer/) and translated using Seaview version 5.0.4 [(Gouy et al., 2010); https://doua.prabi.fr/software/seaview].

To illustrate length distribution of the SHLP6-encoding sORF, rodent phylogeny was reconstructed with Timetree version 5 [(Kumar et al., 2022); www.timetree.org] and edited in iTOL version 6 [(Letunic and Bork, 2021); https://itol.embl.de/].

2.3 Detection of SHLP6 peptide fragments in public MS data

To screen publicly available MS data for fragments of SHLP6, the commonly accepted amino acid sequences of human, rat and mouse SHLP6 were used as query. We also considered the option of an earlier translational start facilitated by the use of alternative codons for translation initiation used by mitochondria of Vertebrata (Sammet et al., 2010). In detail, evidence for human SHLP6 was searched in MS datasets integrated in the web-based targeted peptide search engine PepQuery 2 that was hosted by the Galaxy server [(Galaxy, 2022); https://usegalaxy.eu/]. PepQuery2 identifies or validates known and novel peptides of interest in any local or publicly available MS-based proteomics datasets [(Wen and Zhang, 2023); http://pepquery2.pepquery.org/]. The integrated datasets contained four PTM types, acetylation, glycosylation, phosphorylation and ubiquitinylation. Six MS datasets of mouse and rat were queried (MSV000083647, MSV000086732, MSV000088206, MSV000089856, MSV000091015, and MSV000091978).

2.4 Analysis of temporal transcript abundance patterns across hibernation states

Several tissues and activity states of the thirteen-lined ground squirrel served as model to analyse hibernation-associated transcript alteration using public RNA-seq data. In detail, RNA-seq reads of the SRA bioprojects PRJNA854159 (adrenal gland), PRJNA418486 (brain), PRJNA226612 (brown adipose tissue) and PRJNA702062 (liver) were downloaded to the Galaxy server. Data sets contained single-end sequence reads (brown adipose tissue: ~100 bp) or paired-end reads (adrenal gland: ~135 bp, brain and liver: ~250 to 280 bp). Transcript abundance of the target genes *mt-Rnr2* (mitochondrially encoded 12S and 16S rRNA genes), sHumanin (Szereszewski and Storey, 2019) abbreviated as *mt-sHn*, and *mt-Shlp6* was quantified using Kallisto quant version 0.46.2 (Bray et al., 2016). To obtain a sufficiently long target RNA that would be compatible with the read length of the RNA-seq library available for brown adipose tissue, we considered the expanded mitochondrial coding potential as outlined in the Introduction. In case of *mt-sHn*, we assumed misreading of the canonical stop codon that would increase the size of the peptide from 21 to 38 amino acids, thus expand the sORF to 114 nucleotides (nt). Details on sORF extension of *mt-Shlp6* (170 nt) are outlined in Section 3.3.

Variance-mean dependence of count data and their differential abundance based on negative binomial distribution were estimated by the DESeq2 software (Love et al., 2014).

2.5 Secondary structure prediction of human 16S rRNA

Secondary structure of the human 16S rRNA sequence (accession number NC_012920.1) was predicted without considering modulation by multiple proteins, in particular RNA-binding proteins (Georgakopoulos-Soares et al., 2022), using The Vienna RNA package RNAfold [(Gruber et al., 2008; Lorenz et al., 2011); http://rna.tbi.univie.ac.at/cgi-bin/RNAWebSuite/RNAfold.cgi] and UNAfold [(Markham and Zuker, 2008); http://www.unafold.org/].

2.6 Hydrophobicity and PTM prediction of SHLP6

The degree of hydrophobicity/hydrophilicity of human, mouse and rat SHLP6 was visualised as hydropathicity plot in Kyte-Doolittle scale [(Kyte and Doolittle, 1982); https://web.expasy.org/protscale/]. PTM was predicted using web servers with lowest threshold settings (phosphorylation: [(Wang et al., 2020); http://gps.biocuckoo.cn/online.php], methylation: [(Devall et al., 2016); https://methylsight.cu-bic.ca], glycosylation: [(Gupta and Brunak, 2002); https://services.healthtech.dtu.dk/services/NetNGlyc-1.0/, https://services.healthtech.dtu.dk/services/NetOGlyc-4.0/]: and small ubiquitin-like modifier (SUMO) addition (SUMOylation), and SUMO-interacting motif [(Beauclair et al., 2015); http://www.jassa.fr/index.php?m=jassa].

2.7 Peptide structure assessment and visualisation

Three-dimensional peptide structure was predicted using the deep-learning approach of ColabFold (Mirdita et al., 2022) that is based on AlphaFold2 (Jumper et al., 2021; Yang et al., 2023). Confidence of prediction was scored and ranked according to the predicted Local Distance Difference Test (*pLDDT*) value (Mariani et al., 2013) that was obtained by computing five models with three recycles for each amino acid sequence. To ensure reproducibility, structure prediction was performed with the default parameters of ColabFold. The top-scoring model was visualised using the structural analysis software iCn3D (Wang et al., 2022). Structures were aligned using the "residue by residue" option.

Alternative prediction of human SHLP6 folding was derived from AlphaFold Protein Structure Database of UniProt [(UniProt, 2023); https://alphafold.ebi.ac.uk].

2.8 Statistical analysis

Distribution of the m.3017C>T polymorphism, SHLP6 sizes and structure predictions across heterothermic and homeothermic rodents were compared using the chi-square test run in RStudio version 4.1.2 (RStudio Team, 2021).

Significance of the relationship between SHLP6 length and T_b or *MR* of the heterothermic mammalian species was evaluated using the Wilcoxon rank-sum test, a nonparametric test for two independent groups. The latter statistical analyses were performed in GraphPad Prism (version 9.5.1; GraphPad Software, Boston, MA, United States).

3 Results

3.1 Extraction and validation of mtDNA sequences from DNA- and RNA-seq data

Public sequencing data were used to extract mtDNA sequences of six heterothermic rodent species, namely *Acomys russatus*, *Otospermophilus beecheyi*, *Otospermophilus variegatus*, *Sicista betulina*, *Zapus hudsonius* and *Zapus princeps* (Table 1). Erroneous sequence assignation, *A. russatus* instead of *A. cahirinus*, was determined for the sequence reads SRR17216041 of the Bioproject PRJNA788430 (details not shown). The extracted mitogenomes were validated by phylogenetic reconstruction (Supplementary Figure S1), annotated and submitted to NCBI's GenBank (Table 1).

3.2 Premature translation termination caused by m.3017C>T and relationship with parameters of heterothermy

SHLP6 coding sequences of monotremes, specifically rodents, were found to be very conserved (Emser et al., 2021; Figures 6, 7). In relation to the mouse, homology at DNA and amino-acid levels ranged from 82% to 100% and 85%–100%, respectively (Supplementary Tables S3, S4). The nucleotide substitution that occurred in 22% of the rodent species currently sequenced, reduced the size of SHLP6 from twenty to nine amino acids. Analysis of sequences available for 34% species of the order Rodentia (686 of ~2,000) including 42 species with proven heterothermy status (Ruf and Geiser, 2015) yielded a significantly higher frequency of the shorter peptide across heterotherms (Chi-square test: $p < 0.001$, Figure 1, Supplementary Tables S3, S4). Two suborders of the taxon Rodentia mirrored this significant relationship between SHLP6 length and endothermic thermoregulation (Myomorpha (mouse-like rodents): $p = 0.0001$ and Sciuromorpha (squirrels): $p = 0.003$). The remaining three taxonomic suborders, Castorimorpha, Anomaluromorpha and Hystricomorpha, lacked a critical number of heterothermic species for statistical analysis ($n = 0$ to 4, Figure 1). In contrast, the two length variants of SHLP6 were not found to be related to rodent's or mammal's cold adaption ($p > 0.1$; Supplementary Table S5) nor to heterothermic or homeothermic thermoregulation across other orders of the taxon Mammalia despite frequent occurrence ($p > 0.1$, Supplementary Table S6).

Next, the physiological parameters minimal T_b, minimum torpor *MR* and the ratio of minimal to basal *MR* of heterothermic mammals (Ruf and Geiser, 2015) were evaluated in relation to their SHLP6 size isoforms. Significances were found between the shorter SHLP6 isoform and minimal T_b ($p = 0.0002$) or minimum torpid *MR* ($p = 0.025$, Figure 2).

Recently, the use of translation from alternative translation initiation codons applied by the mitochondrion got a renaissance, for example, illustrated by the mitochondrially encoded human peptides MTALTND4 and SHLP6 (Kienzle et al., 2023). In the latter case, the authors assumed an involvement of the alternative starts codons ATT and ATA to expand the peptide (33 instead of the canonical twenty amino acids). To deliver experimental evidence for this assumption, we mined publicly available MS/MS datasets of man ($n = 48$), mouse ($n = 5$) and rat ($n = 3$) using a targeted peptide search with the engine PepQuery. While the MS data of the two rodents completely lacked a confidential SHLP6 fragment, we obtained MS support for the existence of human SHLP6. However, there was no evidence for alternative translation initiation that would result in size expansion. In detail, the same confident peptide

TABLE 1 Novel mitogenomes extracted from publicly available sequence data.

Rodent species	SRA accession number	Sequencing technique	Mitogenome size (bp)	Accession ID (this study)
Acomys russatus	ERR4183373	WGS	16,218	BK063162
Otospermophilus beecheyi	SRR4180864	Exon capture	16,472	BK063161
Otospermophilus variegatus	SRR4180883	Exon capture	16,472	BK063160
Sicista betulina[a]	SRR12432355	WGS	16,412	BK063159
Zapus hudsonius	SRR11434656	WGS	16,510	BK063158
Zapus princeps	SRR12430165	RNA-seq	15,740[b]	BK063163

[a]Other mitogenome variants of this species were uploaded to the GenBank in parallel to this study.
[b]Incomplete assembly (95%) due to repeated D-loop segments.
Sequence records provided by this study are accessible at the Third-Party Annotation (TPA) section of DDBJ/ENA/GenBank databases (https://www.ncbi.nlm.nih.gov/genbank/TPA.html).

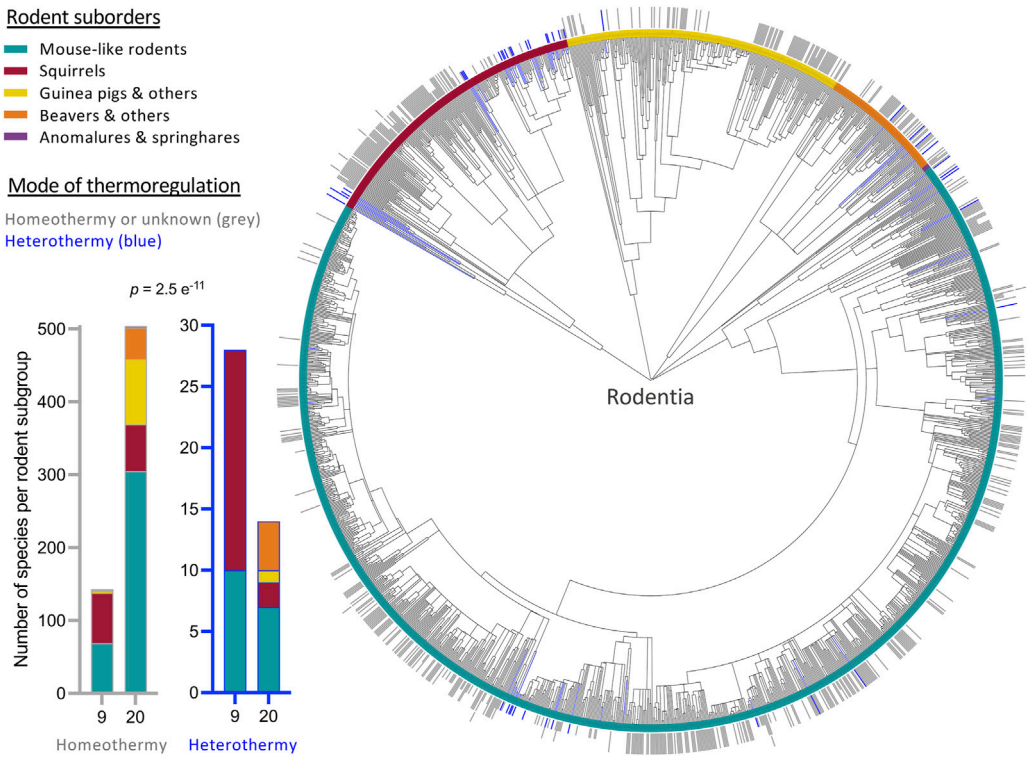

FIGURE 1
Phylogenetic tree depicting the distribution of SHLP6 peptide length across rodent species. Occurrence of heterothermy is highlighted in blue. 20 and 9mers of SHLP6 are depicted by a full bar outside of the tree or a half stroke, respectively. An additional short stroke highlights a species harbouring both length variants. In case no sequences were available at NCBI, the bar is left blank. Further research on little explored rodents is requested to increase the number of species with confidently classified as heterothermic (Ruf and Geiser, 2015). Statistic: chi-square test.

fragment "MLDQDIPMVQPLLK" was identified between one to ten times in four of the human data sets (Figure 3). It completely matched to the first 14 amino acids of the mitochondrially encoded human SHLP6 according to UniProt BLAST or Standard Protein BLAST (primary accession A0A3G1DJN1 of UniProtKB and NCBI's GenBank accession number AMZ80341, respectively), but also to a micropeptide translatable from a NUMT on human chromosome 17 (positions 22,524,419 to 22,524,480 in NC_000017.11).

The PTM datasets contained in PepQuery's database did not yield any confident fragment for SHLP6.

3.3 Steady-state abundance of *mt-Shlp6* transcript during states of hibernation

In general, hibernation-related RNA could be subject to transcriptional and/or post-transcriptional gene regulation (Gillen et al., 2021). Considering the higher incidence of the 9 mer isomer of SHLP6 seen in heterothermic rodents (Section 3.1), we asked whether hibernation would be a phenotype to provide insight into regulation of steady-state RNA level of *mt-Shlp6*. Therefore, we screened a set of public RNA-seq data available for the thirteen-lined ground squirrel. Data covered four tissues, namely, adrenal

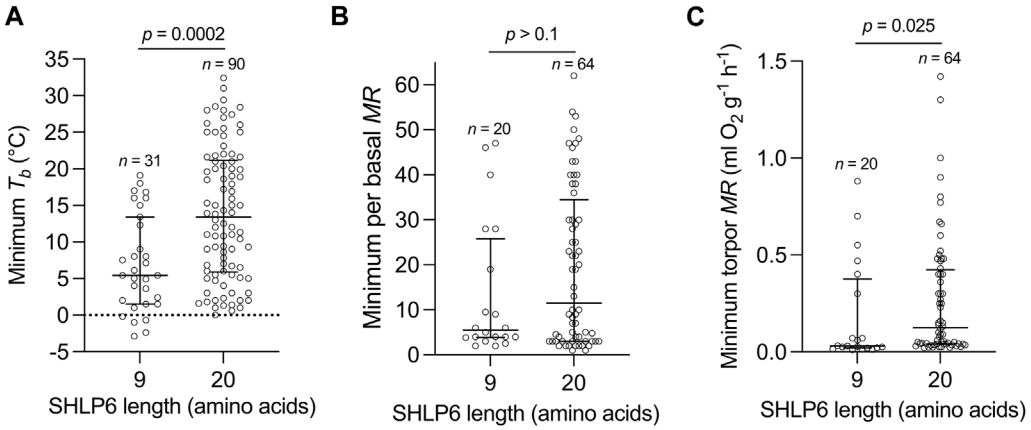

FIGURE 2
Length isoforms of SHLP6 in relation to physiological parameters of hibernation. Distribution of SHLP6 sizes across heterothermic mammals in relation to minimum T_b **(A)**, minimum torpid *MR* **(B)** and ratio of minimal to basal *MR* with T_b and *MR* values taken from Ruf and Geiser (2015) **(C)**. Analysis of significance: Wilcoxon rank-sum test, T_b: body temperature, *MR*: metabolic rate.

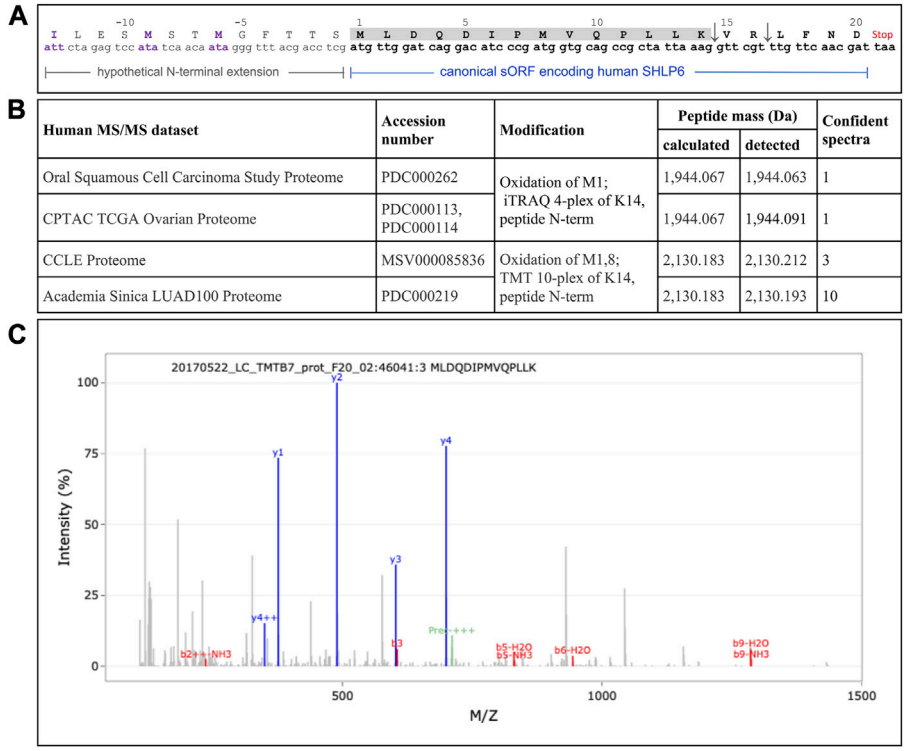

Human MS/MS dataset	Accession number	Modification	Peptide mass (Da)		Confident spectra
			calculated	detected	
Oral Squamous Cell Carcinoma Study Proteome	PDC000262	Oxidation of M1; iTRAQ 4-plex of K14, peptide N-term	1,944.067	1,944.063	1
CPTAC TCGA Ovarian Proteome	PDC000113, PDC000114		1,944.067	1,944.091	1
CCLE Proteome	MSV000085836	Oxidation of M1,8; TMT 10-plex of K14, peptide N-term	2,130.183	2,130.212	3
Academia Sinica LUAD100 Proteome	PDC000219		2,130.183	2,130.193	10

FIGURE 3
Sporadic detection of the non-enriched human SHLP6 using MS analysis **(A)** Hypothetical extension of the canonical human 20mer of SHLP6 predicted by Kienzle et al. (2023). This putative N-terminal extension is depicted by smaller font type. It was hypothesized to result from the use of the alternative translation initiation codons ATT and ATA depicted in violet. Positive or negative numbering refers to the canonical peptide or the hypothetical extension, respectively. The sequence of the cleaved 14mer peptide fragment, "MLDQDIPMVQPLLK", is shaded. The two trypsin cleavage sites contained in the canonical sequence of human SHLP6, but not in the hypothetical N-terminal extension, are shown by the arrows. Origin of coding sequence: NCBI's accession number J01415.2. **(B)** Details on the four human data sets that contained at least a single SHLP6-specific fragment. Notably, the same confident fragment was detected in all cases. **(C)** Example of a MS spectrum depicting the confident fragment "MLDQDIPMVQPLLK". Blue and red signals represent "y" and "b" ions, respectively. Pre: precursor. The exemplary spectrogram was taken from the last of the data sets listed above.

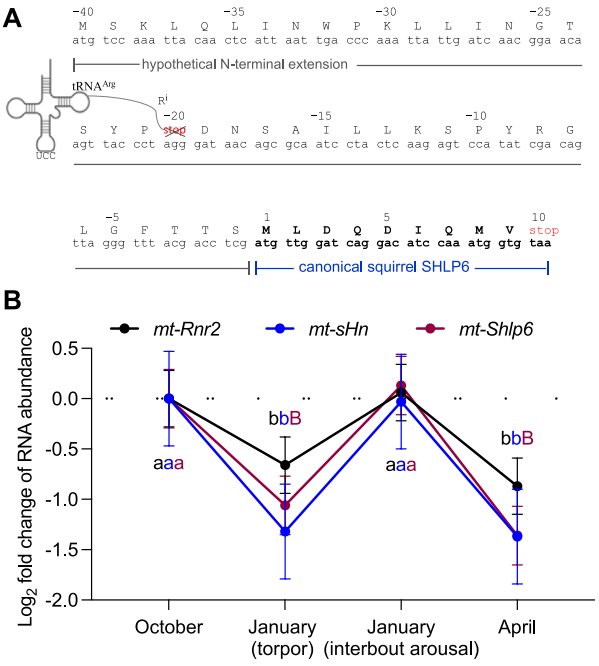

FIGURE 4
Dynamic abundance alteration of SHLP6-encoding RNA in brown adipose tissue of the thirteen-lined ground squirrel during states of hibernation. **(A)** Deduction of SHLP6 ORF used as "query" sequence in the comparison of steady-state RNA levels. Deduction considered the extended coding repertoire of the mitogenome, here, the import of the cytoplasmic $tRNA^{Arg}$ (AGG) into the mitochondrion (Rubio et al., 2008; Jeandard et al., 2019). As a result, the stop codon that divided the two peptides (in red font), gets converted and the putative SHLP6 peptide expanded. Amino acids are depicted by single-letter code and R^{I} denotes the arginine residue resulting from import of cytoplasmic $tRNA^{Arg}$. **(B)** Temporal pattern of the steady-states of transcripts covering the extended SHLP6-encoding ORF. RNA abundance is expressed as transcripts per million. Error bars depict standard deviations. Wald test implemented by DESeq2 was used to assess significance of differential transcript abundance. Difference among a pair of time points is indicated by a different small or capital letter (small letter: $0.05 > p > 0.01$, capital letter: $p < 0.01$). Accession number of the public RNA-seq data used for differential analysis of transcript abundance: PRJNA226612.

gland, brain, liver and brown adipose tissue, a thermogenic tissue that uses uncoupled mitochondrial respiration to generate heat instead of ATP, and four hibernation stages, namely, torpor and interbout arousal as well as the time points before and after hibernation. First, we confirmed the reported differential RNA abundance of *mt-sHn* in brown adipose tissue taken from different states of hibernation [(Szereszewski and Storey, 2019), Figure 4]. Second, we considered that the RNA-seq library available for brown adipose tissue contained a read length of ~100 bp. In order to successfully detect an RNA covering the ORF of *mt-Shlp6*, we questioned whether a longer sequence would exceed the length threshold, thus could serve as appropriate transcript (Figure 4A). For its deduction we considered the extended coding repertoire of the mitogenome. Here, the imported cytoplasmic $tRNA^{Arg}$(AGG) would misread a termination codon that formerly separated two smaller peptides, thus expand the predicted size of the squirrel's SHLP6. Based on this assumption, we found a significantly reduced level during torpor and in spring compared to the time before entering torpor and the state of interbout arousal ($p = 1.07e^{-5}$ and $p = 0.00036$, Figure 4B). Notably, *mt-Shlp6* and its hosting rRNA gene, *mt-Rnr2*, exhibited similar quantitative patterns of transcript alteration. Neither *mt-sHn* nor *mt-Shlp6* transcripts were detectable in the other tissues, likely due to the mismatching (longer) insert size of the RNA-seq libraries used for analysis [~135 bp (adrenal gland) and ~250 to 280 bp (brain and liver) instead of ~100 bp (brown adipose tissue)]. The transcript coding for the short, canonical 9mer of SHLP6 was not detected at all, likely also due to subcritical sequence length for the library. An RNA-seq library composed of shorter sequences that match in length would be a fitting alternative (Chhangawala et al., 2015) to cover the short-sized sORF and sequencing enough of the adapter to be accurately identified and trimmed during data analysis.

3.4 Biochemical parameters of SHLP6: secondary structure, hydrophobicity and PTM

The mitochondrial SNP target m.3017C>T (28C>T of *mt-Shlp6*) is located within a loop of 16S rRNA according to prediction with the algorithms RNAfold3 and UNAfold, hence would likely not impair the folding of the transcript (Figure 5B). PTM prediction for SHLP6 of human, rat and mouse identified indicated lysine methylation and a SUMO-interacting motif in case of human and rat SHLP6 (Figure 5D).

3.5 Prediction of three-dimensional peptide structure for length isoforms of SHLP6

Given the relationship of SHLP6 with endothermic thermoregulation (Sections 3.1, 3.2), we tried to add puzzles for its deeper understanding by three-dimensional peptide structure prediction based on the amino acid sequence. It yielded typical foldings for the 9mer and 20mer isoforms of SHLP6 with longer peptides being slightly more heterogeneous (Figures 6, 7). Except for three 20mer isoforms, a single alpha helix that spanned either the entire or almost the entire peptide was predicted. Most structural positions were predicted with high confidence (*pLDDT* score ≥70). None of the structural positions had a very low confidence (*pLDDT* score <50). The lower structural support obtained for the ends of the 20mers (*pLDDT* score <70) was attributed to intrinsic structural disorder (Necci et al., 2021). Secondary-structure components were not found for the 9mer isoforms (Figure 7). The predicted structural variants, helical or non-helical, were clearly associated with the heterothermic rodents ($p < 0.001$, Supplementary Table S4).

It is currently unclear whether reversible PTMs such as lysine methylation, SUMOylation (Figure 2D) or others, alone or in combination rather than SHLP6 size and/or secondary structure are putative components involved in heterothermy regulation. At least for the prediction of folding, we noted a strong dependency on the software version as indicated by the lack of a N-terminal helix in the human SHLP6 structure provided by the AlphaFold Protein Structure Database of EMBL's European Bioinformatics Institute

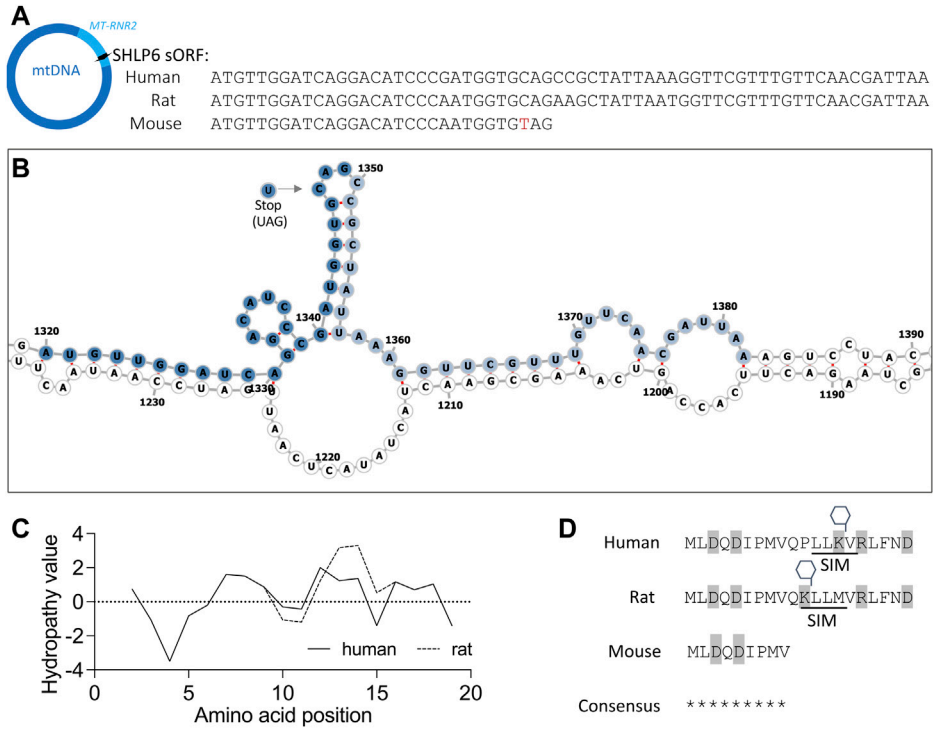

FIGURE 5
Features of SHLP6 **(A)** The sORF of SHLP6 occurs at two size variants exemplarily represented by human, rat and mouse. Polymorphism m.3,017C>T (red letter) introduces a stop codon in the mouse. In azure: hosting gene *MT-RNR2*. Arrow: sORF orientation. **(B)** Secondary structure predicted by RNAFold3 for the human *MT-RNR2* transcript that hosts the sORF of SHLP6 (nucleotides 1,671 to 3,229 in NC_012920.1). m.3,017C>T depicted by the arrow does not affect folding of the hosting transcript. Dark blue: sORF of the 9mer variant of SHLP6 (30 nucleotides including stop codon); light blue: sORF of the 20mer variant of SHLP6 (63 nucleotides including stop codon). A similar secondary structure was predicted with UNAfold (data not shown). **(C)** Degree of hydrophilicity or hydrophobicity analysed for the amino acids of human and rat SHLP6 [hydropathicity plot in Kyte-Doolittle scale (Kyte and Doolittle, 1982)]. Note that the nine amino acids of mouse SHLP6 are shared by the two 20mer variants of the peptide (see sequence consensus). **(D)** Amino-acid sequences of the SHLP6 length isomers with information on charge (grey background) and putative PTM (SIM: SUMO-interacting motif, hexagon: methylation). Asterisk: identical amino-acid residue. We note that the contribution of the PTMs cannot be predicted in relation to daily or multiday torpor *in silico*.

(Supplementary Figure S2). This can be attributed to differences of the AlphaFold2 algorithms and/or to the ambivalent character of the peptide.

It should be noted that predictions of three-dimensional structure for micropeptides such as SHLP6 must be treated with caution. Micropeptides are in general unstructured and potentially fold upon complex formation [(Kubatova et al., 2020) and communication of Prof. Thomas Martinez]. They resemble intrinsically disordered proteins in their hallmark of marked bias in the amino-acid composition, including a relatively low proportion of hydrophobic and aromatic residues as well as a relatively high proportion of charged and polar residues (Dyson, 2016).

4 Discussion

SHLP6 belongs to the class of vertebrate MDPs (Kumagai et al., 2023) and, together with Humanin, it is the second MDP for which the steady-state RNA level was shown to alter in a torpid mammal during hibernation [(Szereszewski and Storey, 2019) and this study].

Here we focussed on the distribution of the *mt-Shlp6* gene polymorphism m.3017C>T across heterothermic and homeothermic species belonging to the taxa Rodentia and Mammalia. It was predicted to cause a length reduction of the MDP from twenty to nine amino acids and to occur at a significantly higher proportion in heterothermic rodents. Mammals in the condition of hibernation or daily torpor showed a significantly higher incidence of the truncating genotype in animals with a lower minimum T_b ($p = 0.0002$). Similarly, non-helical predicted variants of SHLP6 structure were also found to be related to the heterothermic phenotype of the rodents. The concomitant occurrence of length and structural variants hampered clarifying whether alteration of length or structure alone or in combination associates with endothermic thermoregulation. The dichotomy of SHLP6 length was also observed in other orders of the taxon Mammalia (Supplementary Table S5). However, a similar relationship between SHLP6 length and the phenotype of heterothermic thermoregulation was not found ($p > 0.1$). This was attributed to the relatively low number of heterothermic species per order or an alternative adaptive strategy. Summarised, shorter SHLP6 size may mediate tolerance for low minimum T_b and/or better protect during rewarming.

In the future, MDP encoding can more comprehensively be pictured by evaluating the impact of NUMTs (Rubio et al., 2008; Calabrese et al., 2012; Balciuniene and Balciunas, 2019; Lutz-Bonengel et al., 2021; Ng et al., 2022; Wei et al., 2022) and utilization of non-AUG translational

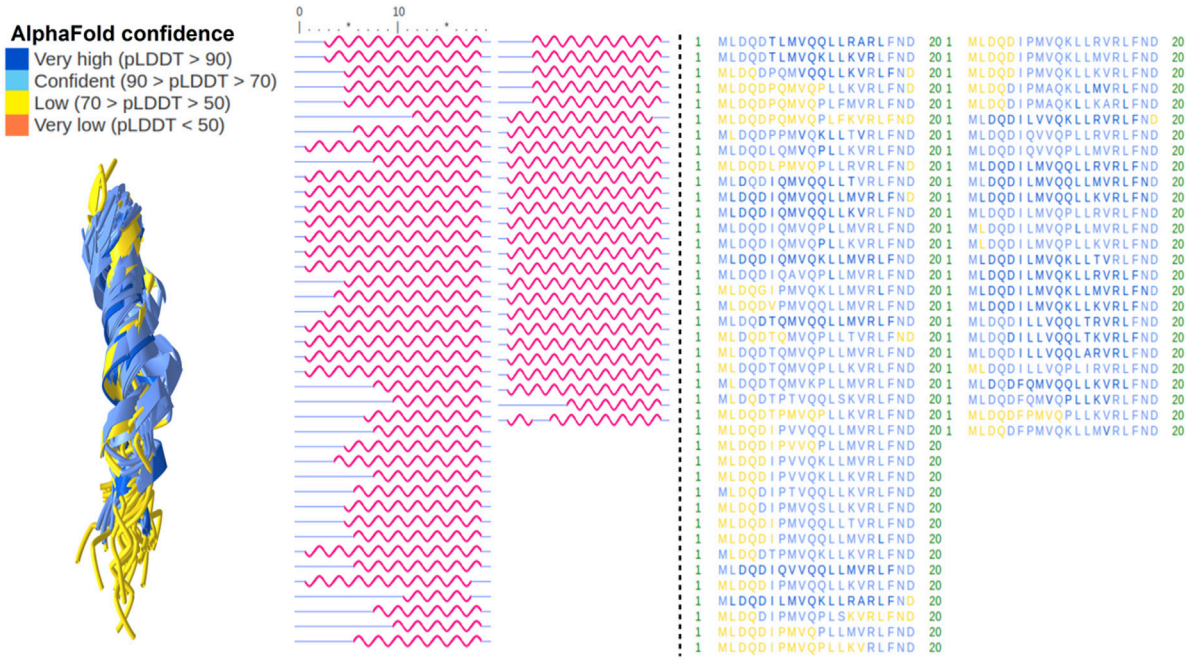

FIGURE 6
Rodent SHLP6 structures with helices. Three-dimensional peptide structures as predicted by the artificial intelligence system AlphaFold2 are shown on the left with prediction confidence per region indicated by color. The secondary structure for each peptide is shown in the middle with alpha helices indicated in red. Amino acid sequences are shown on the right. All peptides with helices had a length of 20 amino acids. Positions five and 15 of the peptide are highlighted by an asterisk.

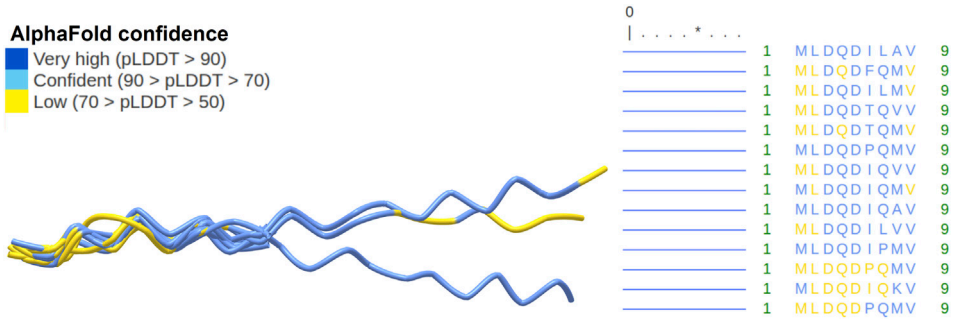

FIGURE 7
Rodent SHLP6 structures without helices. Three-dimensional peptide structures as predicted by AlphaFold2 are shown on the left with prediction confidence per region indicated by color. No secondary structures were predicted as shown by the horizontal, blue lines. Amino acid sequences are shown on the right. A total of three sequences had a length of 20 amino acids. Only the aligned parts of the peptides are shown. The asterisk highlights position five of the peptide.

start sites for example described for MTALTND4 [(Kienzle et al., 2023); https://www.ncbi.nlm.nih.gov/Taxonomy/Utils/wprintgc.cgi], but not indicated in this study for human SHLP6 based on MS/MS data that would shift the N-terminus of the peptide. Resolution of MS analysis could be enhanced by combining immunoprecipitation with MS, hence help to overcome the failure of MS in detecting mouse and rat SHLP6 (see Sections 3). Another MDP-coding issue represents misreading of termination codons (Beier and Grimm, 2001) facilitated by the import of nucleus-encoded tRNAs (Rubio et al., 2008; Ng et al., 2022). Here, this was assumed for translating SHLP6 of the thirteen-lined ground squirrel and awaits validation along with the proof for transcript sizes of other MDPs, for example, by using Nanopore direct RNA sequencing technology that detects the 5' end of a transcript at an accuracy of 10–15 nt (Workman et al., 2019). Moreover, the apparent discrepancy between MDPs sizes determined theoretically and experimentally by Western blotting needs clarification. Unresolved cases comprise Humanin (Woodhead et al., 2020), its counterpart in the rat (Caricasole et al., 2002), murine MOTS-c (Cobb et al., 2016;

Reynolds et al., 2021) and human MTALTND4 (Kienzle et al., 2023) and Gau for which experimental evidence of MDP size is still lacking (Faure et al., 2011). In case of MTALTND4, for example, neither reduction of disulfide bonds, dephosphorylation nor deglycosylation could remove the molecular weight discrepancy (Kienzle et al., 2023). Mitochondrial protein methylation that might be extensive and comparable to the cellular average (Małecki et al., 2022) and other PTMs should be considered when addressing the striking size discrepancy seen in immunoblots for some MDPs. SUMO that adds a theoretical molecular weight of ~12 kDa (Daniel et al., 2017), is one of the putative posttranslational modifiers to be tested in this regard. In case of MTALTND4, the issue of the size discrepancy was attributed to the formation of homomultimers (Kienzle et al., 2023). And last but not least, a better understanding of retrograde signalling mediated by the diverse types of RNA that exit the mitochondrion (Tessier et al., 2017; Mathers and Staples, 2019) would be needed. In principle, this could lead to MDP translation according to the nuclear genetic code (Tessier et al., 2017; Mathers and Staples, 2019). The issue of mitochondrial retrograde signalling should further be extended to non-coding RNA regulators of mitochondrial origin such as ASncmtRNA-1 and ASncmtRNA-2 that together with *MT-SHLP6* map to the same rRNA gene. Theses loop-containing, polyadenylated antisense transcripts are widely abundant in proliferating cells, ubiquitously localised in the nucleus and modulate nuclear gene expression in a retrograde manner (Burzio et al., 2009; Ren et al., 2023). Considering that *mt-Shlp6* was found to be dynamically regulated in brown adipose tissue of the thirteen-lined ground squirrel across hibernation states (Figure 4), the existence of ASncmtRNA-1 and ASncmtRNA-2 in hibernating model species and their abundance changes during daily torpor or the stages of hibernation are of special interest (Burzio et al., 2009). They should also be analysed with regard to the finding that most long non-coding RNAs contain sORFs, hence, the potential to encode functional micropeptides (Pan et al., 2022).

It should also be addressed whether SHLP6 upregulation before torpor and during interbout arousal supports clearance of metabolites that accumulated due to torpor-induced low blood flow considering retrograde signalling by one or several MDPs as well as *cis*-acting regulatory elements and additional mtDNA polymorphisms that are related to heterothermy given the importance of the mitochondrial oxidative phosphorylation system in energy and heat production. Insight into the role of SHLP6 in endothermic thermoregulation can further be substantiated by increasing the number of SHLP6-coding sORFs, the amount of behavioural data with respect to heterothermic or homeothermic thermoregulation of rodents, and by deciphering the detailed mode(s) of action.

5 Conclusion and future perspectives

This study highlighted the conservation and variation of the apoptotic regulator peptide SHLP6 across Rodentia and established the connection between heterothermy and a member of the class of MDPs. It also provided the gold-standard level of proof based on MS for the canonical variant of human SHLP6, and added evidence to the involvement of the peptide in hibernation physiology by demonstrating differential transcript abundance for a hibernating model rodent. SHLP6, putatively an extracellular communicator (Woodhead et al., 2020), has likely a multi-facetted impact. This can be assumed based on its apoptotic function and the variation in micropeptide size, with one isoform being more favourable at a lower minimum T_b of a heterothermic mammal. Reduction of SHLP6 size could modify the potential for oligomerisation (Kienzle et al., 2023), extracellular and/or intracellular signalling (Hartford and Lal, 2020), and/or the number of binding sites for putative PTM switches that could act as a checkpoint to guarantee physiological safeness (Lee et al., 2015; Dai et al., 2022). Further analysis of SHLP6 size variation might focus on the stress perceived during cold exposure. Perceived stress is associated with altered metabolic activity of the amygdala, a brain region involved in stress. It can be measured using ^{18}F-fluorodeoxyglucose positron emission tomography/computed tomography (Tawakol et al., 2017). For example, genetically closely related rodents (e.g., of the genus *Rattus*) that differ in the length of their SHLP6 isomers could be compared. In addition, species such as the gray squirrel (*Sciurus carolinensis*) having size variants encoded by mitochondrial and nuclear DNA, are promising models. *In vivo* experimentation could focus on the metabolic outcome of the 9mer of SHLP6 administered exogenously (Merry et al., 2020; Kim et al., 2023).

A better understanding of SHLP size isomerisation and regulation can be of importance for therapeutic hypothermia, also known as targeted temperature management (Bernard et al., 2002; Garcia-Rubira et al., 2023). It is intentionally used in certain clinical situations to slow the metabolism and help reduce the risk of tissue damage following periods of insufficient blood flow, most commonly after resuscitation from cardiac arrest (Arrich et al., 2023). While therapeutic hypothermia has potential benefits, it also carries risks such as infection, coagulopathy, arrhythmias, and electrolyte imbalances (Geurts et al., 2014; Karnatovskaia et al., 2014; Wang et al., 2015). Therefore, its use must be carefully managed and a protective drug therapy might be of value.

Data availability statement

The datasets presented in this study can be found in online repositories. The names of the repository/repositories and accession number(s) can be found in the article/Supplementary Material.

Author contributions

Study conception: SE, RS. Analysis of sequencing data: SE. Peptide models: CS. Funding: EM. Manuscript writing: SE, RS. Proofreading: CS, EM. All authors contributed to the article and approved the submitted version.

Funding

This study was supported by resources of the University of Vienna.

Acknowledgments

We thank the reviewers for their inspiring input and Ingrid Miller for valuable discussion. Support of the Galaxy Team of the University of Freiburg (Germany) is gratefully acknowledged.

Conflict of interest

The authors declare that the research was conducted in the absence of any commercial or financial relationships that could be construed as a potential conflict of interest.

Publisher's note

All claims expressed in this article are solely those of the authors and do not necessarily represent those of their affiliated organizations, or those of the publisher, the editors and the reviewers. Any product that may be evaluated in this article, or claim that may be made by its manufacturer, is not guaranteed or endorsed by the publisher.

Supplementary material

The Supplementary Material for this article can be found online at: https://www.frontiersin.org/articles/10.3389/fphys.2023.1207620/full#supplementary-material

References

Andrews, M. T. (2019). Molecular interactions underpinning the phenotype of hibernation in mammals. *J. Exp. Biol.* 222, jeb160606. doi:10.1242/jeb.160606

Arrich, J., Schutz, N., Oppenauer, J., Vendt, J., Holzer, M., Havel, C., et al. (2023). Hypothermia for neuroprotection in adults after cardiac arrest. *Cochrane Database Syst. Rev.* 5, CD004128. doi:10.1002/14651858.CD004128.pub5

Balciuniene, J., and Balciunas, D. (2019). A nuclear mtDNA concatemer (Mega-NUMT) could mimic paternal inheritance of mitochondrial genome. *Front. Genet.* 10, 518. doi:10.3389/fgene.2019.00518

Barnes, B. M., Kretzmann, M., Licht, P., and Zucker, I. (1986). The influence of hibernation on testis growth and spermatogenesis in the golden-mantled ground squirrel, *Spermophilus lateralis*. *Biol. Reprod.* 35, 1289–1297. doi:10.1095/biolreprod35.5.1289

Beauclair, G., Bridier-Nahmias, A., Zagury, J.-F., Saïb, A., and Zamborlini, A. (2015). JASSA: a comprehensive tool for prediction of SUMOylation sites and SIMs. *Bioinformatics* 31, 3483–3491. doi:10.1093/bioinformatics/btv403

Beier, H., and Grimm, M. (2001). Misreading of termination codons in eukaryotes by natural nonsense suppressor tRNAs. *Nucleic Acids Res.* 29, 4767–4782. doi:10.1093/nar/29.23.4767

Benayoun, B. A., and Lee, C. (2019). MOTS-c: a mitochondrial-encoded regulator of the nucleus. *BioEssays* 41, 1900046. doi:10.1002/bies.201900046

Bernard, S. A., Gray, T. W., Buist, M. D., Jones, B. M., Silvester, W., Gutteridge, G., et al. (2002). Treatment of comatose survivors of out-of-hospital cardiac arrest with induced hypothermia. *N. Engl. J. Med.* 346, 557–563. doi:10.1056/NEJMoa003289

Bernt, M., Donath, A., Jühling, F., Externbrink, F., Florentz, C., Fritzsch, G., et al. (2013). Mitos: improved de novo metazoan mitochondrial genome annotation. *Mol. Phylogenetics Evol.* 69, 313–319. doi:10.1016/j.ympev.2012.08.023

Bray, N. L., Pimentel, H., Melsted, P., and Pachter, L. (2016). Near-optimal probabilistic RNA-seq quantification. *Nat. Biotechnol.* 34, 525–527. doi:10.1038/nbt.3519

Brown, J. C., Chung, D. J., Belgrave, K. R., and Staples, J. F. (2012). Mitochondrial metabolic suppression and reactive oxygen species production in liver and skeletal muscle of hibernating thirteen-lined ground squirrels. *Am. J. Physiol. Regul. Integr. Comp. Physiol.* 302, R15–R28. doi:10.1152/ajpregu.00230.2011

Brown, J. C. L., and Staples, J. F. (2011). Mitochondrial metabolic suppression in fasting and daily torpor: consequences for reactive oxygen species production. *Physiol. Biochem. Zool.* 84, 467–480. doi:10.1086/661639

Burzio, V. A., Villota, C., Villegas, J., Landerer, E., Boccardo, E., Villa, L. L., et al. (2009). Expression of a family of noncoding mitochondrial RNAs distinguishes normal from cancer cells. *Proc. Natl. Acad. Sci. U. S. A.* 106, 9430–9434. doi:10.1073/pnas.0903086106

Bushmanova, E., Antipov, D., Lapidus, A., and Prjibelski, A. D. (2019). RnaSPAdes: a de novo transcriptome assembler and its application to RNA-seq data. *GigaScience* 8, giz100. doi:10.1093/gigascience/giz100

Bushnell, B. (2014). "BBMap: a fast, accurate, splice-aware aligner," in 9th Annual Genomics of Energy and Environment Meeting, Berkeley, CA.

Calabrese, F. M., Simone, D., and Attimonelli, M. (2012). Primates and mouse NumtS in the UCSC genome browser. *BMC Bioinforma.* 13, S15. doi:10.1186/1471-2105-13-S4-S15

Carey, H. V., Andrews, M. T., and Martin, S. L. (2003). Mammalian hibernation: cellular and molecular responses to depressed metabolism and low temperature. *Physiol. Rev.* 83, 1153–1181. doi:10.1152/physrev.00008.2003

Carey, H. V., Frank, C. L., and Seifert, J. P. (2000). Hibernation induces oxidative stress and activation of NK-kappaB in ground squirrel intestine. *J. Comp. Physiology B-Biochemical Syst. Environ. Physiology* 170, 551–559. doi:10.1007/s003600000135

Caricasole, A., Bruno, V., Cappuccio, I., Melchiorri, D., Copani, A., and Nicoletti, F. (2002). A novel rat gene encoding a Humanin-like peptide endowed with broad neuroprotective activity. *FASEB J.* 16, 1331–1333. doi:10.1096/fj.02-0018fje

Chhangawala, S., Rudy, G., Mason, C. E., and Rosenfeld, J. A. (2015). The impact of read length on quantification of differentially expressed genes and splice junction detection. *Genome Biol.* 16, 131. doi:10.1186/s13059-015-0697-y

Cobb, L. J., Lee, C., Xiao, J., Yen, K., Wong, R. G., Nakamura, H. K., et al. (2016). Naturally occurring mitochondrial-derived peptides are age-dependent regulators of apoptosis, insulin sensitivity, and inflammatory markers. *Aging* 8, 796–809. doi:10.18632/aging.100943

Dai, X., Zhang, J., North, B. J., and Guo, J. (2022). Editorial: post-translational modifications of proteins in cancer immunity and immunotherapy. *Front. Immunol.* 13, 1006145. doi:10.3389/fimmu.2022.1006145

Daniel, J. A., Cooper, B. H., Palvimo, J. J., Zhang, F.-P., Brose, N., and Tirard, M. (2017). Analysis of SUMO1-conjugation at synapses. *Elife.* 6, e26338. doi:10.7554/eLife.26338

Dave, K. R., Christian, S. L., Perez-Pinzon, M. A., and Drew, K. L. (2012). Neuroprotection: lessons from hibernators. *Comp. Biochem. Physiol. B Biochem. Mol. Biol.* 162, 1–9. doi:10.1016/j.cbpb.2012.01.008

Devall, M., Roubroeks, J., Mill, J., Weedon, M., and Lunnon, K. (2016). Epigenetic regulation of mitochondrial function in neurodegenerative disease: new insights from advances in genomic technologies. *Neurosci. Lett.* 625, 47–55. doi:10.1016/j.neulet.2016.02.013

Dyson, H. J. (2016). Making sense of intrinsically disordered proteins. *Biophys. J.* 110, 1013–1016. doi:10.1016/j.bpj.2016.01.030

Emser, S. V., Schaschl, H., Millesi, E., and Steinborn, R. (2021). Extension of mitogenome enrichment based on single long-range PCR: mtDNAs and putative mitochondrial-derived peptides of five rodent hibernators. *Front. Genet.* 12, 685806. doi:10.3389/fgene.2021.685806

Faure, E., Delaye, L., Tribolo, S., Levasseur, A., Seligmann, H., and Barthélémy, R. M. (2011). Probable presence of an ubiquitous cryptic mitochondrial gene on the antisense strand of the cytochrome oxidase I gene. *Biol. Direct* 6, 56–22. doi:10.1186/1745-6150-6-56

Galaxy, C. (2022). The Galaxy platform for accessible, reproducible and collaborative biomedical analyses: 2022 update. *Nucleic Acids Res.* 50, W345–W351. doi:10.1093/nar/gkac247

Galster, W., and Morrison, P. (1975). Gluconeogenesis in arctic ground squirrels between periods of hibernation. *Am. J. Physiol.* 228, 325–330. doi:10.1152/ajplegacy.1975.228.1.325

Garcia-Rubira, J. C., Olivares-Martínez, B., Rivadeneira-Ruiz, M., Fernández-Valenzuela, I., Recio-Mayoral, A., Almendro-Delia, M., et al. (2023). Target temperature in post-arrest comatous patients. Is something changed in the postpandemic era? *Am. J. Emerg. Med.* 71, 14–17. doi:10.1016/j.ajem.2023.06.004

Georgakopoulos-Soares, I., Parada, G. E., and Hemberg, M. (2022). Secondary structures in RNA synthesis, splicing and translation. *Comput. Struct. Biotechnol. J* 20, 2871–2884. doi:10.1016/j.csbj.2022.05.041

Geurts, M., Macleod, M. R., Kollmar, R., Kremer, P. H., and Van Der Worp, H. B. (2014). Therapeutic hypothermia and the risk of infection: a systematic review and meta-analysis. *Crit. Care Med.* 42, 231–242. doi:10.1097/CCM.0b013e3182a276e8

Gillen, A. E., Fu, R., Riemondy, K. A., Jager, J., Fang, B., Lazar, M. A., et al. (2021). Liver transcriptome dynamics during hibernation are shaped by a shifting balance between transcription and RNA stability. *Front. Physiology* 12, 662132. doi:10.3389/fphys.2021.662132

Gouy, M., Guindon, S., and Gascuel, O. (2010). Sea view version 4: a multiplatform graphical user interface for sequence alignment and phylogenetic tree building. *Mol. Biol. Evol.* 27, 221–224. doi:10.1093/molbev/msp259

Granat, L., Hunt, R. J., and Bateman, J. M. (2020). Mitochondrial retrograde signalling in neurological disease. *Philos. Trans. R. Soc. Lond B Biol. Sci.* 375, 20190415. doi:10.1098/rstb.2019.0415

Gruber, A. R., Lorenz, R., Bernhart, S. H., Neuböck, R., and Hofacker, I. L. (2008). The Vienna RNA websuite. *Nucleic Acids Res.* 36, W70–W74. doi:10.1093/nar/gkn188

Gupta, R., and Brunak, S. (2002). Prediction of glycosylation across the human proteome and the correlation to protein function. *Pac. Symposium Biocomput.* 7, 310–322.

Hamilton, M. T., and Booth, F. W. (2000). Skeletal muscle adaptation to exercise: a century of progress. *J. Appl. Physiol.* 88, 327–331. doi:10.1152/jappl.2000.88.1.327

Harber, M. P., Kaminsky, L. A., Arena, R., Blair, S. N., Franklin, B. A., Myers, J., et al. (2017). Impact of cardiorespiratory fitness on all-cause and disease-specific mortality: advances since 2009. *Prog. Cardiovasc. Dis.* 60, 11–20. doi:10.1016/j.pcad.2017.03.001

Hartford, C. C. R., and Lal, A. (2020). When long noncoding becomes protein coding. *Mol. Cell. Biol.* 40, e00528-19. doi:10.1128/MCB.00528-19

Hashimoto, Y., Niikura, T., Tajima, H., Yasukawa, T., Sudo, H., Ito, Y., et al. (2001). A rescue factor abolishing neuronal cell death by a wide spectrum of familial Alzheimer's disease genes and Abeta. *Proc. Natl. Acad. Sci. U. S. A.* 98, 6336–6341. doi:10.1073/pnas.101133498

Hoang, D. T., Chernomor, O., Von Haeseler, A., Minh, B. Q., and Vinh, L. S. (2018). UFBoot2: improving the ultrafast bootstrap approximation. *Mol. Biol. Evol.* 35, 518–522. doi:10.1093/molbev/msx281

Holloszy, J. O., and Coyle, E. F. (1984). Adaptations of skeletal muscle to endurance exercise and their metabolic consequences. *J. Appl. Physiology* 56, 831–838. doi:10.1152/jappl.1984.56.4.831

Hume, I. D., Beiglböck, C., Ruf, T., Frey-Roos, F., Bruns, U., and Arnold, W. (2002). Seasonal changes in morphology and function of the gastrointestinal tract of free-living alpine marmots (Marmota marmota). *J. Comp. Physiology B Biochem. Syst. Environ. Physiology* 172, 197–207. doi:10.1007/s00360-001-0240-1

Humphries, M. U. R. R. A. Y. M., Thomas, D. O. N. A. L. D. W., and Kramer, D. O. N. A. L. D. L. (2003). The role of energy availability in mammalian hibernation: a cost-benefit approach. *Physiol. Biochem. Zool.* 76, 165–179. doi:10.1086/367950

Jeandard, D., Smirnova, A., Tarassov, I., Barrey, E., Smirnov, A., and Entelis, N. (2019). Import of non-coding RNAs into human mitochondria: a critical review and emerging approaches. *Cells* 8, 286. doi:10.3390/cells8030286

Jumper, J., Evans, R., Pritzel, A., Green, T., Figurnov, M., Ronneberger, O., et al. (2021). Highly accurate protein structure prediction with AlphaFold. *Nature* 596, 583–589. doi:10.1038/s41586-021-03819-2

Kalyaanamoorthy, S., Minh, B. Q., Wong, T. K. F., Von Haeseler, A., and Jermiin, L. S. (2017). ModelFinder: fast model selection for accurate phylogenetic estimates. *Nat. Methods* 14, 587–589. doi:10.1038/nmeth.4285

Karnatovskaia, L. V., Wartenberg, K. E., and Freeman, W. D. (2014). Therapeutic hypothermia for neuroprotection: history, mechanisms, risks, and clinical applications. *Neurohospitalist* 4, 153–163. doi:10.1177/1941874413519802

Karpovich, S. A., Toien, O., Buck, C. L., and Barnes, B. M. (2009). Energetics of arousal episodes in hibernating arctic ground squirrels. *J. Comp. Physiol. B* 179, 691–700. doi:10.1007/s00360-009-0350-8

Kienzle, L., Bettinazzi, S., Choquette, T., Brunet, M., Khorami, H. H., Jacques, J. F., et al. (2023). A small protein coded within the mitochondrial canonical gene nd4 regulates mitochondrial bioenergetics. *BMC Biol.* 21, 111. doi:10.1186/s12915-023-01609-y

Kim, K. H., Son, J. M., Benayoun, B. A., and Lee, C. (2018). The mitochondrial-encoded peptide MOTS-c translocates to the nucleus to regulate nuclear gene expression in response to metabolic stress. *Cell Metab.* 28, 516–524. doi:10.1016/j.cmet.2018.06.008

Kim, S. K., Tran, L. T., Namkoong, C., Choi, H. J., Chun, H. J., Lee, Y. H., et al. (2023). Mitochondria-derived peptide SHLP2 regulates energy homeostasis through the activation of hypothalamic neurons. *Nat. Commun.* 14, 4321. doi:10.1038/s41467-023-40082-7

Kubatova, N., Pyper, D. J., Jonker, H. R. A., Saxena, K., Remmel, L., Richter, C., et al. (2020). Rapid biophysical characterization and NMR spectroscopy structural analysis of small proteins from bacteria and archaea. *Chembiochem.* 21, 1178–1187. doi:10.1002/cbic.201900677

Kukat, C., Wurm, C. A., Spahr, H., Falkenberg, M., Larsson, N. G., and Jakobs, S. (2011). Super-resolution microscopy reveals that mammalian mitochondrial nucleoids have a uniform size and frequently contain a single copy of mtDNA. *Proc. Natl. Acad. Sci. U. S. A.* 108, 13534–13539. doi:10.1073/pnas.1109263108

Kumagai, H., Miller, B., Kim, S.-J., Leelaprachakul, N., Kikuchi, N., Yen, K., et al. (2023). Novel insights into mitochondrial DNA: mitochondrial microproteins and mtDNA variants modulate athletic performance and age-related diseases. *Genes* 14, 286. doi:10.3390/genes14020286

Kumar, S., Suleski, M., Craig, J. M., Kasprowicz, A. E., Sanderford, M., Li, M., et al. (2022). TimeTree 5: an expanded resource for species divergence times. *Mol. Biol. Evol.* 39, msac174. doi:10.1093/molbev/msac174

Kurtz, C. C., Otis, J. P., Regan, M. D., and Carey, H. V. (2021). How the gut and liver hibernate. *Comp. Biochem. Physiol. A Mol. Integr. Physiol.* 253, 110875. doi:10.1016/j.cbpa.2020.110875

Kyte, J., and Doolittle, R. F. (1982). A simple method for displaying the hydropathic character of a protein. *J. Mol. Biol.* 157, 105–132. doi:10.1016/0022-2836(82)90515-0

Laukkanen, J. A., and Kujala, U. M. (2018). Low cardiorespiratory fitness is a risk factor for death. *J. Am. Coll. Cardiol.* 72, 2293–2296. doi:10.1016/j.jacc.2018.06.081

Lee, C., Zeng, J., Drew, B. G., Sallam, T., Martin-Montalvo, A., Wan, J., et al. (2015). The mitochondrial-derived peptide MOTS-c promotes metabolic homeostasis and reduces obesity and insulin resistance. *Cell Metab.* 21, 443–454. doi:10.1016/j.cmet.2015.02.009

Letunic, I., and Bork, P. (2021). Interactive tree of life (iTOL) v5: an online tool for phylogenetic tree display and annotation. *Nucleic Acids Res.* 49, W293–W296. doi:10.1093/nar/gkab301

Levesque, D. L., Nowack, J., and Stawski, C. (2016). Modelling mammalian energetics: the heterothermy problem. *Clim. Change Responses* 3, 7. doi:10.1186/s40665-016-0022-3

Liu, Z. C., and Butow, R. A. (2006). Mitochondrial retrograde signaling. *Annu. Rev. Genet.* 40, 159–185. doi:10.1146/annurev.genet.40.110405.090613

Lorenz, R., Bernhart, S. H., Höner Zu Siederdissen, C., Tafer, H., Flamm, C., Stadler, P. F., et al. (2011). ViennaRNA package 2.0. *Algorhithms Mol. Biol.* 6, 26. doi:10.1186/1748-7188-6-26

Love, M. I., Huber, W., and Anders, S. (2014). Moderated estimation of fold change and dispersion for RNA-seq data with DESeq2. *Genome Biol.* 15, 550. doi:10.1186/s13059-014-0550-8

Lu, H., Tang, S., Xue, C., Liu, Y., Wang, J., Zhang, W., et al. (2019). Mitochondrial-derived peptide MOTS-c increases adipose thermogenic activation to promote cold adaptation. *Int. J. Mol. Sci.* 20, 2456. doi:10.3390/ijms20102456

Lutz-Bonengel, S., Niederstätter, H., Naue, J., Koziel, R., Yang, F., Sänger, T., et al. (2021). Evidence for multi-copy Mega-NUMT s in the human genome. *Nucleic Acids Res.* 49, 1517–1531. doi:10.1093/nar/gkaa1271

Małecki, J. M., Davydova, E., and Falnes, P. Ø. (2022). Protein methylation in mitochondria. *J. Biol. Chem.* 298, 101791. doi:10.1016/j.jbc.2022.101791

Mariani, V., Biasini, M., Barbato, A., and Schwede, T. (2013). lDDT: a local superposition-free score for comparing protein structures and models using distance difference tests. *Bioinformatics* 29, 2722–2728. doi:10.1093/bioinformatics/btt473

Markham, N. R., and Zuker, M. (2008). UNAFold: software for nucleic acid folding and hybridization. *Methods Mol. Biol.* 453, 3–31. doi:10.1007/978-1-60327-429-6_1

Mathers, K. E., Mcfarlane, S. V., Zhao, L., and Staples, J. F. (2017). Regulation of mitochondrial metabolism during hibernation by reversible suppression of electron transport system enzymes. *J. Comp. Physiology B Biochem. Syst. Environ. Physiology* 187, 227–234. doi:10.1007/s00360-016-1022-0

Mathers, K. E., and Staples, J. F. (2019). Differential posttranslational modification of mitochondrial enzymes corresponds with metabolic suppression during hibernation. *Am. J. Physiol. Regul. Integr. Comp. Physiol.* 317, R262-R269–R269. doi:10.1152/ajpregu.00052.2019

Merry, T. L., Chan, A., Woodhead, J. S. T., Reynolds, J. C., Kumagai, H., Kim, S. J., et al. (2020). Mitochondrial-derived peptides in energy metabolism. *Am. J. Physiol. Endocrinol. Metab.* 319, E659-E666–e666. doi:10.1152/ajpendo.00249.2020

Miller, B., Kim, S.-J., Mehta, H. H., Cao, K., Kumagai, H., Thumaty, N., et al. (2022). Mitochondrial DNA variation in Alzheimer's disease reveals a unique microprotein called SHMOOSE. *Mol. Psychiatry* 28, 1813–1826. doi:10.1038/s41380-022-01769-3

Mirdita, M., Schütze, K., Moriwaki, Y., Heo, L., Ovchinnikov, S., and Steinegger, M. (2022). ColabFold: making protein folding accessible to all. *Nat. Methods* 19, 679–682. doi:10.1038/s41592-022-01488-1

Morales, J. O., Walker, N., Warne, R. W., and Boyles, J. G. (2021). Heterothermy as a mechanism to offset energetic costs of environmental and homeostatic perturbations. *Sci. Rep.* 11, 19038. doi:10.1038/s41598-021-96828-0

Necci, M., Piovesan, D., Hoque, M. T., Walsh, I., Iqbal, S., Vendruscolo, M., et al. (2021). Critical assessment of protein intrinsic disorder prediction. *Nat. Methods* 18, 472–481. doi:10.1038/s41592-021-01117-3

Nespolo, R. F., Mejías, C., Espinoza, A., Quintero-Galvis, J., Rezende, E. L., Fontúrbel, F. E., et al. (2021). Heterothermy as the Norm, Homeothermy as the Exception: variable Torpor Patterns in the South American Marsupial Monito del Monte (Dromiciops gliroides). *Front. Physiology* 12, 682394. doi:10.3389/fphys.2021.682394

Ng, K. Y., Lutfullahoglu Bal, G., Richter, U., Safronov, O., Paulin, L., Dunn, C. D., et al. (2022). Nonstop mRNAs generate a ground state of mitochondrial gene expression noise. *Sci. Adv.* 8, eabq5234. doi:10.1126/sciadv.abq5234

Nguyen, L. T., Schmidt, H. A., Von Haeseler, A., and Minh, B. Q. (2015). IQ-TREE: a fast and effective stochastic algorithm for estimating maximum-likelihood phylogenies. *Mol. Biol. Evol.* 32, 268–274. doi:10.1093/molbev/msu300

Nowack, J., Levesque, D. L., Reher, S., and Dausmann, K. H. (2020). Variable climates lead to varying phenotypes: "Weird" mammalian torpor and lessons from non-holarctic species. *Front. Ecol. Evol.* 8, 60. doi:10.3389/fevo.2020.00060

Nowack, J., Tarmann, I., Hoelzl, F., Smith, S., Giroud, S., and Ruf, T. (2019). Always a price to pay: hibernation at low temperatures comes with a trade-off between energy savings and telomere damage. *Biol. Lett.* 15, 20190466. doi:10.1098/rsbl.2019.0466

Paharkova, V., Alvarez, G., Nakamura, H., Cohen, P., and Lee, K. W. (2015). Rat Humanin is encoded and translated in mitochondria and is localized to the mitochondrial compartment where it regulates ROS production. *Mol. Cell. Endocrinol.* 413, 96–100. doi:10.1016/j.mce.2015.06.015

Pan, J. F., Wang, R. J., Shang, F. Z., Ma, R., Rong, Y. J., and Zhang, Y. J. (2022). Functional micropeptides encoded by long non-coding RNAs: a comprehensive review. *Front. Mol. Biosci.* 9, 817517. doi:10.3389/fmolb.2022.817517

Ren, B. B., Guan, M. X., Zhou, T. H., Cai, X. J., and Shan, G. (2023). Emerging functions of mitochondria-encoded noncoding RNAs. *Trends Genet.* 39, 125–139. doi:10.1016/j.tig.2022.08.004

Reynolds, J. C., Lai, R. W., Woodhead, J. S. T., Joly, J. H., Mitchell, C. J., Cameron-Smith, D., et al. (2021). MOTS-c is an exercise-induced mitochondrial-encoded regulator of age-dependent physical decline and muscle homeostasis. *Nat. Commun.* 12, 470. doi:10.1038/s41467-020-20790-0

Rice, M. C., Kim, J. S., Imun, M., Jung, S. W., Rice, P. M. C., Park, C. Y., Lai, R. W., et al. (2023). The human mitochondrial genome encodes for an interferon-responsive host defense peptide. *bioRxiv*. 023.03.02.530691. doi:10.1101/2023.03.02.530691

RStudio Team (2021). RStudio: integrated Development for R. RStudio, PBC, Boston, MA, USA. Available at: http://www.rstudio.com/.

Rubio, M. A. T., Rinehart, J. J., Krett, B., Duvezin-Caubet, S., Reichert, A. S., Söll, D., et al. (2008). Mammalian mitochondria have the innate ability to import tRNAs by a mechanism distinct from protein import. *Proc. Natl. Acad. Sci. U. S. A.* 105, 9186–9191. doi:10.1073/pnas.0804283105

Ruf, T., and Geiser, F. (2015). Daily torpor and hibernation in birds and mammals. *Biol. Rev.* 90, 891–926. doi:10.1111/brv.12137

Ruf, T., Giroud, S., and Geiser, F. (2022). Hypothesis and theory: a two-process model of torpor-arousal regulation in hibernators. *Front. Physiol.* 13, 901270. doi:10.3389/fphys.2022.901270

Sammet, S. G., Bastolla, U., and Porto, M. (2010). Comparison of translation loads for standard and alternative genetic codes. *BMC Evol. Biol.* 10, 178. doi:10.1186/1471-2148-10-178

Sangster, G., and Luksenburg, J. A. (2021). Sharp increase of problematic mitogenomes of birds: causes, consequences, and remedies. *Genome Biol. Evol.* 13, evab210. doi:10.1093/gbe/evab210

Schlesinger, D., and Elsasser, S. J. (2022). Revisiting sORFs: overcoming challenges to identify and characterize functional microproteins. *FEBS J.* 289, 53–74. doi:10.1111/febs.15769

Sheriff, M. J., Fridinger, R. W., Tøien, Ø., Barnes, B. M., and Buck, C. L. (2013). Metabolic rate and prehibernation fattening in free-living arctic ground squirrels. *Physiol. Biochem. Zool.* 86, 515–527. doi:10.1086/673092

Siutz, C., Franceschini, C., and Millesi, E. (2016). Sex and age differences in hibernation patterns of common hamsters: adult females hibernate for shorter periods than males. *J. Comp. Physiology B Biochem. Syst. Environ. Physiology* 186, 801–811. doi:10.1007/s00360-016-0995-z

Sousa, M. E., and Farkas, M. H. (2018). Micropeptide. *PLoS Genet.* 14, e1007764. doi:10.1371/journal.pgen.1007764

Staples, J. F., and Brown, J. C. L. (2008). Mitochondrial metabolism in hibernation and daily torpor: a review. *J. Comp. Physiology B Biochem. Syst. Environ. Physiology* 178, 811–827. doi:10.1007/s00360-008-0282-8

Szereszewski, K. E., and Storey, K. B. (2019). Identification of a prosurvival neuroprotective mitochondrial peptide in a mammalian hibernator. *Cell Biochem. Funct.* 37, 494–503. doi:10.1002/cbf.3422

Tawakol, A., Ishai, A., Takx, R. A., Figueroa, A. L., Ali, A., Kaiser, Y., et al. (2017). Relation between resting amygdalar activity and cardiovascular events: a longitudinal and cohort study. *Lancet* 389, 834–845. doi:10.1016/S0140-6736(16)31714-7

Tessier, S. N., Luu, B. E., Smith, J. C., and Storey, K. B. (2017). The role of global histone post-translational modifications during mammalian hibernation. *Cryobiology* 75, 28–36. doi:10.1016/j.cryobiol.2017.02.008

Uniprot, C. (2023). UniProt: the universal protein knowledgebase in 2023. *Nucleic Acids Res.* 51, D523–D531. doi:10.1093/nar/gkac1052

Van Breukelen, F., and Martin, S. L. (2001). Translational initiation is uncoupled from elongation at 18 degrees C during mammalian hibernation. *Am. J. Physiology-Regulatory, Integr. Comp. Physiology* 281, R1374–R1379. doi:10.1152/ajpregu.2001.281.5.R1374

Wagner, P. D. (1991). Central and peripheral aspects of oxygen transport and adaptations with exercise. *Sports Med.* 11, 133–142. doi:10.2165/00007256-199111030-00001

Wang, C. H., Chen, N. C., Tsai, M. S., Yu, P. H., Wang, A. Y., Chang, W. T., et al. (2015). Therapeutic hypothermia and the risk of hemorrhage: a systematic review and meta-analysis of randomized controlled trials. *Med. Baltim.* 94, e2152. doi:10.1097/MD.0000000000002152

Wang, C., Xu, H., Lin, S., Deng, W., Zhou, J., Zhang, Y., et al. (2020). Gps 5.0: an update on the prediction of kinase-specific phosphorylation sites in proteins. *Genomics, Proteomics Bioinforma.* 18, 72–80. doi:10.1016/j.gpb.2020.01.001

Wang, J., Youkharibache, P., Marchler-Bauer, A., Lanczycki, C., Zhang, D., Lu, S., et al. (2022). iCn3D: from web-based 3D viewer to structural analysis tool in batch mode. *Front. Mol. Biosci.* 9, 831740. doi:10.3389/fmolb.2022.831740

Wei, W., Schon, K. R., Elgar, G., Orioli, A., Tanguy, M., Giess, A., et al. (2022). Nuclear-embedded mitochondrial DNA sequences in 66,083 human genomes. *Nature* 611, 105–114. doi:10.1038/s41586-022-05288-7

Wen, B., and Zhang, B. (2023). PepQuery2 democratizes public MS proteomics data for rapid peptide searching. *Nat. Commun.* 14, 2213. doi:10.1038/s41467-023-37462-4

Wenger, H. A., and Bell, G. J. (1986). The interactions of intensity, frequency and duration of exercise training in altering cardiorespiratory fitness. *Sports Med.* 3, 346–356. doi:10.2165/00007256-198603050-00004

Wiersma, M., Beuren, T. M. A., De Vrij, E. L., Reitsema, V. A., Bruintjes, J. J., Bouma, H. R., et al. (2018). Torpor-arousal cycles in Syrian hamster heart are associated with transient activation of the protein quality control system. *Comp. Biochem. Physiology Part B Biochem. Mol. Biol.* 223, 23–28. doi:10.1016/j.cbpb.2018.06.001

Woodhead, J. S. T., D'Souza, R. F., Hedges, C. P., Wan, J. X., Berridge, M. V., Cameron-Smith, D., et al. (2020). High-intensity interval exercise increases humanin, a mitochondrial encoded peptide, in the plasma and muscle of men. *J. Appl. Physiology* 128, 1346–1354. doi:10.1152/japplphysiol.00032.2020

Workman, R. E., Tang, A. D., Tang, P. S., Jain, M., Tyson, J. R., Razaghi, R., et al. (2019). Nanopore native RNA sequencing of a human poly(A) transcriptome. *Nat. Methods* 16, 1297–1305. doi:10.1038/s41592-019-0617-2

Yang, Z. Y., Zeng, X. X., Zhao, Y., and Chen, R. S. (2023). AlphaFold2 and its applications in the fields of biology and medicine. *Signal Transduct. Target. Ther.* 8, 115. doi:10.1038/s41392-023-01381-z

frontiers | Frontiers in Physiology

TYPE Original Research
PUBLISHED 06 September 2023
DOI 10.3389/fphys.2023.1241470

OPEN ACCESS

EDITED BY
Yoshifumi Yamaguchi,
Hokkaido University, Japan

REVIEWED BY
Oliver Otti,
Technical University of Dresden, Germany
Budhan Pukazhenthi,
Smithsonian Conservation Biology Institute (SI), United States

*CORRESPONDENCE
Takahiro Sato,
satoj@tokushima-u.ac.jp

RECEIVED 16 June 2023
ACCEPTED 28 August 2023
PUBLISHED 06 September 2023

CITATION
Sato T, Sugiyama T and Sekijima T (2023), Mating in the cold. Prolonged sperm storage provides opportunities for forced copulation by male bats during winter. *Front. Physiol.* 14:1241470. doi: 10.3389/fphys.2023.1241470

Mating in the cold. Prolonged sperm storage provides opportunities for forced copulation by male bats during winter

Takahiro Sato[1,2]*, Toshie Sugiyama[2] and Tsuneo Sekijima[2]

[1]Graduate School of Technology, Industrial, and Social Sciences, Tokushima University, Tokushima, Japan, [2]Faculty of Agriculture, Niigata University, Niigata, Japan

In a wide range of heterothermic mammals, hibernation interrupts the reproductive cycle by forcing reproductive delays. In hibernating bats with delayed fertilization, an opportunity for sperm competition is enhanced by extending a time-window between copulations and fertilization. In order to achieve greater fertilization success, males are expected to show adaptations for sperm competition by increasing their opportunities for mating over an extended period. We aimed to clarify the physiological and behavioral characteristics of male bats experiencing increased risks of sperm competition. We investigated the characteristics of the reproductive cycle of the little horseshoe bat (*Rhinolophus cornutus*), and examined whether males retain reproductive physiology related to sexual behavior, and attempt to copulate with females even during the hibernation period. Field observations and histological examinations of the reproductive cycle confirmed that females, having mated in the autumn, store spermatozoa in the uterus during hibernation and give birth in the early summer to just one offspring per year, thus males face a low certainty of successful fertilization. Although their testes regressed rapidly and their testosterone levels were lower during winter than in autumn, males stored motile spermatozoa in their cauda epididymides from autumn throughout the winter. During hibernation, we found that males occasionally aroused from torpor and attempted to mate forcibly with torpid females. Forced copulations appear to increase a male's chances of obtaining a mate while avoiding pre-copulatory female choice. Epididymal sperm storage could be advantageous for males in allowing them to extend their potential mating period even though their testes have regressed. We also found that some hibernating nulliparous females were ready for fertilization in spring after hibernation, whereas few parous females appeared in the same roost. In contrast to males, forced copulations would be maladaptive for females because they cannot opt for higher-quality males while in torpor. Females that have experienced sexual coercion when young may subsequently avoid hibernacula where adult males are present.

KEYWORDS

reproductive delay, heterothermy, sperm competition, sexual coercion, Chiroptera

1 Introduction

A wide range of heterothermic mammals conserve energy so as to survive the season of low ambient temperature and scarce prey availability by entering deep, multi-day torpor (i.e., hibernation) (Geiser, 2013). Hibernation is characterized by a regulated reduction in metabolic rate and body temperature resulting in a depression of energy expenditure (Geiser, 2004; Ruf and Geiser, 2015). The physiological state of hibernation slows down many endocrine activities leading to the suppression of circulating levels of reproductive hormones and the suppression of the functions of the reproductive organs (Racey and Swift, 1981; Barnes et al., 1986; Gagnon et al., 2020). Therefore, it has been presumed that hibernation and reproduction are mutually incompatible processes, particularly among rodents (Wimsatt, 1969).

Increasing knowledge of the relationship between thermoregulation and reproductive status has recently shown that hibernation and reproduction can be compatible in some mammal species (McAllan and Geiser, 2014; Geiser, 2021). Among marsupials and bats, females often enter torpor during pregnancy and lactation (Geiser et al., 2005; Körtner et al., 2008; Dzal and Brigham, 2013). Although bouts of torpor during the reproductive season are mostly shallower and shorter than during winter, pregnant hoary bats (*Lasiurus cinereus*) enter multiday torpor, which meets the common definition of hibernation (Willis et al., 2006). Entering torpor temporarily during the reproductive period allows insectivorous species, such as bats, to avoid starvation caused by prey scarcity during extreme weather conditions (Stawski et al., 2014). Reproductive cycles overlap hibernation in Tasmanian echidna (*Tachyglossus aculeatus*) and temperate zone bat species (Crichton, 2000; McAllan and Geiser, 2014). In Tasmanian echidna, males have enlarged testes and are likely to mate with females during hibernation (Morrow and Nicol, 2009; Morrow et al., 2016). Interesting phenomena co-occurring reproduction and hibernation are reproductive delays in bats (Racey and Entwistle, 2000). Among bats, reproductive events are interrupted by prolonged winter torpor, thereby extending the period, either between copulation and fertilization (delayed fertilization) or between fertilization and implantation (delayed implantation) (Oxberry, 1979; Sandell, 1990). The physiological mechanisms that allow bats to maintain reproductive functions during delays have been discussed intensively in terms of the anatomical features of their reproductive organs and the involvement of sex hormones (e.g., androgen for female sperm storage) (Racey and Entwistle, 2000; Ocampo-González et al., 2021). In contrast, their reproductive strategies or tactics during hibernation, which are facilitated by reproductive delays, remain to be discussed.

A unique feature of bats exhibiting reproductive delays is that their opportunities for post-copulatory sexual selection are enhanced (Orr and Zuk, 2014; Orr and Brennan, 2015). In those bat species with delayed fertilization, mating occurs during late-summer and autumn before hibernation, but ovulation and fertilization occur in spring after hibernation (Racey, 1979). During the delay, females store sperm for several months within their reproductive tract (Racey, 1973; Wang et al., 2008). As bats typically bear only one or two offspring per litter (Barclay and Harder, 2003), in those species in which females mate multiple-times, males face reduced certainty of fertilization success. Thus, intense male-male competition is facilitated in the form of sperm competition. Male reproductive traits are under strong selection pressure (Orr and Zuk, 2014). For example, species with delayed fertilization have larger testes than those without delays, indicating that males invest more resources in sperm production (Orr and Zuk, 2013). Bat species in which there is a greater risk of sperm competition, including species with delayed fertilization, have elaborate penile morphology (e.g., the presence of penile spines) and sperm features related to competitive ability (e.g., sperm length and mitochondria quantity) (Hosken, 1997; Fasel et al., 2019). Since delayed fertilization extends the time-window from copulation until fertilization, the hibernating season potentially provides an extended period for mating. In order to achieve greater fertilization success, males are expected to exhibit characteristics that allow them to obtain more mating opportunities. Hibernation certainly inhibits many reproductive processes. However, even under such constraints, physiological and behavioral traits that maximize reproductive success could evolve through sexual selection, particularly in bats with intense sperm competition. If males are able to retain reproductive functions related to sexual behavior even during hibernation, they may be able to copulate over an extended period.

While previous research has often focused on morphological traits (e.g., testes size) as an index of sperm competition, little effort has been made to investigate physiological and behavioral characteristics integrally in the context of male adaptations to sperm competition during hibernation. As a model species to test our predictions, we focused on the cave-dwelling little horseshoe bat (*Rhinolophus cornutus*), which is widely distributed in the Japanese archipelago (Sano and Armstrong, 2009). In this species females give birth to a single offspring in early summer (mainly in late June) (Sano and Armstrong, 2009). Although it was not known whether little horseshoe bat exhibits delayed fertilization or not, sperm competition could be enhanced if females store sperm during hibernation. The anatomical study of male reproductive organs suggested that sperm may be retained within the epididymides during winter (Kurohmaru et al., 2002). Since 2011, we have also monitored the reproductive cycle of a wild population of little horseshoe bat, and we observed torpid males with enlarged external gonads during winter. We expected that males were able to store sperm and attempt to copulate during hibernation.

In this study our first aim was to describe the annual reproductive cycle of the little horseshoe bat, and to investigate whether females store sperm during hibernation, which would be a characteristic of delayed fertilization. Our second aim was to clarify whether or not males retain reproductive conditions enabling them to mate during winter (as well as in autumn). We also tested the prediction that copulation occurs during hibernation. Furthermore, histologically, we determined the reproductive conditions of wintering females to examine whether females were fertilizable in spring, and thus potential mates for males.

2 Materials and methods

2.1 Study site

Our field work was conducted in Osawa cave (37° 40′N, 139° 06′E, 216 m above sea level) located in Gosen City, Niigata Prefecture, Japan. The ambient temperature in the cave was

stable throughout the year (mean ± SD = 9.9°C ± 0.4°C, recorded at 1-h intervals from June 2011 to May 2012 using a temperature data logger). The total number of little horseshoe bats in the cave peaked during summer and winter (700–900 individuals), and was lowest (<10–200 individuals) in late autumn from September to November. Although no other roosts have been found in the vicinity of Osawa cave, it seems that most of bats in the colony disperse to other roosts during autumn. We also collected specimens for experiments assessing male reproductive physiology (section 2.5 in detail) from an abandoned tunnel (37° 08′N, 138° 38′E, 169 m above sea level) located in Tokamachi City, Niigata.

2.2 Ethics statement

All capture, handling and sampling procedures were approved by the Kanto Regional Environmental Office in Saitama, Ministry of the Environment (Permit Number: #1311211, #1405126, #1505111, #16052311 and #1705245), Niigata Prefecture (Permit Number: #148, #208 and #282) and Gosen City (Permit Number: #37). All of the animal experiments were carried out in compliance with procedures reviewed by the Institutional Animal Care and Use Committee and approved by the President of Niigata University (Permit Number: Niigata Univ. Res. 356-2, 356-3, and 356-4).

2.3 Determination of annual reproductive cycle

To determine the annual reproductive cycle of the little horseshoe bat in our study site, preliminary investigations of the hibernation period were conducted from August 2011 to July 2012. We used a Thermo Gear G120 (Nippon Avionics, Kanagawa, Japan) thermal imaging camera for monitoring the surface body temperatures of bats. When possible, we placed the camera on the cave floor 4–7 m away from a group of bats containing >50% of the total number of individuals in the cave, and observed bats for 5–7 days each month. The camera was programmed to take a thermal image (±0.1°C resolution) every 10 min. Thermo Gear G120 has a horizontal field of view of 32° and a vertical field of view of 24° with 1.78 mrad spatial resolution (17.8 mm/pixel at 10 m from a target). Thermal images were confirmed and analyzed using InfRec Analyzer NS9500 Lite software (Nippon Avionics). The camera was powered by a 12V100Ah sealed battery.

The sensitivity of a thermal imaging camera decreases with distance due to absorption of radiant energy from an object, particularly in an environment with high relative humidity such as inside a cave. To detect whether bats being observed became euthermic in thermal images, we determined a temperature threshold using the following procedure. First, we captured bats during active (September 2011, 10 males and 10 females) and inactive periods (January 2012, 14 males and 5 females). When capturing bats, we chose individuals making noticeable movements during the active period, and individuals not moving (i.e., torpid) during the inactive period. The rectal temperature of captured bats was measured using a thermometer connected to thermistor probe (active: mean ± SD = 30.7°C ± 2.0°C, range = 26.9°C–33.4°C; torpid: mean ± SD = 11.7°C ± 1.5°C, range = 10.2°C–15.9°C). Then, for each individual, the surface body temperature was immediately measured in the cave at distances of four and 7 m. Second, we compared the surface body temperature of active and torpid bats to test whether they are distinguishable from hibernating bats. The mean surface body temperature of active bats was significantly higher than that of torpid bats (Welch two sample *t*-test at 4 m: $t = 29.67$, $df = 19.33$, $p < 0.0001$, and at 7 m: $t = 28.44$, $df = 19.94$, $p < 0.0001$). The surface temperature range of active bats (14.9°C–21.1°C at 4 m, 13.1°C–18.2°C at 7 m) did not overlap that of torpid bats (7.6°C–8.2°C at 4 m, 7.6°C–8.3°C at 7 m). Therefore, we considered bats to be "aroused" once their surface body temperatures exceeded the minimum value of active bats (14.9°C at 4 m, 13.1°C at 7 m). For our purposes we have defined hibernation as bats in deep multiday torpor without exceeding the temperature threshold for more than 24 h. We recorded the presence or absence of hibernating bats in the observed group in each month. Based on our monthly monitoring, torpid bats fulfilling our definition of hibernation were observed exclusively from December to March, allowing us to classify the little horseshoe bat's annual life cycle as active from April to November and in hibernation from December to March (Supplementary Figure S1).

The reproduction of the bats was studied from June 2011 to March 2017. We captured bats once each month in Osawa cave using a hand-net or a mist-net (2.6 m heigh, 6.0 m wide, 35 mm mesh, Tokyotobari, Tokyo, Japan). Before capture, we took images of bats in the cave using a digital camera (DSC–RX100M2, Sony Corporation, Tokyo, Japan) to record their roosting positions, and to count the total number of individuals. When hand-netting bats, we minimized the duration of our visits to the cave to less than 20 min to avoid excessive disturbance. Bats were handled and processed at the cave entrance. Little horseshoe bats form their nursery colonies from late June to early August. To minimize disturbance to the colony during this period, a single mist-net was positioned near the cave entrance just before sunset, and retrieved 1 h after sunset.

The sex, age class, and reproductive condition of captured bats were identified. Individuals were assigned to three age classes, juveniles, subadults, or adults, based on wing epiphyseal fusion in the finger bones and their degree of sexual maturity. Juveniles are defined as young of the year with incomplete epiphyseal fusion of their finger bones. Subadults have complete ossification of their finger joints but are still sexually immature. Adults have fully developed finger bones and are sexually mature. Identification of sexual maturity was based on observations of the external genitalia of captured individuals. In rhinolophid bats, females with experience of lactation have a pair of pubic nipples (to which the pups cling) at the upper part of the vulva. Thus, we regarded the presence of pubic nipples as a sign of sexual maturity in females (hereafter referred to as "parous"). Females without pubic nipples were identified as nulliparous. We also classified the reproductive condition of subadult and adult females as pregnant, lactating, or indistinguishable, by palpating the abdomen or confirming hair loss and enlargement of nipples and pubic nipples. Males with developed external gonads (testes and cauda epididymides) were identified as sexually mature adults. We were also able to distinguish adults from subadults based on the appearance of developed musculus bulbocavernosus at the base of the penis, which is externally visible throughout the year in males that have attained

sexual maturity. The reproductive condition of males was classified as either reproductively active (testes and/or cauda epididymides enlarged) or inactive (both gonads regressed) (except juveniles). From 2013 to 2017, we also used digital calipers to measure (to the nearest 0.01 mm) the external size, along the major axis, of the testes and of the cauda epididymides. From 2015 to 2017, after measurements, a total of 31 adult males were collected and brought back to the laboratory for further studies (histological examination, hormone assay and sperm observation, Section 2.5 in detail).

To determine whether little horseshoe bat exhibits delayed fertilization, we collected a total of ten adult females for histological examinations in August (post-lactation and at the beginning of the estrus phase, n = 4), December (early-hibernation, n = 3) and March (late-hibernation, n = 3) of 2017 and 2018. These timings were determined based on our annual life cycle surveys and papers describing the schedule of delayed fertilization in other species (Oxberry, 1979; Kawamoto et al., 1998). Furthermore, during the winters of 2016–2017 and 2017–2018, a total of twenty-three hibernating adult (n = 8) and subadult (n = 15) females were collected randomly to examine histologically whether they would be fertilizable the following spring.

2.4 Female histology

Captured females (total n = 33) were carefully transported to the laboratory within 2 h after capture. We euthanized females by intraperitoneal injection of sodium pentobarbital (10 mg/kg) (Morais et al., 2013; Rincón-Vargas et al., 2013). The reproductive tract (ovary, oviduct and uterus) of each individual was extracted and fixed in Bouin's solution for 24 h. After fixation, the reproductive tract was preserved in 70% ethanol, then dehydrated in graded series in ethanol (70%, 80%, 90%, 95%, and 100%), cleared in xylene and embedded in paraffin. Each sample was sectioned at 4 µm, and stained with hematoxylin–eosin for light microscopy.

For each sampling season, we assessed the presence of developed follicles (antral or Graafian stage: follicles containing an antrum) (Gaisler, 1966; van der Merwe, 1979) in either the left or right ovary, and sperm storage in the uterus. If developed follicles and stored spermatozoa were found during both early- and late-hibernation periods, we presumed that the females had a reproductive cycle representative of delayed fertilization (Oxberry, 1979; Orr and Zuk, 2014). It was also presumed that hibernating females with developed follicles and stored spermatozoa were likely to be fertilized the following spring. Furthermore, we confirmed that females had previously been mated by the presence of a vaginal plug (Gaisler, 1966; Lee, 2020).

2.5 Assessing male reproductive physiology

From 2015 to 2017, adult males (total n = 31) were collected for histological examination, hormone assay and sperm mobility observation during May and June (hereafter referred to as the "anestrus" period, n = 8), during September to early November (hereafter referred to as the "estrus" period, n = 10) and during December to March (the hibernation period, n = 13). These sampling timings were determined based on seasonal changes in the external size of gonads (testes and cauda epididymides). Although most samples were collected from the Osawa cave, a few males appeared in the cave during spring and early summer, corresponding to the anestrus period. Therefore, to collect males for the experiments, a total of eight bats were captured in the abandoned tunnel (Tokamachi City) during the anestrus period. Males were carefully transported to the laboratory within 2 h of capture. We collected blood samples by cardiac puncture after euthanasia induction by intraperitoneal injection of sodium pentobarbital (10 mg/kg) (Morais et al., 2013; Rincón-Vargas et al., 2013). Blood was centrifuged at 15,000 rpm (18,800 ×g) for 15 min at 4°C. Separated serum was stored at −80°C for later testosterone assay. After the blood collection, we removed testes, cauda epididymides and accessory sex glands (complex of ampullary glands, prostate gland, urethral gland, and vesicular glands) separately. The weight of testis, cauda epididymis and complex of accessory sex glands was weighed. Then, using digital calipers, we measured (to the nearest 0.01 mm along the major axis) the internal size of the testes and the cauda epididymides. The right cauda epididymis was used for histological examination and the left for sperm mobility observation (n = 4 bats for each season). For males captured during the anestrus period, we could not collect sufficient volume of blood samples for the hormone assay and sperm for the observation.

Testes and cauda epididymides (total n = 12 bats) were fixed in Bouin's solution for 24 h, and embedded in paraffin after dehydration in a graded series of ethanol (70%, 80%, 90%, 95%, and 100%), then cleared in xylene. They were then sectioned at 4 µm, and stained with hematoxylin–eosin for light microscopy. We examined spermatogenesis in the seminiferous tubules and the presence of spermatozoa in the lumen of the cauda epididymis of each male. To extract spermatozoa for mobility observation, the cauda epididymis was dissected in 1.0 mL of pre-warmed (37°C) HTF medium (Nippon Medical and Chemical Instruments Co., Ltd.). The medium containing spermatozoa was immediately transferred to a Petri dish placed on an inverted phase-contrast microscope with a thermoregulator and CO_2 incubator. Sperm observations were conducted under 37°C, 5% CO_2 conditions at ×200 magnification. We randomly chose four spots on the dish, and recorded 5 s videos of each spot to a laptop PC connected with the microscope. At each spot, we counted the number of both motile (swimming) and immotile sperm. A single observer conducted the observation and count of sperm. The testosterone concentration was determined by ELISA Capture/Sandwich using a commercial kit (Testosterone ELISA kit, Item No. 582701, Cayman Chemical, Michigan, United States of America) (Puga et al., 2017). The assay was performed on 12 bats that sufficient serum samples were obtained (anestrus: not applicable, estrus: n = 6 out of 10, hibernation: n = 6 out of 13). Absorbance was measured at 405 nm on a Multiskan FC (Thermo Scientific, Massachusetts, United States of America) microplate reader. The intra-assay coefficient of variation was 7.7%.

2.6 Observation of winter copulation

To determine if copulations occurred during periodic arousals from hibernation, behavioral observations were made at Osawa cave using an infrared night vision camera (Handycam HDR–CX900, Sony Corporation, Tokyo, Japan) from January to early March in 2016 and 2017. The camera was mounted on a tripod with a remotely controllable pan-tilt device, and placed on the cave floor approximately 6 m away from a group of hibernating bats. The camera and pan-tilt device were remotely operated through extension cables using a control-device. Video imagery from the camera was checked on a small portable monitor connected to the control-device. The control-device and monitor were housed in a waterproof box, and placed inside the cave near the entrance in an area not used by bats and accessible during winter without disturbing them. Camera operation was performed by a single observer from the location of the box. All observation devices were powered by a 12V50Ah sealed battery. To confirm that the camera and connected electronics were not producing any noise, we listened directly to the sounds with a bat detector (D240x Ultrasound Detector, Pettersson Elektronik AB, Uppsala, Sweden), which can make ultrasound audible. The devices produced neither audible nor ultrasonic noise, especially in the range of bat echolocation calls (15–110 kHz for bat's vocalization in Japan, 104 kHz for little horseshoe bats). We also observed the devices using the thermal imaging camera (Thermo Gear G120) in the cave, and confirmed that the devices did not emit any noticeable heat (nor light) sufficient to affect bat behavior.

During the hibernation period, little horseshoe bats tended to periodically arouse from torpor around dusk and were active for several hours (Funakoshi and Uchida, 1980). Thus, for each survey night, observations were started at sunset and continued until no active bats were found. We searched for copulating bats at 30 min intervals by aiming the camera toward the hibernating group and its surroundings. To ascertain copulatory behavior, we referred to characteristics described in the existing literature (Thomas et al., 1979). When copulations were noted, video recordings were made so as to be able to describe the behavior in detail. In January and February 2017, when possible, we captured copulating pairs using a small hand-net soon after coitus, this allowed us to examine whether males had ejaculated successfully. Captured bats were identified to sex, age class, and reproductive condition. For females, we sampled vaginal smears to assess the presence or absence of sperm. Vaginal smears were collected by aspirating distilled water introduced into the vagina with plastic Pasteur pipettes. The collected samples were then placed into 1.5 mL microtubes for each bat. The samples were brought back to the laboratory and stained with Giemsa for light microscopy.

2.7 Statistical analysis

To confirm whether external measurements reflect those of internal size or weight of testes and cauda epididymides, correlations between external and internal size, and between external size and weight were analyzed based on Pearson correlation coefficient. For both gonads, external size was significantly correlated with internal size or weight (Supplementary Figure S2; Supplementary Table S1). Thus, we can use external size as a measure of internal condition. The weight of testis, cauda epididymis, and accessory sex glands was compared among seasons (anestrus: n = 8, estrus: n = 10, hibernation: n = 13) using the nonparametric multiple comparison Steel-Dwass test after checking for normality of the data by means of the Shapiro-Wilk test. For statistical comparisons of the testosterone concentration and sperm mobility among seasons, data collected during estrus and hibernation were used. Testosterone concentrations were compared between estrus and hibernation periods using the Wilcoxon signed-rank test (n = 6 males for both seasons). To test for differences in sperm mobility between estrus (n = 3) and hibernation (n = 4) periods, we used the generalized linear model (GLM, family = Poisson). In the GLM, the number of swimming sperm was used as the response variable, and season (estrus and hibernation) was used for the explanatory variable, with the total number of observed sperm as an offset parameter (log-transformed). Furthermore, to compare the composition of female reproductive conditions (determined by histological examination) between bats hibernating solitarily and in groups, we used Fisher's exact test. All analyses were performed using the statistical software R (R Core Team, 2021, version 4.1.0) run within Rstudio (Rstudio Team, 2021, version 1.4.1717) interface.

3 Results

3.1 Annual reproductive cycle with female sperm storage

Pregnancy began after emergence from hibernation, during April to June, and lactating females appeared in the nursery colony with juveniles from July to August (Figure 1A, Supplementary Figure S3A). During 2011–2017, reproductively active males appeared in the cave from autumn through winter (percentage in the captured males: September–November = 64.3%, December–March = 71.2%) (Figure 1A; Supplementary Figure S3B). Histological examination of adult females revealed that post-lactating bats had neither developed ovarian follicles nor spermatozoa, with the exception of one individual with a developing follicle in an ovary (but no spermatozoa) (Figure 1B). During the early- and late-hibernation period, adult females retained developed follicles in their ovaries, and stored spermatozoa in their uteri (Figures 1C, D). Although post-lactating females did not have vaginal plugs, females had plugs during early-hibernation, indicating that follicle development proceeded during autumn, and that copulations had occurred by the beginning of hibernation.

3.2 Seasonal changes in male reproductive conditions

Seasonal changes in the external sizes of the testes and cauda epididymides followed similar patterns among years (Figure 2A). Testes enlarged from August to November, peaked in size in September or October (mean ± SE during estrus = 4.74 ± 0.20 mm), then regressed rapidly in December (not measurable externally) (Figure 2A). The cauda epididymides size also reached maximum between August and November (mean ± SE during estrus = 2.78 ± 0.12 mm), and gradually decreased but not

10.3389/fphys.2023.1241470

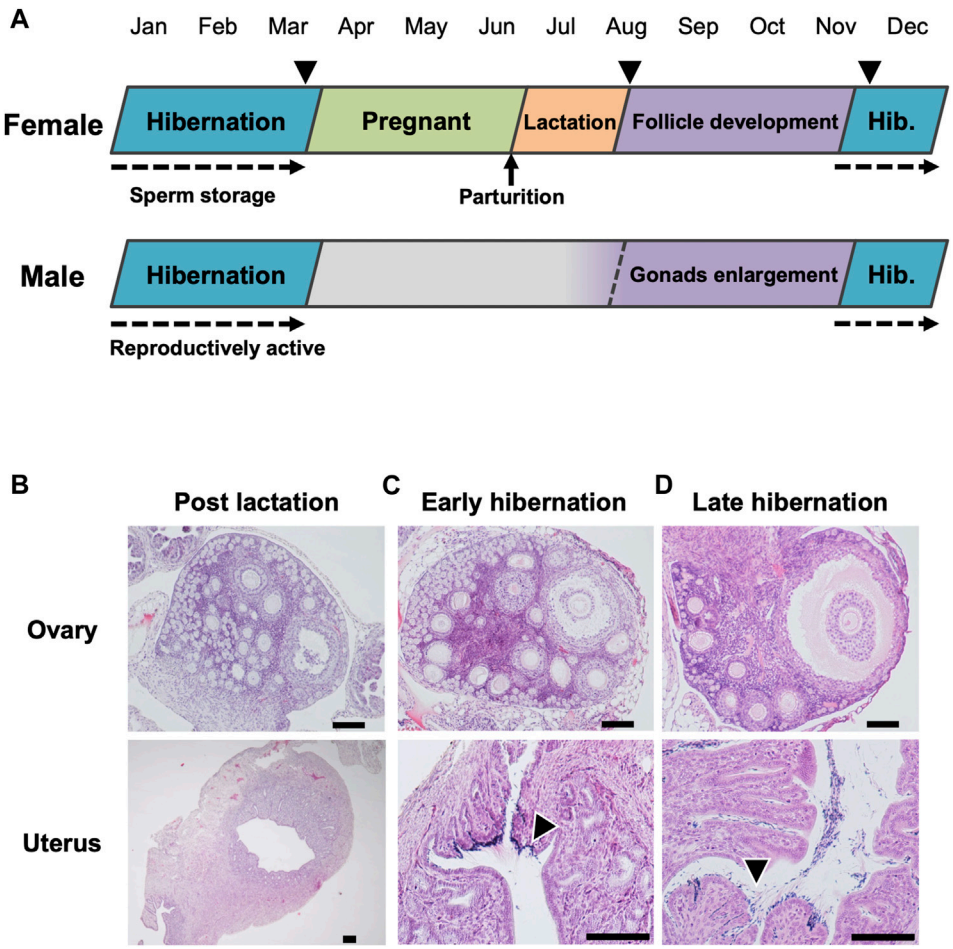

FIGURE 1
Annual reproductive cycle of the little horseshoe bat (*Rhinolophus cornutus*) in Niigata Prefecture. **(A)** denotes reproductive cycle of both sexes determined by monitoring of reproductive conditions and histological examination of females in **(B–D)**. Arrow heads represent the period of capture for female histological study. The beginning of spermatogenesis was not determined. **(B–D)** show ovary and uterus of adult females collected during post-lactation, early hibernation and late hibernation period. Arrow heads in **(C,D)** indicate stored spermatozoa found in the vicinity of the utero-tubal junction. Scale bars on HE stained images are 100 μm.

completely regressed throughout the hibernation period (mean ± SE during hibernation = 2.37 ± 0.05 mm) (Figure 2A). During estrus, spermatogenesis was confirmed in the seminiferous tubules, and the lumen of the cauda epididymides was filled with spermatozoa (Figure 2B). During hibernation, males stored spermatozoa in the cauda epididymis although the testes atrophied and ceased sperm production (Figure 2C). From spring to early summer (anestrus), we confirmed regressed testes with no sperm production, and scarce spermatozoa in the lumen of the cauda epididymides (Figure 2D). Seasonal differences in the weights of testes and cauda epididymides corresponded with seasonal patterns in their external sizes and histological characteristics. Both testes and cauda epididymides were heaviest during estrus (testes: median = 29.29, range = 11.95–42.88 mg, cauda epididymides: median = 5.82, range = 2.34–10.75 mg) (Figures 3A, B). Testis weight differed significantly among all pairs of seasons, whereas there was no significant difference in the weight of the cauda epididymis between estrus and hibernation (Figure 3A, B; Supplementary Table S2). The accessory sex glands weighed more during hibernation than during estrus and anestrus (anestrus: median = 36.58, range = 28.14–50.89 mg, estrus: median = 65.60, range = 32.06–84.41 mg, hibernation: median = 142.83, range = 99.47–205.7 mg) (Figure 3C; Supplementary Table S2). Testosterone concentration was significantly lower during hibernation than during estrus (estrus: median = 1.15, range = 1.07–1.79 ng/mL, hibernation: median = 1.05, range = 0.98–1.19 ng/mL, Wilcoxon signed-rank test: W = 31, p = 0.041) (Figure 3D). There was no significant difference in the proportion of motile spermatozoa between estrus and hibernation (estrus: 85.9%, hibernation: 81.3%, GLM: estimated slope of explanatory variable = −0.054, SE = 0.034, z = −1.566, p = 0.117) (Figure 3E; Supplementary Table S3).

3.3 Winter forced copulation

During hibernation, males arousing from torpor landed beside torpid female bats and attempted to mate with them (Figures 4A, B;

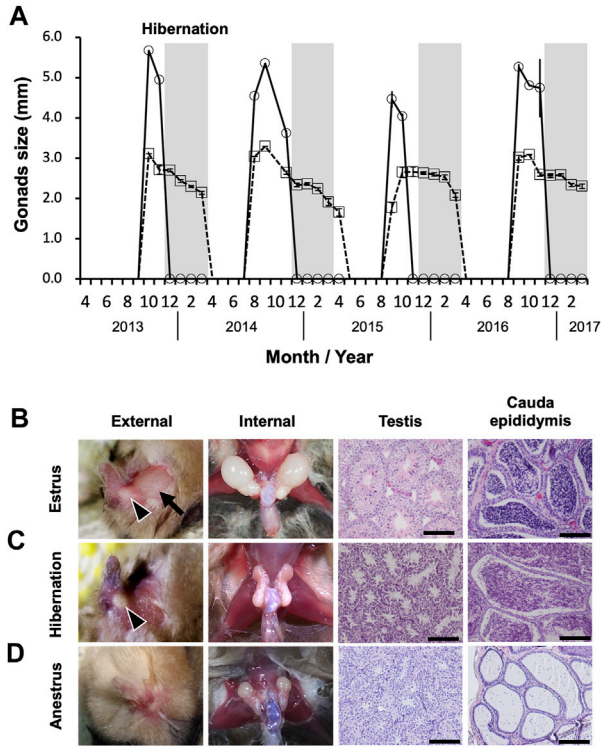

FIGURE 2
Sperm storage in cauda epididymis during hibernation. **(A)** represents seasonal changes in external testicular (solid line) and cauda epididymis size (dashed line). Measurements are shown as means ± SE. Months without symbols indicate that no males were captured. Light-gray bars represent hibernation. **(B–D)** show seasonal changes in external and internal morphology of gonads, and seminiferous tubules of testis and lumen of cauda epididymis. The arrow and arrow heads in **(B,C)** indicate enlarged testis and cauda epididymis, respectively. Scale bars on HE stained images are 100 μm.

Supplementary Video S1), in each case observed copulation was forced. Such events consisted of three behaviors: mounting from the back of the torpid individual, biting the nape of the torpid individual, and attempting intromission (Supplementary Video S1). Recipients often emitted audible vocalizations and struggled. During two survey seasons, amounting to a total of 114 h over 32 days, we observed 70 copulation events of which 29 (41.4%) were successful, including intromission. The remaining 41 events were unsuccessful with males giving up coitus shortly after mounting. We successfully captured seven mating pairs (two of the males escaped) shortly after coitus. All of the males captured after coitus had enlarged cauda epididymides. Five of the seven females were nulliparous in a hibernating group and two were solitary and parous. We confirmed the presence of ejaculated semen on the vaginal opening (Figure 4C) and sperm from smears (Figure 4D; Supplementary Figure S4).

3.4 Hibernating females with fertility

The bats hibernating in the cave formed mixed-sex groups, with groups consistently dominated by adult males (14.1%–69.1% of captured bats) and subadult females (12.9%–56.6% of captured bats) throughout our study period (Supplementary Figure S5; Supplementary Table S4). Twenty-three females (group n = 16; solitary n = 7) were dissected during two hibernating seasons, and their reproductive condition was determined histologically (Figures 5A–C). The composition of reproductive conditions differed significantly between bats hibernating in a group and those hibernating solitarily (Fisher's exact test, p = 0.0035) (Figure 5D). Few parous females were captured from groups during hibernation (0%–7.7% of captured bats) (Supplementary Figure S5; Supplementary Table S4), and when rarely present they were found solitarily in Osawa cave. All of the parous females that were dissected had spermatozoa in their uteri and developed follicles in their ovaries (Figure 5A). In females captured from hibernating groups, 37.5% of those dissected were externally nulliparous (subadult), but their histological examination showed follicle development, sperm storage and vaginal plug formation (Figure 5B). This indicates that these subadult females had attained fertility in the autumn, and had been copulated with. Fifty percent of females collected from hibernating groups showed no signs of insemination or fertility (Figure 5C).

4 Discussion

4.1 Male adaptations for sperm competition

We found that male little horseshoe bats stored spermatozoa in their cauda epididymides, and attempted to copulate despite having regressed testes during the hibernation period. This indicates that epididymal sperm storage during winter allows for extended opportunities for mating. Females hibernating in groups were mainly nulliparous (based on external examination), but some of them were ready for fertilization. For males, fertile females in the hibernaculum appear to be available as potential mates. Females stored spermatozoa during hibernation and gave birth to just one offspring per year, indicating that males experience reduced certainty of successful fertilization. It has been reported that the probability of sperm remaining in the female reproductive tract declines over time as females expels sperm from previous copulations (Krutzsch, 1975; Tidemann, 1993). Therefore, forced copulation during winter may provide additional opportunities for successful fertilization by allowing males to pass more sperm to their mates, and to displace the ejaculates of previous rivals (Edward et al., 2015). Winter copulations may also help to compensate for missed mating opportunities before hibernation (Boyles et al., 2020). Although the number of cases described is still limited, male sperm storage and winter copulations have also been observed in several bat species that have delayed fertilization (Thomas et al., 1979; Boyles et al., 2006). These male characters may reflect adaptations for sperm competition, which is facilitated by delayed fertilization (Orr and Zuk, 2014; Edward et al., 2015). In this study, we were unable to assess the effectiveness of winter copulations in terms of fertilization success; however, the adaptive significance of this behavior seems worthy of further investigation. Future research, clarifying whether winter copulations including physiological mechanisms enabling males to express sexual behavior have evolved widely among species with delayed fertilization, is also needed.

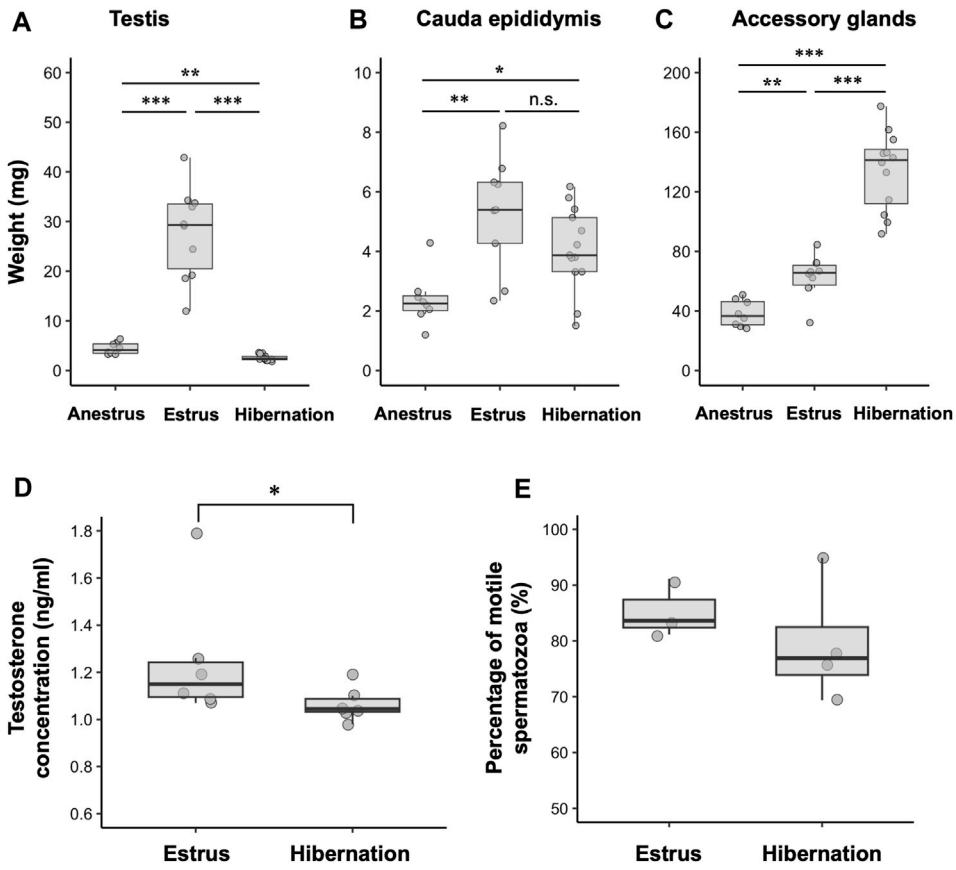

FIGURE 3
Seasonal changes in male reproductive physiology. **(A–C)** show the weight of testis, cauda epididymis and complex of accessory sex glands during anestrus (n = 8), estrus (n = 10) and hibernation (n = 13). **(D,E)** represent seasonal differences in testosterone concentrations (n = 6 for both seasons) and percentages of motile spermatozoa (n = 3 in estrus, n = 4 in hibernation), respectively. Data are shown using boxplots; the top and bottom of the boxes represent the 75th and 25th percentile, respectively, and lines indicate the median. *: 0.01 < p < 0.05, **: 0.001 < p < 0.01, ***: p < 0.001, n.s.: not significant. Statistics for **(E)** are shown in text and Supplementary Table S2.

Two interpretations of the characteristics of males attempting winter copulations are possible. The first interpretation is that a difference in competitiveness among males may be associated with winter copulations. Previous research has shown that competitively dominant males can monopolize females for mating during late summer (Racey and Entwistle, 2000; Senior et al., 2005). Paternity success is also biased towards just a few males in a breeding colony, and success if often determined by age (increased with age) (Watt and Fenton, 1995; Heckel and von Helversen, 2002; Rossiter et al., 2006). If dominant males can out-compete younger and/or inferior males early in the mating season, excluded males might keep attempting to mate during winter. The second interpretation is that it is possible that males in better condition can afford to copulate during winter. For hibernating bats, it is important that they optimize their energy expenditure for successful overwintering (Willis, 2017; Boyles et al., 2020). Arousal from torpor can account for up to 75% of overwintering energy expenditure (Thomas et al., 1990). Euthermic activities following arousal are energetically expensive and lead to fat reserve depletion (Boyles and Willis, 2010). Foraging opportunities outside roosts are drastically reduced during harsh weather conditions and periods of low prey availability. Even though bats are able to forage when periodically arousing from torpor, it may be insufficient for them to fuel their energy reserves, except at low latitudes, in warmer wintering regions (Boyles et al., 2020). Thus, males storing sperm are likely to face a trade-off during hibernation between investing in survival or in mating behavior (energy saving vs. increasing mating opportunities). For example, in the little brown bat (*Myotis lucifugus*), males arouse longer than females in winter, and individuals in better condition exhibit longer periods of arousal (Czenze et al., 2017). Hibernating males with larger fat reserves may be able to invest more energy in copulatory behavior during periodic arousal from torpor.

Females collected during hibernation had copulatory plugs in their vaginas. Such plugs are formed after mating from substances produced by either sex (Devine, 1977; Voss, 1979). In bats with delayed fertilization, copulatory plugs are typically interpreted as a form of "mate guarding" by males to prevent subsequent copulations (Orr and Zuk, 2014). Because male little horseshoe bats can continue to copulate during the period of sperm storage, their previous mates are likely to be re-mated by other males. Thus, mate guarding by means of plugs may be a necessary way of defending their mates and out-competing other males by reducing the mating chances of their rivals (Edward et al., 2015). Additionally, copulatory plugs also play

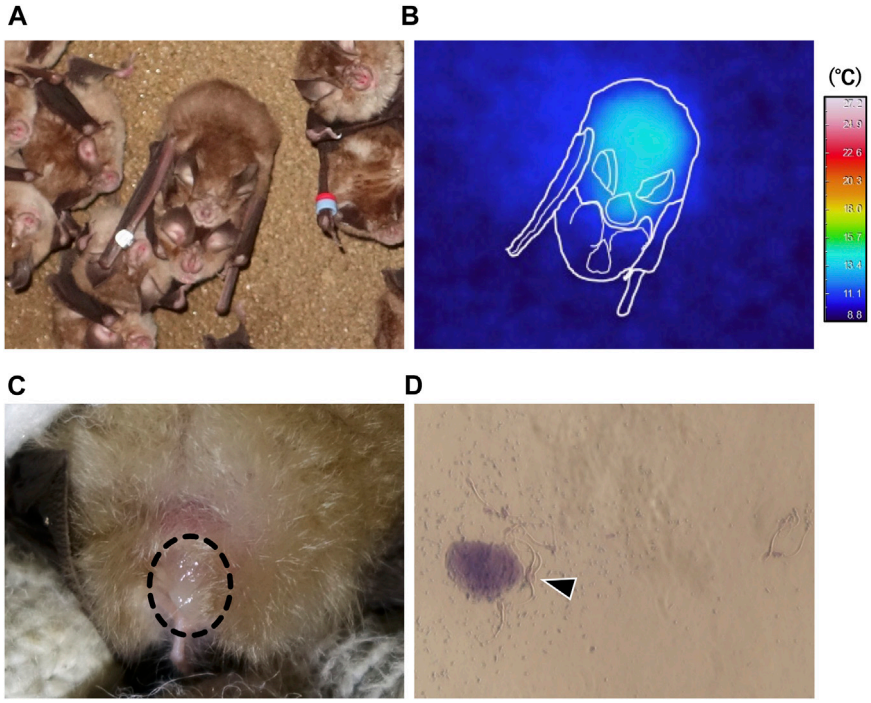

FIGURE 4
Winter forced copulation by males periodically aroused from torpor. **(A)** is a representative image of a copulating pair. **(B)** shows thermal infrared image corresponding to the pair shown in **(A)**, and approximate outlines (white lines) of bats. **(C)** indicates ejaculated semen (dashed circle) found in the vaginal opening of a post-copulatory female. **(D)** represents spermatozoa (arrow head) collected by vaginal smear.

a role in facilitating sperm transport within the reproductive tract by preventing the female from sperm dumping, as, for example, in mice (*Mus musculus*) (Dean, 2013). Copulatory plugs may be beneficial in situations in which early mating can secure advantageous storing positions for the spermatozoa in the vicinity of the oviduct where fertilization occurs (Racey, 1979). However, female bats have often been observed to remove plugs and dump sperm from a previous copulation (Pearson et al., 1952; Phillips and Inwards, 1985), and male bats also have penile weapons, such as spines, which may be used to remove plugs (Armstrong, 2005). It is difficult, therefore, to conclude whether copulatory plugs can completely prevent rival males from later copulations, thus further investigation to facilitate an understanding of the function of such plugs during hibernation is needed.

For male bats, winter forced copulations appear to be advantageous, allowing them to obtain mates while avoiding pre-copulatory female choice. For female bats, it is not possible to determine costs/benefits of forced copulations during hibernation in this study. However, it has been recognized that male sexual coercion could have negative effects on female fitness (Clutton-Brock and Parker, 1995; Cassini, 2020). For example, in mammals, forced copulations increase morbidity and mortality risk of females, and reduce female reproductive success (Smuts and Smuts, 1993; Reale et al., 1996; Linklater et al., 1999; Manguette et al., 2019). These effects are presumed to be caused by increased physical injury or disease transmission during repeated copulations, and by fertilization with sperm of lower-quality males (Edward et al., 2015). To reduce these costs, females often develop counterstrategies (Cassini, 2020). Sexual segregation and avoiding male's territory are interpreted as female responses to sexual coercion by males (Cassini, 2020). In our study site, although subadult females hibernated in groups with adult males, adult females were rarely present in the same hibernaculum. Furthermore, females hibernating in groups often experienced forced copulation. Females having experienced forced copulations as subadults may avoid winter roost sites with adult males. If sexual coercion also detrimentally affects female little horseshoe bats, choosing different hibernacula may develop as a counterstrategy to avoid disturbance by males. However, it should be noted that roost site segregation is also determined by differences in thermoregulatory, microclimatic and energy requirements between sexes (Senior et al., 2005; Angell et al., 2013; Stawski et al., 2014). During hibernation, adult females tend to be more conservative with their energy reserves than either adult males or younger bats (Jonasson and Willis, 2011), because emerging from hibernation in spring in good body condition is important for initiating gestation without delay (Willis, 2017). Thus, adult females may choose their wintering roosts based on the availability of suitable environmental conditions for conserving energy reserves. This might also explain why adult females are scarce at our study site.

4.2 Physiological mechanisms related to winter copulation

Testicular development with spermatogenic activity ceases as winter commences, whereas cauda epididymides and accessory

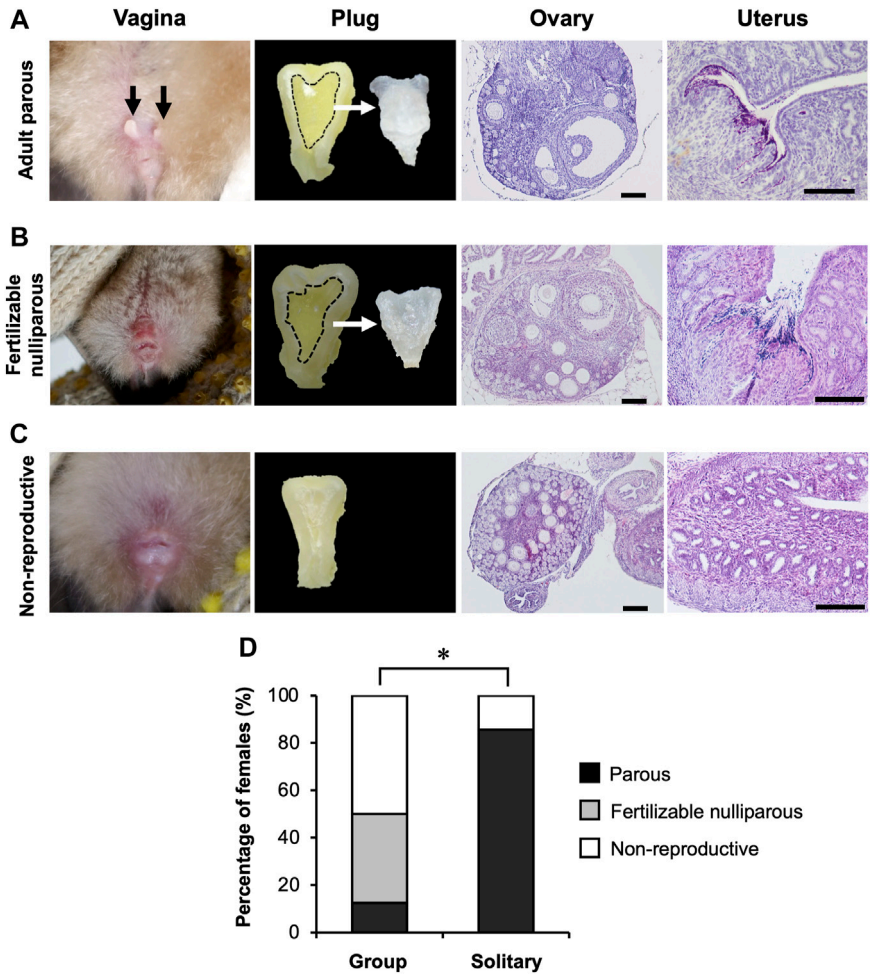

FIGURE 5
Reproductive conditions of hibernating females. **(A–C)** represent adult parous, fertile nulliparous subadults, and non-reproductive females, respectively. Black arrows in the image of vagina **(A)** indicate pubic nipples (sign of lactating experience). Images of plugs show the cross sections of the vagina after preservation in 10% formalin neutral buffer solution, and the extracted plug. All scale bars on these images are 100 μm. **(D)** shows the comparison in percentages of histologically determined reproductive categories between females hibernating in a group and in those hibernating solitarily (see text for statistics). *: $p < 0.05$ (Fisher's exact test).

sex glands are retained during hibernation. Testicular production of gametes is sensitive to cooling temperatures (Komar et al., 2022). Even among heterothermic species, cell growth and steroidogenesis are greatly reduced at lower body temperatures (<20°C), and enzymatic reactions in the testes work efficiently only within limited temperatures (Davis et al., 1963; LeVier and Spaziani, 1968). Multiday torpor during winter is likely to suppress testicular activity in the little horseshoe bat. Conversely, low body temperature during hibernation may be favorable for long-term epididymal sperm storage (Geiser and Brigham, 2012). At low temperatures, the metabolic rate of spermatozoa is reduced, and this inhibits the production of harmful metabolites (e.g., reactive oxygen species), which can damage sperm cells (Gibb and Aitken, 2016; Dziekońska et al., 2020). In bats, the fluid in the epididymal lumen during hibernation shows high levels of osmolarity leading to respiratory reduction, energy conservation, and motility preservation of stored spermatozoa (Crichton et al., 1993; Crichton et al., 1994). Furthermore, it has been suggested that the hyperosmolar environment in the lumen is associated with formation of a blood-epididymal barrier (close relations among epididymal epithelial cells), particularly during the period of sperm storage (Ahiezer et al., 2015). Hibernation-associated epididymal environments may provide suitable conditions for long-term storage and maintenance of viable spermatozoa.

The accessory sex glands of little horseshoe bat weighed most during hibernation. The activities of these glands play an important role in seminal fluid secretion and ejaculation (Clement and Giuliano, 2016). Generally, protein synthesis is suppressed by hibernation (Frerichs et al., 1998; Drew et al., 2007), so in winter glands are likely to be filled with seminal fluid maintained in storage rather than with newly synthesized fluid. In addition, seminal fluid may have remained in the glands simply because of the decreased frequency of copulations during winter compared to the autumn mating season. Although detailed mechanisms have not been described, the innervation

control relating to contractions of the glands may be involved in keeping seminal fluid in accessory sex glands throughout the hibernation period.

Interestingly, male bats engaged in sexual behavior even during testicular regression and while testosterone levels were lowered during hibernation. This suggests that higher levels of gonadal steroid secretion may not be necessary for activation and maintenance of sexual behavior during winter. Our results are in accordance with previous findings obtained from gonadectomized bats. After castration big brown bat (*Eptesicus fuscus*), males continued sexual behavior despite reduced androgen levels (Mendonça et al., 1996). Although possible mechanisms underlying this phenomenon are still unclear in bats, there could be an alternative system for expressing sexual behavior in the regressed gonads. Among non-hibernating animals, such as mice, birds, and nonhuman primates, sexual behaviors are also not completely abolished in the absence of testicular activity (Phoenix et al., 1973; Pradhan et al., 2010; David et al., 2022). One possible explanation for gonadal steroid-independent sexual behavior is that social interactions can induce temporally acute androgen increases (<1 h) (Marler and Trainor, 2020). Importantly, such a transient surge could be of extragonadal origin (Wingfield et al., 2001; Balthazart and Ball, 2006). Detailed mechanisms for the transient synthesis of androgen have been described in seasonal breeding birds. In song sparrows (*Melospiza melodia*), aggressive encounters among males rapidly increase local androgen synthesis in specific regions of the brain during the non-breeding season, when gonads have regressed (Pradhan et al., 2010). This finding also highlights that seasonal breeders can shift from systemic to local sex steroid signaling in the absence of gonadal activity (Pradhan et al., 2010). Local synthesis of steroids appears to be a reasonable mechanism to avoid the energetic cost of maintaining high systemic hormone levels during the non-breeding season (Wingfield et al., 2001). The same may be true for hibernating mammals as these also face seasonal energetic constraints. It has not been shown whether hibernating bats have similar mechanisms, but their extragonadal local steroid synthesis may help to explain why male bats can retain sexual behavior even under the constraints of hibernation.

Data availability statement

The original contributions presented in the study are included in the article/Supplementary Material, further inquiries can be directed to the corresponding author.

Ethics statement

The animal study was approved by the Institutional Animal Care and Use Committee and the President of Niigata University. The study was conducted in accordance with the local legislation and institutional requirements.

Author contributions

TSa and TSe designed this study, conducted field works and collected samples for the experiments. TSa conducted all experiments, and TSu contributed to histological examinations. TSa performed the statistical analysis. TSu and TSe contributed to the discussion of the results. TSa wrote the first draft of the manuscript. All authors contributed to the article and approved the submitted version.

Funding

This study was supported by the grants-in-aid from the Koshiji Nature Foundation (10th in 2011 and 16th in 2017) and the Yamaguchi Educational and Scholarship Foundation (2012, 2013, and 2017) in Niigata Prefecture, Japan.

Acknowledgments

We are sincerely grateful to Prof. Hideo Miguchi and Prof. Hitoshi Sakio, Faculty of Agriculture, Niigata University, and Dr. Dai Fukui, lecturer, Graduate School of Agriculture and Life Sciences, The University of Tokyo, for his helpful suggestions on an early draft of the manuscript, and Prof. Nobuhiko Hoshi, Graduate School of Agricultural Science, Kobe University, for advice on histological examinations. We would also like to thank Dr. Mark Brazil, Scientific Editing Services, for assistance in the preparation of the final draft of the manuscript. We express our thanks to all students of the Laboratory of Animal Ecology, Niigata University, for their support.

Conflict of interest

The authors declare that the research was conducted in the absence of any commercial or financial relationships that could be construed as a potential conflict of interest.

Publisher's note

Supplementary material

The Supplementary Material for this article can be found online at: https://www.frontiersin.org/articles/10.3389/fphys.2023.1241470/full#supplementary-material

References

Ahiezer, R. T., León-Galván Miguel, A., and Edith, A. R. (2015). Epididymal sperm maturation in bats with prolonged sperm storage. *Animal Veterinary Sci.* 3, 1–7. doi:10.11648/j.avs.s.2015030101.11

Angell, R. L., Butlin, R. K., and Altringham, J. D. (2013). Sexual segregation and flexible mating patterns in temperate bats. *PloS One* 8 (1), e54194. doi:10.1371/journal.pone.0054194

Armstrong, K. N. (2005). A description and discussion of the penile morphology of *Rhinonicteris aurantius* (gray, 1845) (microchiroptera: hipposideridae). *Aust. Mammal.* 27 (2), 161–167. doi:10.1071/AM05161

Balthazart, J., and Ball, G. F. (2006). Is brain estradiol a hormone or a neurotransmitter? *Trends. Neurosci.* 29 (5), 241–249. doi:10.1016/j.tins.2006.03.004

Barclay, R., and Harder, L. (2003). "Life histories of bats: life in the slow lane," in *Bat Ecology*. Editors T. H. Kunz and M. B. Fenton (Chicago, IL, USA: The University of Chicago Press), 209–256.

Barnes, B. M., Kretzmann, M., Licht, P., and Zucker, I. (1986). The influence of hibernation on testis growth and spermatogenesis in the golden-mantled ground squirrel, *Spermophilus lateralis*. *Biol. Reprod.* 35 (5), 1289–1297. doi:10.1095/biolreprod35.5.1289

Boyles, J. G., Dunbar, M. B., and Whitaker, J. O. (2006). Activity following arousal in winter in North American vespertilionid bats. *Mamm. Rev.* 36 (4), 267–280. doi:10.1111/j.1365-2907.2006.00095.x

Boyles, J. G., Johnson, J. S., Blomberg, A., and Lilley, T. M. (2020). Optimal hibernation theory. *Mamm. Rev.* 50 (1), 91–100. doi:10.1111/mam.12181

Boyles, J. G., and Willis, C. K. (2010). Could localized warm areas inside cold caves reduce mortality of hibernating bats affected by white-nose syndrome? *Front. Ecol. Environ.* 8 (2), 92–98. doi:10.1890/080187

Cassini, M. H. (2021). Sexual aggression in mammals. *Mamm. Rev.* 51 (2), 247–255. doi:10.1111/mam.12228

Clement, P., and Giuliano, F. (2016). Physiology and pharmacology of ejaculation. *Basic Clin. Pharmacol. Toxicol.* 119, 18–25. doi:10.1111/bcpt.12546

Clutton-Brock, T. H., and Parker, G. A. (1995). Sexual coercion in animal societies. *Anim. Behav.* 49 (5), 1345–1365. doi:10.1006/anbe.1995.0166

Crichton, E. G., Suzuki, F., Krutzsch, P. H., and Hammerstedt, R. H. (1993). Unique features of the cauda epididymidal epithelium of hibernating bats may promote sperm longevity. *Anat. Rec.* 237 (4), 475–481. doi:10.1002/ar.1092370406

Crichton, E. G., Hinton, B. T., Pallone, T. L., and Hammerstedt, R. H. (1994). Hyperosmolality and sperm storage in hibernating bats: prolongation of sperm life by dehydration. *Am. J. Physiol. Regul. Integr. Comp. Physiol.* 267 (5), R1363–R1370. doi:10.1152/ajpregu.1994.267.5.R1363

Crichton, E. G. (2000). "Sperm storage and fertilization," in *Reproductive Biology of bats*. Editors E. G. Crichton and P. H. Krutzsch (San Diego, CA, USA: Academic Press), 295–320.

Czenze, Z. J., Jonasson, K. A., and Willis, C. K. (2017). Thrifty females, frisky males: winter energetics of hibernating bats from a cold climate. *Physiol. Biochem. Zool.* 90 (4), 502–511. doi:10.1086/692623

David, C. D., Wyrosdic, B. N., and Park, J. H. (2022). Strain differences in post-castration sexual and aggressive behavior in male mice. *Behav. Brain Res.* 422, 113747. doi:10.1016/j.bbr.2022.113747

Davis, J. R., Firlit, C. F., and Hollinger, M. A. (1963). Effect of temperature on incorporation of l-lysine-U-C^{14} into testicular proteins. *Am. J. Physiol.* 204 (4), 696–698. doi:10.1152/ajplegacy.1963.204.4.696

Dean, M. D. (2013). Genetic disruption of the copulatory plug in mice leads to severely reduced fertility. *PLoS Genet.* 9 (1), e1003185. doi:10.1371/journal.pgen.1003185

Devine, M. C. (1977). Copulatory plugs, restricted mating opportunities and reproductive competition among male garter snakes. *Nature* 267, 345–346. doi:10.1038/267345a0

Drew, K. L., Buck, C. L., Barnes, B. M., Christian, S. L., Rasley, B. T., and Harris, M. B. (2007). Central nervous system regulation of mammalian hibernation: implications for metabolic suppression and ischemia tolerance. *J. Neurochem.* 102 (6), 1713–1726. doi:10.1111/j.1471-4159.2007.04675.x

Dzal, Y. A., and Brigham, R. M. (2013). The tradeoff between torpor use and reproduction in little brown bats (*Myotis lucifugus*). *J. Comp. Physiol. B Biochem. Syst. Environ. Physiol.* 183, 279–288. doi:10.1007/s00360-012-0705-4

Dziekońska, A., Niedźwiecka, E., Niklewska, M. E., Koziorowska-Gilun, M., and Kordan, W. (2020). Viability longevity and quality of epididymal sperm stored in the liquid state of European red deer (*Cervus elaphus elaphus*). *Anim. Reprod. Sci.* 213, 106269. doi:10.1016/j.anireprosci.2019.106269

Edward, D. A., Stockley, P., and Hosken, D. J. (2015). Sexual conflict and sperm competition. *Cold Spring Harb. Perspect. Biol.* 7 (4), a017707. doi:10.1101/cshperspect.a017707

Fasel, N. J., Kołodziej-Sobocińska, M., Komar, E., Zegarek, M., and Ruczyński, I. (2019). Penis size and sperm quality, are all bats grey in the dark? *Curr. Zool.* 65 (6), 697–703. doi:10.1093/cz/zoy094

Frerichs, K. U., Smith, C. B., Brenner, M., DeGracia, D. J., Krause, G. S., Marrone, L., et al. (1998). Suppression of protein synthesis in brain during hibernation involves inhibition of protein initiation and elongation. *Proc. Natl. Acad. Sci. U.S.A.* 95 (24), 14511–14516. doi:10.1073/pnas.95.24.14511

Funakoshi, K., and Uchida, T. A. (1980). Feeding activity of the Japanese lesser horseshoe bat, *Rhinolophus cornutus cornutus*, during the hibernation period. *J. Mammal.* 61 (1), 119–121. doi:10.2307/1379965

Gagnon, M. F., Lafleur, C., Landry-Cuerrier, M., Humphries, M. M., and Kimmins, S. (2020). Torpor expression is associated with differential spermatogenesis in hibernating eastern chipmunks. *Am. J. Physiol. Regul. Integr. Comp. Physiol.* 319 (4), R455–R465. doi:10.1152/ajpregu.00328.2019

Gaisler, J. (1966). Reproduction in the lesser horseshoe bat (*Rhinolophus hipposideros hipposideros* Bechstein, 1800). *Bijdr. tot Dierkd.* 36 (1), 45–p7. doi:10.1163/26660644-03601003

Geiser, F., and Brigham, R. M. (2012). "The other functions of torpor," in *Living in a seasonal world: Thermoregulatory and metabolic adaptations*. Editors T. Ruf, C. Bieber, W. Arnold, and E. Millesi (Berlin, Germany: Springer), 109–121. doi:10.1007/978-3-642-28678-0_10

Geiser, F. (2013). Hibernation. *Curr. Biol.* 23 (5), R188–R193. doi:10.1016/j.cub.2013.01.062

Geiser, F., McAllan, B. M., and Brigham, R. M. (2005). Daily torpor in a pregnant dunnart (*Sminthopsis macroura* dasyuridae: marsupialia). *Mamm. Biol.* 70 (2), 117–121. doi:10.1016/j.mambio.2004.06.003

Geiser, F. (2004). Metabolic rate and body temperature reduction during hibernation and daily torpor. *Annu. Rev. Physiol.* 66, 239–274. doi:10.1146/annurev.physiol.66.032102.115105

Geiser, F. (2021). "Torpor during reproduction and development," in *Ecological physiology of daily torpor and hibernation. Fascinating life Sciences*. Editor F. Geiser (Switzerland: Springer Nature), 195–223. doi:10.1007/978-3-030-75525-6_8

Gibb, Z., and Aitken, R. J. (2016). The impact of sperm metabolism during *in vitro* storage: the stallion as a model. *Biomed. Res. Int.* 2016, 9380609. doi:10.1155/2016/9380609

Heckel, G., and von Helversen, O. (2002). Male tactics and reproductive success in the harem polygynous bat *Saccopteryx bilineata*. *Behav. Ecol.* 13 (6), 750–756. doi:10.1093/beheco/13.6.750

Hosken, D. J. (1997). Sperm competition in bats. *Proc. R. Soc. B Biol. Sci.* 264 (1380), 385–392. doi:10.1098/rspb.1997.0055

Jonasson, K. A., and Willis, C. K. (2011). Changes in body condition of hibernating bats support the thrifty female hypothesis and predict consequences for populations with white-nose syndrome. *PLoS One* 6 (6), e21061. doi:10.1371/journal.pone.0021061

Kawamoto, K., Kurahashi, S., and Hayashi, T. (1998). Changes in the gonadotropin-releasing hormone (GnRH) neuronal system during the annual reproductive cycle of the horseshoe bat, *Rhinolophus ferrumequinum*. *Rhinolophus Ferrumequinum. Zool. Sci.* 15 (5), 779–786. doi:10.2108/zsj.15.779

Komar, E., Fasel, N. J., Szafrańska, P. A., Dechmann, D. K., Zegarek, M., and Ruczyński, I. (2022). Energy allocation shifts from sperm production to self-maintenance at low temperatures in male bats. *Sci. Rep.* 12 (1), 2138–2211. doi:10.1038/s41598-022-05896-3

Körtner, G., Pavey, C. R., and Geiser, F. (2008). Thermal biology, torpor, and activity in free-living mulgaras in arid zone Australia during the winter reproductive season. *Physiol. Biochem. Zool.* 81 (4), 442–451. doi:10.1086/589545

Krutzsch, P. H. (1975). Reproduction of the canyon bat, *Pipistrellus hesperus*, in southwestern United States. *Am. J. Anat.* 143 (2), 163–200. doi:10.1002/aja.1001430203

Kurohmaru, M., Saruwatari, T., Kimura, J., Mukohyama, M., Watanabe, G., Taya, K., et al. (2002). Seasonal changes in spermatogenesis of the Japanese lesser horseshoe bat, *Rhinolophus cornutus* from a morphological viewpoint. *Okajimas Folia Anat. Jpn.* 79 (4), 93–100. doi:10.2535/ofaj.79.93

Lee, J. H., Shin, D. H., Park, J. Y., Kim, S. Y., and Hwang, C. S., (2020). Vaginal plug formation and release in female hibernating Korean greater horseshoe bat, *Rhinolophus ferrumequinum korai* (Chiroptera: rhinolophidae) during the annual reproductive cycle. *Zoomorphology* 139 (1), 123–129. doi:10.1186/s13000-020-01042-7

LeVier, R. R., and Spaziani, E. (1968). The influence of temperature on steroidogenesis in the rat testis. *J. Exp. Zool. B* 169 (1), 113–120. doi:10.1002/jez.1401690113

Linklater, W. L., Cameron, E. Z., Minot, E. O., and Stafford, K. J. (1999). Stallion harassment and the mating system of horses. *Anim. Behav.* 58 (2), 295–306. doi:10.1006/anbe.1999.1155

Manguette, M. L., Robbins, A. M., Breuer, T., Stokes, E. J., Parnell, R. J., and Robbins, M. M. (2019). Intersexual conflict influences female reproductive success in a female-dispersing primate. *Behav. Ecol. Sociobiol.* 73, 118–214. doi:10.1007/s00265-019-2727-3

Marler, C. A., and Trainor, B. C. (2020). The challenge hypothesis revisited: focus on reproductive experience and neural mechanisms. *Horm. Behav.* 123, 104645. doi:10.1016/j.yhbeh.2019.104645

McAllan, B. M., and Geiser, F. (2014). Torpor during reproduction in mammals and birds: dealing with an energetic conundrum. *Integr. Comp. Biol.* 54 (3), 516–532. doi:10.1093/icb/icu093

Mendonça, M. T., Chernetsky, S. D., Nester, K. E., and Gardner, G. L. (1996). Effects of gonadal sex steroids on sexual behavior in the big brown bat, *Eptesicus fuscus*, upon arousal from hibernation. *Horm. Behav.* 30 (2), 153–161. doi:10.1006/hbeh.1996.0019

Morais, D. B., de Paula, T. A., Barros, M. S., Balarini, M. K., de Freitas, M. B., and da Matta, S. L. (2013). Stages and duration of the seminiferous epithelium cycle in the bat *Sturnira lilium*. *J. Anat.* 222 (3), 372–379. doi:10.1111/joa.12016

Morrow, G. E., Jones, S. M., and Nicol, S. C. (2016). Interaction of hibernation and male reproductive function in wild Tasmanian echidnas *Tachyglossus aculeatus setosus*. *J. Mammal.* 97 (3), 852–860. doi:10.1093/jmammal/gyw013

Morrow, G., and Nicol, S. C. (2009). Cool sex? Hibernation and reproduction overlap in the echidna. *PLoS One* 4 (6), e6070. doi:10.1371/journal.pone.0006070

Ocampo-González, P., López-Wilchis, R., Espinoza-Medinilla, E. E., and Rioja-Paradela, T. M. (2021). A review of the breeding biology of Chiroptera. *Mamm. Rev.* 51 (3), 338–352. doi:10.1111/mam.12236

Orr, T. J., and Brennan, P. L. (2015). Sperm storage: distinguishing selective processes and evaluating criteria. *Trends Ecol. Evol.* 30 (5), 261–272. doi:10.1016/j.tree.2015.03.006

Orr, T. J., and Zuk, M. (2013). Does delayed fertilization facilitate sperm competition in bats? *Behav. Ecol. Sociobiol.* 67, 1903–1913. doi:10.1007/s00265-013-1598-2

Orr, T. J., and Zuk, M. (2014). Reproductive delays in mammals: an unexplored avenue for post-copulatory sexual selection. *Biol. Rev.* 89 (4), 889–912. doi:10.1111/brv.12085

Oxberry, B. A. (1979). Female reproductive patterns in hibernating bats. *J. Reprod. Fert.* 56 (1), 359–367. doi:10.1530/jrf.0.0560359

Pearson, O. P., Koford, M. R., and Pearson, A. K. (1952). Reproduction of the lump-nosed bat (*Corynorhinus rafinesquei*) in California. *J. Mammal.* 33 (3), 273–320. doi:10.2307/1375769

Phillips, W. R., and Inwards, S. J. (1985). The annual activity and breeding cycles of gould's long-eared bat, *Nyctophilus gouldi* (microchiroptera: vespertiionidae). *Aust. J. Zool.* 33 (2), 111–126. doi:10.1071/ZO9850111

Phoenix, C. H., Slob, A. K., and Goy, R. W. (1973). Effects of castration and replacement therapy on sexual behavior of adult male rhesuses. *J. Comp. Physiol. Psych.* 84 (3), 472–481. doi:10.1037/h0034855

Pradhan, D. S., Newman, A. E., Wacker, D. W., Wingfield, J. C., Schlinger, B. A., and Soma, K. K. (2010). Aggressive interactions rapidly increase androgen synthesis in the brain during the non-breeding season. *Horm. Behav.* 57 (4-5), 381–389. doi:10.1016/j.yhbeh.2010.01.008

Puga, C. C., Beguelini, M. R., Morielle-Versute, E., Vilamaior, P. S., and Taboga, S. R. (2017). Structural, ultrastructural and immunohistochemical evidence of testosterone effects and its ablation on the bulbourethal gland of the *Artibeus planirostris* bat (Chiroptera, Mammalia). *Tissue Cell* 49 (4), 470–482. doi:10.1016/j.tice.2017.06.001

R Core Team (2021). *R: A language and environment for statistical computing*. Vienna, Austria: R Foundation for Statistical Computing.

Racey, P. A., and Entwistle, A. C. (2000). "Life-history and reproductive strategies of bats," in *Reproductive Biology of bats*. Editors E. G. Crichton and P. H. Krurzsch (San Diego, CA, USA: Academic Press), 363–414. doi:10.1016/B978-012195670-7/50010-2

Racey, P. A., and Swift, S. M. (1981). Variations in gestation length in a colony of pipistrelle bats (*Pipistrellus pipistrellus*) from year to year. *J. Reprod. Fert.* 61 (1), 123–129. doi:10.1530/jrf.0.0610123

Racey, P. A. (1979). The prolonged storage and survival of spermatozoa in Chiroptera. *J. Reprod. Fert.* 56 (1), 391–402. doi:10.1530/jrf.0.0560391

Racey, P. A. (1973). The viability of spermatozoa after prolonged storage by male and female European bats. *Priod. Biol.* 75, 201–205.

Reale, D., Bousses, P., and Chapuis, J. L. (1996). Female-biased mortality induced by male sexual harassment in a feral sheep population. *Can. J. Zool.* 74 (10), 1812–1818. doi:10.1139/z96-202

Rincón-Vargas, F., Stoner, K. E., Vigueras-Villaseñor, R. M., Nassar, J. M., Chaves, Ó. M., and Hudson, R. (2013). Internal and external indicators of male reproduction in the lesser long-nosed bat *Leptonycteris yerbabuenae*. *J. Mammal.* 94 (2), 488–496. doi:10.1644/11-mamm-a-357.1

Rossiter, S. J., Ransome, R. D., Faulkes, C. G., Dawson, D. A., and Jones, G. (2006). Long-term paternity skew and the opportunity for selection in a mammal with reversed sexual size dimorphism. *Mol. Ecol.* 15 (10), 3035–3043. doi:10.1111/j.1365-294X.2006.02987.x

Rstudio Team (2021). *Integrated development for R. Rstudio, PBC*. Boston, MA, USA: Rstudio.

Ruf, T., and Geiser, F. (2015). Daily torpor and hibernation in birds and mammals. *Biol. Rev.* 90 (3), 891–926. doi:10.1111/brv.12137

Sandell, M. (1990). The evolution of seasonal delayed implantation. *Q. Rev. Biol.* 65 (1), 23–42. doi:10.1086/416583

Sano, A., and Armstrong, K. N. (2009). "*Rhinolophus cornutus* temminck, 1835," in *The wild mammals of Japan*. Editors S. D. Ohdachi, Y. Ishibashi, M. A. Iwasa, and T. Saitoh (Kyoto, Japan: Shoukadoh Book Seller), 60–61.

Senior, P., Butlin, R. K., and Altringham, J. D. (2005). Sex and segregation in temperate bats. *Proc. R. Soc. B Biol. Sci.* 272 (1580), 2467–2473. doi:10.1098/rspb.2005.3237

Smuts, B. B., and Smuts, R. W. (1993). Male aggression and sexual coercion of females in nonhuman primates and other mammals: evidence and theoretical implications. *Adv. Study Behav.* 22 (22), 1–63.

Stawski, C., Willis, C. K. R., and Geiser, F. (2014). The importance of temporal heterothermy in bats. *J. Zool.* 292 (2), 86–100. doi:10.1111/jzo.12105

Thomas, D. W., Dorais, M., and Bergeron, J. M. (1990). Winter energy budgets and cost of arousals for hibernating little brown bats, *Myotis lucifugus*. *J. Mammal.* 71 (3), 475–479. doi:10.2307/1381967

Thomas, D. W., Fenton, M. B., and Barclay, R. M. (1979). Social behavior of the little brown bat, *Myotis lucifugus*: I. Mating behavior. *Behav. Ecol. Sociobiol.* 6, 129–136. doi:10.1007/bf00292559

Tidemann, C. R. (1993). Reproduction in the bats *Vespadelus vulturnus, V. regulus* and *V. darlingtoni* (microchiroptera, vespertilionidae) in coastal south-eastern Australia. *Aust. J. Zool.* 41 (1), 21–35. doi:10.1071/ZO9930021

van der Merwe, M. (1979). Growth of ovarian follicles in the Natal clinging bat. *Afr. Zool.* 14 (3), 112–117. doi:10.1080/02541858.1979.11447659

Voss, R. C. (1979). Male accessory glands and the evolution of copulatory plugs in rodents. *Occas. Pap. Mus. Zoology Univ. Mich.* 689, 1–27.

Wang, Z., Liang, B., Racey, P. A., Wang, Y. L., and Zhang, S. Y. (2008). Sperm storage, delayed ovulation, and menstruation of the female Rickett's big-footed bat (*Myotis ricketti*). *Zool. Stud.* 47 (2), 215–221.

Watt, E. M., and Fenton, M. B. (1995). DNA fingerprinting provides evidence of discriminate suckling and non-random mating in little brown bats *Myotis lucifugus*. *Mol. Ecol.* 4 (2), 261–264. doi:10.1111/j.1365-294X.1995.tb00217.x

Willis, C. K. (2017). Trade-offs influencing the physiological ecology of hibernation in temperate-zone bats. *Integr. Comp. Biol.* 57 (6), 1214–1224. doi:10.1093/icb/icx087

Willis, C. K., Brigham, R. M., and Geiser, F. (2006). Deep, prolonged torpor by pregnant, free-ranging bats. *Naturwissenschaften* 93, 80–83. doi:10.1007/s00114-005-0063-0

Wimsatt, W. A. (1969). "Some interrelations of reproduction and hibernation in mammals," in *Dormancy and survival. Symposia of the society for experimental Biology*. Editor H. W. Woolhouse (Cambridge, MA, USA: Cambridge University Press), 511–549.

Wingfield, J. C., Lynn, S. E., and Soma, K. K. (2001). Avoiding the 'costs' of testosterone: ecological bases of hormone-behavior interactions. *Brain Behav. Evol.* 57 (5), 239–251. doi:10.1159/000047243

frontiers | Frontiers in Physiology

TYPE Original Research
PUBLISHED 07 September 2023
DOI 10.3389/fphys.2023.1251042

OPEN ACCESS

EDITED BY
Sylvain Giroud,
University of Veterinary Medicine Vienna, Austria

REVIEWED BY
Heiko T. Jansen,
Washington State University, United States
Etienne Lefai,
Institut National de Recherche pour l'Agriculture, l'Alimentation et l'Environnement (INRAE), France
Eva Millesi,
University of Vienna, Austria

*CORRESPONDENCE
Marina B. Blanco,
marina.blanco@duke.edu,

†These authors have contributed equally to this work and share first authorship

RECEIVED 30 June 2023
ACCEPTED 23 August 2023
PUBLISHED 07 September 2023

CITATION
Blanco MB, Greene LK, Ellsaesser LN, Williams CV, Ostrowski CA, Davison MM, Welser K and Klopfer PH (2023), Seasonal variation in glucose and insulin is modulated by food and temperature conditions in a hibernating primate. *Front. Physiol.* 14:1251042. doi: 10.3389/fphys.2023.1251042

Seasonal variation in glucose and insulin is modulated by food and temperature conditions in a hibernating primate

Marina B. Blanco [1,2*†], Lydia K. Greene [1,2†], Laura N. Ellsaesser[1], Cathy V. Williams[1], Catherine A. Ostrowski[1], Megan M. Davison[1], Kay Welser[1] and Peter H. Klopfer[2]

[1]Duke Lemur Center, Durham, NC, United States, [2]Department of Biology, Duke University, Durham, NC, United States

Feast-fast cycles allow animals to live in seasonal environments by promoting fat storage when food is plentiful and lipolysis when food is scarce. Fat-storing hibernators have mastered this cycle over a circannual schedule, by undergoing extreme fattening to stockpile fuel for the ensuing hibernation season. Insulin is intrinsic to carbohydrate and lipid metabolism and is central to regulating feast-fast cycles in mammalian hibernators. Here, we examine glucose and insulin dynamics across the feast-fast cycle in fat-tailed dwarf lemurs, the only obligate hibernator among primates. Unlike cold-adapted hibernators, dwarf lemurs inhabit tropical forests in Madagascar and hibernate under various temperature conditions. Using the captive colony at the Duke Lemur Center, we determined fasting glucose and insulin, and glucose tolerance, in dwarf lemurs across seasons. During the lean season, we maintained dwarf lemurs under stable warm, stable cold, or fluctuating ambient temperatures that variably included food provisioning or deprivation. Overall, we find that dwarf lemurs can show signatures of reversible, lean-season insulin resistance. During the fattening season prior to hibernation, dwarf lemurs had low glucose, insulin, and HOMA-IR despite consuming high-sugar diets. In the active season after hibernation, glucose, insulin, HOMA-IR, and glucose tolerance all increased, highlighting the metabolic processes at play during periods of weight gain *versus* weight loss. During the lean season, glucose remained low, but insulin and HOMA-IR increased, particularly in animals kept under warm conditions with daily food. Moreover, these lemurs had the greatest glucose intolerance in our study and had average HOMA-IR values consistent with insulin resistance (5.49), while those without food under cold (1.95) or fluctuating (1.17) temperatures did not. Remarkably low insulin in dwarf lemurs under fluctuating temperatures raises new questions about lipid metabolism when animals can passively warm and cool rather than undergo sporadic arousals. Our results underscore that seasonal changes in insulin and glucose tolerance are likely hallmarks of hibernating mammals. Because dwarf lemurs can hibernate under a range of conditions in captivity, they are an emerging model for primate metabolic flexibility with implications for human health.

KEYWORDS

***Cheirogaleus*, dwarf lemur, hibernation, thermoconforming, torpor**

1 Introduction

Hibernation is a metabolic strategy used to cope with energetic crises like seasonal food scarcity (Ruf and Geiser, 2015). Among mammals, hibernation has evolved independently in members of all major lineages (Carey et al., 2003) with thermolability proposed as the ancestral condition (Lovegrove, 2012a; Lovegrove, 2012b). Depending on the species and local environment there is considerable variation in hibernation "styles" (Canale and Henry, 2010; Geiser and Körtner, 2010; Canale et al., 2012; Staples, 2016). For example, small-bodied, temperate hibernators tend to cycle between multi-day torpor bouts at low temperature and brief arousals to euthermia (Carey et al., 2003; Geiser, 2013); large bears tend to depress metabolism for prolonged periods while maintaining warm body temperature (Tøien et al., 2011); and tropical hibernators can depress metabolism under a range of ambient temperature conditions, from stable cold to those that fluctuate considerably across the day (Canale et al., 2012; Dausmann et al., 2012; van Breukelen and Martin, 2015). Despite this variation in metabolism across species, one commonality shared among fat-storing hibernators is the seasonal cycle between fat deposition and fat depletion (Carey et al., 2003; Giroud et al., 2021). This consistency between feast and fast cycles raises questions about the mammalian mechanisms that regulate switches between carbohydrate and lipid metabolism (Andrews, 2007; Giroud et al., 2021).

At the center of energy balance in mammals is insulin, a peptide hormone that maintains glucose homeostasis and is involved in lipid and protein metabolism (Wilcox, 2005; Keane and Newsholme, 2014). In the broadest terms, glucose enters the bloodstream, which triggers beta cells in the pancreas to secrete insulin, which in turn, promotes the uptake of surplus glucose by muscle or adipose tissues for storage as glycogen or lipids (Keane and Newsholme, 2014). Insulin also inhibits lipolysis (Sears and Perry, 2015). To burn stored lipids, target tissues can become insulin insensitive or insulin resistant (Sears and Perry, 2015). Thus insulin, directly or indirectly, affects how both carbohydrate- and lipid-based energy is synthesized, stored, and metabolized over a lifetime (Wilcox, 2005). In addition to insulin, other hormones and signaling molecules play essential roles in metabolic regulation (e.g., glucagon, ghrelin, leptin, *etc.*) (Healy et al., 2010; Amitani et al., 2013; Weitten et al., 2013). For hibernators, however, there is considerable literature on glucose, insulin, and reversible insulin resistance, in large part, to probe how hibernators can naturally withstand seasonal obesity and starvation, conditions that can be detrimental in non-hibernators, like humans (Martin, 2008; Wu et al., 2013).

In certain hibernating rodents, the fattening season prior to hibernation is characterized by greater concentrations of circulating glucose and insulin (Florant and Greenwood, 1986; Tokuyama et al., 1991; Martin, 2008), as well as insulin insensitivity (Melnyk et al., 1983; Florant et al., 1985; Florant and Greenwood, 1986; Tokuyama et al., 1991). In these systems, insulin sensitivity is then restored after hibernation has ended (Martin, 2008; Wu et al., 2013). Hedgehogs and bears, by contrast, show reduced circulating glucose and/or insulin during the fattening season, as well as increased insulin sensitivity (Laurila and Suomalainen, 1974; Rigano et al., 2017). Like rodents, bears are also sensitive to insulin after hibernation (Rigano et al., 2017). These differences between species during the fattening season could perhaps be related to differences in seasonal diets, the degree of fat deposition at the time of sampling, or experimental study design.

During hibernation, hibernators generally show more consistent patterns of glucose, insulin, and insulin sensitivity. For animals cycling between torpor and arousal, circulating glucose and insulin levels increase as animals rewarm and ratchet-up metabolism (Konttinen et al., 1964; Tashima et al., 1970; Galster and Morrison, 1975; Hoo-Paris et al., 1978; Castex and Sutter, 1979; Hoo-Paris and Sutter, 1980; Al-Badry and Taha, 1983). During hibernation, a time when significant lipolysis is essential to fuel metabolism, insulin insensitivity is common to rodents (Moreau-Hamsany et al., 1988), hedgehogs (Hoo-Paris et al., 1978), and bears (McCain et al., 2013; Rigano et al., 2017). The idea that greater insulin insensitivity in mammalian heterotherms is necessary for lipolysis is further supported from studies using rodents that normally hibernate, but that were artificially kept under warm conditions, constant photoperiod, and with food year-round: During periods of weight loss (i.e., fat burn), the animals did not differ in circulating glucose or insulin relative to periods of weight gain, but they did show greater insulin insensitivity (Grimes et al., 1981; Melnyk et al., 1983; Melnyk and Martin, 1985). Likewise, mouse lemurs that are facultative hibernators from Madagascar and gain weight seasonally in captivity without expressing hibernation, showed greater insulin sensitivity and insensitivity respectively during periods of weight gain and loss (Terrien et al., 2018; Giroud et al., 2021). These primates also had the greatest concentrations of circulating insulin when losing weight, with no correlational change in glucose (Terrien et al., 2018), perhaps due to the continued availability of food.

The fat-tailed dwarf lemur (*Cheirogaleus medius;* 150–300 g) is a larger cousin of the mouse lemur and presents a fascinating system for probing heterothermic flexibility and metabolic correlates in an obligate hibernator. Fat-tailed dwarf lemurs are endemic to the dry deciduous forests of western Madagascar, where they hibernate during the dry season (Fietz and Dausmann, 2006). In anticipation of hibernation, these lemurs almost double their body mass during the ~2-month fattening period by eating ripe fruits and converting the fruit sugar into fat that is deposited primarily around their tail (Fietz and Ganzhorn, 1999). As tropical hibernators, fat-tailed dwarf lemurs can hibernate under a range of conditions, from stable temperatures of 12°C–20°C to those that fluctuate daily from 10°C–30°C. Under stable temperatures, fat-tailed dwarf lemurs cycle between multi-day torpor bouts (in which body temperature approximates ambient) and periodic arousals. Under fluctuating conditions, they thermoconform, i.e., passively track warming and cooling ambient temperatures without fully arousing, for weeks at a time (Dausmann et al., 2004; Dausmann et al., 2005).

The Duke Lemur Center (DLC) in Durham, NC houses the only reproductive population of fat-tailed dwarf lemurs outside of Madagascar. Unlike mouse lemurs, fat-tailed dwarf lemurs can hibernate under appropriate laboratory conditions (Blanco et al., 2021; Blanco et al., 2022a). During the lean season, DLC dwarf lemurs can be maintained in warm rooms with available food, which maximally allows only shallow metabolic depression, or in temperature-controlled "hibernacula" rooms where food can be

offered or withheld, depending on the experimental setup. The hibernacula can be set to different temperature profiles, including stable or fluctuating conditions. Taken together, this setup allows for experimental studies to track metabolic signatures across seasons and within the lean season relative to environmental condition.

In the present study, we add to the literature on glucose and insulin dynamics in hibernators using the natural metabolic flexibility of the fat-tailed dwarf lemur and the experimental setup at the DLC. Specifically, we combine data on circulating glucose and insulin assayed from the DLC dwarf lemur colony during the fattening, lean, and active seasons of two years. During the lean season, we measured these analytes in animals housed under various temperature and food regimens, and thus expressing a range of metabolic strategies. Lastly, we conducted glucose tolerance tests on a subset of subjects across seasons. Under the hypothesis that glucose intolerance and insulin insensitivity are hallmarks of lipid-based metabolism and seasonally required for fat-storing hibernators, we predict that dwarf lemurs will show signatures consistent with lean-season insulin insensitivity, with variation across metabolic strategies and states.

2 Materials and methods

2.1 Subjects and housing

The subjects were 28 fat-tailed dwarf lemurs that ranged in age from 0.3–16 years and were studied in 2021–2022 and 2022–2023. In year 1, the subjects included 23 lemurs (10 adult males; 5 adult females; 5 juvenile males; 3 juvenile females); in year 2, the subjects included 20 lemurs (11 adult males; 4 adult females; 1 juvenile male; and 4 juvenile females). A subset of 15 subjects participated in both years. We define juveniles as animals under 3 years of age (Blanco and Godfrey, 2013).

DLC dwarf lemurs are housed in small family units or solitarily in indoor enclosures year-round. Water is always freely available. They are all maintained under an artificial, North Carolina-like photoperiod (Blanco et al., 2021) with the onset of the light cycle occurring at 11:30a.m. To accommodate for a changing photoperiod, the light phase is shortened or lengthened by ~15–30 min every other week, with the shortest light:dark cycle being 9.5 h:14.5 h (starting in late fall) and longest 14.5 h:9.5 h (starting in late spring).

We define mid-September to mid-November as the core of the fattening season, December-February as the core of the lean season, and March-May as the active season.

During the fattening and active seasons, dwarf lemurs are maintained under stable warm conditions (22°C–25°C). During the fattening season, they are fed a high-sugar diet (~15 g fresh fruit, ~3 g monkey biscuit, 2 g dried fruit), whereas during the active season they are fed a high-fat diet (~12 g fruit and veggie mix, 6 g monkey biscuit, 2 mealworms) (Blanco et al., 2022b). This regimen mimics the natural foraging patterns of wild populations (Fietz and Ganzhorn, 1999) and helps mediate seasonal fat deposition and depletion (Blanco et al., 2022b).

During the lean season, six of our subjects remained under stable warm conditions and were fed a calorie-reduced, high-fat diet (Blanco et al., 2022b). The remaining subjects were transferred to hibernacula rooms. Of these, 16 were housed under stable cold conditions (~15°C) and underwent food deprivation: These animals cycled between multiday torpor bouts and periodic arousals, i.e., they hibernated (Blanco et al., 2022a). An additional 9 subjects were housed under stable cold conditions but offered food daily: These subjects routinely ate and showed daily torpor expression (Blanco et al., unpublished data). The remaining 10 subjects were housed under fluctuating temperature conditions that cycled from 12°C–30°C daily. These subjects were food deprived and consistently thermoconformed (Blanco et al., unpublished data) (Figure 1).

Dwarf lemurs are endangered primates: In line with the DLC's mission, we designed our study to be minimally invasive and non-harmful to the animals, which understandably limited our experimental options. This study was approved by the DLC's Research Committee and Duke University's Institutional Animal Care and Use Committee (protocol A213-20-11).

2.2 Glucose tolerance tests

We conducted glucose tolerance tests in year 1 on a subset of animals during the fattening (4 adults; 4 juveniles), lean (3 adults; 1 juvenile), and active (6 adults; 5 juveniles) seasons, as well as control tests in the fattening (4 adults), lean (2 adults), and active (5 adults; 1 juvenile) seasons. Animals were assigned to either test or control conditions and always underwent the same experimental procedure when studied at different timepoints. Because of concerns to animal welfare, we only performed lean-season tolerance tests on animals maintained under warm conditions with food.

Glucose and control tests were conducted in the morning hours in the DLC's veterinary clinic during the final hours of the light phase (~8:00–11:30a.m.) following an overnight fast. Individuals were manually restrained and anesthetized. We chose Telazol (10.5 mg/kg, IM) because it has minimal interference with glucose metabolism (Gresl et al., 2000; Vaughan et al., 2014). Once the lemurs were anesthetized, we collected a fasting blood sample in EDTA from the tail or saphenous vein for insulin, from which we aliquoted two drops of whole blood to measure blood glucose in duplicate using a handheld glucometer (Contour next EZ, Ascensia, Inc.). The remaining whole blood was promptly spun to plasma and stored at −80°C until analysis.

We waited 15 min after anesthesia administration to begin tests. For the glucose tests, we administered 5% dextrose in sterile water (40 mL/kg, subcutaneous injection); for the control tests, we used sterile saline solution (0.9% NaCl, subcutaneous injection), with the volume adjusted per individual weight. We collected serial blood drops at the 15-, 30-, 60-, and 90-min marks to measure glucose in duplicate using the glucometer. Once the tests were completed, animals recovered in transport kennels and were returned to their home enclosure during the first part of their active phase.

2.3 Biological sampling

We collected blood samples for glucose and/or insulin from study lemurs not undergoing tolerance tests in year 1 and all animals in year 2. During the fattening and active seasons, and for animals

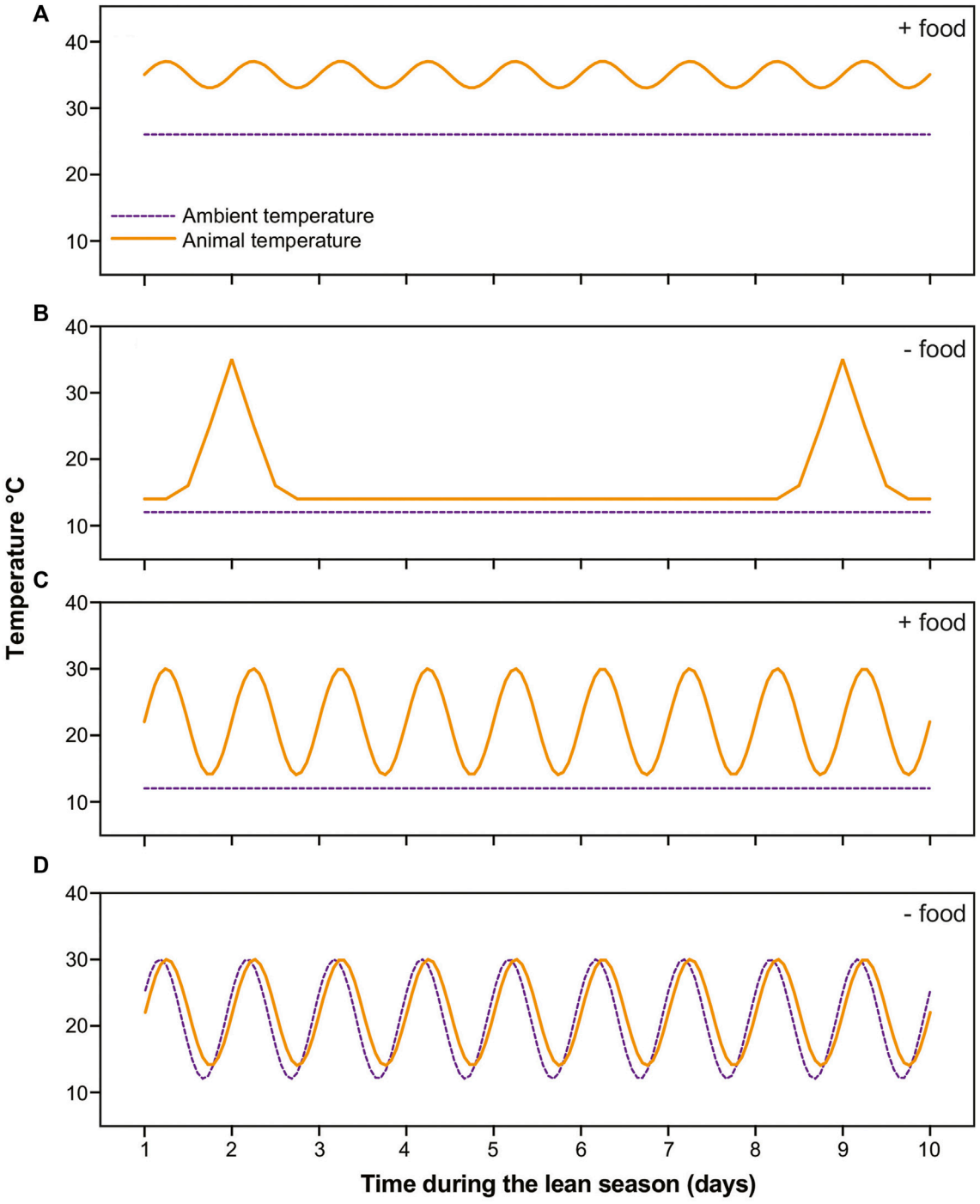

FIGURE 1
Schematics of temperature profiles in dwarf lemurs (solid orange lines) and rooms (dashed purple lines) in the four categories during 10 days in the lean season. **(A)** Lemurs under stable warm conditions with food undergo shallow torpor; **(B)** Lemurs under stable cold conditions without food cycle between multiday bouts of torpor and brief arousals; **(C)** Lemurs under stable cold conditions with food availability undergo daily torpor; **(D)** Lemurs under fluctuating daily conditions thermoconform, that is, passively track ambient temperatures without consistently using thermogenesis to arouse.

kept under warm conditions during the lean season, dwarf lemurs were sampled during the final hours of their light phase following an overnight fast. They were manually restrained and anesthetized (Ketamine; 10 mg/kg IM). We collected a blood sample in EDTA, aliquoted drops to measure glucose, and stored the remainder as plasma, as described above.

For lean-season dwarf lemurs in the hibernacula rooms of year 1, we measured glucose from animals under stable cold conditions with and without food while animals were torpid and aroused. In the early morning (7:00a.m.), we confirmed if study animals were torpid by checking temperature recordings from lemurs' external transmitters. Dwarf lemurs in the hibernacula rooms wore

TABLE 1 The number of samples across seasons, conditions, and metabolic states analyzed for glucose and insulin.

Assay type	Fattening	Lean						Active
		Cold; no food		Cold; food		Fluctuating; no food	Warm; food	
		Torpid	Aroused	Torpid	Aroused			
Glucose	36	8	16	5	8	10	6	40
Insulin	32	NA	8	NA	1	10	5	32
HOMA-IR	32	NA	8	NA	1	10	5	32

temperature-sensitive radiocollars that allowed us to determine individuals' metabolic status (for more details on radiocollars, see Blanco et al., 2021). If torpid, we restrained dwarf lemurs close to their home enclosure without anesthesia for rapid sampling of blood drops to measure glucose. These animals were placed in transport kennels in warm rooms for several hours. Once aroused, they were anesthetized for an additional blood draw to measure blood glucose. For lean-season dwarf lemurs in the hibernacula rooms of year 2, we brought lemurs to the clinic in transport kennels in the early morning (7:00a.m.), where they were housed for several hours. Once aroused, they underwent full blood sampling under anesthesia for glucose and insulin as described above.

All animals were allowed to recover from anesthesia in transport kennels and warm rooms. Animals were returned to their home enclosures during the first part of their active phase.

2.4 Sample and statistical analyses

For glucose, we averaged values across duplicate droplets. In total, we measured blood glucose in 36 samples from animals during the fattening season, in 53 samples from animals during the lean season, and in 40 samples from animals during the active season (Table 1). For collected plasma, we submitted 50 μL aliquots for insulin assays to Eurofins SF Analytical DBA Craft Technologies (ELISA NBP2-60076-1 kit). In total, we measured insulin in 32 samples from animals during the fattening season, in 24 samples from aroused/active animals during the lean season, and in 32 samples from animals during the active season (Table 1). All insulin values had a paired glucose value: We calculated the homeostatic model assessment for insulin resistance (HOMA-IR) following the formula = fasting insulin [μIU/mL] × fasting glucose [mg/dL])/405 (Terrien et al., 2018).

We implemented a series of linear mixed models (LMMs) via the lmerTest (version 3.1–3; Kuznetsova et al., 2017) package in Rstudio (version 2022.07.2; RStudio Team, 2022) with R software (version 4.2.1; R Core Team, 2022). We used log-transformed data, as they improved model fit as assessed by reduced AIC scores. For glucose, insulin, and HOMA-IR, we first computed models within the fattening season to determine whether animals placed under different conditions during the ensuing lean season showed any differences. We used glucose, insulin, or HOMA-IR as the dependent variable, lean-season condition, study year, animal sex and age (in years) as the independent variables, and individual lemur as a random term.

Next, we compared differences across seasons, regardless of what condition animals were placed under during the lean season. We excluded glucose values from torpid animals. We included glucose, insulin or HOMA-IR as the dependent variable, season, animal sex and age as the independent variables, and lemur as a random term. Within the lean season, we compared differences across conditions. We computed LMMs by entering glucose, insulin, or HOMA-IR as the dependent variable, lean-season condition as the independent variable, and lemur as a random term. We excluded sex and age as explanatory variables for models within seasons, given the reduced sample sizes. We excluded glucose values from torpid animals, and the single insulin value from the individual under cold conditions with food.

We asked if glucose differed between torpid and aroused animals. We ran a LMM for the lemurs kept under cold conditions with and without food, using glucose as the dependent variable, metabolic state (torpid *versus* aroused) nested within lean-season condition (cold, with *versus* without food) as the independent variable, and lemur as the random term.

For the glucose and control tolerance tests, we computed the area under the curve (AUC) across sampling timepoints per test in GraphPad Prism (version 9.5.0). We used log (AUC) values as they improved model fit. We compared experimental vs control tests using a LMM in which AUCs were entered as the dependent variable, treatment status as the independent variable, and lemur as the random term. Next, we looked within experimental subjects to ask if AUCs differed across seasons. We computed a LMM with AUC entered as the dependent variable, season as the independent variable, and lemur as the random term. Lastly, we asked if there was an effect of age. Due to sampling sizes, we restricted this model to only the fattening and active seasons: We included AUCs as the dependent variable, age category (adult vs juvenile) nested within season as the independent variable, and lemur as a random term.

3 Results

3.1 Results in the fattening season

Within the fattening season, neither fasting blood glucose ($t = 0.168$, $p = 0.868$), insulin ($t = 1.228$, $p = 0.254$), nor HOMA-IR ($t = 0.955$, $p = 0.364$) varied by study year. Likewise, forthcoming lean-season condition was not significantly associated to glucose ($t < 1.555$, $p > 0.131$ for all pairwise comparisons) or HOMA-IR ($t < 1.714$, $p > 0.112$ for all pairwise comparisons). Insulin showed no

10.3389/fphys.2023.1251042

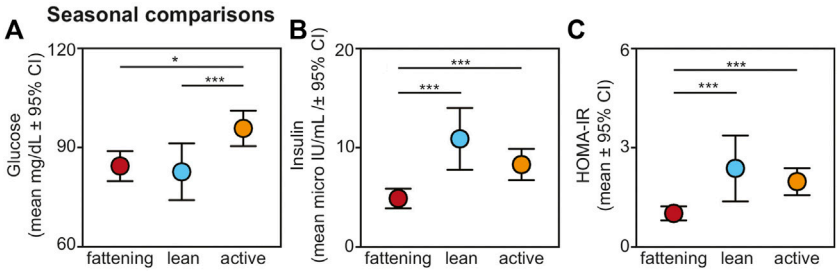

FIGURE 2
Fasting **(A)** glucose, **(B)** insulin, and **(C)** HOMA-IR values from non-torpid dwarf lemurs sampled across the fattening (red), lean (blue), and active (orange) seasons. All metrics are graphed as mean units ± 95% confidence intervals. *$p < 0.05$; ***$p < 0.001$.

difference during the fattening season in lemurs that would experience cold conditions without vs with food (t = 1.604, p = 0.145) or vs fluctuating conditions without food (t = 1.475, p = 0.154). We did find a difference during the fattening season between lemurs that would experience cold conditions with food and fluctuating conditions without food (t = 2.384, p = 0.039).

During the fattening season, males had significantly greater glucose than did females (t = 2.919, p = 0.007), and older animals trended towards having decreasing glucose (t = −1.833, p = 0.077). We found no such associations between insulin and animal sex (t = 1.216, p = 0.243) and age (t = 0.633, p = 0.534) or between HOMA-IR and animal sex (t = 0.537, p = 0.601) and age (t = 0.129, p = 0.899).

3.2 Results across seasonal timepoints

We found an overall, strong effect of season on glucose, insulin, and HOMA-IR values (Figure 2). Regarding glucose, lemurs during the active season had greater values compared to the fattening (t = 2.474, p = 0.015) and lean (t = 3.660, $p < 0.001$) seasons (Figure 2A). There was no difference in blood glucose between the fattening and lean seasons (t = 1.088; p = 0.279).

Insulin varied across seasons, with significantly reduced values in the fattening season compared to the lean (t = −4.484, $p < 0.001$) and active (t = −3.767, $p < 0.001$) seasons (Figure 2B). There was no difference in insulin between the lean and active seasons (t = 1.005, p = 0.318). HOMA-IR varied seasonally similarly to insulin: HOMA-IR was lower in the fattening season compared to the lean (t = 3.483, $p < 0.001$) and active (t = 4.120, $p < 0.001$) seasons (Figure 2C), and there was no difference between the lean and active seasons (t = 0.323, p = 0.747). Average HOMA-IR values were 0.99 for the fattening season, 2.36 for the lean season, and 1.96 for the active season.

For glucose, sex remained a significant effect in this seasonal model, with males having greater glucose values compared to females (t = 2.236; p = 0.027), but when considering this fuller sample set, we found no effect of animal age (t = −0.818, p = 0.415). Neither sex nor age were significantly associated with either insulin or HOMA-IR in these fuller models (t < 0.985, $p > 0.336$ for all comparisons).

3.3 Results across lean-season conditions

Within the lean season, we found effects of ambient temperature and food availability on glucose, insulin, and HOMA-IR values from non-torpid animals (Figure 3). Regarding glucose, lemurs without provisioned food did not differ in blood glucose when housed under cold *versus* fluctuating temperatures (t = 0.721; p = 0.476); however, lemurs under cold conditions without food had significantly reduced glucose compared to lemurs housed under cold conditions with food (t = −4.271; $p < 0.001$) and compared to those housed under warm conditions with food (t = −7.211; $p < 0.001$) (Figure 3A). Likewise, lemurs under fluctuating conditions without food had reduced glucose values compared to lemurs under cold conditions with food (t = −3.356, p = 0.005) and compared to those under warm conditions with food (t = −6.324, $p < 0.001$). Lemurs housed under cold conditions with food had reduced glucose compared those under warm conditions with food (t = −3.026, p = 0.005).

From non-torpid animals within the lean season, insulin was significantly reduced in lemurs maintained under fluctuating conditions without food compared to those under cold conditions without food (t = −2.480, p = 0.022) and under warm conditions with food (t = −2.718, p = 0.013) (Figure 3B). There was no difference in insulin between animals under cold conditions without food and warm conditions with food (t = 0.548, p = 0.590) and both groups showed considerable variation in fasting insulin.

Regarding HOMA-IR, values were significantly greater in animals maintained under warm conditions with food compared to those under cold conditions without food (t = 2.482, p = 0.022) and fluctuating conditions without food (t = 3.974, $p < 0.001$) (Figure 3C). We found no difference in HOMA-IR values between lemurs under cold and fluctuating conditions without food (t = 1.606, p = 0.124). Importantly, average HOMA-IR values were 1.95 for non-torpid lemurs under cold conditions without food, 1.17 for non-torpid lemurs under fluctuating conditions without food, and 5.49 for non-torpid lemurs under warm conditions with daily food. Thus, HOMA-IR values in dwarf lemurs housed in warm rooms with food are well above the standard threshold of 2.0 for insulin resistance.

Lastly, for animals housed under cold conditions, we found greater glucose values in aroused *versus* torpid animals for those without (t = 3.956, $p < 0.001$) and with (t = 3.080, p = 0.005) available food (Figure 4).

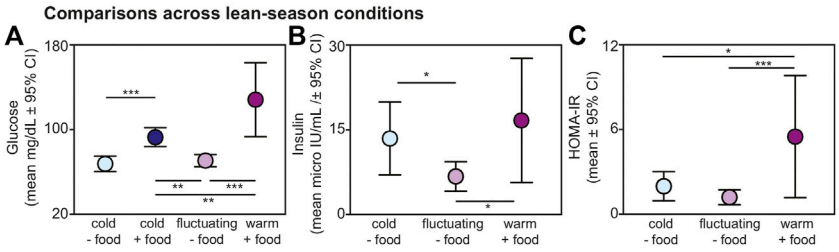

FIGURE 3
Fasting **(A)** glucose, **(B)** insulin, and **(C)** HOMA-IR values from non-torpid dwarf lemurs under different conditions during the lean season, including cold conditions without food (light blue), cold conditions with food (dark blue), fluctuating conditions without food (light purple), and warm conditions with food (dark purple). All metrics are graphed as mean units ± 95% confidence intervals. *$p < 0.05$; **$p < 0.01$; ***$p < 0.001$.

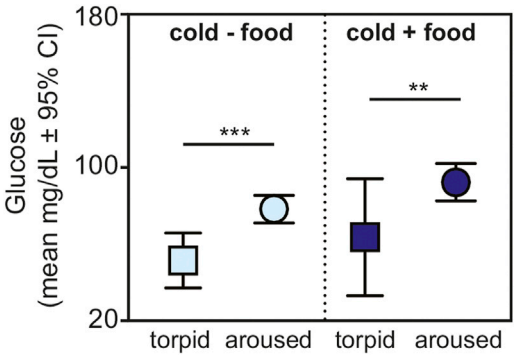

FIGURE 4
Fasting glucose in torpid (square) and aroused (circle) dwarf lemurs during the lean season maintained under cold conditions without food (light blue) and with food (dark blue). All metrics are graphed as mean units ± 95% confidence intervals. **$p < 0.01$; ***$p < 0.001$.

3.4 Results of glucose tolerance tests

Relative to animals receiving glucose tests, those receiving control tests had significantly smaller AUCs (t = −9.709; $p < 0.001$) (Figure 5A). Within experimental subjects, we found an effect of season in the response to glucose tests. Specifically, we found significantly larger AUCs during the lean *versus* active season (t = 2.313; $p = 0.034$), albeit we found no such differences between the fattening and lean season (t = 1.082; $p = 0.293$) or between the fattening and active season (t = −1.506; $p = 0.160$) (Figure 5B). When considering only the fattening (Figure 6A) and active (Figure 6B) seasons, we found that juveniles have a significantly smaller AUC compared to adults during the fattening season (t = −2.833, $p = 0.013$), but not during the active season (t = −1.022, $p = 0.323$) (Figure 6C).

4 Discussion

In the first study of glucose and insulin dynamics in dwarf lemurs, we find seasonal patterns that are broadly consistent with those known from other hibernating mammals. Like rodents, bears, and hedgehogs (Hoo-Paris et al., 1978; Melnyk et al., 1983; Moreau-Hamsany et al., 1988; Tokuyama et al., 1991; Rigano et al., 2017), dwarf lemurs can show signatures of lean-season insulin resistance, including elevated fasting insulin and HOMA-IR values, lower fasting glucose, and reduced glucose tolerance compared the fattening and/or active seasons. Despite variation between individuals, sexes, and age classes, dwarf lemurs during the fattening season showed patterns that bore greater resemblance to the dynamics of bears, hedgehogs, and mouse lemurs (Laurila and Suomalainen, 1974; Rigano et al., 2017; Terrien et al., 2018) compared to hibernating rodents (Tokuyama et al., 1991; Wu et al., 2013) during the same time of year; namely, they had relatively low

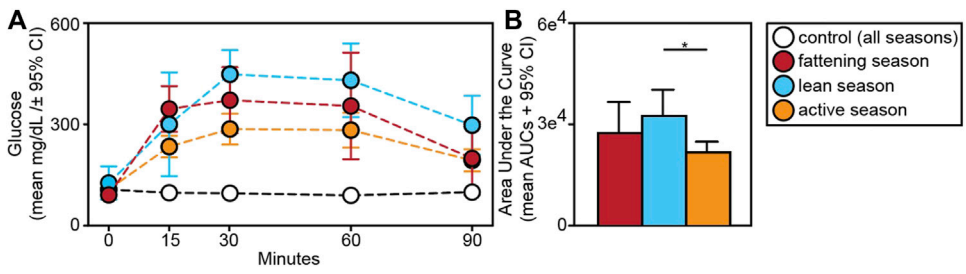

FIGURE 5
(A) Glucose tolerance test profiles from dwarf lemurs given a dextrose challenge during the fattening, lean and active season or given a control saline solution; **(B)** Area under the curve for dwarf lemurs sampled across seasons. *$p < 0.05$.

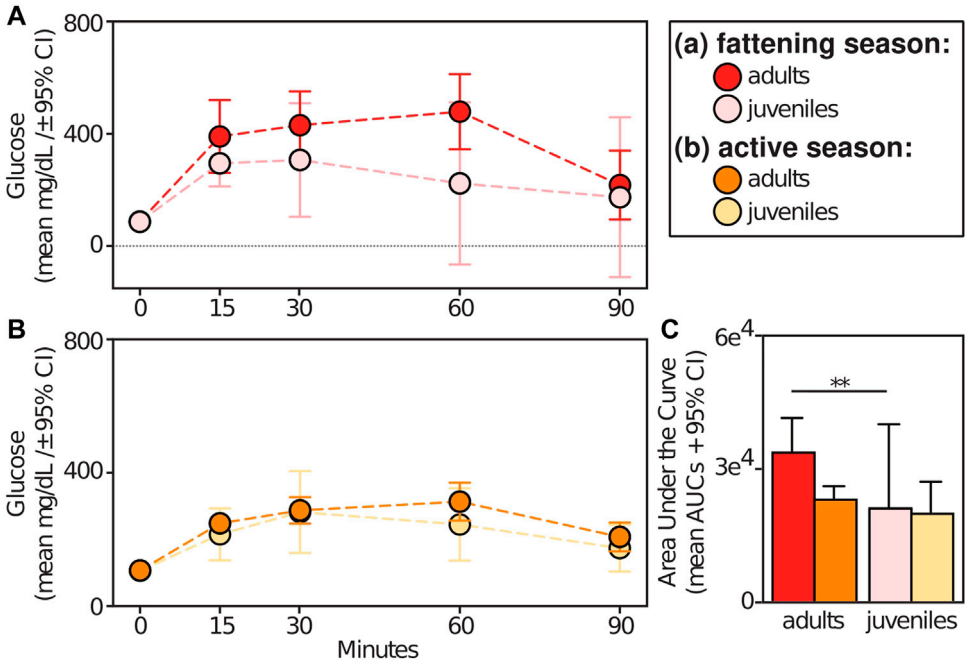

FIGURE 6
Glucose tolerance test profiles from adult vs juvenile dwarf lemurs given a dextrose challenge during the **(A)** fattening and **(B)** active seasons; **(C)** Area under the curve for adult and juveniles dwarf lemurs sampled between fattening and active seasons. $^{**}p \leq 0.01$.

values of glucose, insulin, and HOMA-IR. By contrast in the active season after hibernation, the lemurs showed greater fasting glucose, insulin, and HOMA-IR, as well as the greatest glucose tolerance of any timepoint. These seasonal differences highlight the processes at play during periods of weight gain *versus* loss, as animals balance carbohydrate and lipid-based metabolism. Notably during fattening, insulin likely responded to the glucose from food carbohydrates needed to deposit lipids. During the active season, insulin was likely also regulated by the adipose-tissue insensitivity needed for lipolysis to deplete any residual fat reserves.

During the lean season, two of our study conditions mimic the natural settings for wild dwarf lemurs in Madagascar- stable ambient temperatures or daily fluctuating temperatures, both without food (Dausmann et al., 2004). Under the former, dwarf lemurs cycle between torpor and arousal and showed fasting glucose and insulin dynamics that were most consistent with those from temperate hibernators: Glucose values were lowest during torpor and increased during arousals and fasting insulin was variable across individuals, likely because they were at different stages of the arousal process when sampled. Thermoconforming lemurs likewise had low fasting glucose, but curiously also had consistently low fasting insulin. This insulin result raises interesting questions about lipid-based metabolism in hibernators under fluctuating temperatures that allow them to passively cool and warm daily rather than rely on expensive and sporadic arousals from cold temperatures. Interestingly, HOMA-IR values did not differ significantly between these two conditions and remained under the standard threshold of 2.0 for insulin sensitivity, albeit the average value of 1.95 for animals under cold conditions approached this threshold, while the average value of 1.17 for animals under fluctuating conditions did not.

The other two lean-season conditions in our study are unlike anything wild dwarf lemurs would experience and involve the provisioning of daily food under stable temperature conditions. As would be expected, fasting glucose values were greater in both study groups with food compared to those without food; and fed animals under warm *versus* cold conditions had the greatest values of all. Indeed, we found HOMA-IR values well above the threshold for insulin resistance, as well as the greatest glucose intolerance, in animals kept under warm conditions with food during the lean season, highlighting that those with the greatest insulin insensitivity were also those under the least "natural" conditions. Although we were unable to perform glucose tolerance tests in food-restricted animals under different regimes during the lean season, we would expect that any dwarf lemur, like mouse lemurs (Terrien et al., 2018), undergoing weight loss and lipid metabolism to experience some insulin insensitivity, albeit perhaps to varying degrees.

Although our results from the lean season paint a relatively clear picture of glucose and insulin dynamics, those from the other two seasons are somewhat noisier. Notably, both the fattening and active seasons are times of transition: At any single timepoint, animals will show individual differences in food intake, degree of fattening, and activity levels. Such variation could explain the difference in glucose tolerance we found between adults and juveniles during the fattening season: Juveniles that were still prioritizing growth while also depositing fat were likely more sensitive to insulin to regulate glucose uptake (Boswell et al., 1994). In contrast, adults nearing their full capacity for fat stores were perhaps already showing signs of the insulin insensitivity that would characterize the forthcoming lean season. Future studies could beneficially culture adipose tissues from dwarf lemurs collected across seasons and age classes, and grown under different temperature

and endocrine environments (e.g., Moreau-Hamsany et al., 1988), to more directly measure insulin resistance and the finely tuned relationships between glucose, lipids, and insulin. Moreover, monitoring of insulin levels after controlled injections could aid in the discussion of insulin resistance in these lemurs, although techniques will need to be refined to allow for sequential blood draws in these small-bodied and critically endangered animals.

While acknowledging the constraints of our study system and limits to acceptable experimentation, our results demonstrate the promise of dwarf lemurs for investigating timely questions in hibernation metabolism, including elucidating the proximate mechanisms that regulate feast-fast cycles. Like all hibernators, dwarf lemurs have circannual rhythms that establish seasonal and consistent cycles of insulin sensitivity and insensitivity. Unlike temperate hibernators, however, dwarf lemurs show metabolic flexibility during the lean season that is intrinsically linked to environmental heterogeneity (Dausmann et al., 2004; Blanco et al., 2018). This flexibility includes capacity to depress metabolism, and even hibernate, under relatively warm and fluctuating conditions. Understanding the metabolic processes at play in thermoconforming dwarf lemurs, where significant lipolysis occurs without animals having to undergo costly arousals, may yield new insights into the role of insulin and other hormones in mediating lipid-based metabolism more broadly. As primate models, hibernating dwarf lemurs add another layer to the conversation about how insulin resistance can be reversed, with clear implications for human health.

Data availability statement

The raw data supporting the conclusions of this article will be made available by the authors, without undue reservation.

Ethics statement

The animal study was approved by Duke University's Institutional Animal Care and Use Committee (protocol A213-20-11). The study was conducted in accordance with the local legislation and institutional requirements.

Author contributions

MB conceived and design the project with LG, KW, and PK; LE, CW, CO, MD developed methods for glucose tolerance tests, and collected all samples; MB and LG analyzed the data; MB and LG wrote the manuscript. All authors contributed to the article and approved the submitted version.

Funding

MB was supported by the Duke Lemur Center.

Acknowledgments

We thank the DLC husbandry and research departments for their help in implementing this study. We also thank Julie Ter Beest and Lana Fox for their assistance with biological sampling. This is Duke Lemur Center publication #1573.

Conflict of interest

The authors declare that the research was conducted in the absence of any commercial or financial relationships that could be construed as a potential conflict of interest.

Publisher's note

Supplementary material

The Supplementary Material for this article can be found online at: https://www.frontiersin.org/articles/10.3389/fphys.2023.1251042/full#supplementary-material

References

Al-Badry, K. S., and Taha, H. M. (1983). Hibernation-hypothermia and metabolism in hedgehogs. Changes in some organic components. *Comp. Biochem. Physiol.* 74A, 143–148. doi:10.1016/0300-9629(83)90725-9

Amitani, M., Asakawa, A., Amitani, H., and Inui, A. (2013). The role of leptin in the control of insulin-glucose axis. *Front. Neurosci.* 7, 51. doi:10.3389/fnins.2013.00051

Andrews, M. T. (2007). Advances in molecular biology of hibernation in mammals. *Bioessays* 29, 431–440. doi:10.1002/bies.20560

Blanco, M. B., Dausmann, K. H., Faherty, S. L., and Yoder, A. D. (2018). Tropical heterothermy is "cool": the expression of daily torpor and hibernation in primates. *Evol. Anthropol.* 27, 147–161. doi:10.1002/evan.21588

Blanco, M. B., and Godfrey, L. R. (2013). Does hibernation slow the "pace of life" in dwarf lemurs (*Cheirogaleus* spp.)? *Int. J. Primatol.* 34, 130–147. doi:10.1007/s10764-012-9653-9

Blanco, M. B., Greene, L. K., Ellsaesser, L. N., Schopler, B., Davison, M., Ostrowski, C., et al. (2022b). Of fruits and fats: high-sugar diets restore fatty acid profiles in the white adipose tissue of captive dwarf lemurs. *Proc. R. Soc. B* 289, 20220598. doi:10.1098/rspb.2022.0598

Blanco, M. B., Greene, L. K., Klopfer, P. H., Lynch, D., Browning, J., Ehmke, E. E., et al. (2022a). Body mass and tail girth predict hibernation expression in captive dwarf lemurs. *Physiol. Biochem. Zool.* 95, 122–129. doi:10.1086/718222

Blanco, M. B., Greene, L. K., Williams, C. V., Lynch, D., Browning, J., et al. (2021). On the modulation and maintenance of hibernation in captive dwarf lemurs. *Sci. Rep.* 11, 5740. doi:10.1038/s41598-021-84727-3

Boswell, T., Woods, S. C., and Kenagy, G. J. (1994). Seasonal changes in body mass, insulin, and glucocorticoids of free-living golden-mantled ground squirrels. *Gen. Comp. Endocrinol.* 96, 339–346. doi:10.1006/gcen.1994.1189

Canale, C. I., and Henry, P-Y. (2010). Adaptive phenotypic plasticity and resilience of vertebrates to increasing climatic unpredictability. *Clim. Res.* 43, 135–147. doi:10.3354/cr00897

Canale, C. I., Levesque, D. L., and Lovegrove, B. G. (2012). "Tropical heterothermy: does the exception prove the rule or force a re-definition?," in *Living in a seasonal world*. Editors T. Ruf, C. Bieber, W. Arnold, and E. Millesi (Berlin: Springer), 29–40.

Carey, H. V., Andrews, M. T., and Martin, S. L. (2003). Mammalian hibernation: cellular and molecular responses to depressed metabolism and low temperature. *Physiol. Rev.* 83, 1153–1181. doi:10.1152/physrev.00008.2003

Castex, C., and Sutter, B. C. (1979). Seasonal variations of insulin sensitivity in edible dormouse (*Glis glis*) adipocytes. *Gen. Comp. Endocrinol.* 38, 365–369. doi:10.1016/0016-6480(79)90071-6

Dausmann, K., Glos, J., Ganzhorn, J., and Heldmaier, G. (2004). Physiology: hibernation in a tropical primate. *Nature* 429, 825–826. doi:10.1038/429825a

Dausmann, K. H., Glos, J., Ganzhorn, J. U., and Heldmaier, G. (2005). Hibernation in the tropics: lessons from a primate. *J. Comp. Physiol. B* 175, 147–155. doi:10.1007/s00360-004-0470-0

Dausmann, K. H., Nowack, J., Kobbe, S., and Mzilikazi, N. (2012). "Afrotropical heterothermy: A continuum of possibilities," in *Living in a seasonal world*. Editors T. Ruf, C. Bieber, W. Arnold, and E. Millesi (Berlin, Heidelberg: Springer). doi:10.1007/978-3-642-28678-0_2

Fietz, J., and Dausmann, K. H. (2006). "Big is beautiful: fat storage and hibernation as a strategy to cope with marked seasonality in the fat-tailed dwarf lemurs (*Cheirogaleus medius*)," in *Lemurs: Ecology and adaptation*. Editors L. Gould and M. L. Sauther (Berlin, Heidelberg: Springer), 97–111.

Fietz, J., and Ganzhorn, J. U. (1999). Feeding ecology of the hibernating primate *Cheirogaleus medius*: how does it get so fat? *Oecologia* 121, 157–164. doi:10.1007/s004420050917

Florant, G. L., and Greenwood, M. R. C. (1986). "Seasonal variations in pancreatic functions in marmots: the role of pancreatic hormones and lipoprotein lipase in fat deposition," in *Living in the cold*. Editors H. C. Heller, X. J. Musacchia, and L. C. H. Wang (New York: Elsevier).

Florant, G. L., Lawrence, A. K., Williams, K., and Bauman, W. A. (1985). Seasonal changes in pancreatic B-cell function in euthermic yellow-bellied marmots. *Am. J. Physiol.* 249, R159–R165. doi:10.1152/ajpregu.1985.249.2.R159

Galster, W., and Morrison, P. R. (1975). Gluconeogenesis in arctic ground squirrels between periods of hibernation. *Am. J. Physiol.* 228, 325–330. doi:10.1152/ajplegacy.1975.228.1.325

Geiser, F., and Körtner, G. (2010). Hibernation and daily torpor in Australian mammals. *Aust. Zool.* 35, 204–215. doi:10.7882/az.2010.009

Geiser, F. (2013). Hibernation. *Curr. Biol.* 23, R188–R193. doi:10.1016/j.cub.2013.01.062

Giroud, S., Habold, C., Nespolo, R. F., Mejías, C., Terrien, J., Logan, S. M., et al. (2021). The torpid state: recent advances in metabolic adaptations and protective mechanisms. *Front. Physiol.* 11, 623665. doi:10.3389/fphys.2020.623665

Gresl, T. A., Baum, S. T., and Kemnitz, J. W. (2000). Glucose regulation in captive *Pongo pygmaeus* abeli, P. p. pygmaeus, and P. p. abeli x P. p. pygmaeus orangutans. *Zoo. Biol.* 19, 193–208. doi:10.1002/1098-2361(2000)19:3<193::aid-zoo3>3.0.co;2-m

Grimes, L. J., Melnyk, R. B., Martin, J. M., and Mrosovsky, N. (1981). Infradian cycles in glucose utilization and lipogenic enzyme activity in dormouse (*Glis glis*) adipocytes. *Gen. Comp. Endocrinol.* 45, 21–25. doi:10.1016/0016-6480(81)90163-5

Healy, J. E., Ostrom, C. E., Wilkerson, G. K., and Florant, G. L. (2010). Plasma ghrelin concentrations change with physiological state in a sciurid hibernator (*Spermophilus lateralis*). *Gen. Comp. Endocrinol.* 166, 372–378. doi:10.1016/j.ygcen.2009.12.006

Hoo-Paris, R., Castex, C., and Sutter, B. C. (1978). Plasma glucose and insulin in the hibernating hedgehog. *Diabete Metab.* 4, 13–18.

Hoo-Paris, R., and Sutter, B. C. (1980). Role of glucose and catecholamines in the regulation of insulin secretion in the hibernating hedgehog (*Erinaceus europaeus*). *Gen. Comp. Endocrinol.* 41, 62–65. doi:10.1016/0016-6480(80)90032-5

Keane, K., and Newsholme, P. (2014). Metabolic regulation of insulin secretion. *Vitam. Horm.* 95, 1–33. doi:10.1016/B978-0-12-800174-5.00001-6

Konttinen, A., Rajasalmi, M., and Sarajas, H. S. (1964). Fat metabolism of the hedgehog during the hibernating cycle. *Am. J. Physiol.* 207, 845–848. doi:10.1152/ajplegacy.1964.207.4.845

Kuznetsova, A., Brockhoff, P. B., and Christensen, R. H. B. (2017). lmerTest package: tests in linear mixed effects models. *J. Stat. Softw.* 82, 1–26. doi:10.18637/jss.v082.i13

Laurila, M., and Suomalainen, P. (1974). Studies in the physiology of the hibernating hedgehog. 19. The changes in the insulin level induced by seasons and hibernation cycle. *Ann. Acad. Sci. Fenn. Biol.* 201, 1–40.

Lovegrove, B. G. (2012a). "A single origin of heterothermy in mammals," in *Living in a seasonal world*. Editors T. Ruf, C. Bieber, W. Arnold, and E. Millesi (Berlin: Springer), 3–11.

Lovegrove, B. G. (2012b). The evolution of endothermy in cenozoic mammals: A plesiomorphic-apomorphic continuum. *Biol. Rev.* 87, 128–162. doi:10.1111/j.1469-185X.2011.00188.x

Martin, S. L. (2008). Mammalian hibernation: A naturally reversible model for insulin resistance in man? *Diab Vasc. Dis. Res.* 5, 76–81. doi:10.3132/dvdr.2008.013

McCain, S., Ramsay, E., and Kirk, C. (2013). The effects of hibernation and captivity on glucose metabolism and thyroid hormones in American black bear (*Ursus americanus*). *J. Zoo. Wildl. Med.* 44, 324–332. doi:10.1638/2012-0146R1.1

Melnyk, R. B., and Martin, J. M. (1985). Insulin and central regulation of spontaneous fattening and weight loss. *Am. J. Physiol.* 249, R203–R208. doi:10.1152/ajpregu.1985.249.2.R203

Melnyk, R. B., Mrosovsky, N., and Martin, J. M. (1983). Spontaneous obesity and weight loss: insulin action in the dormouse. *Am. J. Physiol.* 245, R396–R402. doi:10.1152/ajpregu.1983.245.3.R396

Moreau-Hamsany, C., Castex, C., Hoo-Paris, R., Kacemi, N., and Sutter, B. (1988). Hormonal control of lipolysis from the white adipose tissue of hibernating jerboa (*Jaculus orientalis*). *Comp. Biochem. Physiol.* 91, 665–669. doi:10.1016/0300-9629(88)90945-0

R Core Team (2022). *R: A language and environment for statistical computing*. Vienna, Austria: R Foundation for Statistical Computing.

Rigano, K. S., Gehring, J. L., Evans Hutzenbiler, B. D., Chen, A. V., Nelson, O. L., Vella, C. A., et al. (2017). Life in the fat lane: seasonal regulation of insulin sensitivity, food intake, and adipose biology in brown bears. *J. Comp. Physiol. B* 187, 649–676. doi:10.1007/s00360-016-1050-9

RStudio Team (2022). *RStudio*. Boston, MA: Integrated Development Environment for R. RStudio, PBC.

Ruf, T., and Geiser, F. (2015). Daily torpor and hibernation in birds and mammals. *Biol. Rev.* 90, 891–926. doi:10.1111/brv.12137

Sears, B., and Perry, M. (2015). The role of fatty acids in insulin resistance. *Lipids Health Dis.* 14, 121. doi:10.1186/s12944-015-0123-1

Staples, J. F. (2016). Metabolic flexibility: hibernation, torpor, and estivation. *Compr. Physiol.* 6, 737–771. doi:10.1002/cphy.c140064

Tashima, L. S., Adelstein, S. J., and Lyman, C. P. (1970). Radioglucose utilization by active, hibernating, and arousing ground squirrels. *Am. J. Physiol.* 218, 303–309. doi:10.1152/ajplegacy.1970.218.1.303

Terrien, J., Gaudubois, M., Champeval, D., Zaninotto, V., Roger, L., Riou, J. F., et al. (2018). Metabolic and genomic adaptations to winter fattening in a primate species, the grey mouse lemur (*Microcebus murinus*). *Int. J. Obes.* 42, 221–230. doi:10.1038/ijo.2017.195

Tøien, Ø., Blake, J., Edgar, D. M., Grahn, D. A., Heller, H. C., and Barnes, B. M. (2011). Hibernation in black bears: independence of metabolic suppression from body temperature. *Science* 331, 906–909. doi:10.1126/science.1199435

Tokuyama, K., Galantino, H. L., Green, R., and Florant, G. L. (1991). Seasonal glucose uptake in marmots (*Marmota flaviventris*): the role of pancreatic hormones. *Comp. Biochem. Physiol.* 100, 925–930. doi:10.1016/0300-9629(91)90316-5

van Breukelen, F., and Martin, S. L. (2015). The hibernation continuum: physiological and molecular aspects of metabolic plasticity in mammals. *Physiology* 30, 273–281. doi:10.1152/physiol.00010.2015

Vaughan, K. L., Szarowicz, M. D., Herbert, R. L., and Mattison, J. A. (2014). Comparison of anesthesia protocols for intravenous glucose tolerance testing in rhesus monkeys. *J. Med. Primatol.* 43, 162–168. doi:10.1111/jmp.12104

Weitten, M., Robin, J. P., Oudart, H., Pévet, P., and Habold, C. (2013). Hormonal changes and energy substrate availability during the hibernation cycle of Syrian hamsters. *Horm. Behav.* 64, 611–617. doi:10.1016/j.yhbeh.2013.08.015

Wilcox, G. (2005). Insulin and insulin resistance. *Clin. Biochem. Rev.* 26, 19–39.

Wu, C. W., Biggar, K. K., and Storey, K. B. (2013). Biochemical adaptations of mammalian hibernation: exploring squirrels as a perspective model for naturally induced reversible insulin resistance. *Braz J. Med. Bio Res.* 46, 1–13. doi:10.1590/1414-431x20122388

frontiers | Frontiers in Physiology

TYPE Original Research
PUBLISHED 22 November 2023
DOI 10.3389/fphys.2023.1298505

OPEN ACCESS

EDITED BY
James Harper,
Sam Houston State University,
United States

REVIEWED BY
Carola Sanpera,
University of Barcelona, Spain
Alessandra Occhinegro,
University of Bologna, Italy

*CORRESPONDENCE
Steve Smith,
steve.smith@vetmeduni.ac.at

†These authors have contributed equally to this work

§These authors share last authorship

RECEIVED 21 September 2023
ACCEPTED 07 November 2023
PUBLISHED 22 November 2023

CITATION
Galindo-Lalana C, Hoelzl F, Zahn S, Habold C, Cornils JS, Giroud S and Smith S (2023), Seasonal variation in telomerase activity and telomere dynamics in a hibernating rodent, the garden dormouse (*Eliomys quercinus*). *Front. Physiol.* 14:1298505. doi: 10.3389/fphys.2023.1298505

Seasonal variation in telomerase activity and telomere dynamics in a hibernating rodent, the garden dormouse (*Eliomys quercinus*)

Carlos Galindo-Lalana [1‡], Franz Hoelzl [1‡], Sandrine Zahn [2], Caroline Habold [2], Jessica S. Cornils [3], Sylvain Giroud [3,4§] and Steve Smith [1*§]

[1]Department of Interdisciplinary Life Sciences, Konrad Lorenz Institute of Ethology, University of Veterinary Medicine, Vienna, Austria, [2]University of Strasbourg, Centre National de la Recherche Scientifique, Institut Pluridisciplinaire Hubert Curien, Strasbourg, France, [3]Research Institute of Wildlife Ecology, Department of Interdisciplinary Life Sciences, University of Veterinary Medicine, Vienna, Austria, [4]Energetics Lab, Department of Biology, Northern Michigan University, Marquette, MI, United States

Telomere dynamics in hibernating species are known to reflect seasonal changes in somatic maintenance. Throughout hibernation, the periodic states of rewarming, known as inter-bout euthermia or arousals, are associated with high metabolic costs including shortening of telomeres. In the active season, if high energetic resources are available, telomere length can be restored in preparation for the upcoming winter. The mechanism for telomere elongation has not been clearly demonstrated, although the action of the ribonucleoprotein complex, telomerase, has been implicated in many species. Here we tested for levels of telomerase activity in the garden dormouse (*Eliomys quercinus*) at different seasonal time points throughout the year and across ages from liver tissues of male juveniles to adults. We found that telomerase is active at high levels across seasons (during torpor and inter-bout euthermia, plus in the active season) but that there was a substantial decrease in activity in the month prior to hibernation. Telomerase levels were consistent across age groups and were independent of feeding regime and time of birth (early or late born). The changes in activity levels that we detected were broadly associated with changes in telomere lengths measured in the same tissues. We hypothesise that i) telomerase is the mechanism used by garden dormice for maintenance of telomeres and that ii) activity is kept at high levels throughout the year until pre-hibernation when resources are diverted to increasing fat reserves for overwintering. We found no evidence for a decrease in telomerase activity with age or a final increase in telomere length which has been detected in other hibernating rodents.

KEYWORDS

torpor, euthermia, oxidative damage, biological ageing, somatic maintenance

Introduction

Understanding the complexity of telomere dynamics in non-model organisms has become a burgeoning field of research in ecology and evolution (see reviews in (Monaghan and Ozanne, 2018; Smith et al., 2022). In contrast to early research in humans and cancer models, where telomeres typically shorten with age as a result of the end replication problem and oxidative stress

(Harley et al., 1990; Blasco, 2007; Aubert, 2014), recent research has shown that in some organisms telomeres can lengthen as individuals become older and that telomeres can even have a complex and dynamic role in life histories (Monaghan and Ozanne, 2018; Marasco et al., 2022). Such findings of active telomere maintenance struggled to find traction initially but repeated examples across many taxa have led to a general acceptance that the process is not uncommon non-model species (Hoelzl et al., 2016b; Criscuolo et al., 2020; Panasiak et al., 2020; Tissier et al., 2022; Giroud et al., 2023). The underlying mechanisms for telomere repair, however, remain poorly understood.

Telomeres in hibernating rodents, particularly, have been shown to cycle through periods of loss and periods of maintenance (Hoelzl et al., 2016a; Giroud et al., 2023). The gain and loss of telomeres seems tightly bound to seasonal variation in energy availability and to phases characterized by marked changes in metabolic demands, such as those observed during torpor and hibernation (Hoelzl et al., 2016a). Active periods are time points when telomeres can be elongated but the underlying process for elongation is unclear and seemingly energy costly. In a supplemental feeding experiment on edible dormice (*Glis glis*) it was shown that elongation was possible in the active season but only when extra food resources were made available in the form of energy rich sunflower seeds (Hoelzl et al., 2016a). Similarly, telomere elongation is possible in hibernating garden dormice (*Eliomys quercinus*) if food is available (Giroud et al., 2023). Telomerase, the ribo-nucleoprotein complex, is a prime candidate as the mechanism for telomere extension but little is known of its activity in non-model species. In experimental settings telomerase has been shown to act to increase telomere length in these examples (de Jesus et al., 2011; Reichert et al., 2014; Tomás-Loba et al., 2008; see review here; Criscuolo et al., 2018).

Telomerase activity (TA) is problematic to measure in many wild populations due to difficulties in collecting appropriate samples and processing them in a time-efficient manner. The situation is compounded by the lack of knowledge about when and how long telomerase should be active to generate a detectable increase in telomere length. It is vitally important to resolve this problem to allow researchers to disentangle the complex mechanisms of telomere maintenance and the relationships with energy balances that may constrain life histories. Previous research has shown that hibernating rodents suffer a loss of telomere length throughout hibernation and that this loss is intricately linked to the number and length of interbout euthermia phases (IBE) across the hibernation period (Hoelzl et al., 2016a). All hibernation periods are typified by periods of extreme reduction in metabolism and body temperature (torpor) interspersed with short bursts of euthermia where individuals return to normal metabolism and body temperature before returning into the torpor phase (Lyman et al., 1982; Carey et al., 2003; Heldmaier et al., 2004; Hoelzl et al., 2015). Telomere attrition across hibernation has been shown in both edible dormice (*Glis glis*) and garden dormice (*E. quercinus*) as well as in other hibernating rodents such as Columbian ground squirrels (*Urocitellus columbianus*), eastern chipmunks (*Tamias striatus*), and also in some bat species (Hoelzl et al., 2016b; Foley et al., 2018; Nowack et al., 2019; Giroud et al., 2022; Tissier et al., 2022; Viblanc et al., 2022). In garden dormice however, individuals were able to maintain or increase relative telomere length (RTL) during hibernation when provided with food *ad libitum* (Giroud et al., 2023). Further, Hoelzl et al. (2016a) showed that telomere loss was most closely related to the number of IBE episodes during hibernation. Combined, this evidence suggests that IBE is highly energy demanding and that it involves bursts of reactive oxygen species (ROS) generation that are hugely damaging to telomeres. It further suggests that telomerase activity is reduced throughout hibernation and thus telomere repair does not take place during this period at least when animals lack food supply.

The most likely candidate period for telomere maintenance is during the early active season when energy is abundant and individuals emerge from the period of high ROS damage during hibernation. Alternatively, telomere maintenance may occur immediately prior to hibernation when body fat reserves are increasing dramatically in preparation for the winter months. Although, during this time the costs of lipogenesis are likely very high and may not allow investment into telomere maintenance and increased TA, especially in the liver. While research has shown that telomeres can be elongated in edible dormice in the active season when food availability is high (Hoelzl et al., 2016a) and also with chronological age in Eastern chipmunks (Tissier et al., 2022), telomerase activity was not measured in the same individuals, so the mechanism for telomere repair is still unclear. Sampling individuals throughout the entire active season and also throughout hibernation, including during deep torpor and IBE, and measuring telomerase activity as well as telomere length, is the only way to resolve the timing and likely mechanism of telomere maintenance. Such sampling requires a well-managed population where all individuals are monitored for age, body mass, body temperature and food intake.

In this study, we used a long-term captive colony of garden dormice as an experimental system to understand the timing and activation of telomerase and how it relates directly to telomere maintenance. By using a closely monitored population we were able to very accurately determine the state of individuals throughout hibernation as well as their body mass and energy intake throughout the active season. The colony, housed at the Research Institute of Wildlife Ecology in Vienna, contained individuals of different ages and sexes, from which life-history parameters could be closely monitored. By sampling liver tissues of individuals at the distinct timepoints of interest, we were able to measure both the level of TA relative to total protein amount as well as RTL of the very same tissue samples. We made measurements of RTL and TA from liver tissues as this organ has been shown in pilot studies to exhibit high levels of TA and is expected to be highly active during lipogenesis and "lipid-mobilisation" to provide energy during hibernation. This provides a very powerful method to determine the interplay between TA, RTL, season and age while accounting for sex and body mass in the same models. We hypothesise that TA will be low throughout all points during hibernation and will peak early in the active season, when food availability is high, but will decrease substantially pre-hibernation when individuals are building fat reserves. Due to high metabolic demands in the liver (lipogenesis), increased foraging activity and associated extensive ROS production, telomeres are not likely to be elongated in autumn. We therefore expect a cyclical seasonal dynamic for RTL with loss over winter and a regeneration early in the active season.

The advantage of our well monitored study system is that we have a deep knowledge of their physiology as well as detailed data on the use of torpor and IBE, food intake, age, and body mass of all sampled individuals. Further by measuring RTL and TA from the same tissues, we can access simultaneous estimates of these inter-related parameters to clearly assess the effect of enzymatic repair on telomeres.

Materials and methods

Ethical note

All procedures have been discussed and approved by the institutional ethics and animal welfare committee in accordance with GSP guidelines and national legislation (ETK-046/03/2020, ETK-108/06/2022, and ETK-150/09/2022), and the national authority according to §§29 of Animal Experiments Act, Tierversuchsgesetz 2012 - TVG 2012 (BMBWF-68.205/0175-V/3b/2018).

Study species and sampling

The samples for this study came from an ongoing project on torpor use in garden dormice and were made available for assessment of TA and RTL at relevant seasonal timepoints (early active season, pre-hibernation, torpor bout in hibernation season, IBE in hibernation season). Due to logistic constraints, only juvenile male individuals were available and monitored over the hibernation season but both sexes as adults were available for measurements over the active season.

We used 107 individuals in this study including 80 (43 females and 37 males) adult garden dormice from the active season (including the early active season and the pre-hibernation fattening phase), ages ranging between 11 and 62 months and having undergone at least one complete hibernation; and a further 27 juvenile males sampled during their first hibernation (13 in torpor and 12 in IBE) at the age of 10 months. These groups will be called "adult" and "juvenile" respectively for the remainder of the text. Adult individuals in the early active season group contained animals that were born early in the season (March/April) and others that were late born (July). All individuals were fed *ad libitum* except for 13 juvenile individuals in the hibernation group that were on a food restriction regime (see Supplementary Table S10). Of the active season individuals, the animals were born in captivity and raised under natural climatic conditions in outdoor enclosures at the Research Institute of Wildlife Ecology (FIWI) of the University of Veterinary Medicine Vienna, Austria (48°15′N, 16°22′E). The study individuals were euthanized and the liver was flash frozen in liquid nitrogen within 5 min after death of the animals. All samples were stored at −80°C upon processing.

Torpid animals were sacrificed by immediate decapitation. Euthermic animals during hibernation, pre-hibernation and summer were euthanized by incrementally exposure to carbon dioxide (CO2, 100%) until loss of consciousness followed by decapitation, as previously described (Huber et al., 2021). Once individuals were euthanized, the liver was flash frozen in liquid nitrogen within 5 min after death of the animals. All samples were stored at −80°C upon processing.

Temperature recording and torpor pattern

We used nest temperature as a proxy for T_b to estimate torpor use, as described by Willis et al. (2005) and used in previous studies in garden dormice (Giroud et al., 2012; Giroud et al., 2014; Mahlert et al., 2018; Nowack et al., 2019). In brief, the nest box was equipped with a customized temperature data logger (FIWI, Vienna, Austria; resolution: 0.2°C, accuracy: ±0.06°C), which recorded the temperature of the nest every minute. Nests were big enough for one dormouse to fit completely inside but small enough that it had to sit directly on the thermologger. The floors of the nests were covered with a thin layer of hay to provide familiar nesting conditions but to still ensure the contact between the animal and data loggers. To mimic normal conditions during hibernation, animals were kept under constant darkness and at a near stable temperature in the cooling units. In their housing setup dormice were exposed to environmental temperatures of 13.5±3.8°C at pre-hibernation and 24.5±1.8°C during the summer just prior to and during sacrifices.

Molecular procedures

A small portion of liver tissue was harvested from euthanized individuals as part of standard colony management measures. For the TA and RTL analysis, samples were stored immediately at −80°C until analysis. To estimate TA we used a modified version of the droplet digital telomere repeat amplification protocol (ddTRAP) of (Ludlow et al., 2014). In brief, approximately 0.5 mg of frozen liver was powdered in liquid nitrogen for 20 s at 50 osc/sec in a Tissue Lyser (Qiagen, Germany). TRAP lysis buffer (80 µL) was added to each sample and incubated on ice for 2 hours (10 mM Tris-HCl, pH 8.0, 1mM $MgCl_2$, 1 mM EDTA, 1% (vol/vol) NP-40, 0.25 mM sodium deoxycholate, 10% (vol/vol) glycerol, 150 mM NaCl, 5 mM β-mercaptoethanol; 0.1 mM AEBSF (4-(2-aminoethyl)benzenesulfonyl fluoride hydrochloride). One microlitre of lysed sample was then used in the TRAP reaction containing 1x TRAP buffer (10x concentration: 200 mM Tris-HCl, pH 8.3, 15 mM $MgCl_2$), 0.4 mg/mL BSA, TS primer (HPLC purified, 200nM; 5' AATCCGTCGAGCAGAGTT), dNTPs (2.5 mM each) and purified water to a volume of 50 µL. The TRAP reaction was performed in a thermal cycler with the lid heating deactivated. To test if temperature had an effect on TA we incubated the lysate at 25°C (as in Ludlow et al., 2014) and 5°C (to mimic torpor body temperature) for 40 min and then heated to 95°C for 6 min before cooling to 4°C. Two µl of the TRAP product was then added to the ddPCR reaction mix containing 1xEvaGreen ddPCR Supermix v2.0 (Bio-Rad, Hercules, CA, United States), 50 nM TS primer, 50 nM of the ACX primer and purified water to a volume of 20 µL. After droplet generation (QX200 drop generator, Bio-Rad), 40 µL of the generated emulsion was transferred to a 96-well PCR plate (twin-tec 96-well plate, Eppendorf, Fisher) and sealed with foil (Thermo Scientific, AB0757). PCR was performed (GeneAmp® PCR System 9,700, Applied Biosystems, Foster City, CA) with a temperature increase of 2.5°C/s between all steps. Activation of Taq polymerase (95°C for 5 min) was followed by 40 cycles of 95°C for 30s, 54°C for 30 s, 72°C for 30 s, then held at 12°C. Fluorescence was read on the droplet reader (QX200, Bio-Rad) after PCR (using the 6-Fam channel Nucleic Acids Research, 2014 e104 (channel 1 on the software)). One no-template lysis buffer control sample and one control sample without primers but with lysate were added to determine the threshold between positive and negative results. The output was given in number of molecules of extension products per microliter of ddPCR reaction, indicating the number of extended TS molecules and therefore telomerase activity. All values were normalised to total protein content in each sample (a proxy for the number of cells in each assay) as determined via a standard Bradford assay of 30 µL of the remaining lysate.

DNA was extracted from the same lysate generated for the ddTRAP measurement of TA. To 30 µL lysate we added 500 µL TNES buffer and 15 µL Proteinase K. Samples were vortexed and incubated for 20 min at

TABLE 1 Summary of individuals analysed for telomerase activity (TA) and relative telomere length (RTL) from the study colony of garden dormice at the Research Institute for Wildlife Ecology, Vienna.

	Early active season				Prehibernation		Torpor	IBE
	Male		Female		Male	Female	Male	
	Early born	Late born	Early born	Late born	Early born			
Adults (*ad libitum*)	8	6	12	8	23	23	-	-
Juveniles (*ad libitum*)	-	-	-	-	-	-	8	6
Juveniles (fasted)	-	-	-	-	-	-	7	6

55°C while shaking. Then 180 µL of 5M NaCl was added before vortexing and centrifugation for 20 min at 12,000 rpm. Supernatant was transferred to a new 1.5 mL tube (containing 1 µL Glycogen). Precipitation was performed with chilled isopropanol incubated at −80°C for 30 min. DNA was then pelleted and resuspended in 100 µL TE buffer. Concentration and quality (260/280 ratio) of the extracted DNA was determined using a NanoDrop 2000c (Peqlab Biotechnologie GmbH, Erlangen, Germany).

Relative telomere length

An 54 bp portion of the cMYC proto-oncogene was used as the non-variable copy number (non-VCN) gene. Primer sequences for the non-VCN gene were 5'-GAG GGC CAA GTT GGA CAG TG-3'(cMYC_F) and 5'-TTG CGG TTG TTG CTG ATC TG-3' (cMYCR), and telomeric primer sequences were 5′-CGG TTT GTT TGG GTT TGG GTT TGG GTT TGG GTT TGG GTT-3′ (tel 1b) and 5′-GGC TTG CCT TAC CCT TAC CCT TAC CCT TAC CCT TAC CCT-3′ (tel 2b) RTL was estimated via qPCR as described by Hoelzl et al. (2016b). Non-VCN gene and telomere PCRs were carried out in separate runs with 20 ng DNA per reaction, 400 nmol l−1 of each primer in a final volume of 20 µL containing 10 µL of Promega BRYT Green GoTaq® qPCR Master Mix (Cat. Nr. A6001/2; Promega, Madison, United States). PCR conditions for cMYC were 10 min at 95°C followed by 40 cycles of 10 s at 95°C, 20 s at 63°C and 20 s at 72°C. PCR conditions for the telomere primers were 10min at 95°C followed by 40 cycles of 10 s at 95°C, 20 s at 56°C and 20 s at 72°C. In each run, a final melting step was included with the temperature ramping from 65°C to 95°C, at 1°C steps. Two reference standard samples (standard A and standard B) were included in every run and compared with all ratios of telomere to non-VCN gene. A non-template control was included as well in every run. To minimize pipetting errors, reactions were prepared using the Qiagility PCR robot (Qiagen, Germany). Cycling was conducted on a Rotorgene Q quantitative thermocycler (Qiagen, Germany). For analysis of the non-baseline corrected raw qPCR data, the software LinRegPCR (2012.0) was used. RTL was calculated using a modified formula from Ruijter et al. (2009), where E is the qPCR efficiency and Ct the cycle threshold. The subscript ST refers to the telomere reaction of the standard sample, SC to the control gene reaction of the standard sample, T to the telomere reaction of the target sample and C to the control gene (cMYC) reaction of the target sample: RTL = $(E_T^{CtT}/E_{ST}^{CtST})/(E_c^{CtC}/E_{SC}^{CtSC})$.

The mean qPCR efficiency was calculated via the amplification plot method (Ramakers et al., 2003) which gives lower but more accurate estimates of efficiency than standard curve based methods (Morinha et al., 2020; Spießberger et al., 2022). For the non-VCN gene and telomere reactions, mean qPCR efficiencies were 91.0% and 78.6%, respectively.

Statistics

All analyses were carried out in R 4.3.1 (R Core Team, 2023). A Wilcoxon rank test was performed on the assay temperature comparison between TA at 5°C and 25°C. For comparison between groups the package emmeans was used (Lenth, 2023). Analyses were split in two groups adult females and males in the active and prehibernation season and juvenile male garden dormice during hibernation in torpor and IBE. In case of the adult/yearling group, we used Generalized linear models to analyze the influence of the state (active/prehibernation), body mass, sex, age in month and the time point of birth (early/late) in the season as explanatory variables for the square root transformed TRAP assay concentration at 25°C (Gamma distribution), as well as the RTL ratio (Gaussian distribution) in a separate model. For the juvenile garden dormice, we used the state (torpor/IBE), body mass and the food regime (*ad libitum*/restricted) to explain TRAP assay concentration at 25°C (Gaussian distribution) and RTL ratio (Gamma distribution). We checked regression diagnostics with the built-in visual inspection function in base R 4.3.1 (R Core Team, 2023). The model with the best fit, was chosen by comparing AICc values for different model specifications, the models with the lowest AICc, per analysis, were used for calculation of the Relative Variable Importance (Barton, 2023). Variables with values over 0.7 for RVI were defined as being important for the respective model. In the case of the TRAP assay model for the adult animals, we had one case with no change in TRAP assay concentration, to avoid losing samples for modeling we added 0.001 to all TRAP assay concentration values, because for the Gamma distribution exclusively positive values are needed. We used the ggeffects package (Lüdecke, 2018) to create the estimated marginal means at the specific values of the model terms, to create partial plots (Figure 3).

Results

Out of 107 animals in the study (Table 1), for the ddTRAP assay, six adults failed (three females in prehibernation, and one female in the active season; one male in prehibernation, and one in the active season), and two juveniles failed (one male in torpor, and one male in IBE). A further two adults failed for the RTL

analysis (one female and one male, both in prehibernation). This left data for 99 individuals for the ddTRAP assay (74 adults and 25 juveniles) and for 105 individuals for RTL (78 adults and 27 juveniles).

The standard temperature to assess TA is 25°C (Ludlow et al., 2014). To test if telomerase from garden dormice is able to elongate the substrate at low temperatures (comparable to the body temperature during deep torpor), we used the elongation temperature of 5°C (see Figure 1). A Wilcoxon rank test confirmed a significant difference between the two temperatures ($W = 9{,}907$, $p < 0.01$). Thus, even if telomerase is present at low temperatures common during deep torpor in garden dormice, TA is minimal and telomere elongation is unlikely to occur via this mechanism. All further comparisons are for TA at 25°C.

A comparison between the four different seasons showed lower TRAP activity in active and prehibernation phases, compared to Torpor and IBE (see Figure 2A). Be aware though, that in torpor and IBE animals were not older than 10 months, namely, "juveniles".

The generalized linear model with TRAP assay at 25°C in the adult dormice group showed that the difference between active and prehibernation season had the strongest effect on telomerase activity per mg protein, with values being higher in the active season compared to prehibernation (Figure 3A, Supplementary Tables S1, 2). All other predictors had no meaningful influence in the model (Supplementary Tables S1, 2).

The model for RTL in adult individuals, with the same predictors as in the TRAP model, showed that seasonal state (active/prehibernation) had the same very strong effect (see Figure 2B) with animals in prehibernation having much shorter RTL than those in the active season (all early born). However, for this model, also the sex of the animals was important with males having longer RTL compared to females in both seasons. The late born individuals (only measured in the active season) had much shorter RTL compared to animals born early in the season (Figure 3B, Supplementary Tables S3, 4). All other variables, body mass and the age of the animals did not have an influence on the model (Supplementary Tables S3, 4).

None of the predictor variables for the models that included the measurements of juvenile males during torpor and IBE (body mass and the feeding regime) had any meaningful influence for the TRAP assay or the RTL ratio. The only variable that stood out, but still had no relative variable importance over 0.7, was body mass in the model including the TRAP assay measurements (Supplementary Tables S5–8).

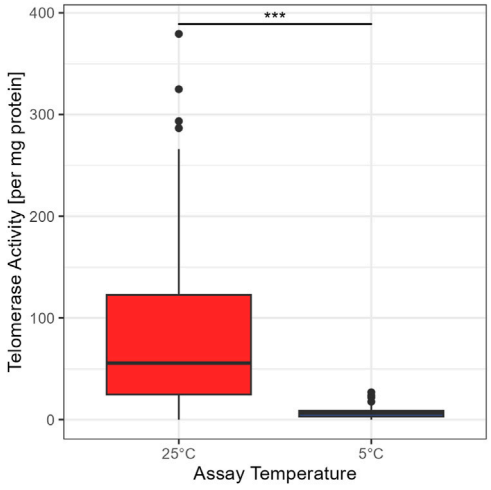

FIGURE 1
Comparison between TRAP assay concentrations at 25°C and 5°C, for 99 animals in the 25°C group and 105 animals in the 5°C group, the boxes show the 25th percentile, the median, and the 75th percentile (Interquartile Range/IQR), whiskers represent the 25th/75th percentile −/+ 1.5 * IQR; points outside of that range are outliers, asterisks indicate significant differences between groups: '***' <0.001 '**' <0.01 '*' <0.05.

Discussion

The clearest and most surprising result from our study is that telomerase is detectable and is maintained at relatively high levels not only during the early active season but also during the two hibernation sampling points, including deep torpor. This runs contrary to our original hypothesis that telomerase activation is costly and unable to be sustained during periods of low energy expenditure such as torpor. It is possible, however, that the TA that we detected is a carry-over of telomerase activated in the period of IBE and, although present, is not active at the low body temperatures experienced during torpor. Our finding that TA is significantly lower when the TRAP phase of the assay is run at 5°C compared to 25°C supports this argument. It is important to note, however, that TA is much lower at 5°C but it was not completely absent (see Figure 1), suggesting that some telomere elongation may still be possible even at such a low temperature. An estimated half-life for the telomerase complex of just 24 h underscores that residual telomerase created during IBE may not be sufficient to maintain activity during deep torpor and that new expression of hTERT would be needed (Holt et al., 1997). This leaves open the intriguing possibility that telomerase can be activated and some telomere elongation is still possible even during torpor, an idea supported by previous research showing an increase in RTL for some individuals over torpor and the hibernation season (Turbill et al., 2013; Giroud et al., 2014). That telomerase is active during IBE is also a novel finding (see Figure 2A) and may shed further light on the need for all hibernating species to periodically return to euthermia. Further research is needed to determine whether TA induced during IBE is purely a consequence of the intense and damaging ROS output generated in this phase of hibernation or a necessary requirement to maintain telomeres as they gradually erode across hibernation. Keeping telomere lengths above a certain threshold and avoiding extreme shortening of telomeric DNA might represent an important strategy in terms of cancer avoidance in animal species living in highly seasonal environments.

Our results show a clear seasonal effect for RTL in garden dormice that has previously been reported in this species (Giroud et al., 2014; Nowack et al., 2019; Giroud et al., 2023) and other species (Hoelzl et al., 2016a; Foley et al., 2018), with a depletion during the hibernation period that is quickly recovered in the active season when food resources are plentiful. This result fits well with our original expectations of a cyclical relationship between RTL and season in the garden dormouse. In the active season, there was also a strong

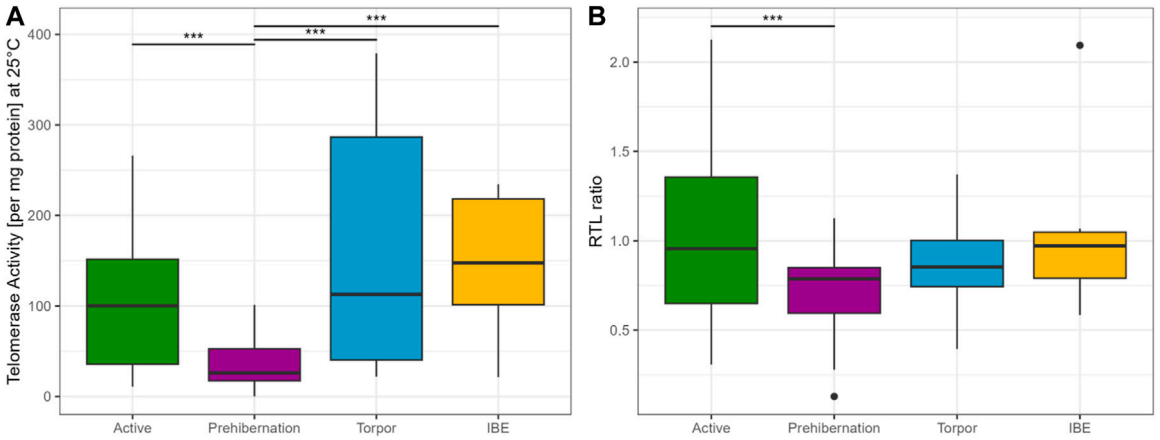

FIGURE 2
(A) TRAP assay concentration at 25°C for all four different seasons, showing that telomerase is present in all phases of the cycle and potentially active. Results represent the glm model (Gaussian distribution), with the response variable telomerase activity at 25°C (square root transformed) and state as the only explanatory variable. For visualisation purposes the plot is on the original scale representing the raw data. **(B)** RTL ratio for all four different seasons. Active and prehibernation seasons only include adult female and male garden dormice, torpor and IBE timepoints only include juvenile males. We cannot compare the different timepoints in a full model, due to these constraints. The R package emmeans (Lenth, 2023) was used for comparisons between groups, asterisks indicate significant differences: "***" <0.001 "**" <0.01 "*" <0.05. The boxes show the 25th percentile, the median, and the 75th percentile (Interquartile Range/IQR), whiskers represent the 25th/75th percentile −/+ 1.5 * IQR, points outside of that range are outliers.

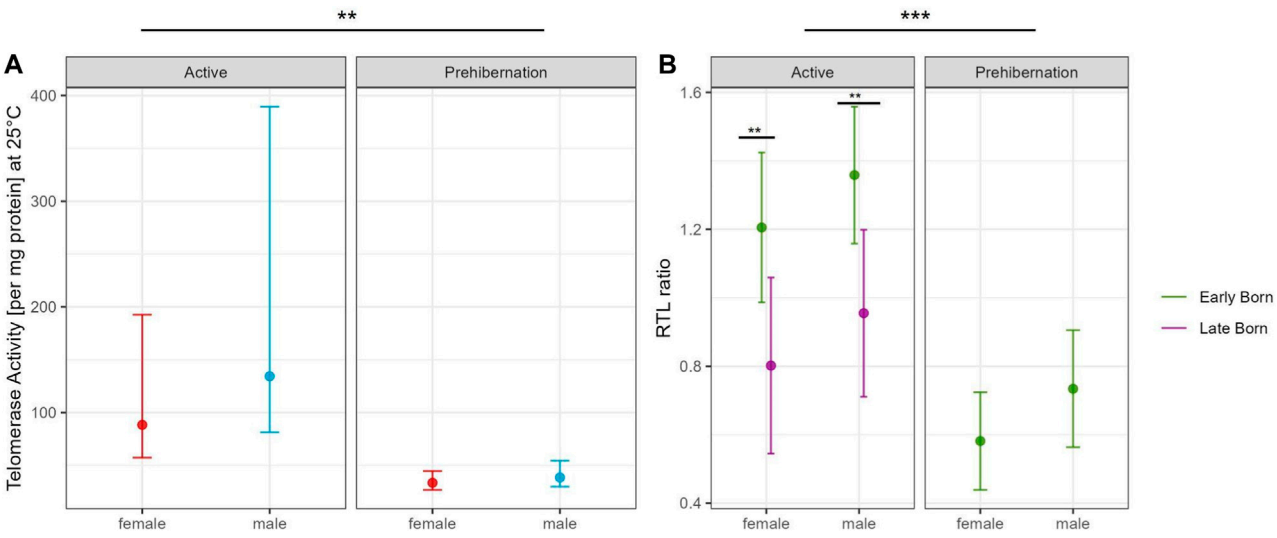

FIGURE 3
Comparison of **(A)** Partial residual plot of the effect of male (blue) and female (red) adult garden dormice on the TA at 25°C compared between the active and prehibernation season. The underlying model accounts for the effects of body mass, early/late born and age of the animals in months and **(B)** Partial residual plot of the effect of early (green) and late (violet) born garden dormice on RTL comparing the active and prehibernation season, underlying model accounts for the effects of body mass and age of the animals in months. Predictions are back-transformed to the original response scale, whiskers show the standard errors, for each group on square root scale for the telomerase activity plot, asterisks indicate significant differences between groups: "***" <0.001 "**" <0.01 "*" <0.05.

influence of early/late born individuals on RTL. For both sexes, late born individuals had significantly shorter RTL than early born. This result is in line with the costs of catch-up growth previously reported for late born garden dormice (Giroud et al., 2014; Mahlert et al., 2018) and likely reflects a carry-over signature of telomere loss from more frequent IBE phases in their first season of hibernation. We also detected, however, a tendency for RTL to decrease immediately prior to hibernation at a time when individuals are investing intensively in accruing body fat for the winter period (see Figure 2B). This interesting finding confirms that the early active season is the important timepoint for individuals to invest in telomere repair and that, directly before hibernation, energy seems to be diverted to other processes such as lipogenesis and fat storage. It may be, however, that this effect is specific to liver tissue which is the prime

organ involved in lipid metabolism and storage. Further tests on other tissue types will help to resolve this question. Interestingly, in our study we were also able to show a corresponding and marked drop in TA at the prehibernation timepoint, which strongly suggests a central role for telomerase in telomere maintenance in this species of hibernating rodent. This finding is incredibly interesting and has important consequences for our understanding of somatic maintenance in general and the energetic costs of telomere repair in particular.

Telomere repair mechanisms have long been postulated to be active in many species (Smith et al., 2022) but the exact nature of these mechanisms has been unclear to date. While telomerase has been the prime candidate, other mechanisms such as ALT (alternative lengthening of telomeres) have also been suggested (Neumann et al., 2013; Shay and Wright, 2019). We show here that, in garden dormice at least, telomerase is closely linked to telomere maintenance and when TA drops we can detect a corresponding drop in RTL. Given the generally high levels of TA at most sampling points however, it is possible that telomerase has other non-canonical functions in this species (Arndt and MacKenzie, 2016). It has been suggested previously that telomerase may be involved in processes as diverse as mitochondrial function (Ahmed et al., 2008; Haendeler et al., 2009; Moslehi et al., 2012), reproduction (Hapangama et al., 2008; Tan et al., 2012; Čapková Frydrychová, 2023), and immunity (Allsopp et al., 2002; Blasco, 2002). Garden dormice may be a good model for investigating such non-canonical functions given the high activity we have detected in this study and their life history which is strongly linked to seasonal fluctuations in energy availability, temperature, and predator avoidance.

Only juvenile male individuals were available for TA measurement during hibernation in this study and they had similar levels of activity to adults in the active season, which was clearly higher than adults in the prehibernation season. This result should be treated with caution given that no juveniles were included in the early active or the prehibernation group. As significant telomere shortening in the first year of life is reported in many species (Monaghan and Ozanne, 2018), it may be that, for juveniles, telomerase is activated at a relatively early timepoint to counteract this loss and TA could be maintained at a high level throughout the active season right up to entering the first hibernation. Our model also highlighted a sex difference in RTL throughout the entire active season (early and immediately prior to hibernation). This finding hints towards a gender biased difference in energy balance during the active season perhaps as a result of reproductive effort. Indeed, male energy requirements for reproduction differ in timing to females in the closely related species *Glis glis*. In males of that species, a large energy demand is related to gonadal development immediately prior and after emergence from hibernation, whereas in females, the main cost is associated with birth and lactation during the main active season (Lebl et al., 2010). The difference in TA that we detected in the active season may reflect an increased investment by females into reproduction and a trade-off in energy balance away from telomere repair. A corresponding trade-off in males likely comes earlier in the active season, immediately prior or right at emergence, and was therefore not captured with our sampling regime. Further studies with additional sampling points should help clarify this issue.

Data availability statement

The raw data supporting the conclusion of this article will be made available by the authors, without undue reservation.

Ethics statement

The animal study was approved by the Ethics and animal welfare committee of the University of Veterinary Medicine, Vienna. The study was conducted in accordance with the local legislation and institutional requirements.

Author contributions

CG-L: Methodology, Validation, Writing–original draft, Writing–review and editing. FH: Conceptualization, Investigation, Methodology, Supervision, Validation, Writing–original draft, Writing–review and editing. SZ: Methodology, Validation, Writing–review and editing. CH: Conceptualization, Writing–review and editing. JC: Formal Analysis, Methodology, Writing–review and editing. SG: Conceptualization, Investigation, Project administration, Writing–review and editing. SS: Conceptualization, Investigation, Project administration, Supervision, Writing–original draft, Writing–review and editing.

Acknowledgments

The authors thank the Austrian Science Fund (FWF, Grant No. P31577-B25) and the Austrian Agency for International Cooperation in Education and Research (OeAD Scientific and Technological Cooperation, Grant No. FR 09/2020) for supporting this research. Further, the authors thank Peter Steiger for the help with animal care.

Conflict of interest

The authors declare that the research was conducted in the absence of any commercial or financial relationships that could be construed as a potential conflict of interest.

Publisher's note

Supplementary material

The Supplementary Material for this article can be found online at: https://www.frontiersin.org/articles/10.3389/fphys.2023.1298505/full#supplementary-material

References

Ahmed, S., Passos, J. F., Birket, M. J., Beckmann, T., Brings, S., Peters, H., et al. (2008). Telomerase does not counteract telomere shortening but protects mitochondrial function under oxidative stress. *J. Cell Sci.* 121, 1046–1053. doi:10.1242/jcs.019372

Allsopp, R. C., Cheshier, S., and Weissman, I. L. (2002). Telomerase activation and rejuvenation of telomere length in stimulated T cells derived from serially transplanted hematopoietic stem cells. *J. Exp. Med.* 196, 1427–1433. doi:10.1084/jem.20021003

Arndt, G. M., and MacKenzie, K. L. (2016). New prospects for targeting telomerase beyond the telomere. *Nat. Rev. Cancer* 16, 508–524. doi:10.1038/nrc.2016.55

Aubert, G. (2014). Chapter four - telomere dynamics and aging. *Prog. Mol. Biol. Transl. Sci.* 125, 89–111. doi:10.1016/B978-0-12-397898-1.00004-9

Barton, K. (2023). MuMIn: multi-model inference. R package version 1.47.5. Available at: https://CRAN.R-project.org/package=MuMIn.

Blasco, M. A. (2002). Immunosenescence phenotypes in the telomerase knockout mouse. *Springer Semin. Immunopathol.* 24, 75–85. doi:10.1007/s00281-001-0096-1

Blasco, M. A. (2007). Telomere length, stem cells and aging. *Nat. Chem. Biol.* 3, 640–649. doi:10.1038/nchembio.2007.38

Čapková Frydrychová, R. (2023). Telomerase as a possible key to bypass reproductive cost. *Mol. Ecol.* 32, 2134–2143. doi:10.1111/mec.16870

Carey, H. V., Andrews, M. T., and Martin, S. L. (2003). Mammalian hibernation: cellular and molecular responses to depressed metabolism and low temperature. *Physiol. Rev.* 83, 1153–1181. doi:10.1152/physrev.00008.2003

Criscuolo, F., Pillay, N., Zahn, S., and Schradin, C. (2020). Seasonal variation in telomere dynamics in African striped mice. *Oecologia* 194, 609–620. doi:10.1007/s00442-020-04801-x

Criscuolo, F., Smith, S., Zahn, S., Heidinger, B. J., and Haussmann, M. F. (2018). Experimental manipulation of telomere length: does it reveal a corner-stone role for telomerase in the natural variability of individual fitness? *Philos. Trans. R. Soc. B Biol. Sci.* 373, 20160440. doi:10.1098/rstb.2016.0440

de Jesus, B. B., Schneeberger, K., Vera, E., Tejera, A., Harley, C. B., and Blasco, M. A. (2011). The telomerase activator TA-65 elongates short telomeres and increases health span of adult/old mice without increasing cancer incidence. *Aging Cell* 10, 604–621. doi:10.1111/j.1474-9726.2011.00700.x

Foley, N. M., Hughes, G. M., Huang, Z., Clarke, M., Jebb, D., Whelan, C. V., et al. (2018). Growing old, yet staying young: the role of telomeres in bats' exceptional longevity. *Sci. Adv.* 4, eaao0926. doi:10.1126/sciadv.aao0926

Giroud, S., Habold, C., Vetter, S., Painer, J., Four-Chaboussant, A., Smith, S., et al. (2022). Living in a changing world: physiological and behavioural flexibility of juvenile Garden Dormice. *ARPHA Conf. Abstr.* 5, e81850. doi:10.3897/aca.5.e81850

Giroud, S., Ragger, M.-T., Baille, A., Hoelzl, F., Smith, S., Nowack, J., et al. (2023). Food availability positively affects the survival and somatic maintenance of hibernating garden dormice (Eliomys quercinus). *Front. Zool.* 20, 19. doi:10.1186/s12983-023-00498-9

Giroud, S., Turbill, C., and Ruf, T. (2012). "Torpor use and body mass gain during pre-hibernation in late-born juvenile garden dormice exposed to food shortage," in *Living in a seasonal world: thermoregulatory and metabolic adaptations*. Editors T. Ruf, C. Bieber, W. Arnold, and E. Millesi (Berlin, Heidelberg: Springer), 481–491. doi:10.1007/978-3-642-28678-0_42

Giroud, S., Zahn, S., Criscuolo, F., Chery, I., Blanc, S., Turbill, C., et al. (2014). Late-born intermittently fasted juvenile garden dormice use torpor to grow and fatten prior to hibernation: consequences for ageing processes. *Proc. R. Soc. B Biol. Sci.* 281, 20141131. doi:10.1098/rspb.2014.1131

Haendeler, J., Dröse, S., Büchner, N., Jakob, S., Altschmied, J., Goy, C., et al. (2009). Mitochondrial telomerase reverse transcriptase binds to and protects mitochondrial DNA and function from damage. *Arterioscler. Thromb. Vasc. Biol.* 29, 929–935. doi:10.1161/ATVBAHA.109.185546

Hapangama, D. K., Turner, M. A., Drury, J. A., Martin-Ruiz, C., Von Zglinicki, T., Farquharson, R. G., et al. (2008). Endometrial telomerase shows specific expression patterns in different types of reproductive failure. *Reprod. Biomed. Online* 17, 416–424. doi:10.1016/s1472-6483(10)60227-1

Harley, C. B., Futcher, A. B., and Greider, C. W. (1990). Telomeres shorten during ageing of human fibroblasts. *Nature* 345, 458–460. doi:10.1038/345458a0

Heldmaier, G., Ortmann, S., and Elvert, R. (2004). Natural hypometabolism during hibernation and daily torpor in mammals. *Respir. Physiol. Neurobiol. Hypoxic Hypometabolism* 141, 317–329. doi:10.1016/j.resp.2004.03.014

Hoelzl, F., Bieber, C., Cornils, J. S., Gerritsmann, H., Stalder, G. L., Walzer, C., et al. (2015). How to spend the summer? Free-living dormice (Glis glis) can hibernate for 11 months in non-reproductive years. *J. Comp. Physiol. B* 185, 931–939. doi:10.1007/s00360-015-0929-1

Hoelzl, F., Cornils, J. S., Smith, S., Moodley, Y., and Ruf, T. (2016a). Telomere dynamics in free-living edible dormice (Glis glis): the impact of hibernation and food supply. *J. Exp. Biol.* 219, 2469–2474. doi:10.1242/jeb.140871

Hoelzl, F., Smith, S., Cornils, J. S., Aydinonat, D., Bieber, C., and Ruf, T. (2016b). Telomeres are elongated in older individuals in a hibernating rodent, the edible dormouse (Glis glis). *Sci. Rep.* 6, 36856. doi:10.1038/srep36856

Holt, S. E., Aisner, D. L., Shay, J. W., and Wright, W. E. (1997). Lack of cell cycle regulation of telomerase activity in human cells. *Proc. Natl. Acad. Sci.* 94, 10687–10692. doi:10.1073/pnas.94.20.10687

Huber, N., Vetter, S., Stalder, G., Gerritsmann, H., and Giroud, S. (2021). Dynamic function and composition shift in circulating innate immune cells in hibernating garden dormice. *Front. Physiol.* 12, 620614. doi:10.3389/fphys.2021.620614

Lebl, K., Kürbisch, K., Bieber, C., and Ruf, T. (2010). Energy or information? The role of seed availability for reproductive decisions in edible dormice. *J. Comp. Physiol. B* 180, 447–456. doi:10.1007/s00360-009-0425-6

Lenth, R. (2023). Emmeans: estimated marginal means, aka least-squares means. R package version 1.8.7. Available at: https://CRAN.R-project.org/package=emmeans.

Lüdecke, D. (2018). Ggeffects: tidy data frames of marginal effects from regression models. *J. Open Source Softw.* 3, 772. doi:10.21105/joss.00772

Ludlow, A. T., Robin, J. D., Sayed, M., Litterst, C. M., Shelton, D. N., Shay, J. W., et al. (2014). Quantitative telomerase enzyme activity determination using droplet digital PCR with single cell resolution. *Nucleic Acids Res.* 42, e104. doi:10.1093/nar/gku439

Lyman, C. P., Willis, J. S., Malan, A., and Wang, L. C. H. (1982). *Hibernation and torpor in mammals and birds*. Elsevier Science.

Mahlert, B., Gerritsmann, H., Stalder, G., Ruf, T., Zahariev, A., Blanc, S., et al. (2018). Implications of being born late in the active season for growth, fattening, torpor use, winter survival and fecundity. *eLife* 7, e31225. doi:10.7554/eLife.31225

Marasco, V., Smith, S., and Angelier, F. (2022). How does early-life adversity shape telomere dynamics during adulthood? Problems and paradigms. *BioEssays* 44, 2100184. doi:10.1002/bies.202100184

Monaghan, P., and Ozanne, S. E. (2018). Somatic growth and telomere dynamics in vertebrates: relationships, mechanisms and consequences. *Philos. Trans. R. Soc. Lond. B. Biol. Sci.* 373, 20160446. doi:10.1098/rstb.2016.0446

Morinha, F., Magalhães, P., and Blanco, G. (2020). Standard guidelines for the publication of telomere qPCR results in evolutionary ecology. *Mol. Ecol. Resour.* 20, 635–648. doi:10.1111/1755-0998.13152

Moslehi, J., DePinho, R. A., and Sahin, E. (2012). Telomeres and mitochondria in the aging heart. *Circ. Res.* 110, 1226–1237. doi:10.1161/CIRCRESAHA.111.246868

Neumann, A. A., Watson, C. M., Noble, J. R., Pickett, H. A., Tam, P. P. L., and Reddel, R. R. (2013). Alternative lengthening of telomeres in normal mammalian somatic cells. *Genes Dev.* 27, 18–23. doi:10.1101/gad.205062.112

Nowack, J., Tarmann, I., Hoelzl, F., Smith, S., Giroud, S., and Ruf, T. (2019). Always a price to pay: hibernation at low temperatures comes with a trade-off between energy savings and telomere damage. *Biol. Lett.* 15, 20190466. doi:10.1098/rsbl.2019.0466

Panasiak, L., Dobosz, S., and Ocalewicz, K. (2020). Telomere dynamics in the diploid and triploid rainbow trout (*Oncorhynchus mykiss*) assessed by Q-FISH analysis. *Genes* 11, 786. doi:10.3390/genes11070786

Ramakers, C., Ruijter, J. M., Deprez, R. H. L., and Moorman, A. F. M. (2003). Assumption-free analysis of quantitative real-time polymerase chain reaction (PCR) data. *Neurosci. Lett.* 339, 62–66. doi:10.1016/S0304-3940(02)01423-4

R Core Team (2023). *R: a language and environment for statistical computing*.

Reichert, S., Bize, P., Arrivé, M., Zahn, S., Massemin, S., and Criscuolo, F. (2014). Experimental increase in telomere length leads to faster feather regeneration. *Exp. Gerontol.* 52, 36–38. doi:10.1016/j.exger.2014.01.019

Ruijter, J. M., Ramakers, C., Hoogaars, W. M. H., Karlen, Y., Bakker, O., Van Den Hoff, M. J. B., et al. (2009). Amplification efficiency: linking baseline and bias in the analysis of quantitative PCR data. *Nucleic Acids Res.* 37, e45. doi:10.1093/nar/gkp045

Shay, J. W., and Wright, W. E. (2019). Telomeres and telomerase: three decades of progress. *Nat. Rev. Genet.* 20, 299–309. doi:10.1038/s41576-019-0099-1

Smith, S., Hoelzl, F., Zahn, S., and Criscuolo, F. (2022). Telomerase activity in ecological studies: what are its consequences for individual physiology and is there evidence for effects and trade-offs in wild populations. *Mol. Ecol.* 31, 6239–6251. doi:10.1111/mec.16233

Spießberger, M., Hoelzl, F., Smith, S., Vetter, S., Ruf, T., and Nowack, J. (2022). The tarnished silver spoon? Trade-off between prenatal growth and telomere length in wild boar. *J. Evol. Biol.* 35, 81–90. doi:10.1111/jeb.13954

Tan, T. C. J., Rahman, R., Jaber-Hijazi, F., Felix, D. A., Chen, C., Louis, E. J., et al. (2012). Telomere maintenance and telomerase activity are differentially regulated in asexual and sexual worms. *Proc. Natl. Acad. Sci. U. S. A.* 109, 4209–4214. doi:10.1073/pnas.1118885109

Tissier, M. L., Bergeron, P., Garant, D., Zahn, S., Criscuolo, F., and Réale, D. (2022). Telomere length positively correlates with pace-of-life in a sex- and cohort-specific way and elongates with age in a wild mammal. *Mol. Ecol.* 31, 3812–3826. doi:10.1111/mec.16533

Tomás-Loba, A., Flores, I., Fernández-Marcos, P. J., Cayuela, M. L., Maraver, A., Tejera, A., et al. (2008). Telomerase reverse transcriptase delays aging in cancer-resistant mice. *Cell* 135, 609–622. doi:10.1016/j.cell.2008.09.034

Turbill, C., Ruf, T., Smith, S., and Bieber, C. (2013). Seasonal variation in telomere length of a hibernating rodent. *Biol. Lett.* 9, 20121095. doi:10.1098/rsbl.2012.1095

Viblanc, V. A., Criscuolo, F., Sosa, S., Schull, Q., Boonstra, R., Saraux, C., et al. (2022). Telomere dynamics in female Columbian ground squirrels: recovery after emergence and loss after reproduction. *Oecologia* 199, 301–312. doi:10.1007/s00442-022-05194-9

Willis, C. K. R., Goldzieher, A., and Geiser, F. (2005). A non-invasive method for quantifying patterns of torpor and activity under semi-natural conditions. *J. Therm. Biol.* 30, 551–556.

frontiers | Frontiers in Physiology

TYPE Mini Review
PUBLISHED 25 April 2024
DOI 10.3389/fphys.2024.1377986

OPEN ACCESS

EDITED BY
Paschalis-Thomas Doulias,
University of Ioannina, Greece

REVIEWED BY
Kelly Drew,
University of Alaska Fairbanks, United States

*CORRESPONDENCE
Yoshifumi Yamaguchi,
bunbun@lowtem.hokudai.ac.jp

RECEIVED 28 January 2024
ACCEPTED 08 April 2024
PUBLISHED 25 April 2024

CITATION
Sone M and Yamaguchi Y (2024), Cold resistance of mammalian hibernators ~ a matter of ferroptosis?
Front. Physiol. 15:1377986.
doi: 10.3389/fphys.2024.1377986

Cold resistance of mammalian hibernators ~ a matter of ferroptosis?

Masamitsu Sone[1,2] and Yoshifumi Yamaguchi[1,2]*

[1]Hibernation Metabolism, Physiology and Development Group, Institute of Low Temperature Science, Hokkaido University, Sapporo, Japan, [2]Graduate School of Environmental Science, Hokkaido University, Sapporo, Japan

Most mammals adapt thermal physiology around 37°C and large deviations from their range, as observed in severe hypothermia and hyperthermia, resulting in organ dysfunction and individual death. A prominent exception is mammalian hibernation. Mammalian hibernators resist the long-term duration of severe low body temperature that is lethal to non-hibernators, including humans and mice. This cold resistance is supported, at least in part, by intrinsic cellular properties, since primary or immortalized cells from several hibernator species can survive longer than those from non-hibernators when cultured at cold temperatures. Recent studies have suggested that cold-induced cell death fulfills the hallmarks of ferroptosis, a type of necrotic cell death that accompanies extensive lipid peroxidation by iron-ion-mediated reactions. In this review, we summarize the current knowledge of cold resistance of mammalian hibernators at the cellular and molecular levels to organ and systemic levels and discuss key pathways that confer cold resistance in mammals.

KEYWORDS

cold resistance, hibernation, torpor, homeotherm, cell death, ferroptosis

Life in the cold

In a cold environment, homeotherms including birds and mammals can maintain their core body temperature (Tb) higher than ambient temperature because of the homeostatic system of body temperature and high thermogenic capacity, thereby being able to operate at night and expand ecological niches into temperate and even polar climates. However, most homeotherms are vulnerable to drastic changes in the Tb. The core Tb of homeotherms is maintained within a value of 1°C, and in many cases, around 37°C. If an insufficient energy source for maintaining Tb homeostasis is obtained for the long term, it finally results in lowered Tb and subsequently malfunction of organs and the whole body system, threatening their lives in strict homeotherms. In contrast, some homeotherms can dynamically change their Tb in a highly regulated manner by being liberated from the restriction of keeping Tb constant and are called heterotherms because of this feature (Ruf and Geiser, 2015). Among heterothermic events, torpor and hibernation are the most prominent examples of drastic changes in Tb (Ruf and Geiser, 2015; Giroud et al., 2020). During torpor, animals suppress their basal metabolic rate and exhibit a very low Tb. Torpor that occurs for a short period (less than 24 h) in response to fasting (starvation) or

Abbreviations: ROS, reactive oxygen species; ETC, electron transport complexes; αT, α-tocopherol; 13LGS, thirteen-lined ground squirrels; AGS, arctic ground squirrels.

other environmental fluctuations that demand animals to reduce energy consumption in an opportunistic manner is classified as daily torpor. Torpor that lasts over 24 h with a very low Tb (often defined below 10°C or 15°C) is called a deep torpor. When deep torpor occurs repeatedly and seasonally for a long period, it is called hibernation. Torpor and hibernation have been observed across all mammalian clades as adaptive mechanisms to cope with fluctuating environments. Hereafter, we use the words "hibernators" for mammals that are able to hibernate among heterotherm and "non-hibernators" for mammals other than hibernators. How torpor and hibernation were acquired during evolution and what discriminates hibernators from non-hibernators or heterotherms from homeotherms are long-lasting questions and are still a matter of debate (Grigg et al., 2004; Canale et al., 2012; Boyles et al., 2013; Ruf and Geiser, 2015; Giroud et al., 2020). Dissecting the physiological, genetic, and molecular mechanisms of torpor and hibernation would help clarify these questions.

Cell-intrinsic cold resistance

One of the important factors that enables hibernation and discrimination of hibernators from non-hibernators is cold resistance, the ability to endure extreme and prolonged low Tb experienced during a long hibernation period. It has long been known that cold resistance is not observed in non-hibernators, including strict homeotherms, such as humans, and heterotherms, such as mice, not only at whole body level but also at tissues and cellular levels (Lyman et al., 1982); When exposed to extreme cold temperatures lower than 10°C, primary cultured cells or tumor cells from non-hibernators such as humans, mice, and rats die within a day or several days, but those from hibernators can survive for over 5 days (Hendriks et al., 2017; Ou et al., 2018; Hendriks et al., 2020; Anegawa et al., 2021). Such difference in cold resistance between hibernators and non-hibernators is also observed in neurons and hepatocytes differentiated from induced pluripotent stem cells (iPSC) derived from a hibernator thirteen-lined ground squirrels (13LGS) (*Ictidomys tridecemlineatus*), highlighting the cell-intrinsic properties of cold resistance and cellular homeostasis in hibernators (Ou et al., 2018; Zhang et al., 2022). Interestingly, such cell-intrinsic properties to sustain cellular homeostasis under cold conditions may also be observed in embryonic stem (ES) cells of mice (*Mus musculus*), which do not hibernate but do fasting-induced torpor (FIT), and are therefore classified as heterotherms. Distinct mouse strains exhibit FIT with different torpor depths depending on the strains; the STM2 strain (*Mus musculus molossinus*) exhibits the lowest Tb of 23°C, whereas B6J (*Mus musculus musculus*) and MYS/Mz (*Mus musculus castaneus*) exhibit Tb of 31°C and 34°C, respectively (Suita et al., 2023). Interestingly, ES cells and liver cells from STM2 strains can sustain oxidative phosphorylation (OxPhos) and higher oxygen consumption at lower temperatures (31°C), whereas those from B6J or MYS/Mz inactivate OxPhos and metabolically incline to glycolysis, suggesting that the cell-intrinsic ability of STM2 mice to maintain mitochondrial activity at low temperatures may enable its lowest Tb in FIT. Thus, the lowest temperature limit that animals can withstand at the cellular level may be a genetically defined intrinsic trait in heterotherms, including both hibernators and non-hibernators.

Dying in cold ~ a matter of ferroptosis?

Why, in the first place, do most mammalian cells die when exposed to low temperature for long duration, though duration and temperature for triggering cold-induced cell death differs among animals and cell types? A classical scheme of how prolonged low temperature leads to cell death was proposed long ago (Hochachka, 1986; Aloia and Raison, 1989; Boutilier, 2001; Rubinsky, 2003). At low temperatures, the lipid membrane bilayers of cells undergo a phase transition into undesired forms, such as a gel phase, leading to segregation of membrane lipids and proteins, and membrane damage. Because of such chronic membrane damage and leakage, ion gradients across cell membranes cannot be sustained, resulting in an increased net Na^+ influx and K^+ efflux. Dysregulation of Na^+/K^+ homeostasis by low temperature was proposed to be caused by failure of ATP homeostasis (Boutilier, 2001) and differences in the temperature coefficient between ion-channel-mediated efflux of K^+ and Na^+/K^+ -ATP pump-dependent influx of K^+ (Hochachka, 1986). As a result, voltage-dependent calcium channels open, and calcium ion concentrations increase within cells. The increased calcium ion concentration further activates calcium ion-dependent phospholipases and proteases and causes remodeling of the plasma membranes, leading to cell death (Hochachka, 1986). Biochemical studies on key metabolic enzymes involved in ion homeostasis, such as Na^+ -K^+ -ATPase, identified differences in the kinetics of hibernators such as ground squirrels and non-hibernators such as rats (Lyman et al., 1982). However, such differences do not sufficiently explain the remarkable cell-intrinsic cold resistance of hibernators. Living organisms also adopt a mechanism called "homeoviscous adaptation," which is the phenomenon of cells adjusting the viscosity of the membrane lipids and thereby compensating membrane fluidity to different temperatures. It includes cold-induced decreases in the length and/or increases in the unsaturation of the fatty acyl chains and shifts in phospholipid composition (Aloia and Raison, 1989). However, little is known about the exact contribution of homeoviscous adaptation to hibernators' cold resistance. Resistance to various other stresses such as hypoxia/reoxygenation and ischemia/reperfusion are also observed in hibernators (Dave et al., 2012). Thus, there is much room for considering the additional mechanisms of why and how mammalian cells are sensitive to cold temperatures from the current perspective.

Cell death can be classified into many types according to the molecular, cellular, and morphological features during the dying process and functional assessment with genetic and/or pharmaceutical inhibition of each cell death type (Galluzzi et al., 2018). Cold-induced cell death in cancer cell lines and primary hepatocytes can be regarded as ferroptosis, a form of necrotic cell death with hallmarks such as necrotic morphology, iron dependency, and extensive lipid peroxidation (Hattori et al., 2017; Hendriks et al., 2017; Hendriks et al., 2020; Anegawa et al., 2021). Ferroptosis was formally named in 2012 as a novel form of cell death, which was induced in certain types of cancers by the anti-cancer drug erastin, which targets the xCT system to transport

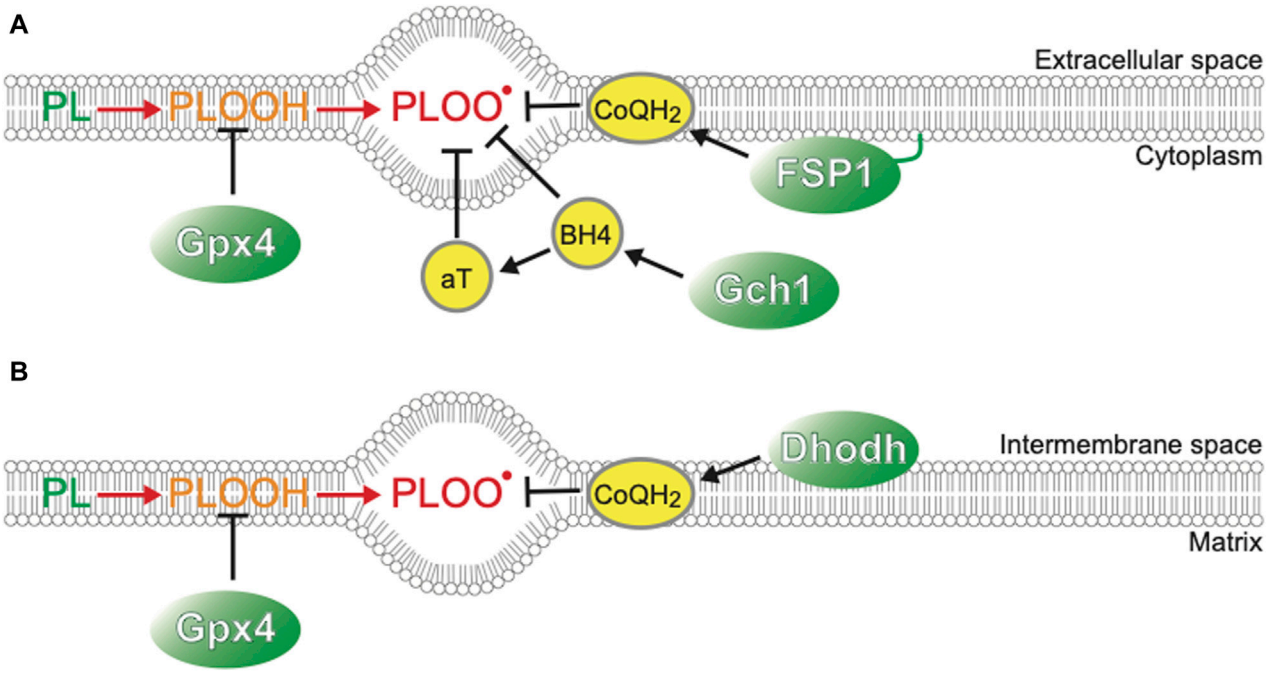

FIGURE 1
Players suppressing ferroptosis **(A)** Plasma membrane. **(B)** Mitochondrial inner membrane.

cystine into cells and has distinct features from other types of cell death, such as apoptosis or classical necrosis (Seiler et al., 2008; Dixon et al., 2012; Stockwell and Jiang, 2020). Cystine is a source of glutathione synthesis, and inhibition of this system results in inadequate activity of glutathione peroxidase 4 (GPx4), which reduces lipid peroxide to lipid alcohol and thereby acts as a repair system for damaged cellular membranes. GPx4 deficiency gives rise to ferroptosis in an iron-dependent manner (Figure 1). First, hydrogen extraction occurs in phospholipids containing polyunsaturated fatty acyl tails by reactive oxygen species (ROS), such as hydrogen peroxide (H_2O_2) and superhydroxyl radical (-OH), or iron-dependent peroxidation enzymes, such as lipoxygenases (Yang et al., 2016; Wenzel et al., 2017) and cytosolic cytochrome P450s (Zou et al., 2020; Yan et al., 2021), leading to further oxidization of lipid radicals by O_2 into lipid peroxyl radicals. Once lipid peroxyl radicals are formed, they extract hydrogen from nearby unsaturated fatty acids, resulting in the formation of lipid radicals and lipid peroxides. Although lipid peroxides are relatively stable, they can facilitate iron-mediated Fenton reactions or other reactions that generate new lipid radicals. As a result, two molecules of lipid radicals are produced from one molecule per cycle, leading to an exponential increase in the number of lipid radicals. This chain reaction of lipid oxidation propagates to the cell membrane or organelle membrane and finally destroys membrane structures, resulting in necrotic morphology (Yan et al., 2021). As labile Fe^{2+} in cytoplasm mediates harmful Fenton reaction, its concentration is tightly regulated to be as low as <5% of total cellular iron, the rest of which is incorporated into Ferritin, a protein that oxidizes Fe^{2+} to Fe^{3+} irons and store them in its cage-like structure, Fe-S clusters, and heme (Kakhlon and Cabantchik, 2002; Galy et al., 2024). Extracellular iron is imported into cells mainly through an iron-carrier protein Transferrin and its receptor TfR, or alternatively through other routes such as metal cation symporter ZIP14 (Galy et al., 2024). Modulation of these Fe^{2+} regulatory systems leads to the changes of cellular susceptibility to ferroptosis inducers; for example, inhibition of NCOA4, which mediates autophagic degradation of Ferritin and therefore increases availability of labile Fe^{2+}, leads to resistance to a ferroptosis inducing drug, erastin (Gao et al., 2016; Hou et al., 2016). The mechanisms of ferroptosis have been extensively studied in the field of cancer biology, because some cancer cells exhibit susceptivity to ferroptosis and revealing its mechanisms may provide novel therapeutic approaches against tumors that are resistant to conventional anti-cancer drugs that target well-known regulated cell death pathways such as apoptosis. Several crucial pathways to prevent/accelerate ferroptosis have been found (Figure 1).

Possible mechanisms of cold-induced ferroptosis

As mentioned above, clues to the molecular mechanisms of cold-induced ferroptosis have come from human cancer studies. Cold stress (4°C) activates the apoptosis signal-regulating kinase 1 (ASK1)-p38 MAPK signaling cascade, which is activated by oxidative stress and reactive oxygen species (ROS). Inhibition of the ASK1-p38 pathway delays cell death under cold temperatures in multiple human cancer cell lines (Hattori et al., 2017). Cold-induced cell death in human cancer cells is not inhibited by inhibitors of apoptosis, a well-known regulated cell death mediated by the activation of caspases, which are evolutionarily conserved cysteine proteases, but is inhibited by an iron-chelator

deferoxamine and ferrostatin-1, potent inhibitors of ferroptosis, leading to the notion that cell death could be regarded as cold-induced ferroptosis. Loss-of-function screening for suppressors of cold-induced ferroptosis in human cancer cell lines identified mitochondrial calcium uptake protein 1 (MICU1), a protein located in the inner mitochondrial membrane that is involved in the transport of Ca^{2+} to the mitochondrial matrix (Nakamura et al., 2021). Human cancer cell lines lacking the MICU1 gene do not exhibit an increase in Ca^{2+} concentration in the mitochondrial matrix under short-term (16 h) cold (4°C) culture and suppress mitochondrial membrane potential (MMP) hyperpolarization just after cold exposure, lipid peroxidation, and subsequent cell death, all of which are triggered by cold. Thus, MICU1 is involved in cold-induced ferroptosis in certain types of cancer cells. The mechanism by which MICU1 deficiency suppresses cold-induced ferroptosis has not been fully elucidated, but one possible scenario proposed is as follows: cold induces calcium influx into the cytosol, leading to an increase in Ca^{2+} concentration in the cytosol and subsequently in the mitochondria via MICU1. This Ca^{2+} influx causes an increase in the activity of electron transport complexes (ETC), leading to mitochondrial membrane (MMP) hyperpolarization, which facilitates ROS generation at multiple steps of, ETC, resulting in lipid peroxidation. A similar scenario was proposed for cultured neurons (Ou et al., 2018). Neurons differentiated from human iPSC exhibit MMP hyperpolarization after cold exposure, then lose MMP and finally die, but depolarization by inhibitors of, ETC complexes, ionophores, or overexpression of mitochondrial uncoupler proteins that cause proton leak suppresses cell death. Thus, it is likely that a cascade of cytosolic calcium increases, and mitochondrial hyperpolarization, subsequent ROS generation, and lipid peroxidation is vital for cold-induced ferroptosis.

On the other hand, studies in cancer cells cultured at normothermia suggest that ferroptosis can be triggered by lipid peroxidation not only in mitochondria but also at other sites within cells or at the plasma membrane at 37°C. First, two enzymes, NADPH-dependent flavin mononucleotide-containing cytochrome P450 oxidoreductase (POR) and NADH-cytochrome b5 reductase (CYB5R1), are necessary for ferroptosis in cancer cells that are susceptible to cell death (Zou et al., 2020; Yan et al., 2021). POR constitutes the cytochrome P450 (CYP) enzyme system and takes electrons from NADPH to donate it to CYPs, including cytochrome b5 or other redox partners, such as heme oxidase (HO1) and squalene monooxidase. However, the interactions between these proteins may not be essential for inducing ferroptosis. It has been proposed that POR and CYB5R1 directly donate electrons from NADPH/NADH to oxygen to generate H_2O_2, leading to lipid peroxidation of polyunsaturated fatty acid (PUFA) on the cellular membrane (Yan et al., 2021). Other organelles, such as peroxisomes or lysosomes, could also be the origin of ferroptosis triggers (Shintoku et al., 2017; Wenzel et al., 2017; Shah et al., 2018). Moreover, plasma membrane itself is a site of accumulation of lipid peroxides formed during ferroptosis, and the accumulated lipid peroxides facilitates cation permeability of the plasma membrane via the activation of the mechanosensitive non-selective cation channels, including piezo-type mechanosensitive ion channel component 1 (Piezo1) and the transient receptor potential (TRP) channel family, and inhibition of Na^+/K^+ -ATPase (Hirata et al., 2023). Clarifying the involvement of the plasma membranes and organelles other than mitochondria in cold-induced ferroptosis and cold resistance in hibernators awaits further investigation.

Genetic basis of defenses against cold in hibernators

Accumulating evidence suggests that even at low temperatures, ROS can be generated within the cells of non-hibernators, leading to lipid peroxidation and cold-induced ferroptosis. Since mitochondria are thought to be the main source of ROS under cold conditions, it has long been studied whether mitochondria of mammalian hibernators exhibit different properties under cold stress in comparison with those of non-hibernators (Lyman et al., 1982; Brown et al., 2012; Mathers and Staples, 2019; Jensen et al., 2021). There are excellent reviews on the biochemical and metabolic properties of hibernators' mitochondria and potential ROS management via sulfide metabolism (Giroud et al., 2020; Jensen and Fago, 2021). However, the exact mechanisms by which and to what extent hibernators suppress ROS generation and cold-induced ferroptosis still remains elusive.

One promising and powerful solution for clarifying the mechanisms of cold resistance is to directly manipulate genes. Comparative metabolomic analysis of hepatocyte-like cells derived from 13LGS-iPSCs revealed that 5-aminolevulinate (5-ALA), a metabolite produced in the first step of the heme synthesis pathway from glycine and succinyl-CoA, increased after 4 h of cold treatment, and is seemingly required for cold resistance of these cells because knockdown of 5-aminolevulinate synthase 1 (ALAS1) led to overproduction of ROS from mitochondria during cooling and rewarming (Zhang et al., 2022). Moreover, the authors demonstrated that liver organs harvested from rats treated at 4°C for 48 h with 5-ALA decreased cell stress and cell death markers in the process of rewarming compared to those without it. They suggested that 5-ALA enhances the activity of Complex III of mitochondrial, ETC, and thereby suppresses reverse electron transfer from Complex II to Complex I during the rewarming process. Thus, functional assessment of candidate genes that are identified by omics approaches could be a promising approach to elucidate mechanisms of cold resistance.

To identify and manipulate genes that can render cold resistance to hibernators and non-hibernators more directly, two pioneering papers conducted a gain-of-function screening using cDNA library generated from hibernators (Singhal et al., 2020; Sone et al., 2023). These gain-of-function strategies hypothesize that hibernators express genes that can render cold resistance even when heterologously expressed in non-hibernators that do not exhibit cold resistance. One study using a cDNA library from arctic ground squirrels (AGS) (*Spermophilus parryii*) tried to identify genes that confer resistance to mild cold (31°C) stress as well as ischemic stress and inhibition of the respiratory complex by the chemical inhibitor Rotenone in mouse neural precursor cells. An identified candidate was ATP5G1, which is a component of the ATP synthase complex in the mitochondria. AGS-ATP5G1 has multiple AGS-specific amino acid substitutions, and the human ATP5G1 protein, whose proline residue at position 32 is replaced with leucine mimicking the AGS gene (Hu ATP5G1P32L) confers resistance to mild cold stress (31°C)

when overexpressed in mouse neural precursor cells. Replacement of the 32nd leucine of ATP5G1 in AGS neural precursor cells with a human-like amino acid (ATP5G1L32P) resulted in a slight decrease in stress resistance. Although the mechanism by which AGS ATP5G1 confers stress resistance is unknown, it is suggested to be related to an increase in the mitochondrial reserve respiratory capacity. It is unclear to what extent AGS-ATP5G1 contributes to the severe cold below 10°C that is experienced during hibernation, because the study used very mild cold stress (31°C) as a stressor. The 32nd leucine of ATP5G1 is not conserved in other hibernators, including Syrian hamsters (*Mesocricetus auratus*) (unpublished observation according to the uniport database), suggesting that it is the family sciuridae-specific mutation.

Another gain-of-function study identified genes that confer resistance to severe cold and rewarming experienced during hibernation (Sone et al., 2023). Through gain-of-function screening using a cDNA library prepared from Syrian hamster cancer cells that can survive even when exposed to severe cold (4°C) for more than 5 days and subsequent rewarming to 37°C, this study identified GPx4 as a strong suppressor of cold-induced ferroptosis in a non-hibernating human cancer cell line. As mentioned above, GPx4 is a protein that removes lipid hydroperoxides by reducing them with glutathione to lipid alcohol and plays a crucial role in suppressing ferroptosis. A cold-vulnerable human cancer cell line becomes resistant to severe cold (4°C) exposure and rewarming by heterologous expression of Syrian hamster GPx4, which suppresses lipid peroxidation. On the other hand, disruption of GPx4 in Syrian hamster cancer cells, a loss of function strategy, results in cold-induced ferroptosis after 3 days of cold exposure, judging from the hallmarks of ferroptosis, such as accumulation of lipid peroxides, necrotic morphology, and inhibition of cell death by iron chelators. Such a loss of cold resistance was rescued by overexpression of either hamster GPx4 or human GPx4. This study also demonstrates that GPx4 activity is necessary only under cold conditions because treatment with chemical inhibitors of GPx4 kills hamster cells only under cold treatment. These lines of evidence suggest that 1) GPx4 is an essential component of cold resistance in hibernator Syrian hamsters, and 2) both non-hibernator human GPx4 and hibernator Syrian hamster GPx4 are able to suppress cold-induced ferroptosis when overexpressed.

This study further identifies the factors that play a crucial role in cold resistance. Although GPx4-knock out (KO) hamster cells die after 5 days of cold conditions (4°C), they survive for 2 days at 4°C. This is in striking contrast to human cancer cells or mouse primary hepatocytes that die within 1 day under cold conditions. Such "short-term" cold resistance of GPx4-KO hamster cells is supported by other ferroptosis-suppressing pathways such as CoQ reducing system, biopterin synthesis system, and α-tocopherol (αT) (Sone et al., 2023). Single disruption of ferroptosis suppressor protein-1 (FSP1), dihydroorotate dehydrogenase (Dhodh), or GTP Cyclohydrolase 1 (Gch1), which are genes involved in $CoQH_2$ or biopterin synthesis (Figure 1) (Bersuker et al., 2019; Doll et al., 2019; Kraft et al., 2020; Mao et al., 2021; Nakamura et al., 2023), does not cause cell death either at 37°C or at 4°C, but co-treatment with GPx4 inhibitors results in a massive increase in cell death at 4°C, particularly in the case of Gch1 disruption. These observations suggest that 1) ferroptosis-suppressing pathways act to inhibit cold-induced ferroptosis in an additive manner both in hibernators and non-hibernator cells, and that 2) among them, GPx4 is a central component of cold resistance in hibernators.

Extrinsic and systemic factors that support cold resistance of hibernators

In addition to the above-mentioned cell-intrinsic mechanisms to prevent lipid peroxidation and cell death, hibernators also utilize extrinsic and systemic mechanisms supporting cold resistance to combat many types of oxidative stress *in vivo* accompanying hibernation. During both deep torpor and interbout arousal in 13LGS, the oxidation of lipids and proteins increases in various organs (Duffy and Staples, 2022). In AGS, the levels of antioxidant enzymes and low molecular weight ROS scavengers increase in the blood and cerebrospinal fluid during hibernation (Drew et al., 2002), and Vitamin C (ascorbate), a water-soluble antioxidant, increases 3- to 5-fold in the blood and 2-fold in the cerebrospinal fluid during deep torpor, whereas glutathione, another antioxidant, remains unchanged (Drew et al., 1999). More specifically, ascorbate levels decline during arousal from deep torpor (Toien et al., 2001). This occurs with the increase in urea, which is a degradation product of nucleic acids by xanthine oxidase, accompanied by the generation of free radicals and H_2O_2. This suggests that ascorbate is used to scavenge ROS in the blood and cerebrospinal fluid during arousal. Consistent with this hypothesis, a microdialysis analysis in hibernating Syrian hamsters demonstrated that the injection of an inhibitor of xanthine oxidase into the brain suppresses the consumption of ascorbate in the cerebrospinal fluid during the arousal period (Osborne and Hashimoto, 2007). Catalase activity to degrade H_2O_2 also increases in hamster blood during the mid-awake state and inhibits H_2O_2-induced cell death (Ohta et al., 2006). In contrast, it was reported that the levels of plasma ascorbate and urate are lowest during torpor and increase gradually during the arousal process in Syrian hamsters (Okamoto et al., 2006). The αT level peaked during deep torpor and declined during arousal. Because αT can be reduced from αT radicals by ascorbate, the opposite kinetics of ascorbate and αT in Syrian hamsters suggest that ascorbate may reduce αT radicals in the plasma during rewarming.

Ascorbate is synthesized mainly in the liver of most mammals, except primates, guinea pigs, and numerous bats (Duque et al., 2022). Ascorbate also regulates the iron homeostasis via intestinal iron absorption and promotion of cellular uptake of iron ion through Transferrin-TfR system (Lane and Richardson, 2014). Total iron levels in bones or livers in Daurian ground squirrels during DT is lower than those during summer (He et al., 2022; Yin et al., 2022). Transcriptomic analysis of white adipose tissues in Crossley's dwarf lemurs and proteomic analysis of livers in 13LGSs demonstrated that expression levels of Ferritin is higher in torpor or the entry into torpor, respectively, when compared with those in active seasons (Rose et al., 2011; Faherty et al., 2018). Although the biological significance of these seasonal changes is unclear, such changes may help sequestering Fe^{2+} and contribute to inhibition of ferroptosis during torpor in hibernators.

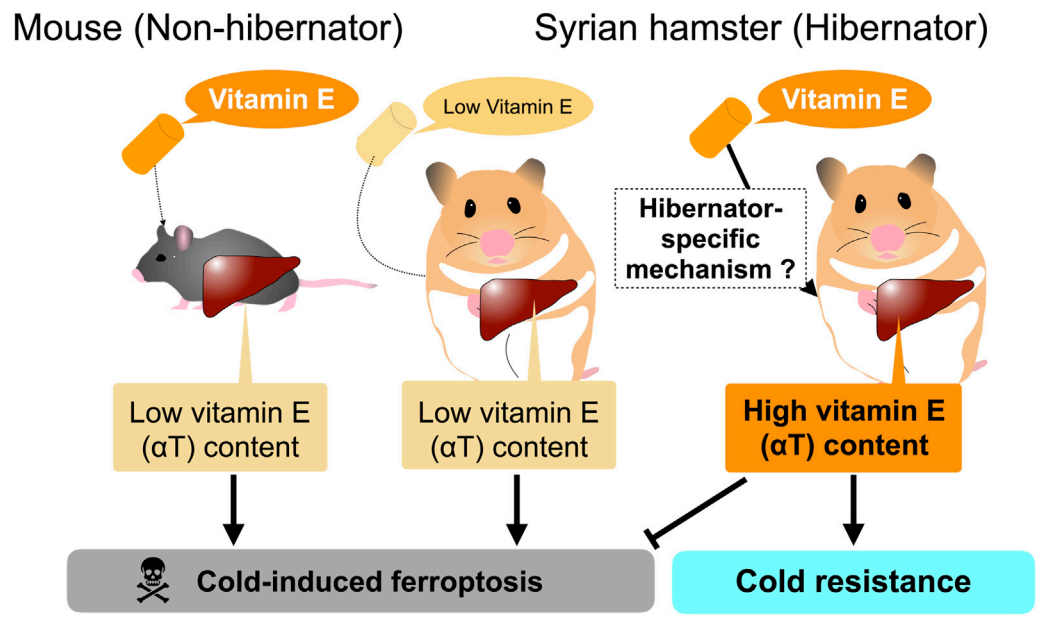

FIGURE 2
In vitro hepatic cold resistance affected by diet and species.

However, careful consideration is required to interpret the dynamics of systemic factors and their contribution to systemic cold resistance and redox status of animals. Most of the above-mentioned systemic factors are nutrients, metabolites, and minerals that are taken from diets and are synthesized, regenerated, and recycled within bodies, suggesting that their amounts could be affected by diets provided to the animals. For instance, the amount of αT in the liver and plasma of Syrian hamsters is largely affected by their diets given to them. αT is a major form of vitamin E obtained from the diet and plays a crucial role in rendering cold resistance to cells and organs by preventing lipid peroxidation. The liver is the primary organ responsible for storing and redistributing diet-derived αT from the portal vein into the systemic circulation. Redistribution of αT from the liver is achieved by αT transfer protein (α-TTP) in mammals, and loss-of-function mutations in humans result in low circulating vitamin E concentrations and many pathological symptoms related to vitamin E deficiency, such as neurodegenerative disorders (Di Donato et al., 2010; Kono et al., 2013). Primary cultured hepatocytes from Syrian hamsters survive for more than 5 days at 4°C, regardless of whether they are during the hibernation period or the non-hibernation period (Anegawa et al., 2021). Under the same conditions, primary cultured mouse hepatocytes die within 1–2 days at 4°C by cold-induced ferroptosis. The cold resistance of Syrian hamster hepatocytes depends on the diet of the animals used for and prior to hepatocyte culture (Figure 2). Diets containing relatively higher amounts of total vitamin E (more than >150 mg/kg; hereafter high αT diets) support hepatic cold resistance *in vitro*, while diets containing lower amounts of total vitamin E (less than <70 mg/kg; hereafter medium αT diets) fail to do so; Primary hepatocytes prepared from animals fed a medium vitamin E diet underwent cold-induced ferroptosis at 4°C. This loss of hepatic cold resistance was rescued by oral administration of αT. Hepatic αT content correlated well with cold resistance of hepatocytes. Interestingly, the high αT diets used in this study failed to increase hepatic αT content and render cold resistance in mouse hepatocytes, as mentioned above, indicating species differences in the hepatic ability to store dietary αT derived from diets. Thus, the cold resistance of primary cells prepared from tissues, at least in the liver, can be easily affected by species and diet fed to animals (Figure 2). Consideration of the possible effects of nutrients taken from diets on cold resistance may be useful in clinical applications, because αT could prevent lipid peroxidation that occurs not only in the deep torpor but also in the rewarming process during arousal, which is similar to the cold-rewarming process of cold-stored organs in the case of organ transplantation (Talaei et al., 2011; Vettel et al., 2014; Tolouee et al., 2022).

Contrary to the *in vitro* significance of αT in cold resistance, the *in vivo* significance of αT in hibernation is not yet clear. Vitamin E insufficiency causes many pathological conditions, hampering the examination of its role of vitamin E in hibernation. One preliminary study reported the negative effects of higher amounts of αT on torpor expression in golden-mantled ground squirrels (*Spermophilus lateralis*) using two diets that differ in tocopherol content (Frank et al., 2000), but it is difficult to conclude the role of tocopherols in torpor and hibernation because these diets are not chemically formulated and must differ in the content of many ingredients other than tocopherols, such as fatty acids and lipids. This is also true for the roles of other nutrients in torpor and hibernation in many literatures. For instance, it was hypothesized that omega-3 and omega-6 fatty acids play different roles in torpor and hibernation, based on studies in which phenotypes of torpor and hibernation are examined in animals fed diets containing different amounts of these fatty acids (Ruf and Arnold, 2008; Giroud et al., 2013; Arnold et al., 2015; Giroud et al., 2018; Giroud et al., 2020). However, such studies cannot be supported by fully chemically

defined diets, and several reports contradict this hypothesis (Trefna et al., 2017; Rice et al., 2021). Obviously, as in the case of vitamin E, there must be many differences in its ingredients. Thus, future studies with strategies that directly manipulate the amount of these nutrients and redox factors within bodies, for instance, by genetic manipulation of genes responsible for the uptake, transport, or metabolism of specific nutrients and metabolites, are required to dissect the mechanisms of cold resistance at the whole-body level.

Open questions and future perspectives

Owing to recent technological advances, it is now possible to address the mechanisms of cold resistance as well as other properties of hibernation from the functional assessment of genes in cells tissues, and hibernators (Singhal et al., 2020; Sone et al., 2023). It opens up new avenues for answering several fundamental and classic questions, as follows:

Q1: What genes are necessary and sufficient for cold resistance of hibernators?
Q2: Is it possible to confer cold resistance to non-hibernator cells?
Q3: Is cold resistance achieved either by a few specific genes or by the sum of modifications of the functions of many genes?
Q4: Are there common or diverse mechanisms for cold resistance among various hibernators?

Regarding Q1 and Q2, Sone et al. (2023) demonstrated that GPx4 is necessary for cell-intrinsic cold resistance in Syrian hamster cells and is sufficient to confer cold resistance heterologously to non-hibernator human and mouse cells when overexpressed. However, GPx4 is highly conserved among mammals, including non-hibernators, raising the question of why non-hibernators are vulnerable to cold, despite the presence of GPx4. Further investigation is needed to elucidate why non-hibernators are cold-vulnerable, and whether GPx4 function is specifically modified in hibernators. GPx4 is essential for survival of mice and humans. GPx4-deficient mice die during early development and mutations in GPx4 allele can be neonatally lethal (Imai et al., 2003; Yant et al., 2003; Cheff et al., 2021). GPx4 is also necessary for the survival of certain types of cancer cells (Yang et al., 2014), but GPx4-KO hamster pancreatic cancer cells can survive at 37°C, suggesting that other ferroptosis-suppressing pathways or redox pathways work to compensate for the loss of GPx4 in the cells at 37°C as well as under cold (Sone et al., 2023). Thus, hibernators may develop superior ability to non-hibernators in terms of redox regulation via ferroptosis-suppressing redox pathways such as GPx4 and its co-factors glutathione, $CoQH_2$, BH4, and systemically supplied anti-oxidative factors such as αT or vitamin K (Mishima et al., 2022), thereby building up cold resistance. This idea may favor the later notion in Q3, when considering together with the report that diminishment of cold sensitivity in 13LGS and Syrian hamsters is due to species-specific amino acid substitutions of a cold-activated non-selective cation channel, TRPM8 (Matos-Cruz et al., 2017). Alternatively, the cellular membrane composition of hibernators may be intrinsically distinct from that of non-hibernators, or seasonally adapted to achieve cold resistance and maintain membrane fluidity under cold conditions, which could affect the structure of membrane proteins that are vital for maintaining cellular ion homeostasis (Aloia and Raison, 1989; Giroud et al., 2013; Cheff et al., 2021). Further efforts to answer these questions in detail will be necessary in specific model hibernators such as Syrian hamsters, in which the causal relationship between genes and phenomena can be functionally addressed, in combination with candidate genes and candidate molecules accumulated through the latest bioinformatics, omics, and comparative approaches in various hibernators, including ground squirrels, marmots, dormice, chipmunks, bats, and bears (Fedorov et al., 2014; Villanueva-Canas et al., 2014; Ferris and Gregg, 2019; Grabek et al., 2019; Jansen et al., 2019; Gillen et al., 2021; Chen and Mao, 2022; Bao et al., 2023; Christmas et al., 2023; Haugg et al., 2023; Heinis et al., 2023; Takamatsu et al., 2023; Thienel et al., 2023; Yang et al., 2023). Based on these studies, we will further clarify Q4 and its related question whether cold resistance associated with hibernation originates from a common ancestral trait or as a result of convergent evolution across distinct mammalian clades. In either case, understanding the mechanisms of cold resistance will expand our knowledge of thermal adaptation in mammals and merit possible medical applications to organ preservation and therapeutic hypothermia.

Author contributions

MS: Writing–original draft, Writing–review and editing, Funding acquisition. YY: Funding acquisition, Writing–original draft, Writing–review and editing.

Funding

The author(s) declare that financial support was received for the research, authorship, and/or publication of this article. This work was supported by grants from the Ministry of Education, Culture, Sports, Science, and Technology (MEXT)/Japan Society for the Promotion of Science KAKENHI (22K19320, 23H04940) and Inamori Research Institute for Science.

Acknowledgments

We thank A. Yamauchi and members of hibernation, physiology, metabolism, and development group at institute of low temperature science, Hokkaido University for valuable comments on the manuscript.

Conflict of interest

The authors declare that the research was conducted in the absence of any commercial or financial relationships that could be construed as a potential conflict of interest.

The author(s) declared that they were an editorial board member of Frontiers, at the time of submission. This had no impact on the peer review process and the final decision.

Publisher's note

References

Aloia, R. C., and Raison, J. K. (1989). Membrane function in mammalian hibernation. *Biochim. Biophys. Acta* 988, 123–146. doi:10.1016/0304-4157(89)90007-5

Anegawa, D., Sugiura, Y., Matsuoka, Y., Sone, M., Shichiri, M., Otsuka, R., et al. (2021). Hepatic resistance to cold ferroptosis in a mammalian hibernator Syrian hamster depends on effective storage of diet-derived α-tocopherol. *Commun. Biol.* 4, 796. doi:10.1038/s42003-021-02297-6

Arnold, W., Giroud, S., Valencak, T. G., and Ruf, T. (2015). Ecophysiology of omega Fatty acids: a lid for every jar. *Physiol. (Bethesda)* 30, 232–240. doi:10.1152/physiol.00047.2014

Bao, Z., Guo, C., Chen, Y., Li, C., Lei, T., Zhou, S., et al. (2023). Fatty acid metabolization and insulin regulation prevent liver injury from lipid accumulation in Himalayan marmots. *Cell Rep.* 42, 112718. doi:10.1016/j.celrep.2023.112718

Bersuker, K., Hendricks, J. M., Li, Z., Magtanong, L., Ford, B., Tang, P. H., et al. (2019). The CoQ oxidoreductase FSP1 acts parallel to GPX4 to inhibit ferroptosis. *Nature* 575, 688–692. doi:10.1038/s41586-019-1705-2

Boutilier, R. G. (2001). Mechanisms of cell survival in hypoxia and hypothermia. *J. Exp. Biol.* 204, 3171–3181. doi:10.1242/jeb.204.18.3171

Boyles, J. G., Thompson, A. B., McKechnie, A. E., Malan, E., Humphries, M. M., and Careau, V. (2013). A global heterothermic continuum in mammals. *Glob. Ecol. Biogeogr.* 22, 1029–1039. doi:10.1111/geb.12077

Brown, J. C., Chung, D. J., Belgrave, K. R., and Staples, J. F. (2012). Mitochondrial metabolic suppression and reactive oxygen species production in liver and skeletal muscle of hibernating thirteen-lined ground squirrels. *Am. J. Physiol. Regul. Integr. Comp. Physiol.* 302, R15–R28. doi:10.1152/ajpregu.00230.2011

Canale, C., Levesque, D., and Lovegrove, B. (2012). "Tropical heterothermy: does the exception prove the rule or force a Re-definition?," in *Living in a seasonal world*. Editors T. Ruf, C. Bieber, W. Arnold, and E. Millesi (Springer Science and Business Media).

Cheff, D. M., Muotri, A. R., Stockwell, B. R., Schmidt, E. E., Ran, Q., Kartha, R. V., et al. (2021). Development of therapies for rare genetic disorders of GPX4: roadmap and opportunities. *Orphanet J. Rare Dis.* 16, 446. doi:10.1186/s13023-021-02048-0

Chen, W., and Mao, X. (2022). Impacts of seasonality on gene expression in the Chinese horseshoe bat. *Ecol. Evol.* 12, e8923. doi:10.1002/ece3.8923

Christmas, M. J., Kaplow, I. M., Genereux, D. P., Dong, M. X., Hughes, G. M., Li, X., et al. (2023). Evolutionary constraint and innovation across hundreds of placental mammals. *Science* 380, eabn3943. doi:10.1126/science.abn3943

Dave, K. R., Christian, S. L., Perez-Pinzon, M. A., and Drew, K. L. (2012). Neuroprotection: lessons from hibernators. *Comp. Biochem. Phys. B* 162, 1–9. doi:10.1016/j.cbpb.2012.01.008

Di Donato, I., Bianchi, S., and Federico, A. (2010). Ataxia with vitamin E deficiency: update of molecular diagnosis. *Neurol. Sci.* 31, 511–515. doi:10.1007/s10072-010-0261-1

Dixon, S. J., Lemberg, K. M., Lamprecht, M. R., Skouta, R., Zaitsev, E. M., Gleason, C. E., et al. (2012). Ferroptosis: an iron-dependent form of nonapoptotic cell death. *Cell* 149, 1060–1072. doi:10.1016/j.cell.2012.03.042

Doll, S., Freitas, F. P., Shah, R., Aldrovandi, M., da Silva, M. C., Ingold, I., et al. (2019). FSP1 is a glutathione-independent ferroptosis suppressor. *Nature* 575, 693–698. doi:10.1038/s41586-019-1707-0

Drew, K. L., Osborne, P. G., Frerichs, K. U., Hu, Y., Koren, R. E., Hallenbeck, J. M., et al. (1999). Ascorbate and glutathione regulation in hibernating ground squirrels. *Brain Res.* 851, 1–8. doi:10.1016/s0006-8993(99)01969-1

Drew, K. L., Toien, O., Rivera, P. M., Smith, M. A., Perry, G., and Rice, M. E. (2002). Role of the antioxidant ascorbate in hibernation and warming from hibernation. *Comp. Biochem. Physiol. C Toxicol. Pharmacol.* 133, 483–492. doi:10.1016/s1532-0456(02)00118-7

Duffy, B. M., and Staples, J. F. (2022). Arousal from torpor increases oxidative damage in the hibernating thirteen-lined ground squirrel (ictidomys tridecemlineatus). *Physiol. Biochem. Zool.* 95, 229–238. doi:10.1086/719931

Duque, P., Vieira, C. P., Bastos, B., and Vieira, J. (2022). The evolution of vitamin C biosynthesis and transport in animals. *BMC Ecol. Evol.* 22, 84. doi:10.1186/s12862-022-02040-7

Faherty, S. L., Villanueva-Canas, J. L., Blanco, M. B., Alba, M. M., and Yoder, A. D. (2018). Transcriptomics in the wild: hibernation physiology in free-ranging dwarf lemurs. *Mol. Ecol.* 27, 709–722. doi:10.1111/mec.14483

Fedorov, V. B., Goropashnaya, A. V., Stewart, N. C., Toien, O., Chang, C., Wang, H., et al. (2014). Comparative functional genomics of adaptation to muscular disuse in hibernating mammals. *Mol. Ecol.* 23, 5524–5537. doi:10.1111/mec.12963

Ferris, E., and Gregg, C. (2019). Parallel accelerated evolution in distant hibernators reveals candidate cis elements and genetic circuits regulating mammalian obesity. *Cell Rep.* 29, 2608–2620. doi:10.1016/j.celrep.2019.10.102

Frank, C. L., Gibbs, A. G., Dierenfeld, E. S., and Kramer, J. V. (2000). *The effects of alpha-tocopherol on mammalian torpor*. Berlin, Heidelberg: Springer Berlin Heidelberg, 207–213.

Galluzzi, L., Vitale, I., Aaronson, S. A., Abrams, J. M., Adam, D., Agostinis, P., et al. (2018). Molecular mechanisms of cell death: recommendations of the nomenclature committee on cell death 2018. *Cell Death Differ.* 25, 486–541. doi:10.1038/s41418-017-0012-4

Galy, B., Conrad, M., and Muckenthaler, M. (2024). Mechanisms controlling cellular and systemic iron homeostasis. *Nat. Rev. Mol. Cell Biol.* 25, 133–155. doi:10.1038/s41580-023-00648-1

Gao, M., Monian, P., Pan, Q., Zhang, W., Xiang, J., and Jiang, X. (2016). Ferroptosis is an autophagic cell death process. *Cell Res.* 26, 1021–1032. doi:10.1038/cr.2016.95

Gillen, A. E., Fu, R., Riemondy, K. A., Jager, J., Fang, B., Lazar, M. A., et al. (2021). Liver transcriptome dynamics during hibernation are shaped by a shifting balance between transcription and RNA stability. *Front. Physiol.* 12, 662132. doi:10.3389/fphys.2021.662132

Giroud, S., Frare, C., Strijkstra, A., Boerema, A., Arnold, W., and Ruf, T. (2013). Membrane phospholipid fatty acid composition regulates cardiac SERCA activity in a hibernator, the Syrian hamster (*Mesocricetus auratus*). *PloS one* 8, e63111. doi:10.1371/journal.pone.0063111

Giroud, S., Habold, C., Nespolo, R. F., Mejias, C., Terrien, J., Logan, S. M., et al. (2020). The torpid state: recent advances in metabolic adaptations and protective mechanisms†. *Front. Physiol.* 11, 623665. doi:10.3389/fphys.2020.623665

Giroud, S., Stalder, G., Gerritsmann, H., Kubber-Heiss, A., Kwak, J., Arnold, W., et al. (2018). Dietary lipids affect the onset of hibernation in the garden dormouse (eliomys quercinus): implications for cardiac function. *Front. Physiol.* 9, 1235. doi:10.3389/fphys.2018.01235

Grabek, K. R., Cooke, T. F., Epperson, L. E., Spees, K. K., Cabral, G. F., Sutton, S. C., et al. (2019). Genetic variation drives seasonal onset of hibernation in the 13-lined ground squirrel. *Commun. Biol.* 2, 478. doi:10.1038/s42003-019-0719-5

Grigg, G. C., Beard, L. A., and Augee, M. L. (2004). The evolution of endothermy and its diversity in mammals and birds. *Physiological Biochem. zoology PBZ* 77, 982–997. doi:10.1086/425188

Hattori, K., Ishikawa, H., Sakauchi, C., Takayanagi, S., Naguro, I., and Ichijo, H. (2017). Cold stress-induced ferroptosis involves the ASK1-p38 pathway. *EMBO Rep.* 18, 2067–2078. doi:10.15252/embr.201744228

Haugg, E., Borner, J., Stalder, G., Kubber-Heiss, A., Giroud, S., and Herwig, A. (2023). Comparative transcriptomics of the garden dormouse hypothalamus during hibernation. *FEBS Open Bio* 14, 241–257. doi:10.1002/2211-5463.13731

He, Y., Kong, Y., Yin, R., Yang, H., Zhang, J., Wang, H., et al. (2022). Remarkable plasticity of bone iron homeostasis in hibernating daurian ground squirrels (Spermophilus dauricus) may Be involved in bone maintenance. *Int. J. Mol. Sci.* 23, 15858. doi:10.3390/ijms232415858

Heinis, F. I., Alvarez, S., and Andrews, M. T. (2023). Mass spectrometry of the white adipose metabolome in a hibernating mammal reveals seasonal changes in alternate fuels and carnitine derivatives. *Front. Physiol.* 14, 1214087. doi:10.3389/fphys.2023.1214087

Hendriks, K. D. W., Joschko, C. P., Hoogstra-Berends, F., Heegsma, J., Faber, K. N., and Henning, R. H. (2020). Hibernator-derived cells show superior protection and survival in hypothermia compared to non-hibernator cells. *Int. J. Mol. Sci.* 21, 1864. doi:10.3390/ijms21051864

Hendriks, K. D. W., Lupi, E., Hardenberg, M. C., Hoogstra-Berends, F., Deelman, L. E., and Henning, R. H. (2017). Differences in mitochondrial function and morphology during cooling and rewarming between hibernator and non-hibernator derived kidney epithelial cells. *Sci. Rep.* 7, 15482. doi:10.1038/s41598-017-15606-z

Hirata, Y., Cai, R., Volchuk, A., Steinberg, B. E., Saito, Y., Matsuzawa, A., et al. (2023). Lipid peroxidation increases membrane tension, Piezo1 gating, and cation permeability to execute ferroptosis. *Curr. Biol.* 33, 1282–1294 e5. doi:10.1016/j.cub.2023.02.060

Hochachka, P. W. (1986). Defense strategies against hypoxia and hypothermia. *Science* 231, 234–241. doi:10.1126/science.2417316

Hou, W., Xie, Y., Song, X., Sun, X., Lotze, M. T., Zeh, H. J., 3rd, et al. (2016). Autophagy promotes ferroptosis by degradation of ferritin. *Autophagy* 12, 1425–1428. doi:10.1080/15548627.2016.1187366

Imai, H., Hirao, F., Sakamoto, T., Sekine, K., Mizukura, Y., Saito, M., et al. (2003). Early embryonic lethality caused by targeted disruption of the mouse PHGPx gene. *Biochem. Biophys. Res. Commun.* 305, 278–286. doi:10.1016/s0006-291x(03)00734-4

Jansen, H. T., Trojahn, S., Saxton, M. W., Quackenbush, C. R., Evans Hutzenbiler, B. D., Nelson, O. L., et al. (2019). Hibernation induces widespread transcriptional remodeling in metabolic tissues of the grizzly bear. *Commun. Biol.* 2, 336. doi:10.1038/s42003-019-0574-4

Jensen, B. S., and Fago, A. (2021). Sulfide metabolism and the mechanism of torpor. *J. Exp. Biol.* 224, jeb215764. doi:10.1242/jeb.215764

Jensen, B. S., Pardue, S., Duffy, B., Kevil, C. G., Staples, J. F., and Fago, A. (2021). Suppression of mitochondrial respiration by hydrogen sulfide in hibernating 13-lined ground squirrels. *Free Radic. Biol. Med.* 169, 181–186. doi:10.1016/j.freeradbiomed.2021.04.009

Kakhlon, O., and Cabantchik, Z. I. (2002). The labile iron pool: characterization, measurement, and participation in cellular processes(1). *Free Radic. Biol. Med.* 33, 1037–1046. doi:10.1016/s0891-5849(02)01006-7

Kono, N., Ohto, U., Hiramatsu, T., Urabe, M., Uchida, Y., Satow, Y., et al. (2013). Impaired α-TTP-PIPs interaction underlies familial vitamin E deficiency. *Science* 340, 1106–1110. doi:10.1126/science.1233508

Kraft, V. A. N., Bezjian, C. T., Pfeiffer, S., Ringelstetter, L., Muller, C., Zandkarimi, F., et al. (2020). GTP Cyclohydrolase 1/tetrahydrobiopterin counteract ferroptosis through lipid remodeling. *ACS Cent. Sci.* 6, 41–53. doi:10.1021/acscentsci.9b01063

Lane, D. J., and Richardson, D. R. (2014). The active role of vitamin C in mammalian iron metabolism: much more than just enhanced iron absorption. *Free Radic. Biol. Med.* 75, 69–83. doi:10.1016/j.freeradbiomed.2014.07.007

Lyman, C. P., Willis, J. S., Malan, A., and Wang, L. C. H. (1982). *Hibernation and torpor in mammals and birds*. New York: Academic Press.

Mao, C., Liu, X., Zhang, Y., Lei, G., Yan, Y., Lee, H., et al. (2021). DHODH-mediated ferroptosis defence is a targetable vulnerability in cancer. *Nature* 593, 586–590. doi:10.1038/s41586-021-03539-7

Mathers, K. E., and Staples, J. F. (2019). Differential posttranslational modification of mitochondrial enzymes corresponds with metabolic suppression during hibernation. *Am. J. Physiol. Regul. Integr. Comp. Physiol.* 317, R262–R269. doi:10.1152/ajpregu.00052.2019

Matos-Cruz, V., Schneider, E. R., Mastrotto, M., Merriman, D. K., Bagriantsev, S. N., and Gracheva, E. O. (2017). Molecular prerequisites for diminished cold sensitivity in ground squirrels and hamsters. *Cell Rep.* 21, 3329–3337. doi:10.1016/j.celrep.2017.11.083

Mishima, E., Ito, J., Wu, Z., Nakamura, T., Wahida, A., Doll, S., et al. (2022). A non-canonical vitamin K cycle is a potent ferroptosis suppressor. *Nature* 608, 778–783. doi:10.1038/s41586-022-05022-3

Nakamura, T., Mishima, E., Yamada, N., Mourao, A. S. D., Trumbach, D., Doll, S., et al. (2023). Integrated chemical and genetic screens unveil FSP1 mechanisms of ferroptosis regulation. *Nat. Struct. Mol. Biol.* 30, 1806–1815. doi:10.1038/s41594-023-01136-y

Nakamura, T., Ogawa, M., Kojima, K., Takayanagi, S., Ishihara, S., Hattori, K., et al. (2021). The mitochondrial Ca(2+) uptake regulator, MICU1, is involved in cold stress-induced ferroptosis. *EMBO Rep.* 22, e51532. doi:10.15252/embr.202051532

Ohta, H., Okamoto, I., Hanaya, T., Arai, S., Ohta, T., and Fukuda, S. (2006). Enhanced antioxidant defense due to extracellular catalase activity in Syrian hamster during arousal from hibernation. *Comp. Biochem. Physiol. C Toxicol. Pharmacol.* 143, 484–491. doi:10.1016/j.cbpc.2006.05.002

Okamoto, I., Kayano, T., Hanaya, T., Arai, S., Ikeda, M., and Kurimoto, M. (2006). Up-regulation of an extracellular superoxide dismutase-like activity in hibernating hamsters subjected to oxidative stress in mid-to late arousal from torpor. *Comp. Biochem. Physiol. C Toxicol. Pharmacol.* 144, 47–56. doi:10.1016/j.cbpc.2006.05.003

Osborne, P. G., and Hashimoto, M. (2007). Brain ECF antioxidant interactions in hamsters during arousal from hibernation. *Behav. Brain Res.* 178, 115–122. doi:10.1016/j.bbr.2006.12.006

Ou, J., Ball, J. M., Luan, Y., Zhao, T., Miyagishima, K. J., Xu, Y., et al. (2018). iPSCs from a hibernator provide a platform for studying cold adaptation and its potential medical applications. *Cell* 173, 851–863. doi:10.1016/j.cell.2018.03.010

Rice, S. A., Mikes, M., Bibus, D., Berdyshev, E., Reisz, J. A., Gehrke, S., et al. (2021). Omega 3 fatty acids stimulate thermogenesis during torpor in the Arctic Ground Squirrel. *Sci. Rep.* 11, 1340. doi:10.1038/s41598-020-78763-8

Rose, J. C., Epperson, L. E., Carey, H. V., and Martin, S. L. (2011). Seasonal liver protein differences in a hibernator revealed by quantitative proteomics using whole animal isotopic labeling. *Comp. Biochem. Physiol. Part D. Genomics Proteomics* 6, 163–170. doi:10.1016/j.cbd.2011.02.003

Rubinsky, B. (2003). Principles of low temperature cell preservation. *Heart Fail Rev.* 8, 277–284. doi:10.1023/a:1024734003814

Ruf, T., and Arnold, W. (2008). Effects of polyunsaturated fatty acids on hibernation and torpor: a review and hypothesis. *Am. J. physiology. Regul. Integr. Comp. physiology* 294, R1044–R1052. doi:10.1152/ajpregu.00688.2007

Ruf, T., and Geiser, F. (2015). Daily torpor and hibernation in birds and mammals. *Biol. Rev. Camb Philos. Soc.* 90, 891–926. doi:10.1111/brv.12137

Seiler, A., Schneider, M., Forster, H., Roth, S., Wirth, E. K., Culmsee, C., et al. (2008). Glutathione peroxidase 4 senses and translates oxidative stress into 12/15-lipoxygenase dependent- and AIF-mediated cell death. *Cell Metab.* 8, 237–248. doi:10.1016/j.cmet.2008.07.005

Shah, R., Shchepinov, M. S., and Pratt, D. A. (2018). Resolving the role of lipoxygenases in the initiation and execution of ferroptosis. *ACS Cent. Sci.* 4, 387–396. doi:10.1021/acscentsci.7b00589

Shintoku, R., Takigawa, Y., Yamada, K., Kubota, C., Yoshimoto, Y., Takeuchi, T., et al. (2017). Lipoxygenase-mediated generation of lipid peroxides enhances ferroptosis induced by erastin and RSL3. *Cancer Sci.* 108, 2187–2194. doi:10.1111/cas.13380

Singhal, N. S., Bai, M., Lee, E. M., Luo, S., Cook, K. R., and Ma, D. K. (2020). Cytoprotection by a naturally occurring variant of ATP5G1 in Arctic ground squirrel neural progenitor cells. *Elife* 9, e55578. doi:10.7554/eLife.55578

Sone, M., Mitsuhashi, N., Sugiura, Y., Matsuoka, Y., Maeda, R., Yamauchi, A., et al. (2023). Identification of genes supporting cold resistance of mammalian cells: lessons from a hibernator. bioRxiv 2023.12.27.573489. doi:10.1101/2023.12.27.573489

Stockwell, B. R., and Jiang, X. (2020). The chemistry and biology of ferroptosis. *Cell Chem. Biol.* 27, 365–375. doi:10.1016/j.chembiol.2020.03.013

Suita, K., Ishikawa, K., Kaneko, M., Wataki, A., Takahashi, M., Kiyonari, H., et al. (2023). Mouse embryonic stem cells embody organismal-level cold resistance. *Cell Rep.* 42, 112954. doi:10.1016/j.celrep.2023.112954

Takamatsu, N., Shirahata, Y., Seki, K., Nakamaru, E., Ito, M., and Tsukamoto, D. (2023). Heat shock factor 1 induces a short burst of transcription of the clock gene Per2 during interbout arousal in mammalian hibernation. *J. Biol. Chem.* 299, 104576. doi:10.1016/j.jbc.2023.104576

Talaei, F., Bouma, H. R., Van der Graaf, A. C., Strijkstra, A. M., Schmidt, M., and Henning, R. H. (2011). Serotonin and dopamine protect from hypothermia/rewarming damage through the CBS/H2S pathway. *PloS one* 6, e22568. doi:10.1371/journal.pone.0022568

Thienel, M., Muller-Reif, J. B., Zhang, Z., Ehreiser, V., Huth, J., Shchurovska, K., et al. (2023). Immobility-associated thromboprotection is conserved across mammalian species from bear to human. *Science* 380, 178–187. doi:10.1126/science.abo5044

Toien, O., Drew, K. L., Chao, M. L., and Rice, M. E. (2001). Ascorbate dynamics and oxygen consumption during arousal from hibernation in Arctic ground squirrels. *Am. J. Physiol. Regul. Integr. Comp. Physiol.* 281, R572–R583. doi:10.1152/ajpregu.2001.281.2.R572

Tolouee, M., Hendriks, K. D. W., Lie, F. F., Gartzke, L. P., Goris, M., Hoogstra-Berends, F., et al. (2022). Cooling of cells and organs confers extensive DNA strand breaks through oxidative stress and ATP depletion. *Cell Transpl.* 31, 9636897221108705. doi:10.1177/09636897221108705

Trefna, M., Goris, M., Thissen, C. M. C., Reitsema, V. A., Bruintjes, J. J., de Vrij, E. L., et al. (2017). The influence of sex and diet on the characteristics of hibernation in Syrian hamsters. *J. Comp. Physiol. B* 187, 725–734. doi:10.1007/s00360-017-1072-y

Vettel, C., Hottenrott, M. C., Spindler, R., Benck, U., Schnuelle, P., Tsagogiorgas, C., et al. (2014). Dopamine and lipophilic derivates protect cardiomyocytes against cold preservation injury. *J. Pharmacol. Exp. Ther.* 348, 77–85. doi:10.1124/jpet.113.207001

Villanueva-Canas, J. L., Faherty, S. L., Yoder, A. D., and Alba, M. M. (2014). Comparative genomics of mammalian hibernators using gene networks. *Integr. Comp. Biol.* 54, 452–462. doi:10.1093/icb/icu048

Wenzel, S. E., Tyurina, Y. Y., Zhao, J., St Croix, C. M., Dar, H. H., Mao, G., et al. (2017). PEBP1 wardens ferroptosis by enabling lipoxygenase generation of lipid death signals. *Cell* 171, 628–641. doi:10.1016/j.cell.2017.09.044

Yan, B., Ai, Y., Sun, Q., Ma, Y., Cao, Y., Wang, J., et al. (2021). Membrane damage during ferroptosis is caused by oxidation of phospholipids catalyzed by the oxidoreductases POR and CYB5R1. *Mol. Cell* 81, 355–369 e10. doi:10.1016/j.molcel.2020.11.024

Yang, W. S., Kim, K. J., Gaschler, M. M., Patel, M., Shchepinov, M. S., and Stockwell, B. R. (2016). Peroxidation of polyunsaturated fatty acids by lipoxygenases drives ferroptosis. *Proc. Natl. Acad. Sci. U. S. A.* 113, E4966–E4975. doi:10.1073/pnas.1603244113

Yang, W. S., SriRamaratnam, R., Welsch, M. E., Shimada, K., Skouta, R., Viswanathan, V. S., et al. (2014). Regulation of ferroptotic cancer cell death by GPX4. *Cell* 156, 317–331. doi:10.1016/j.cell.2013.12.010

Yang, Y., Hao, Z., An, N., Han, Y., Miao, W., Storey, K. B., et al. (2023). Integrated transcriptomics and metabolomics reveal protective effects on heart of hibernating Daurian ground squirrels. *J. Cell Physiol.* 238, 2724–2748. doi:10.1002/jcp.31123

Yant, L. J., Ran, Q., Rao, L., Van Remmen, H., Shibatani, T., Belter, J. G., et al. (2003). The selenoprotein GPX4 is essential for mouse development and protects from radiation and oxidative damage insults. *Free Radic. Biol. Med.* 34, 496–502. doi:10.1016/s0891-5849(02)01360-6

Yin, R., Zhang, J., Xu, S., Kong, Y., Wang, H., and Gao, Y. (2022). Resistance to disuse-induced iron overload in Daurian ground squirrels (Spermophilus dauricus) during extended hibernation inactivity. *Comp. Biochem. Physiol. B Biochem. Mol. Biol.* 257, 110650. doi:10.1016/j.cbpb.2021.110650

Zhang, X., Chen, L., Liu, W., Shen, J., Sun, H., Liang, J., et al. (2022). 5-Aminolevulinate improves metabolic recovery and cell survival of the liver following cold preservation. *Theranostics* 12, 2908–2927. doi:10.7150/thno.69446

Zou, Y., Li, H., Graham, E. T., Deik, A. A., Eaton, J. K., Wang, W., et al. (2020). Cytochrome P450 oxidoreductase contributes to phospholipid peroxidation in ferroptosis. *Nat. Chem. Biol.* 16, 302–309. doi:10.1038/s41589-020-0472-6

Frontiers in Physiology

Understanding how an organism's components work together to maintain a healthy state

The second most-cited physiology journal, promoting a multidisciplinary approach to the physiology of living systems - from the subcellular and molecular domains to the intact organism and its interaction with the environment.

Discover the latest Research Topics

See more →

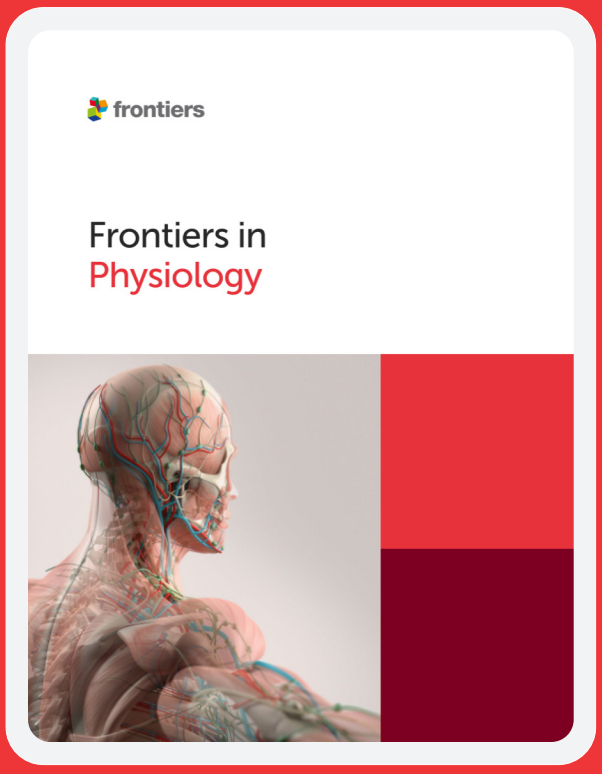

Frontiers

Avenue du Tribunal-Fédéral 34
1005 Lausanne, Switzerland
frontiersin.org

Contact us

+41 (0)21 510 17 00
frontiersin.org/about/contact